ARS JOURNAL

A PUBLICATION OF THE AMERICAN ROCKET SOCIETY

FORMERLY JET PROPULSION

BIND

March 1959 Volume 29 Number 3

forging a renaissance in COPPER

THE BETTMANN ARCHIVE

Forging "new metals" has been routine procedure at Wyman-Gordon for 75 years. Contrasting the modern marvels of metallurgical development is the oldest metal employed by man—copper. Here you see the largest copper closed die forging ever produced—a Re-entry Shield weighing 1875 pounds (67-1/2" x 21-1/2"). Unexcelled know-how, with the availability of the most modern forging equipment, assures the ultimate in forging quality to meet the constantly expanding demands of progress—man's quest for greater speeds and power in his unending exploration farther and farther into yesterday's unknown.

WYMAN-GORDON COMPANY

Established 1883

FORGINGS OF ALUMINUM • MAGNESIUM • STEEL • TITANIUM
Also Beryllium • Molybdenum • Columbium and other unusual metals

WORCESTER 1, MASSACHUSETTS
HARVEY, ILLINOIS • DETROIT, MICHIGAN

the Pioneer in space

To send the U.S. Pioneer more than 60,000 miles into interplanetary space, Space Technology Laboratories in seven months designed, developed, assembled, and tested an 88-foot combination of three integrated stages with a payload incorporating 36 separate ignition systems. STL's Astrovehicles Laboratory focused on the payload itself and the sensitively related problems of propulsion, weight, and stability. These are in addition to the overall complexities of the structural configuration.

Pioneer, setting new apogees in science and missilery, typifies the achievements STL is making in the advancement of space technology. Those who are able to contribute to and benefit from these developments are invited to consider joining our staff.

Space Technology Laboratories

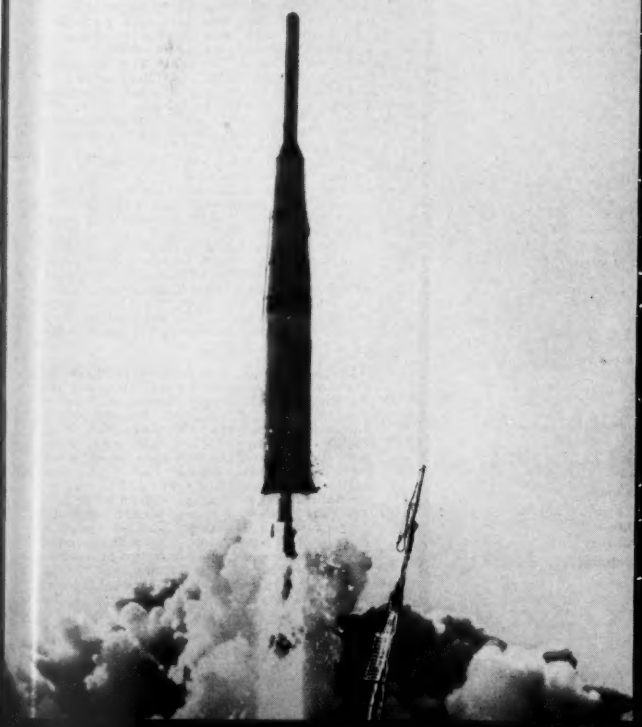

Space Technology Laboratories, Inc.
5730 Arbor Vitae Street, Los Angeles 45, California

ARS JOURNAL

A PUBLICATION OF THE AMERICAN ROCKET SOCIETY

FORMERLY JET PROPULSION

American Rocket Society

500 Fifth Avenue, New York 36, N. Y.

Founded 1930

Scope of ARS JOURNAL

This Journal is devoted to the advancement of astronautics through the dissemination of original papers disclosing new scientific knowledge and basic applications of such knowledge. The sciences of astronautics are understood here to embrace selected aspects of jet and rocket propulsion, space flight mechanics, high-speed aerodynamics, flight guidance, space communications, atmospheric and outer space physics, materials and structures, human engineering, overall system analysis, and possibly certain other scientific areas. The selection of papers to be printed will be governed by the pertinence of the topic to the field of astronautics, by the current or probable future significance of the research, and by the importance of distributing the information to the members of the Society and to the profession at large.

Information for Authors

Manuscripts must be as brief as the proper presentation of the ideas will allow. Exclusion of dispensable material and conciseness of expression will influence the Editors' acceptance of a manuscript. In terms of standard-size double-spaced typed pages, a typical maximum length is 22 pages of text (including equations), 1 page of references, 1 page of abstract and 12 illustrations. Fewer illustrations permit more text, and vice versa. Greater length will be acceptable only in exceptional cases.

Short manuscripts, not more than one quarter of the maximum length stated for full articles, may qualify for publication as Technical Notes or Technical Comments. They may be devoted to new developments requiring prompt disclosure or to comments on previously published papers. Such manuscripts are usually published within two months of the date of receipt.

Sponsored manuscripts are published occasionally as an ARS service to the industry. A manuscript that does not qualify for publication, according to the above-stated requirements as to subject, scope or length, but which nevertheless deserves widespread distribution among jet propulsion engineers, may be printed as an extra part of the Journal or as a special supplement, if the author or his sponsor will reimburse the Society for actual publication costs. Estimates are available on request. Acknowledgment of such financial sponsorship appears as a footnote on the first page of the article. Publication is prompt since such papers are not in the ordinary backlog.

Manuscripts must be double spaced on one side of paper only with wide margins to allow for instructions to printer. Include a 100 to 200 word abstract. State the authors' positions and affiliations in a footnote on the first page. Equations and symbols may be handwritten or typewritten; clarity for the printer is essential. Greek letters and unusual symbols should be identified in the margin. If handwritten, distinguish between capital and lower case letters, and indicate subscripts and superscripts. References are to be grouped at the end of the manuscript and are to be given as follows: For journal articles: authors first, then title, journal, volume, year, page numbers; for books: authors first, then title, publisher, city, edition and page or chapter numbers. Line drawings must be clear and sharp to make clear engravings. Use black ink on white paper or tracing cloth. Lettering should be large enough to be legible after reduction. Photographs should be glossy prints, not matte or semi-matte. Each illustration must have a legend; legends should be listed in order on a separate sheet.

Manuscripts must be accompanied by written assurance as to security clearance in the event the subject matter lies in a classified area or if the paper originates under government sponsorship. Full responsibility rests with the author.

Submit manuscripts in duplicate (original plus first carbon, with two sets of illustrations) to the Editor, Martin Summerfield, Professor of Aeronautical Engineering, Princeton University, Princeton, N. J. Preprints of papers presented at ARS national meetings are automatically considered for publication.

ARS JOURNAL is published monthly by the American Rocket Society, Inc. and the American Interplanetary Society at 20th & Northampton Sts., Easton, Pa., U. S. A. Editorial offices: 500 Fifth Ave., New York 36, N. Y. Price: $12.50 per year, $2.00 per single copy. Second-class mail privileges authorized at Easton, Pa. This Publication is authorized to be mailed at the special rates of postage prescribed by Section 132.122. Notice of change of address should be sent to the Secretary, ARS, at least 30 days prior to publication. Opinions expressed herein are the authors and do not necessarily reflect the views of the Editors or of the Society.

NO CHILD'S PLAY

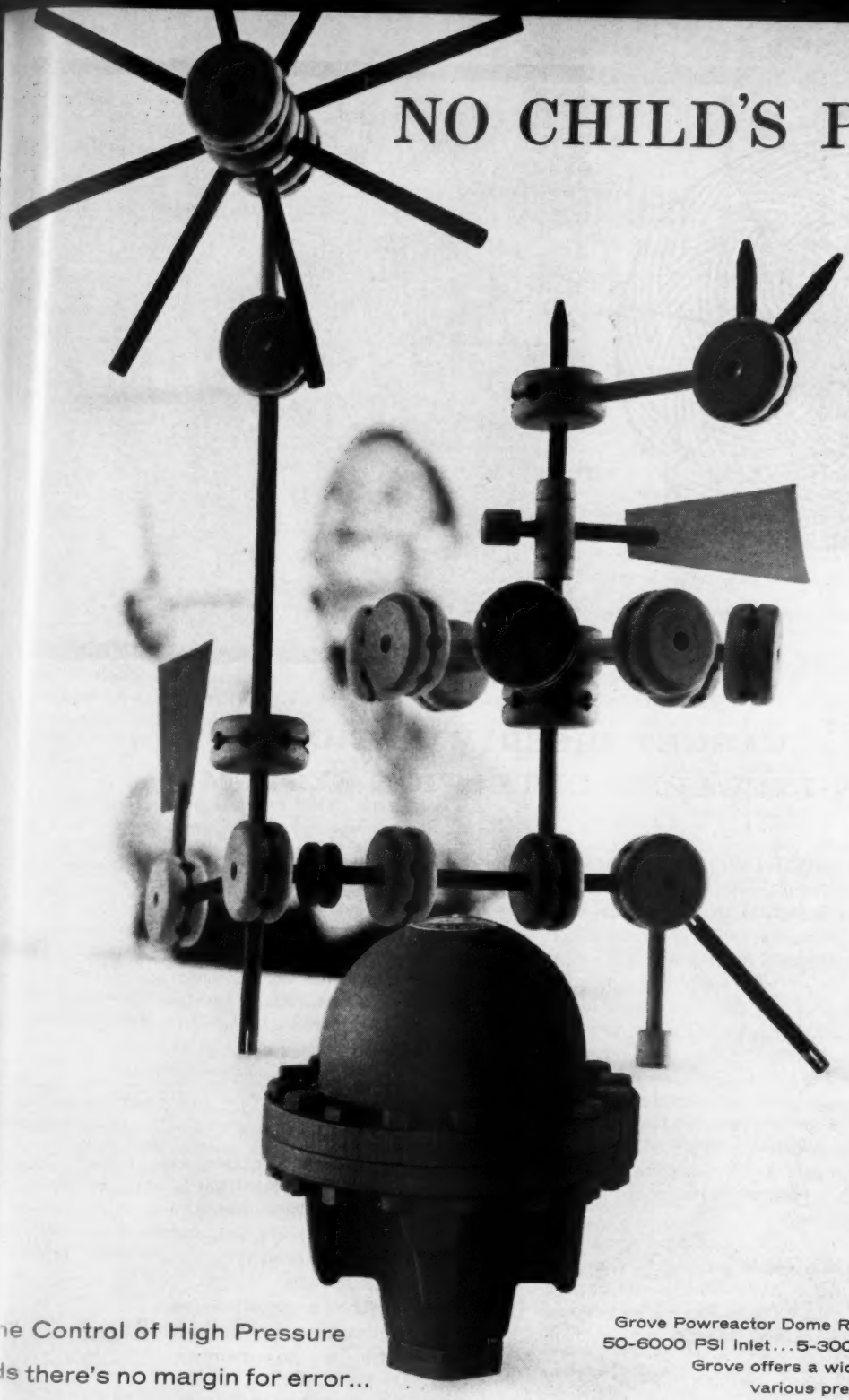

Grove Powreactor Dome Regulator Model GH-408... 50-6000 PSI Inlet...5-3000 PSI Reduced Pressure. Grove offers a wide variety of regulators for various pressure and flow conditions.

n The Control of High Pressure luids there's no margin for error...

his is no child's play. Response must be instantaneous...accuracy absolute...dependability ositive. This is why for over a quarter of a century, Grove Regulators have been the No. 1 hoice for the critical control of high pressure fluids. Here at Grove—unmatched experience nd unique design/engineering skills that can work for you. See or call your Grove man today.

GROVE VALVE and REGULATOR COMPANY

529 Hollis St., Oakland 8, California · 2559 W. Olympic Blvd., Los Angeles 6, California
ffices in other principal cities

5156

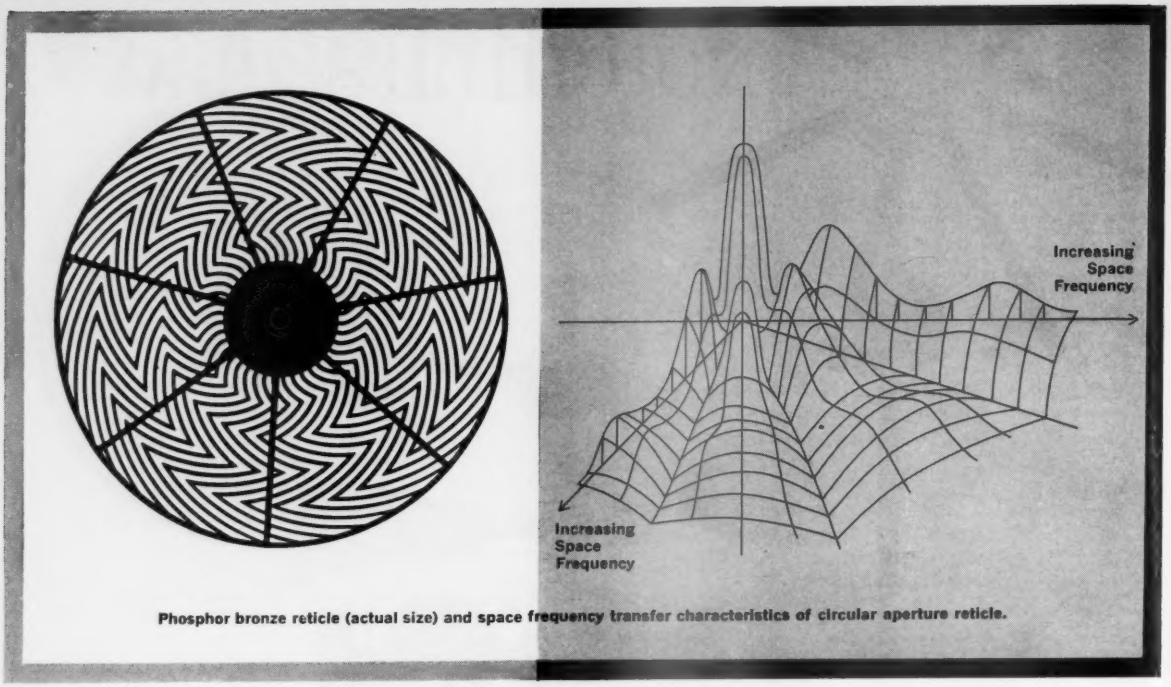

Phosphor bronze reticle (actual size) and space frequency transfer characteristics of circular aperture reticle.

TARGET DISCRIMINATION IN INFRARED DETECTION SYSTEMS

The pioneering field of infrared detection offers many challenging opportunities to scientists and engineers at Ramo-Wooldridge for advanced studies in the solution of target discrimination problems. Research is continually under way at Ramo-Wooldridge in the integrating of infrared detection devices with the latest electronic systems techniques for enhanced target detection on the ground and in the air.

The phosphor bronze reticle, or image chopper, illustrated above was developed by Ramo-Wooldridge. It indicates a marked stride in space filtering discrimination concepts, and is used for target signal enhancement in guided missiles, anti-aircraft fire control and air collision warning applications.

The reticle is used in the focal plane of an infrared optical system and is rotated to chop the target image for the desired space filtering. It is also employed in time filtering, such as pulse length discrimination, or pulse bandwidth filtering.

Space filtering is critical to infrared systems, because of its ability to improve the detection of objects located in the midst of background interference. In a manner similar to that used in the modification of electronic waveforms by electrical filtering, space filtering enhances the two-dimensional space characteristics of a target. The size and features of the target are highlighted and the undesired background eliminated.

Scientists and engineers with backgrounds in infrared systems—or any of the other important areas of research and development listed below—are invited to inquire about current opportunities at Ramo-Wooldridge.

Electronic reconnaissance and countermeasures systems
Analog and digital computers
Air navigation and traffic control
Antisubmarine warfare
Basic research
Electronic language translation
Information processing systems
Advanced radio and wireline communications
Missile electronics systems

RAMO-WOOLDRIDGE
P. O. BOX 90534 AIRPORT STATION • LOS ANGELES 45, CALIFORNIA
a division of *Thompson Ramo Wooldridge Inc.*

Recent Advances in Gaseous Detonation[1]

R. A. GROSS
Fairchild Engine Division
Deer Park, N. Y.

A. K. OPPENHEIM
University of California
Berkeley, Calif.

A review of recent work in gaseous detonation is presented. Early work is briefly mentioned and treatises listed. Theoretical calculations of Chapman-Jouguet detonations are reviewed, compared and the ambiguity concerning the speed of sound in a reacting gas mixture discussed. Experimental Chapman-Jouguet measurements are reviewed. Recent studies of the interior of a detonation wave are presented. Standing detonation wave research, detonation limits, two-dimensional detonations, spectra, ionization and magnetohydrodynamic treatments are brought to the reader's attention. A qualitative description of the development of a flame to a detonation is presented. Experimental observations are examined and recent theoretical attempts to explain these observations are reviewed.

Dr. Gross, Chief Research Engineer at the Fairchild Engine Division, is currently doing fundamental research in high temperature gas dynamics, supersonic combustion and plasma physics. He received his B.S. degree in Mechanical Engineering from the University of Pennsylvania (1949) and his Ph.D. in Engineering Sciences and Applied Physics from Harvard (1952), where he was a teaching fellow. Since 1954 he has been working in advanced propulsion engineering at Fairchild, and during 1959–1960 will be on leave of absence as a National Science Foundation Senior Post Doctoral Fellow. Dr. Gross has written numerous papers on advanced propulsion and problems associated with detonation and is a fellow of the American Rocket Society.

Dr. Oppenheim is now Professor of Aeronautical Sciences at the University of California, Berkeley, where he has taught since 1950; and is also consultant for the Shell Development Company. He received the Dipl. Ing. in Aeronautical Engineering from the Warsaw Institute of Technology (1943), the Ph.D. from the University of London and the D.I.C. from Imperial College (1945). He has served on the faculties of City and Guilds College, London, 1945–1948, and Stanford University, 1948–1950. An active member of the American Rocket Society, Dr. Oppenheim is a past president of the Northern California Section and has recently been elected to the National Board of Directors.

Steady-State Phenomena

A DETONATION is a wave in which an exothermal reaction takes place and which moves with supersonic velocity with respect to the undetonated (reactant) gas. It is characterized by this supersonic propagation velocity and a large pressure and temperature increase across the wave. A detonation differs from a flame (deflagration) in that a flame moves with subsonic velocity. The propagation rate of a detonation is determined mainly by aerothermodynamic considerations, whereas flame speeds appear to be determined by a complex interaction between high temperature chemical kinetics, heat transfer and diffusion.

Received Jan. 16, 1959.

[1] This review was prepared with the support of the Air Force Office of Scientific Research, ARDC, Washington 25, D. C., under Contracts AF 49(638)-15 and AF 496(38)-166. The section Steady State Phenomena was written by R. A. Gross, and the Development of Detonation was prepared by A. K. Oppenheim.

History

The phenomenon of detonation was discovered concurrently by Berthelot (1)[2] and Mallard and LeChatelier (2) in 1881. Chapman (3) and Jouguet (4,5) independently postulated that the steady-state detonation commonly observed in experiments is distinguished by the fact that the fluid flow immediately behind the detonation wave has a Mach number exactly equal to one relative to the wave. Such a detonation wave has subsequently been called a "Chapman-Jouguet" detonation or simply "C-J" detonation. Following these pioneering works, the literature has carried a steady stream of research reports by chemists, physicists, mathematicians and engineers who became interested in this phenomenon. Reviews of this work can be obtained by referring to books or treatises that present comprehensive information on detonation (6 to 13). Work in this field transcends national boundaries; important contributions having been made by French, English, German, U. S. and Russian scientists.

Classification of Flows

Combustion is distinguished by the numerous and often complex types of phenomena that occur in nature. To obtain a qualitative understanding of some, examine the solutions of the one-dimensional steady flow equations of motion where thermal energy is added to the flow. In Fig. 1 are shown the solutions of the equations representing conservation of mass, momentum and energy. V_1 is the velocity (relative to the wave) ahead of the detonation, V_2 the product velocity and M_1 the approach Mach number. Details concerning these equations and their solutions can be found in (11, 13, 14). Important points in this figure are labeled, and their physical implications noted. Points 6, 7 and 10 are

[2] Numbers in parentheses indicate References at end of paper.

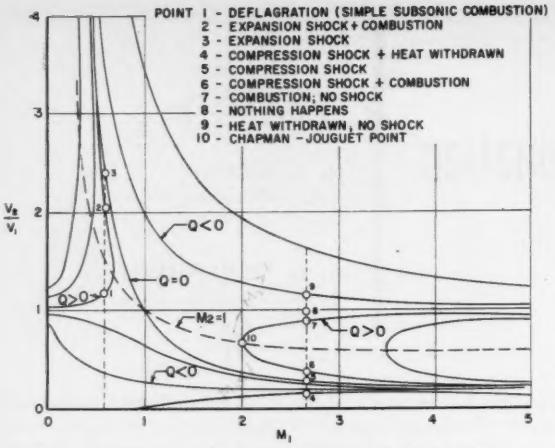

Fig. 1 One-dimensional steady flow with heat addition

detonations. Point 10 is the C-J point and represents the singular solution of the equations. Point 6 is a "strong" detonation and is characterized by the fact that the product flow is subsonic. Point 7 is a "weak" detonation and has the property of a supersonic product flow. A strong detonation has a larger pressure ratio across the wave than a weak detonation at the same value of M_1. The C-J point is the coalescing of the strong and weak detonation branches and has a product Mach number of 1, or "choked" flow. There is a corresponding subsonic C-J point, although it does not usually bear this name. Between the two C-J points, for a given amount of heat addition, there are no steady flow solutions to the equations of motion. For a given quantity of heat addition, the C-J points represent a minimum supersonic wave propagation rate and a maximum subsonic wave propagation rate, respectively.

Detonation Wave Propagation Calculations

The fundamental physical problem in combustion is the determination of the combustion wave propagation rate or speed and the attendant change in the properties of the gases. Since the early work of Chapman (3) and Jouguet (4), scientists have been able to predict C-J detonation velocities with fair precision. The equations of conservation of mass, momentum, energy, chemical equilibrium of the product flow and the fact that the product flow Mach number is 1 constitute a determinant problem. These equations consist of a large simultaneous set of nonlinear algebraic equations. Because of the labor involved in obtaining solutions, the majority of published reports concern relatively simple two atom chemical systems, such as hydrogen-oxygen.

Complete detonation calculations which include dissociation of a three or more atom system are given in (4,9,14,15,23 and 24). All detonation computations have been concerned with the same system of equations, although the numerical methods of solution have varied. Progress has been made primarily in the use of improved thermodynamic data (14 to 23) and care in the proper use of the appropriate sound speed for the C-J point. Recently (14,23,24) electronic digital computers have been employed to solve more complex systems with high accuracy, and we can expect considerable future contributions in this field from such devices.

Recently there has been considerable concern about the uniqueness of the definition of the C-J point. This involves the question of the velocity of sound in a reacting gaseous medium. Surprisingly, nearly all theoretical calculations of the C-J point contain a theoretical error that arises from the ambiguity of the speed of sound definition at the C-J plane. This point is amplified in the next section.

To see how such present computations compare, consider the relatively simple case of the stoichiometric hydrogen-oxygen C-J detonation data of Table 1. Unfortunately, many authors describe the source of their thermodynamic data inadequately, and they do not give the chemical composition of the product flow. Such data are presented, however, in references such as (14,15 and 17).

Speed of Sound in a Reacting Gaseous Medium

The question of the appropriate sound speed in high temperature gas mixtures was raised by Brinkley and Richardson (25) and has been followed by an interesting literature debate recently summarized by Wood and Kirkwood (26). The problem centers about the difference between an equilibrium sound speed and a frozen sound speed. Consider a gas whose equation of state is given by

$$p = p(\rho, s, \beta_i \ldots \beta_n) \qquad [1]$$

where p is the pressure, ρ the density, s the entropy and β_i the mole fraction of the ith chemical constituent of the mixture. Then the equilibrium speed of sound a_e is defined

$$a_e^2 = \left(\frac{\partial p}{\partial \rho}\right)_{s,\,\Delta F\,=\,0} = \left(\frac{\partial p}{\partial \rho}\right)_{s,\,\beta_i} + \sum_{i\,=\,1}^{n} \left(\frac{\partial p}{\partial \beta_i}\right)_{s,\,\beta_i} \left(\frac{\partial \beta_i}{\partial \rho}\right)_{s,\,\Delta F\,=\,0} \qquad [2]$$

where

$$\Delta F_\alpha = \sum \nu_i^\alpha \mu_i$$

ΔF_α is the Gibbs free energy; μ_i is the chemical potential of substance i, and ν_i^α is the stoichiometric coefficient of the ith substance in the αth chemical reaction.

The term $(\partial p/\partial \rho)_{s,\,\beta_i}$ is the frozen speed of sound, i.e., the sound speed in a gas mixture of constant chemical composition. This is the sound speed familiar in low speed aerodynamics. The summation in Equation [2] corresponds to the contribution to the sound speed by the slight change in chemical composition associated with the change in pressure and temperature in the sound wave itself. For a fixed chemical composition, the sound speed of an ideal gas is given by

$$a_f^2 = \left(\frac{\partial p}{\partial \rho}\right)_{s,\,\beta_i} = \gamma \frac{R}{m} T \qquad [3]$$

where T is the temperature, γ the ratio of specific heats and R the gas constant. When the fluid is a mixture of ideal gases

$$\gamma = \frac{\Sigma \beta_i C_{pi}}{\Sigma \beta_i \left(C_{pi} - \dfrac{R}{m}\right)} \qquad [4]$$

where C_{pi} is the specific heat at constant pressure of the ith species, and m is the molecular weight of the mixture. Most calculations of the C-J point, a priori, set the product flow Mach number equal to unity using Equation [3]. However, the classical C-J point, which is the singular point, has the product Mach number equal to unity only if the product Mach number is defined in terms of Equation [2]. To illustrate this point consider Fig. 2. Here is shown the classical Hugoniot curve which is interesting because the coordinates are purely thermodynamic (velocities having been eliminated). The data shown here for a hydrogen-oxygen detonation were computed using the computer program of (14) and

thermodynamic data of (24). Point B is the classical C-J point in which the equilibrium product Mach number is unity. It is the singular point, i.e., point of tangency on the product Hugoniot curve, and has the additional property that $ds = 0$ where the derivative of the entropy s is evaluated along the product Hugoniot curve (10). C is the point found in all theoretical calculations using Equation [3]. The value of V_1, the detonation speed, the quantity most often experimentally measured, is quite similar between B and C, but the pressure, temperature and composition are significantly different.

The frozen speed of sound at point B is, for most C-J stoichiometric fuel air mixtures (14), larger than the equilibrium speed of sound and of the order of $a_e/a_f \approx 0.96$.

Experimental Measurements of C-J Detonations

Shock and detonation tubes have been used to measure the velocity of propagation of C-J detonations (17,27,29). Experimental work in this area is difficult because of the very fast response instrumentation required. Most hydrocarbon-air stoichiometric mixtures under room conditions detonate with velocities of the order of 6000 ft per sec or a Mach number of about 5 (14). The use of piezoelectric, ionization and resistance gages have been the usual techniques employed. Kistiakowsky (32) and Duff (35,36) have succeeded in making density ratio measurements across detonation waves using x-ray absorption techniques. The effect of initial pressure and temperature upon detonation speed were experimentally examined by Cannon (33) and Hoelzer (34).

The question concerning the product gas sound speed mentioned previously appears difficult to resolve experimentally. Relaxation effects (37) cause some doubt on the question of equilibrium. More important, however, is the fact that the flow field behind a detonation gives evidence of two-dimensional effects. A Schlieren photograph of such

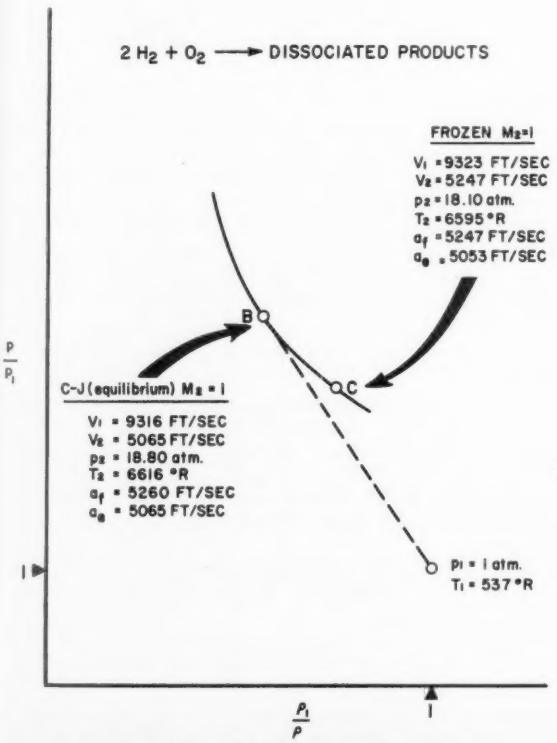

Fig. 2 Stoichiometric hydrogen-oxygen detonation

Table 1 Stoichiometric hydrogen-oxygen detonation

$p_1 = 1.0$ atm
$T_1 = 70$ F
$2H_2 + O_2 \rightarrow$ dissociated products

Source	Measured Velocity V_1, ft/sec	Calculated Velocity V_1, ft/sec	Calculated Pressure p_2, atm	Calculated Temperature T_2, F
(14)	...	9342	18.90	6175
(17)[a]	9268	9357	18.06	6160
(100)[a]	9100	8961	17.22	5908
(15)[a]	9249	9206	18.05	5989
Eisen and Gross[b]	...	9316	18.80	6156
(28)	9072	...	...	...
(27)	8800	...	...	...

[a] These data should be compared with the frozen speed of sound solution shown in Fig. 2.

[b] In (14) some of the thermodynamic data used are outdated. Consequently the calculation has been redone using the latest thermodynamic information available. This accounts for the difference between (14) and the more recent Eisen-Gross data given in Table 1. The sources of thermodynamic data used in this latest calculation can be found in (24).

effects was recently published by Fay (38) wherein weak shocks are seen originating from the wall, and he suggests that this is the effect of the viscous boundary layer and heat transfer. It has been known for some time that the diameter of the experimental tube has an effect upon the detonation velocity; elementary analyses have been offered by Kistiakowsky (23, 30) and Zeldovich (39), and partially confirmed by experiment (30).

Again, it is interesting to compare some experimental results for the hydrogen-oxygen detonation. These are shown also in Table 1. It can be seen that the experimental results cluster near the computed values, but the theoretical values are slightly higher. It is suspected that this results from the aforementioned two-dimensional effects.

Finally, some interest has been focused upon the flow behind the C-J plane by Taylor (40). A rarefaction wave propagates upstream behind the C-J plane so as to establish conditions which satisfy the boundary conditions from which the detonation originated. Kistiakowsky (41) has made some measurements which confirm the Taylor analysis.

Interior of a Detonation Wave

Although the detonation speed can with good precision be determined solely from aerothermodynamic considerations across the wave, considerable interest exists in the wave interior. In this region the chemical changes take place. Von Neumann (42), Doring (43), Zeldovich (39) and others analyzed this problem assuming that the detonation wave consists of a normal shock wave followed by a deflagration. The flame was thought to be initiated by the high temperature created by the shock wave. Unfortunately, many of these early works obscured the real problem by their failure to consider gradients within the wave. The concept of a shock followed by a deflagration implies the existence of a pressure peak immediately behind the shock and prior to the thermal acceleration of the flow to a Mach number of 1. This maximum pressure is sometimes referred to as the von Neumann "spike." Kistiakowsky (44) and Duff (35) looked for this peak, and, although their measurements showed qualitative agreement with this theory, they failed to find the required maximum spike height.

Recently Hirschfelder et al. (45,46) have made a vigorous attack upon this problem. They solve numerically the differential equations in the wave interior under some simplifying chemical kinetic assumptions and obtain composition, temperature and pressure as a function of distance. The effects of viscosity, diffusion and thermal conductivity were included. In the examples Hirschfelder studied, there was a strong coupling between the reaction zone and the shock zone so that the solutions never exhibited the height of the von Neumann spike.

The physical results of Hirschfelder's analysis are summarized in Fig. 3. Here again is shown the Hugoniot curve. The loci of the von Neumann solution and Hirschfelder solutions are indicated. The von Neumann model is like a zero order solution to the more general problem treated by Hirschfelder.

Non-C-J Detonations

Under certain conditions a detonation propagating along a tube will exhibit nonsteady effects ascribed mostly to spin. Gordon et al. (47) recently published some experimental data on conditions under which such spinning occurs. Fay (48) and Chu (49) have developed theories which predict spin frequency and pitch. These theories are based upon acoustic (linearized) treatments of the problem, in which the heat release is phased to reinforce the oscillation. The actual phenomena are nonlinear, and observed waves are often different and frequently complex.

Steady strong or weak detonation waves have never, until recently, been observed either in nature or created in the laboratory. Although there are many statements in the literature claiming that steady non-C-J detonations do not exist, suggestions that they might exist are given by Reed (50), Hayes (51) and others (52,54). Gross (55) recently reported on the first laboratory observations of steady, strong detonations using hydrogen and air in a specially designed high temperature, steady flow, supersonic research tunnel. Repeated experiments and measurements have demonstrated the existence, stability and reproducibility of steady strong detonations. This research has opened up a large supersonic flow regime in which steady combustion can be achieved.

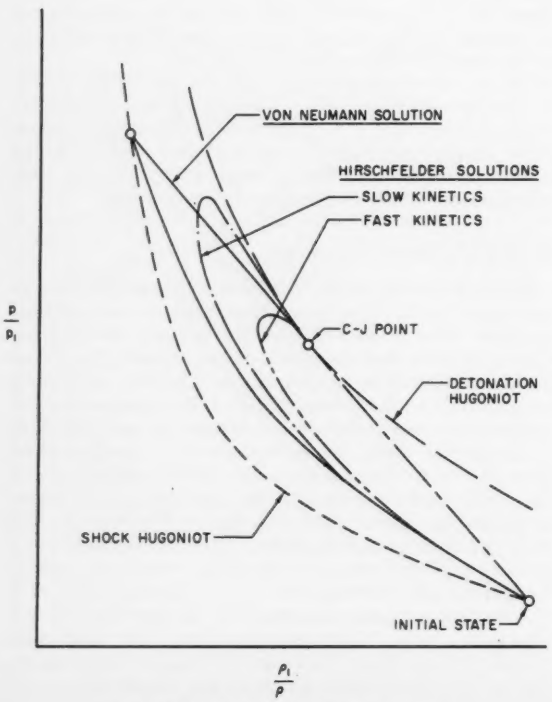

Fig. 3 Interior of a detonation wave

Standing Detonation Research

Recently, efforts have been made to obtain a detonation wave that is stationary in laboratory coordinates. In 1956 von Behrens (56) reported on the diffusion burning of partially burned rocket fuel with air in the flow field of a rocket exhaust. Nicholls et al. (57,58) have succeeded in burning a preheated mixture of hydrogen and air when it flows through the Mach reflected shock existing in open space downstream of an underexpanded nozzle. It is not clear whether this can be called a classical detonation, since light emission from apparent combustion took place for large distances downstream of the wave. However, this represented a real step forward in aerothermodynamic research.

The strong detonations reported by Gross (55) are steady standing waves and have been held stationary in the laboratory for time periods of up to 1 hr; longer times could be obtained with increased fuel storage capacity. The waves are less than one quarter of an inch thick, one-dimensional, and stationary in a Mach 3 premixed stream of hydrogen and air. Thermal ignition takes place through a normal shock wave when the stagnation temperature is above about 1370 F. Once the detonation has been established, unusual properties, hitherto unreported, have been observed. Mixtures of hydrogen-air have been burned under conditions far leaner than previously reported ignition, flammability and detonation limits. Of considerable interest theoretically is the fact that once the detonation wave is established, the upstream stagnation temperature can be reduced greatly without apparent effect upon the combustion process in the wave. For example, the upstream stagnation temperature of the system has been reduced to the order of 500 F and the detonation maintained. The degree to which the stagnation temperature can be so reduced is a function of the fuel-air ratio. These experimental observations give strong support to the thesis that transport properties within a detonation wave are important (see Hirschfelder (45,46)) since the conditions behind a shock wave at these stagnation temperatures are far too low to produce thermal ignition. This work will be reported on in detail in the literature in the near future.

As this work progresses we may see the first purposeful applications of detonation. Hypersonic detonative ramjets were first discussed by Roy (59) and recently by others (60 to 63). Such developments may extend the Mach number of air-breathing propulsion systems. The control of detonation may also open up some interesting chemical production methods.

Miscellaneous

It is not always possible to generate a detonation. Data on detonation limits were reported by Fay (64) and Steinberg (65) using shock tube methods. More recently Belles (66) proposed an analytical method for the prediction of the detonation limits of hydrogen-oxygen. This problem appears closely tied to chemical kinetics, a subject which is still evolving.

Some analytical aspects of steady detonation in two dimensions have been reported by Manson (67), Zeldovich (68), Sedov (69) and others.

Detonation spectra have recently been studied by Wagner (70) and Gaydon (71). Fay (72) has made some shock tube ionization measurements behind detonation waves, and Chinitz et al. (24) have presented extensive calculations of the aerodynamic, chemical and electrical properties behind air shocks and H_2-air and C_2H_2-air detonations.

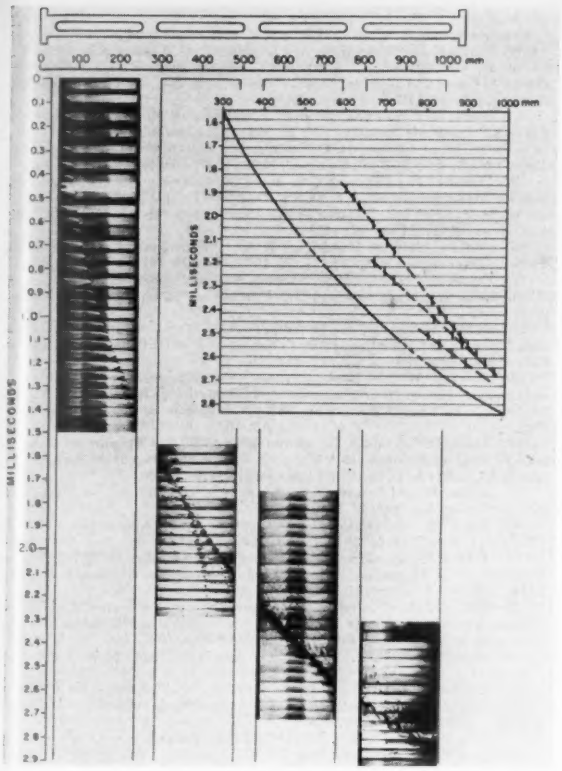

Fig. 4 Schlieren photographs of the development of detonation

A study of the electromagnetic effects on exothermal waves has been made by Gross et al. (73,101). They study the interaction of a transverse magnetic field with a one-dimensional detonation. (The latter report contains an error in section B and is being revised.)

Development of Detonation

The problem of the onset of detonation has baffled the scientist for a long time. It was, in fact, this problem—brought to focus by accidents in coal mines and laboratories—that gave the start to the prolific research on the properties of the steady-state detonation described in the first part of this paper.

The development of detonation is, by definition, an unsteady process. Understanding and exploration of it has been handicapped by the lack of instrumentation with sufficiently fast response characteristics to study the transient wave phenomena which control its progress. Such instrumentation is now available. It was developed by improvements at first of Schlieren techniques combined with microsecond light sources and rotating drum or mirror cameras, and more recently of electronic apparatus which resulted from the progress in shock tube technology. The insight gained into the details of the phenomena gave rise to modern theories on the mechanism of the processes leading to the development of detonation.

Experiment

Fig. 4 represents the type of records obtained some 15 years ago by Schmidt, Steinicke and Neubert (74). It consists of a series of Schlieren photographs of a flame accelerating into detonation in a constant area tube. It was obtained by means of four Schlieren systems using intermittent spark gap light sources and a camera with four rotating drums. The record reveals not only the time-space trace (world-line) of the flame front, but also world-lines of shockfronts which sweep through the combustible mixture ahead of the flame. On the basis of Fig. 4 and similar observations, a phenomenological description of the process can be construed as follows.

The laminar flame front accelerates at first due to the thermal expansion of the burned gases. At the same time the unburned mixture immediately ahead of the flame is set in motion by a series of Mach waves which are generated in the course of combustion. The laminar flame front becomes first curved, then wrinkled, and finally it breaks into a turbulent flame brush. In the case of ignition at a closed end, the wrinkling is initially due to the fact that the flame is pushed from behind by the expanding hot products and is consequently exposed to cold gas flow at an increased rate. In the meantime the Mach waves coalesce into shock fronts, and the flow ahead of the flame induced by their action reaches a supercritical velocity and also becomes turbulent, intensifying still more the process of flame acceleration.

The breakdown of the laminar flame front into a cellular structure, which occurs under the gentle conditions prevailing in the vicinity of the flammability limit, is a well-known phenomenon. Under the more intense conditions of an explosive mixture, this process is so rapid and the wrinkling so fast that the combustion zone itself becomes a strong source of turbulence and a generator of finite pressure waves.

Thus, in rapid succession, the reaction zone is subjected first to the effects of turbulence and then to effects of elevated pressure which increase the density, and consequently the volumetric rate of energy release and of high temperature; this produces dissociation and, in some cases, even partial ionization of the unburned mixture, yielding radicals which increase the speed of the combustion reaction.

The phenomenological description of the development of detonation is due to the observation of many investigators. Besides Schmidt et al., the more recent contributions worth mentioning are those of Turin and Huebler (75), Evans et al. (76), Bollinger and Edse (77), Brinkley and Lewis (78), Cook (79), Laffitte and Bouchet (80), Martin (81,82) and Kistiakowsky (31). The attention given this problem in the USSR is especially significant, as evidenced by the numerous articles of Zeldovich (83), Shchelkin (84), Sokolik (85), the coverage given it in the recent text of Zeldovich and Kompaneets (86), and the very recent experimental studies of Bazhenova et al. (87) and Salamandra et al. (88).

A more sophisticated study than that of flames in pipes concerns the problem of spherical explosions. Here especially worth noting are the recent experimental studies of Manson (89), Freiwald and Ude (90) and Zeldovich, Kogarko and Simonov (91).

The understanding of the process is inadequate yet for the establishment of a predictive theory. That is, having been given all the initial conditions, we are still unable to derive from the theory a specific description of the subsequent development of the process. The state of our knowledge is such that the most prolific effort is still spent on the rationalization of experimental results and on the performance of more elucidating experiments.

The study of the development of detonation is concerned primarily with wave interaction phenomena—the most important feature of unsteady flow processes.

The most idealized model of a combustion system developing into detonation consists of a shock wave which is followed by a flame front. In considering such an unsteady double discontinuity, Oppenheim (92,93) pointed out that the states of the products immediately behind the combustion front are not represented by the classical Hugoniot curve, and consequently that the classical theory is insufficient for the

study of the unsteady phenomena associated with detonation, such as its stability. For this purpose, he developed the theory of the Q-curve, that is, the locus of states attained behind a double discontinuity system under conditions similar to those of the Hugoniot curve (constant heat release per unit mass and given pressure and density of reactants), with the additional stipulation that the products of combustion move with respect to the flame front at a velocity equal to the local velocity of sound.

The model provides the basis for an idealized description of a continuous, dynamically compatible transition from deflagration to detonation. Of particular interest in this connection is an intermediate state reached by the products when they move at the same velocity as the undisturbed reactant mixture. At lower temperatures and pressures, the products move in the opposite direction, at higher temperatures and pressures, in the same direction as the shock-flame system. One of the significant results of the analysis is the conclusion that, in order for the detonation to be established in a dynamically compatible manner as a result of the coalescence of the combustion front with the shock just before coalescing, both fronts must move at a higher velocity than the final steady-state value, and the intermediate pressure between the two fronts must be considerably higher than the final one of the upper Chapman-Jouguet state.

The algebra of the plane double discontinuity system has been explored recently by Troshin (94), while Adams and Pack (95) presented a discussion of the dynamic compatibility which governs the coexistence of shocks, flame fronts and rarefaction waves in a nonsteady combustion system which develop into detonation. Popov (96) used the method of characteristics to rationalize the experimental records of the development of detonation in closed tubes, and, in particular, to demonstrate that the observed fluctuations of the flame front are due to reflections of waves from the closed ends.

Especially noteworthy is the thorough algebraic and arithmetic analysis of the double discontinuity system presented by Taylor and Tankin (97). In their exposition, they restrict their attention to only two points of the Q-curve: The state corresponding to the case in which the velocity of the products is the same as that of the undisturbed reactant mixture, and the upper Chapman-Jouguet state which—they confirm—has to be exceeded in the course of the development of the process as a necessary condition for the flame to catch up with the shock wave. They also analyze the case of dynamic compatibility of a spherical deflagration following a spherical shock wave and obtain some interesting specific solutions for such a double discontinuity system.

In a recent report based on lectures given by von Kármán at the Sorbonne, Millan (98) describes the development of the process following the account of Zeldovich (83). His approach to the problem is essentially descriptive, but special emphasis is given to the action of the shock front preceding the accelerating combustion wave. A more detailed discussion of the transition from normal combustion to detonation is in section 18 of the text of Zeldovich and Kompaneets (86).

The wave interaction phenomena occurring during the development of detonation which have been observed by Schmidt et al. (Fig. 4) were analyzed recently by Oppenheim and Stern (99) who rationalize the results and demonstrate how they could be exploited for the study of reaction kinetics of accelerating flames.

References

1 Berthelot, M., "Sur la Vitesse de Propagation des Phenomenes Explosifs dans les gas," Comptes Rendus, de l'Academic des Sciences, Paris, pp. 18–22.

2 Mallard, E. and LeChatelier, H., "Sur la Vitesse de Propagation de L'inflammation dans les Melanzes Explosifs," Comptes Rendus, de l'Academic des Sciences, Paris, pp. 145–148, July 18, 1881.

3 Chapman, "On the Rate of Explosion in Gases," *Phil. Mag.*, 1899, vol. 47, p. 90.

4 Jouguet, "Sur la Propagation des Reaction Chimiques dans les Gas," *J. Mathematique*, vol. 6, no. 1, 1905, p. 347; vol. 6, no. 2, 1906, p. 6.

5 Jouguet, E. "Mecanique des Explosifs," O. Doin, Paris, 1917.

6 Hirschfelder, J. O. Curtiss, C. F. and Bird, R. B., "Molecular Theory of Gases and Liquids," John Wiley & Sons, Inc., N. Y., 1954, chapter 11, sec. 9, pp. 797–813.

7 Lewis, B. L. and von Elbe, G., "Combustion, Flames and Explosions of Gases," Academic Press Inc., N. Y., 1951, pp. 579–627.

8 Jost, W. and Croft, H. O., "Explosion and Combustion Processes in Gases," McGraw-Hill Book Co., Inc., N.Y., 1946, chapter V, pp. 160–209.

9 Manson, N., "Propagation des Detonations et des Deflagrations dans les Melanges Gazeux," ONERA, Institute Franc. Petroles Rep., 1947; *also* (Eng. trans.) Tech. Inf. and Library Services, Ministry of Supply, England, Nov. 1956; ASTIA, AD 132808.

10 Courant, R. and Friedrichs, K. O., "Supersonic Flow and Shock Waves," Interscience Pub. Inc., N. Y., 1948, pp. 204–234.

11 Emmons, H. W., "Fundamentals of Gas Dynamics," Vol. III, in "High Speed Aerodynamics and Jet Propulsion," Princeton Univ. Press, 1958, pp. 574–686.

12 Lewis, B., Pease, R. N. and Taylor, H. S., "Combustion Processes," Vol. II, in "High Speed Aerodynamics and Jet Propulsion," Princeton Univ. Press, 1956, Part 5, pp. 577–612.

13 Doering, W. and Burkhardt, G., "Contributions to the Theory of Detonation" (trans. from German), Tech. Rep. no. F-TS-1227-IA (GDAM A9-7-46) Air Material Command, Wright-Patterson Air Force Base, May 1949.

14 Eisen, C. L., Gross, R. A. and Rivlin, T. J., "Theoretical Calculations in Gaseous Detonations," Fairchild Engine Division, Deer Park, N. Y., March 15, 1958; AFOSR TN 58-326; ASTIA AD 154230.

15 Lewis, B. and Friauf, J., "Explosions in Detonating Gas Mixtures," *J. Amer. Chem. Soc.*, vol. 52, 1930.

16 Edse, R., "Calculations of Detonation Velocity in Gases," WADC TR 54-416, March 1956; ASTIA AD 94173.

17 Berets, D. J., Greene, E. F. and Kistiakowsky, G. B., "Gaseous Detonations I. Stationary Waves in Hydrogen-Oxygen Mixtures," *J. Amer. Chem. Soc.*, vol. 72, March 1950.

18 Huff, V. H., Gordon, S. and Morrell, V. E., "General Method and Thermodynamic Tables for Computation of Equilibrium Composition and Temperature of Chemical Reactions," NACA Rep. 1037, Jan. 26, 1950.

19 Wendtlandt, R. Z., *Phys. Chem.* vol. 110, 1924, p. 637; vol. 116, 1925, p. 227.

20 Zeldovich, Y. B. and Ratner, S. B., "Calculating and Speed of Detonation in Gases," *J. Exper. and Theoret. Phys.*, (USSR), vol. 11, no. 1, 1941; ASTIA AD 144658.

21 Moyle, M. P., "The Effect of Temperature on the Detonation Characteristics of H_2-O_2 Mixtures," Univ. of Michigan Rep., Dec. 1956.

22 Gealer, R. L., "The Influence of High Pressure on the Properties of H_2-O_2 Detonation Waves," Univ. of Michigan Rep., June 1958.

23 Kistiakowsky, G. B. and Zinman, W. G., "Gaseous Detonations VII. A Study of Thermodynamic Equilibrium in Acetylene-Oxygen Waves," *J. Chem. Phys.*, vol. 23, no. 10, Oct. 1955, pp. 1889–1894. (Calculations by Duff.)

24 Chinitz, W., Eisen, C. L. and Gross, R. A., "Aerothermodynamic and Electrical Properties of Some Gas Mixtures to Mach 20," ARS preprint 706-58, N. Y., 1958.

25 Brinkley, S. R., Jr. and Richardson, J. M., "On the Structure of Plane Detonation Waves with finite Reaction Velocity," Fourth Symposium on Combustion, 1953, Williams & Wilkins Co., pp. 450–457.

26 Wood, W. W. and Kirkwood, J. G., "Present Status of Detonation Theory," *J. Chem. Phys.*, vol. 29, no. 4, Oct. 1958, pp. 957–958.

27 Morrison, R. B., "A Shock Tube Investigation of Detonative Combustion," Univ. of Michigan Rep. UMM-97, Jan. 1952.

28 Moyle, M. P., "The Effect of Temperature on the Detonation Characteristics of H_2-O_2 Mixtures," Univ. of Mich., Dec. 1956. Velocity given is averaged from original data taken from Table 8, p. 111.

29 Berets, D. J., Greene, E. F. and Kistiakowsky, G. B., "Gaseous Detonations II—Initiation by Shock Waves," *J. Amer. Chem. Soc.*, vol. 72, no. 1086, 1950, pp. 1086–1091.

30 Kistiakowsky, G. B., Knight, H. T. and Malin, M. E., "Gaseous Detonation III, Dissociation Energies of Nitrogen and Carbon Monoxide," *J. Chem. Phys.* vol. 20, no. 5, May 1952, pp. 876–883.

31 Kistiakowsky, G. B. and Mangelsdorf, P., "Gaseous Detonation VII, Two Stage Detonations in Acetylene-Oxygen Mixtures," *J. Chem. Phys.*, vol. 25, no. 3, Sept. 1956, pp. 516–519.

32 Kistiakowsky, G. B., "Density Measurements in Gaseous Detonation Waves," *J. Chem. Phys.*, vol. 19, no. 12, Dec. 1951, pp. 1611–1612.

33 Cannon, C. D. and Jewell, L. D., "Preliminary Study of the Effect of Initial Temperature on Detonation Parameters," ASTIA AD 26804, March 1954, WADC.

34 Hoelzer, C. A. and Stobaugh, W. K., "Influence of Initial Pressure on Detonation Parameters in Combustible Gases," ASTIA AD 26709, March 1954, WADC.

35 Duff, R. E. and Knight, H. T., "Precision Flash X-Ray Determination of Density Ratio in Gaseous Detonations," *J. Chem. Phys.*, vol. 25, Dec. 1956, p. 1301.

36 Duff, R. E., Knight, H. T. and Rink, J. P., "Precision Flash X-Ray Determination of Density Ratio in Gaseous Detonations," *Phys. Fluids*, vol. 1, no. 5, Sept.-Oct. 1958, pp. 393–398.

37 Resler, E. L., Jr., "Sound Speed in a Reacting Medium," *J. Chem. Phys.*, vol. 25, Dec. 1956, pp. 1287–1288.

38 Fay, J. A. and Opel, G., "Two-Dimensional Effects in Gaseous Detonation Waves," *J. Chem. Phys.*, vol. 29, no. 4, Oct. 1958, p. 955.

39 Zeldovich, Y. B., "Theory of Propagation of Detonations in Gaseous Systems," *J. Exper. and Theoret. Phys.* (USSR), vol. 10, 1940, p. 542.

40 Taylor, G. I., "The Dynamics of the Combustion Products Behind Plane and Spherical Detonation Fronts in Explosives," *Proc. Royal Soc.*, London, Series A-200, 1950, pp. 235–247.

41 Kistiakowsky, G. B., "Gaseous Detonations VI—The Rarefaction Wave," *J. Chem. Phys.*, vol. 23, no. 2, Feb. 1955, pp. 271–274.

42 Von Neumann, J., "Theory of Detonation Waves," Prog. Rep. 238, to April 1, 1942, OSRD Rep. 549, 1942, Ballistic Research Lab. File no. X-122, Inst. for Adv. Study, May 4, 1942.

3 Doring, W., "Uder den Detonationsvorgang in Gasen," *Annalen de Physik*, vol. 43, 1943, p. 421.

44 Kistiakowsky, G. B. and Kydd, P. H., "Gaseous Detonations IX—A Study of the Reaction Zone by Gas Density Measurements," *J. Chem. Phys.*, vol. 25, no. 5, Nov. 1956, pp. 824–835.

45 Hirschfelder, J. O. and Curtiss, C. F., "Theory of Detonations I—Irreversible Unimolecular Reaction," *J. Chem. Phys.*, vol. 28, no. 6, June 1958, pp. 1130–1146.

46 Linder, B., Curtiss, C. F. and Hirschfelder, J. O., "Theory of Detonations II—Reversible Unimolecular Reaction," *J. Chem. Phys.*, vol. 28, no. 6, June 1958.

47 Gordon, W. E., Mooradian, A. T. and Harpes, S. A., "Limit and Spin Effects in Hydrogen-Oxygen Detonations," Seventh Symposium on Combustion, London, Buttersworth Sci. Pub., pp. 487–494.

48 Fay, J. A., "A Mechanical Theory of Spinning Detonation," *J. Chem. Phys.*, vol. 20, no. 6, June 1952, pp. 942–950.

49 Chu, Boa-Teh, "Vibration of the Gaseous Column Behind a Strong Detonation Wave," Proc. Gas Dynamics Symposium on Aerothermochemistry, Northwestern Univ., Aug. 1955, pp. 95–111.

50 Reed, S. G., Jr., "Some Examples of Weak Detonations," *J. Chem. Phys.*, vol. 20, 1952, pp. 1823–1833.

51 Hayes, W. D., "The Basic Theory of Gasdynamic Discontinuities," in "Fundamentals of Gas Dynamics," Vol. III, "High Speed Aerodynamics and Jet Propulsion," Princeton Univ. Press, 1958, pp. 417–481.

52 Taylor, G. I. and Tankin, R. S., "Gas Dynamical Aspects of Combustion," in "Fundamentals of Gas Dynamics," Vol. III, "High Speed Aerodynamics and Jet Propulsion," Princeton Univ. Press, pp. 622–686.

53 Ubbelohde, A. R., "The Possibility of Weak Detonation Waves," Fourth Symposium on Combustion, Williams & Wilkins Co., 1953, pp. 464–467.

54 Heybeg, W. H. and Reed, S. G., Jr., "Condensation Shocks, Weak Detonations, and Related Phenomena," NAVord Rep. 2779, Aeroballistic Research Rep. 156, ASTIA AD 18800, June 8, 1953.

55 Gross, R. A., "Research on Supersonic Combustion," ARS JOURNAL, vol. 29, no. 1, Jan. 1959, pp. 63–64.

56 Von Behrens, H. and Rossler, F. "Uberschallflammen durch Sekundarverbrennung von Raketenstrahlen in Luft," *Zeitschrift fur Angwandte Physik*, vol. 8, 1956, pp. 237–244.

57 Nicholls, J. A., Dabora, E. K. and Gealer, R. L., "Studies in Connection with Stabilized Detonation Waves," Seventh Symposium on Combustion, London, Buttersworth, Sci. Pub., pp. 144–150.

58 Rutkowski, J. and Nicholls, J. A., "Considerations for the Attainment of a Standing Detonation Wave," Proc. Gas Dynamics Symposium on Aerothermochemistry, Aug. 1955, Northwestern Univ.

59 Roy, M. Maurice, Comptes Rendus de l'Academic des Sciences, Feb. 1, 1946, Paris.

60 Dunlap, R., Brehm, R. L. and Nicholls, J. A., "A Preliminary Study of the Application of Steady-State Detonative Combustion to a Reaction Engine," JET PROPULSION, vol. 28, no. 7, July 1958, pp. 451–456.

61 Nicholls, J. A., Wilkinson, H. R. and Morrison, R. B., "Intermittent Detonation as a Thrust-Producing Mechanism," JET PROPULSION, May 1957, pp. 534–541.

62 Roy, M. Maurice, "Propulsion Supersonique par Turboreacteurs et par Statoreacteurs, "Proc. First Int. Congress in the Aeronautical Sciences, Madrid, Spain, Sept. 1958, to be published, Pergamon Press.

63 Partel, G., "General Round-up in the Ramjet Field and Its Significance to Astronautics," Ninth Congress, IAF, Amsterdam, Aug. 1958, to be published.

64 Fay, J. A., "Some Experiments on the Initiation of Detonation in $2H_2$-O_2 Mixtures by Uniform Shock Waves," Fourth Symposium on Combustion, Williams & Wilkins Co., 1953, pp. 501–507.

65 Steinberg, M. and Kaskan, N. E., "The Ignition of Combustible Mixtures by Shock Waves," Fifth Symposium on Combustion, Reinhold Pub. Co., N. Y., 1955, pp. 664–672.

66 Belles, F. E., "Detonability and Chemical Kinetics—Prediction of Limits of Detonability of Hydrogen," Seventh Symposium on Combustion, London, Buttersworths Sci. Pub., pp. 86–92.

67 Manson, N. and Ferrie, F., "Contribution to the Study of Spherical Detonation Waves," Fourth Symposium on Combustion, Williams & Wilkins Co., Baltimore, 1953, pp. 486–494.

68 Zeldovich, J. B., *JETP* (USSR), vol. 112, no. 389, 1942.

69 Sedov, L. I., "Detonation in Media of Variable Density," Sixth Symposium on Combustion, Reinhold Pub. Co., N. Y., 1956, pp. 639–641.

70 Wagner, H., "Spectra of the Detonation of Oxygen with H_2, CO and Hydrocarbons," Sixth Symposium on Combustion, Reinhold Pub. Co., N. Y., 1956, pp. 366–371.

71 Fairbairn, A. R. and Gaydon, A. G., "Spectra Produced by Shock Waves, Flames and Detonations," *Proc. Royal Soc.*, London, Ser. A, April 9, 1957, pp. 464–475.

72 Fay, J. A. and Basu, S., "Ionization in Detonation Waves," Dept. of Mechanical Engineering, MIT, Cambridge, Mass., March 1958, 7th Symposium on Combustion, Butterworth Sci. Pub., pp. 175–179.

73 Gross, R. A., "A Note on One Dimensional Plasma Motion," *J. Aero/Space Sci.*, vol. 25, no. 12, Dec. 1958, pp. 788–789.

74 Schmidt, E., Steinicke, H. and Neubert, U., "Flame and Schlieren Photographs of Combustion Waves in Tubes," Fourth Symposium (Int.) on Combustion, Williams & Wilkins Co., Baltimore, 1953, pp. 658–666; *see also* "Flame and Schlieren Photographs of the Combustion of Gas-Air Mixtures in Tubes," VDI-Forschungsheft 431 (in German), Part B, vol. 17, Deutscher Ingenieur-Verlag, Dusseldorf, 1951.

75 Turin, J. J. and Huebler, J., "Advanced Studies in the Combustion of Industrial Gases," Report to Commission on Industrial and Commercial Gas Research, American Gas Association, Project IGR-59, April 1951, p. 14.

76 Evans, M. W., Given, F. I. and Richeson, W. E., "Effect of Attenuating Materials on Detonation Induction Distance in Gases," *J. Appl. Phys.*, vol. 26, no. 9, Sept. 1955, pp. 1111–1113.

77 Bollinger, L. E. and Edse, R., "Measurement of Detonation Induction Distances in Hydrogen-Oxygen and Acetylene-Oxygen-Nitrogen Mixtures at Normal and Elevated Initial Pressures and Temperatures," WADC Tech. Rep. 57-414, ASTIA D AD 130874, June 1957.

78 Brinkley, S. R. and Lewis, B., "The Transition from Deflagration to Detonation," Preprints of Papers Presented at the Seventh Symposium (Int.) on Combustion, Butterworths Sci. Pub., London, 1958, pp. 383–387.

79 Cook, M. A., Pack, D. H. and Gey, W. A., "Deflagration to Detonation Transition," Preprints of Papers Presented at the Seventh Symposium (Int.) on Combustion, Butterworths Sci. Pub., London, 1958, pp. 702–718.

80 Laffitte, P. and Bouchet, R., "Suppression of Explosion Waves in Gaseous Mixtures by Means of Fine Powders," Preprints of Papers Presented at the Seventh Symposium (Int.) on Combustion, Butterworths Sci. Publ., London, 1958, pp. 363–367.

81 Martin, F. J. and White, D. R., "The Formation and Structure of Gaseous Detonation Waves," Preprints of Papers Presented at the Seventh Symposium (Int.) on Combustion, Butterworths Sci. Pub., London, 1958, pp. 229–238.

82 Martin, F. J., "Transition from Slow Burning to Detonation in Gaseous Mixtures," *Phys. Fluids*, vol. 1, no. 5, Sept.-Oct. 1958, pp. 399–407.

83 Zeldovich, Y. B., "Theory of Detonation Onset in Gases," (in Russian), *Zhurnal Teknicheskoi Fiziki, USSR*, vol. 17, 1947, pp. 3–26.

84 Shchelkin, K. I., "Phenomena in the Vicinity of Detonation Formation in a Gas," *Soviet Physics JETP*, no. 2, March 1956, pp. 296–300. Translated from *Zhurnal Eksperimentalnoi i Teoreticheskoi Fiziki*, vol. 29, Aug. 1955, pp. 221–226.

85 Sokolik, A. S., "On the Mechanism of Predetonative Acceleration of Flames" (in Russian), *Zhurna Eksperimentalnoi i Teoreticheskoi Fiziki*, vol. 21, no. 10, 1951, pp. 1163–1179.

86 Zeldovich, Y. B. and Kompaneets, A. S., "Theory of Detonation" (in Russian), Gosudarstvennoe Isdatel'stvo Tekhnika-Teoreticheskoi Literatury, Moskow, 1955.

87 Bazhenova, T. V. and Soloukhin, R. I., "Gas Ignition Behind the Shock Wave," Preprints of Papers Presented at the Seventh Symposium (Int.) on Combustion, Butterworths Sci. Pub., London, 1958, pp. 613–622.

88 Salamandra, G. D., Bazhenova, T. V. and Naboko, I. M., "Formation of Detonation Wave During Combustion of Gas in Combustion Tube," Preprints of Papers Presented at the Seventh Symposium (Int.) on Combustion, Butterworths Sci. Pub., London, 1958, pp. 206–210.

89 Manson, N., "Formation and Velocity of Spherical Explosion Waves in Gaseous Mixtures," *Revue de l'Institute Francais du Petrole et Annales des Combustibles Liquides*, vol. 9, no. 4, April 1954, pp. 133–143.

90 Freiwald, H. and Ude, H., "Untersuchungen an kugelformige detonationswellen in Gasgemischen," *Zeitschrift fur Elektrochemie*, vol. 61, no. 5, 1957, pp. 663–672.

91 Zeldovich, Y. B., Kogarko, S. M. and Simonov, N. N., "An Experimental Investigation of Spherical Detonation of Gases," *Zhurnal Tekhnicheskoi Fiziki*, vol. 26, no. 8, 1956, 1744–1768. Translated in *Sov. Phys.-Tech. Phys.*, vol. 1, no. 8, Aug. 1957, pp. 1689–1713.

92 Oppenheim, A. K., "A Contribution to the Theory of the Development and Stability of Detonation in Gases," *J. Appl. Mech.*, vol. 19, no. 1, 1952, pp. 63–71.

93 Oppenheim, A. K., "Gasdynamic Analysis of the Development of Gaseous Detonation and Its Hydraulic Analogy," Fourth Symposium (Int.) on Combustion, Williams & Wilkins Co., Baltimore, 1953, pp. 471–480.

94 Troshin, Y. K., "The Generalized Hugoniot Adiabatic Curve," Preprints of Papers Presented at the Seventh Symposium (Int.) on Combustion, Butterworths Sci. Pub., London, 1958, pp. 827–836.

95 Adams, G. K. and Pack, D. C., "Some Observations on the Problem of Transition Between Deflagration and Detonation," Preprints of Papers Presented at the Seventh Symposium (Int.) on Combustion, Butterworths Sci. Pub., London, 1958, pp. 198–205.

96 Popov, V. A., "On the Pre-Detonation Period of Flame Propagation," Preprints of Papers Presented at the Seventh Symposium (Int.) on Combustion, Butterworths Sci. Pub., London, 1958, pp. 398–405.

97 Taylor, G. I. and Tankin, R. S., "Transformation from Deflagration to Detonation," in "Fundamentals of Gas Dynamics," Vol. III, "High Speed Aerodynamics and Jet Propulsion," Princeton Univ. Press, 1958, pp. 645–656.

98 Millan, G., "Transition from Deflagration to Detonation," Section 7, Chapter V, Aerothermochemistry, ARDC Rep., U. S. Air Force, Jan. 1958, pp. V34–V38.

99 Oppenheim, A. K. and Stern, R. A., "On the Development of Gaseous Detonation—Analysis of Wave Interaction Phenomena," Preprints of Papers Presented at the Seventh Symposium (Int.) on Combustion, Butterworths Sci. Pub., London, 1958, pp. 62–75.

100 Dunn, R. and Wolfson, B. T., "Generalized Equations and Procedures for the Calculation of Detonation Parameters," WADC TN 54-13, March 1956.

101 Gross, R. A., Chinitz, W. and Rivlin, T. J., "Magnetohydrodynamic Effects in Combustion," AFOSR TN 58-120, ASTIA AD 152-028, Feb. 15, 1958, to be published *J. Aero/Space Sci.*

Performance Calculations for Hybrid Nuclear-Chemical Rocket Propulsion Systems

LEON GREEN Jr.[1]
and JAMES M. CARTER[2]

Aerojet-General Corp.
Azusa, Calif.

Preliminary performance calculations for propulsion systems in which water and light metal propellant components are vaporized by nuclear heat prior to chemical reaction indicate that the hybrid system can remove limitations due to high heats of vaporization on the capacity of light metals to generate combustion products with high available enthalpy, and avoid the limitations placed on gas temperatures achievable by pure heat transfer systems by material strength requirements. The hybrid system can thus reconcile high specific impulse performance with high propellant density and avoid the use of cryogenic propellants. A semiquantitative comparison of the relative cost and feasibility of achieving a given flight performance with various propellant systems indicates that the hybrid water-metal systems compare favorably with high energy chemical and pure heat transfer systems. A qualitative discussion of the engineering difficulties faced by the various nuclear systems indicates that, by virtue of avoiding the material protection problem, development of a low-cost hybrid water-magnesium system requires no major technological advances beyond today's achievement, although systems employing lithium promise higher performance. It is concluded that the indicated performance achievable with hybrid systems is attractive enough to warrant more detailed consideration of such systems for possible application to ambitious missions.

THE CONSTANT demand for increased rocket performance has prompted several evaluations of the ultimate specific impulse which can be derived from chemical propulsion systems, notably those of Carter (1),[3] Zwicky (2) and Tormey (3). These studies generally agree that the upper limit of specific impulse values achievable by the ambient temperature reaction of molecular chemical species will be about 400 lbf sec/lbm,[4] if not lower. To attain impulses beyond this value, use of nuclear heating, free radicals or still more exotic methods would be required, and the limitations of all such schemes have not yet been fully assessed. The purpose of the present paper is to compare briefly some limitations of the two methods of thrust generation which are practical in today's technology, namely, chemical and nuclear heating of a working fluid, and to suggest that hybrid nuclear-chemical propulsion systems may deserve more detailed consideration than they have hitherto received.

Performance Limitations of Chemical Systems

It is recognized that to achieve high specific impulse a chemical propellant system should have a high energy content (to yield a high stagnation enthalpy), a low molecular weight and a high effective value of specific heat ratio $\gamma = c_p/c_v$ for the nozzle expansion process.[5] High γ-values are promoted by the presence of monatomic products in the exhaust. Tormey suggested the use of the light metals lithium, beryllium and boron as propellant components because of their low atomic weight, and Zwicky recommended their use (together with that of magnesium, aluminum and silicon) because of their high heat of reaction with oxygen or fluorine. Carter, however, noted that these extremely high heat releases per unit weight cannot be fully exploited in conventional rocket systems, because of the high heat of phase change required for conversion into the vapor state. This fact is illustrated by Table 1, which presents pertinent physical property data for lithium, magnesium and aluminum for comparison with those of more conventional propellant components.

Table 1 Pertinent physical properties of selected propellant components

Fluid	Melting point, C	Boiling point, C	L_v, cal/g	d_{mp}, g/cc	L_v cal/cc	Approx. cost, $/lb
H_2	−259	−253	108	0.07	7.6	1.5[a]
F_2	−223	−187	41.1	1.14	46.8	4.0
O_2	−218	−183	50.9	1.13	57.5	0.05
NH_3	−78	−33	327	0.69	226	0.15
H_2O	0	100	539	1.00	517	0
N_2H_4	1.4	113	335	1.01	337	2 5
Li	179	1317	4680	0.51	2380	8.0[b]
Mg	650	1103	1137	1.57	1790	0.36
Al	660	2450	3050	2.2	6700	0.26

[a] Hypothetical value based on arbitrary assumption that present cost of about $15/lb in laboratory scale production by NBS can be reduced by about a factor of 10 in quantity production.
[b] In large quantity production.

Presented at the ARS Spring Meeting, Dallas, Texas, March 1958.

[1] Head, Applied Mechanics, Corporate Research Division. Member ARS.

[2] Corporate Research Advisor. Member ARS.

[3] Numbers in parentheses indicate References at end of paper.

[4] All specific impulse values in this paper are referred to a pressure expansion ratio of 34 to 1.

[5] On the basis of an interpretation of the idealized specific impulse equation in which the γ-value for the combustion condition (introduced by the perfect gas approximation for enthalpy in terms of temperature) was not distinguished from the effective γ-value governing the expansion process, Tormey states imprecisely that a low γ-value is desirable.

It is apparent that if the latent heat of vaporization were supplied by some external source, the high heat of reaction of the light metals could be manifested in the production of superheated combustion products with high values of enthalpy available for expansion work, and thus exploited for propulsion. This observation immediately suggests the use of a nuclear reactor for purpose of propellant vaporization and superheating to a vapor pressure level sufficient for thrust chamber operation. In this fashion, one energy content limitation on light metal chemical propellants could be removed.

Performance Limitations of Nuclear Systems

The use of a nuclear reactor to heat a working fluid for rocket propulsion purposes has been widely discussed, and a description of a conceptual design for such a heat transfer rocket, together with a good bibliography of the open literature on nuclear rocket propulsion, has recently been provided by Rosenblum, Rinehart and Thompson (4). In the presently practical case wherein heat is generated by a fission process within solid fuel elements, the principal factor limiting achievable performance is the temperature which can be tolerated by the fuel element without structural failure and at which chemical attack by the propellant is not too severe. A closely allied limitation results from the problem of heat removal from the fuel element by a gas of low molecular weight without suffering either too great a difference between the maximum solid temperature and the bulk gas temperature, incurring a performance sacrifice, or too great a pressure drop in the core, incurring a penalty in the form of increased pumping power necessary and increased turbomachinery weight.

The design outlined by Rosenblum et al. is the often mentioned type employing fuel elements fabricated from graphite, a moderator material of exceptional strength vs. temperature behavior in that its short-time breaking strength reaches a maximum value at a temperature of about 2500 C (5), and which even at temperatures of incandescence is not susceptible to erosion by high velocity flows of chemically inert fluids free of particulate matter (6). At temperatures of this order, however, graphite is subject to deformation by creep, and no experimental information is available concerning the degree to which the rate of the thermally-activated, diffusional processes which are manifested by creep may be increased by a high neutron flux[6] or under the bombardment by relatively massive and highly charged fission fragments which would be experienced by fuel-loaded material. In any event, it is doubtful that a graphite fuel-element structure can withstand temperatures of more than about 2400 C for even a relatively short time, without suffering creep deformation in excess of acceptable design limits. When the temperature drop in the solid and gas film is considered (as will be discussed later), it appears that a bulk gas temperature of about 4500 R (about 2230 C) represents the most optimistic value which can be envisaged in conjunction with a graphite reactor.

Thus the concept of a reactor used as a vaporizer of a light metal chemical propellant again suggests itself. By such means, the temperature limitation imposed by the reactor core material could be avoided, the core operated at a more conservative temperature at which an increased variety of possible cladding materials is usable, and combustion flame temperatures far in excess of the stagnation temperatures achievable by a solid-to-gas heat transfer system could be realized. In contrast to the case where heat generated within a solid must be removed at high rates and the material must be operated at its maximum usable temperature, high temperatures generated by gas phase reactions can be contained in thrust chambers of conventional materials by employing efficient wall cooling methods, such as porous wall transpiration.

[6] An order-of-magnitude estimate by G. Schoek (*J. Appl. Phys.*, vol. 29, 1958, p. 112, indicates that the creep rate of graphite at temperature $T_m/2$ would be increased by a factor of 2 at a flux of about 10^{13} fast neutrons/cm^2 sec.

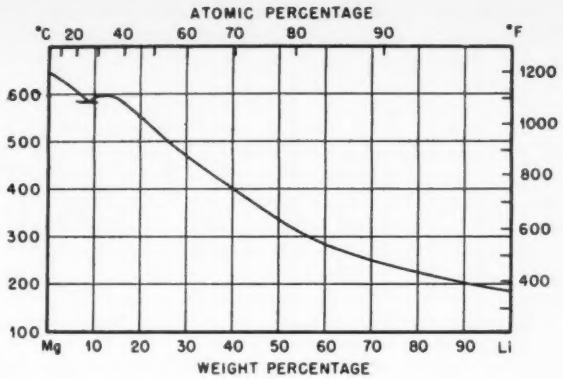

Fig. 1 Liquidus curve for lithium-magnesium (from "Liquid Metals Handbook")

Chemical Performance of Vaporized Metal-Water Systems

The foregoing discussion has suggested the possibility that the principal performance limitation of high energy, light metal chemical propellant systems (i.e., low available enthalpy of combustion products due to high heat of vaporization for the metals) and of nuclear heating systems (i.e., attainable gas temperatures limited by material strength considerations) could be obviated in a hybrid nuclear-chemical system in which the propellant components are vaporized by nuclear heat and then reacted chemically to yield high enthalpy combustion products. In order to investigate the potential performance achievable by such a scheme, sample performance calculations for the systems lithium-water (with an excess of lithium as working fluid) and magnesium-water (with an excess of water as working fluid) were made. In addition, a calculation for a mixed lithium-magnesium fuel system was included, since the two metals form a continuous solid solution of variable melting point over a wide range of composition, as shown in Fig. 1. In this system, magnesium and water were in stoichiometric proportions for reaction, and lithium served as the principal working fluid. Water was arbitrarily selected as an oxidizer in preference to fluorine or oxygen, because of its obvious cost and availability advantages, because it provides some free hydrogen in the exhaust because of its noncryogenic nature, and because its dissociation permits the existence of high enthalpy combustion products without excessively high flame temperatures. If these considerations are not governing, the substitution of fluorine would yield higher flame temperatures and possibly higher specific impulse values.

As a comparative basis for the calculations, it was assumed that both the metal and water were heated to a temperature of 1500 C (an arbitrary figure, 1000 C below the maximum strength point of graphite) before reaction. (Actually it would not be desirable to superheat water any higher than is necessary to obtain a sufficient pressure level.) The calculations also assume that the reaction products are expanded isentropically over a pressure ratio of 34 to 1, so that the results might be compared with published performance data for various chemical systems under expansion from 500 to 14.7 psia. Assumption of such a relatively low expansion ratio actually tends to penalize the water-metal propellant system in comparison to some of the other systems, since a

more complete expansion, such as would prevail at high altitude conditions, would permit greater recovery of the energy in any dissociated water or hydrogen fraction for useful nozzle work.

In this latter regard, Tormey (3) states that only the translational portion of the energy in rocket combustion gases is available for mechanical work, and that all energy present in the form of rotational and vibrational modes, as well as that due to dissociation and ionization, is not available. This statement is equivalent to saying that in a rocket nozzle, expansion time is so short that all products behave as monatomic gases, with a "frozen" specific heat ratio of 1.67 during expansion. For sufficiently rapid expansions (very small nozzles with very high expansion ratios), this statement may be accurate. In actual rocket nozzles for motors of thrust levels of 1000 lbf and greater, it may be inaccurate. Effective exhaust velocities may be about 10,000 ft/sec, and nozzle lengths will vary from a few inches for 1000-lb thrust to a few feet at 100,000l-b thrust. Assuming an average velocity one-half the effective exhaust value, nozzle lengths of 1 to 2 ft correspond to total residence time in the nozzle of 2 to 4×10^{-4} sec (7,8,9). Relaxation times for rotational and vibrational energies are of the order of 10^{-10} sec at high temperatures. Specific reaction rates under rocket nozzle conditions are such that substantially complete reaction (reassociation) occurs in about 10^{-8} to 10^{-9} sec, and ionization rates and the reverse are of the same order (10,11). Under these conditions, then, there is ample time for these other forms of energy to contribute to the work done by the gases in the nozzle. Altman and Carter (11) state that reassociation during expansion may effect increases in the exhaust velocity as high as 10 per cent for the O_2-H_2 and F_2-H_2 systems, and a similar effect would be expected for water-metal systems with excess water.

There is at present considerable discussion concerning the participation of these various nontranslational energies in the expansion process (12). It should, however, be kept in mind that although relaxation times for vibrational energy, for instance, of a pure gas of homopolar molecules may be relatively long, these times may be greatly shortened by the presence of other molecules, particularly if they are heteropolar, such as water. The question of contribution of nontranslational energy to increase of velocity in a nozzle must be regarded as debatable, at least insofar as the completeness of this energy conversion is concerned. Present evidence provided by performance tests with conventional propellants indicates the conversion is at least a large fraction of what would be predicted on a complete equilibrium basis. If, as is proposed for some spaceflight programs, combustion pressures are dropped to near normal atmosphere, and pressure expansion ratios are increased to 100 or more, the question would become much more serious. This is so because of the larger fraction of nontranslational energy, due to vibration and dissociation, and to the predictable decrease of conversion of this energy, due to lower density during expansion.

The calculations also assumed that thermal and kinetic equilibrium is maintained during the expansion process. Dissociation of metal oxides was neglected. The thermodynamic data from (13 and 14) were used where applicable. The heat content and entropy values of magnesium oxide (assumed solid over the entire temperature range) were based on specific heat data given by Kelley (15). The heat content and entropy of lithium oxide were calculated by one of the authors (JMC). In this calculation, specific heats of the vapor were estimated from those of steam, using differences in force constants and in atomic masses to estimate vibrational specific heats. The heat of vaporization was estimated from scanty vapor pressure data, and by comparison with the entropy of vaporization for other substances boiling at about the same temperature. In view of uncertainties, no heat recoverable by condensation of lithium oxide was assumed in calculating performance.

The results of the calculations are presented in Figs. 2, 3 and 4. From these curves, typical performance points at one mixture ratio for each system were selected for comparison with the high energy chemical and nuclear systems included in Table 2. In this selection, no attempt was made to optimize the water-metal mixture ratio by means other

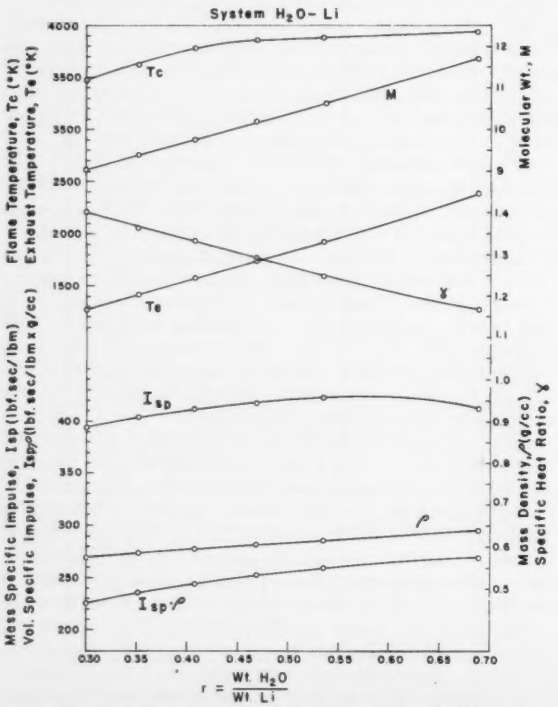

Fig. 2 Performance data for system water-lithium

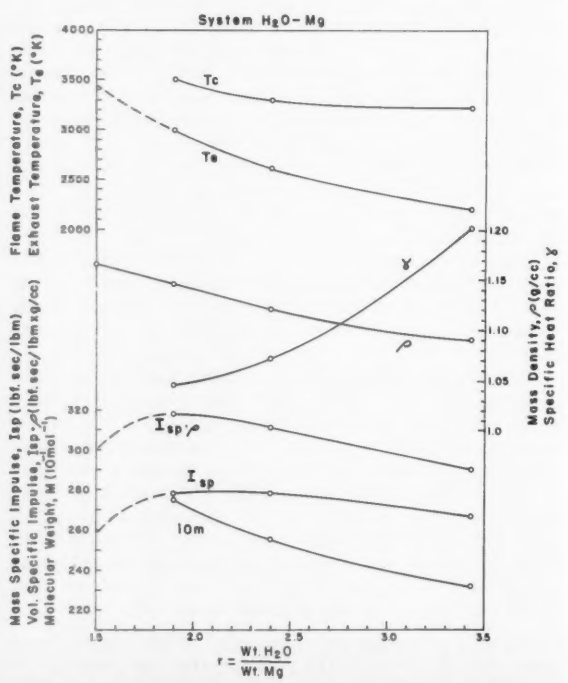

Fig. 3 Performance data for system water-magnesium

Table 2 Propellant system comparison (pressure expansion ratio 34 to 1)

Type →	Chemical						Nuclear-Chemical			Nuclear	
Propellant system →	O_2-H_2		F_2-H_2		F_2-NH_3	F_2-N_2H_4	H_2O-Li	H_2O-Li-Mg	H_2O-Mg	H_2	NH_3
mixture ratio, (wt. oxidizer/wt. fuel)	8.0	3.5	1.9	4.5	3.0	2.0	0.60	0.39	1.9	...	...
chamber stagnation temperature, T_c (R)	6630	4960	8990	5460	7730	8200	7040	6080	6300	4500	4500
molecular weight in chamber, M (mol^{-1})	16	9.0	18	8.9	19	19	11.1	12.2	27.5	2	8.5
effective specific heat ratio in expansion, γ	1.22	1.26	1.34	1.33	1.33	1.33	1.21	1.13	1.05	1.4	1.3
bulk propellant density, ρ(g/cc)	0.43	0.26	0.75	0.32	1.16	1.30	0.625	0.842	1.15	0.07	0.69
(lbm/ft³)	26.8	16.7	46.8	20	72.3	81.0	39.0	52.5	71.5	4.4	43.0
mass specific impulse, I_{sp} (lbf sec/lbm)	317	364	338	373	305	316	423	362	278	722	351
vol. specific impulse (lbf sec/lbm × g/cc)	136	94.6	25.3	119	354	411	264	305	318	50.5	242
(10^3 lbf sec/ft³)	8.50	6.07	15.8	7.46	22.1	25.6	16.5	19.0	19.9	3.18	15.1
mass flow rate for thrust of 500,000 lbf (lbm/sec)	1580	1370	1480	1340	1640	1580	1180	1380	1740	692	1420
vol. flow rate for thrust of 500,000 lbf (ft³/sec)	58.8	82.2	31.7	67.0	22.6	19.5	30.3	26.3	22.0	157	33.1
propellant cost rate for above thrust ($/sec)	334	990	5740	4760	4980	5540	5900	3920	216	1040	213
reactor power to heat propellants (10^6 btu/sec)	...	...	...	...	...	...	9.2	7.4	4.3	15	8.2
propellant wt. fraction for burnout vel. of 25,000 fps	0.91	0.88	0.90	0.87	0.92	0.91	0.84	0.88	0.94	0.66	0.89
feasibility parameter $\left(\frac{1}{\zeta} - 1\right)\rho$	0.043	0.036	0.082	0.045	0.10	0.13	0.11	0.12	0.075	0.036	0.084

than visual inspection. The data for pure chemical systems were obtained from (3, 16 and 17).

It may be seen from Table 2 that, in terms of mass specific impulse, the H_2O-Li system appears highly attractive, its value of 423 lbf sec/lbm surpassed only by the nuclear heated H_2 system at 722 lbf sec/lbm. The system H_2O-Mg ranks lowest on this scale with a value of 278 lbf sec/lbm, and the system H_2O-Li-Mg shows an intermediate value of 362 lbf sec/lbm, which surpasses the nuclear NH_3 system and compares favorably with the O_2-H_2 and F_2-H_2 chemical systems. In terms of volume specific impulse, the order shifts considerably, with the high density F_2-N_2H_4 and F_2-NH_3 chemical systems heading the list at 25,600 and 22,100 lbf sec/ft³, respectively, followed by the hybrid system H_2O-Mg at 19,900 lbf sec/ft³. On the volume specific impulse basis, all the low density systems employing substantial fractions of elemental hydrogen compare unfavorably.

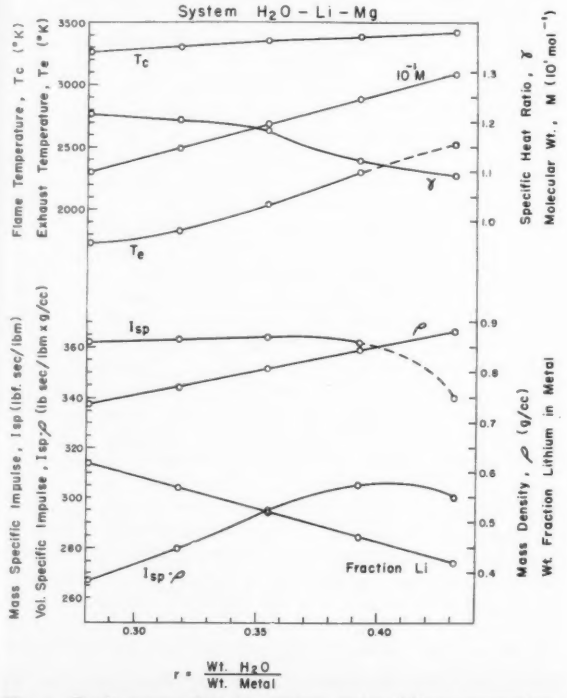

Fig. 4 Performance data for system water-lithium-magnesium

In view of the approximations noted above, necessitated by the general meagerness of high temperature data for metals and oxides, it is not claimed that the performance data presented are the results of rigorous calculations. Nevertheless, they are believed accurate enough to permit the following semiquantitative comparisons of the feasibility of achieving a given flight performance.

Comparison of Chemical, Nuclear and Hybrid Systems for a Given Flight Performance

As illustrated by the trend of the above data, the relative attractiveness of a propulsion system cannot be assessed by consideration of specific impulse values alone; flight performance and cost data are required for this purpose. For a truly quantitative comparison of flight performances, detailed mission analyses and preliminary vehicle design studies are necessary, but interesting semiquantitative comparisons can be made by assuming arbitrary levels of thrust and burnout velocity. Since it is evident a priori that nuclear powered vehicles will compete with chemically powered ones only for ambitious missions requiring high thrust levels, a thrust of 500,000 lbf and a burnout velocity of 25,000 ft/sec were selected for comparison purposes.

Relative Propellant Cost

Specification of the thrust level determined the values of propellant mass flow rate and approximate cost rate compared

in Table 2. For the systems employing nuclear heating, the approximate reactor power levels required to achieve the specified temperatures (1500 C for the hybrid systems and 2230 C for the pure nuclear systems) are also determined. Together with knowledge of the mass specific impulse, specification of the burnout velocity fixes the required propellant mass fraction of the loaded vehicle, as determined by the simplified expression of Fig. 5. This expression neglects drag and gravity effects, but some compensation for the error is provided by use of the specific impulse values for a 34 to 1 pressure expansion ratio, which will be improved in expansion under actual high altitude flight conditions.

Comparison of the flow rate figures does not lead to any new observations but does serve to illustrate the relatively large volumetric rates required for the hydrogen systems, especially the nuclear heat transfer system, which will in turn require turbopumps larger than those needed for the higher density propellants. Also illustrated is the large variation in reactor power requirement among the various nuclear systems (lowest for the water-magnesium hybrid, highest for the hydrogen heat transfer system), which will be reflected as a significant variation in reactor weight and fuel investment.

The relative propellant cost rate figures indicate that the hybrid water-magnesium and pure nuclear ammonia systems are the most economical. Although these figures are relatively firm, there is considerable uncertainty about the costs of the systems using hydrogen, which are based upon a crudely extrapolated cost value[7] as indicated in Table 1. Most nebulous of all are the costs of the hybrid lithium systems, since the lithium cost figure of Table 1 is for the commercial material, 92.5 per cent Li^7 with a thermal neutron capture cross section of 0.033 barn, and 7.5 per cent Li^6 with a thermal cross section of 945 barns. Any application of lithium as a reactor coolant would thus require either the use of at least partially purified Li^7 with an increased per-lb cost, or of a reactor with a fast or epithermal neutron energy spectrum. It is possible that the use of completely purified Li^7 may not be desirable, since the presence of Li^6 in the stream (if tolerable from control and fuel investment standpoints) can provide both a mechanism for direct energy transfer to the fluid and a source of a low molecular weight exhaust components by the slow neutron (n, α) reaction

$$ {}_3Li^6 + {}_0n^1 \rightarrow {}_1H^3 + {}_2He^4 \qquad [1] $$

[7] An estimated cost of about $0.55 per lb at the liquefaction plant has recently been quoted by the Linde Co., but the extrapolated value of $1.50 per lb used here is probably more representative of the cost at the firing site.

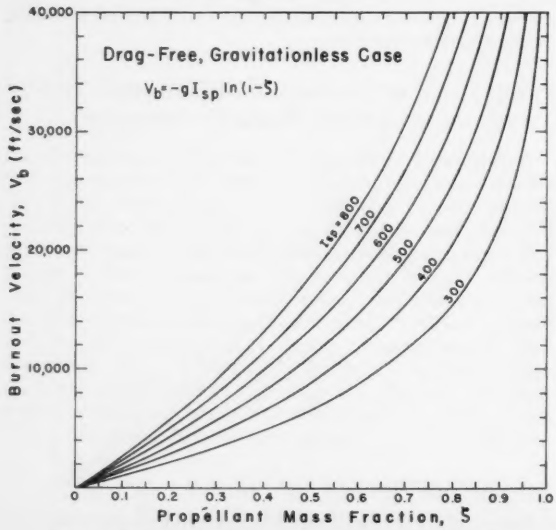

Fig. 5 Burnout velocity vs. propellant mass fraction

The magnitude of these possibly beneficial effects has not been estimated, but will probably not be great.

Relative Engineering Feasibility

Despite the considerable difference between the derived values of Table 2, it is not possible to evaluate the relative attractiveness or feasibility of the various propellant systems for the selected mission without an additional criterion. The question which needs to be answered is "How feasible is it to build a vehicle of the required propellant mass fraction using propellants of the density indicated?" Obviously, any precise answer would require a detailed preliminary design, but it has been suggested that a rough figure of merit may be derivable from simple, qualitative considerations (18). By definition of propellant mass fraction $\zeta = m_p/(m_v + m_p)$, where m_p = mass of propellant, and m_v = mass of dry vehicle

$$ m_v = m_p\left(\frac{1}{\zeta} - 1\right) \qquad [2] $$

Since we are seeking a basis for gross comparison only, the admittedly gross approximation[8] that the mass of the propellant tank constitutes a certain constant proportion of the dry vehicle mass seems admissible

$$ m_v \propto m_t \qquad [3] $$

Introduction of a second rough approximation that, for a given mass of propellant, the mass of the propellant tank varies inversely as the mass density of the propellant

$$ m_t \propto 1/\rho \qquad [4] $$

leads to the result that

$$ \left(\frac{1}{\zeta} - 1\right)\rho = \text{constant} \qquad [5] $$

It should again be emphasized that this result permits only gross comparisons in view of the crudeness of the approximations of Equations [3 and 4], but even these comparisons appear significant.

In order to use Equation [5], it is necessary to evaluate the constant involved. Since only a rough rule is desired, it appears legitimate to use the statement of Sutton (16) that "It requires extremely careful design to exceed a mass ratio of 0.80; mass ratios approaching 0.90 appear to be the probable practical limit." Although this statement might not be rigorously exact, it provides a useful basis for comparison. It is presumed that Sutton's judgment applies to single-stage vehicles using propellants with a specific gravity of the order of unity, in which case a maximum propellant fraction of 0.90 would correspond to a value of 0.11 for the constant in Equation [5]. Values higher than this (i.e., low propellant fraction coupled with high propellant density) may be considered easily feasible, whereas the achievement of lower values (i.e., high propellant fractions using low density propellants) would seem relatively formidable tasks. If, from a still more optimistic viewpoint, a value of $\zeta = 0.95$ is considered the upper limit using propellants of unit specific gravity, the corresponding value of the feasibility parameter would be 0.052. In view of the highly approximate nature of this feasibility criterion, however, comparisons to more than one significant figure are not warranted.

On the basis of this criterion, it is possible to estimate the relative feasibility of achieving the desired performance (25,000 ft/sec burnout velocity) using the various propellant systems listed in Table 2. It may be observed that the systems fall into three categories. Those carrying a substantial fraction of their fuel in the form of elemental hydrogen (both O_2-H_2 systems, the low mixture ratio F_2-H_2 system and the nuclear H_2 system) show a feasibility parameter of the order of 0.04, a value which may be considered too low to warrant

[8] Equation [3] disregards the fact that thrust transmission structures do not scale directly with tank weight.

serious consideration. The chemical systems F_2-NH_3 and F_2-N_2H_4, together with the hybrid systems H_2O-Li and H_2O-Li-Mg, yield a relatively attractive value of the order of 0.1, with a spread too small to permit a preference without more detailed consideration. The high mixture ratio F_2-H_2 chemical system, the hybrid H_2O-Mg system and the nuclear NH_3 system show an intermediate value of the order of 0.08, which may be interpreted as indicating marginal feasibility requiring evaluation by more detailed study.

It must be emphasized that these gross observations apply only to the mission assumed. Ambitious spaceflight missions would demand increased specific impulse performance, and the relative attractiveness of the nuclear H_2 system would be improved.

Engineering Problems of Pure and Hybrid Nuclear Systems

Although the present paper is primarily concerned with the relative performance of the various propellant systems considered, it may be briefly noted that the water-metal hybrid systems can avoid some of the engineering problems encountered in the pure heat transfer systems.

Materials

It was emphasized earlier that the material strength problem which limits the gas temperature levels achievable by a pure heat transfer system using a graphite reactor may be obviated in the hybrid scheme. The problem of chemical attack by the propellant, and its prevention, was only noted in passing. It is well-known that ammonia seriously attacks graphite at temperatures of 1500 C and above, whereas hydrogen is less reactive. The resistance of graphite to reduction by hydrogen can be improved by refractory carbide coatings (19), but protection against ammonia attack is more difficult.

In the hybrid systems, the use of lithium also involves a protection problem, but there are indications that the refractory metals molybdenum, columbium and tantalum show good resistance up to 1000 C (20), and their use at still higher temperatures may be possible. No data on the resistance of tungsten, rhenium or high melting intermetallic compounds to lithium attack is known to the authors. In the use of magnesium with graphite there does not appear to be any serious corrosion problem (20). Water may be handled by limiting the temperature levels to relatively low values sufficient to give the required steam pressure, i.e., by using water as the reflector coolant and the liquid metal for the high temperature core coolant.

It is worth noting that, in the event that the solid-temperature limit could be raised by use of some material other than graphite, the relative standing of the pure and hybrid systems here considered would not be affected. It appears that the only system which might show a relative improvement would be a mixed-metal hybrid system, which could then substitute aluminum (with an increased heat of combustion and increased mass density) for magnesium. Aluminum was not considered here because of the estimate (on a highly extrapolated basis) that temperatures of the order of 3000 C would be required to yield a usable high vapor pressure. As shown in Fig. 6, aluminum is also miscible in lithium.

Heat Removal

The data of Table 2 indicate that operation of nuclear systems requires high rates of heat removal from the core, although this demand is reduced somewhat in the hybrid scheme. It is evident that the removal of heat at total rates of the order of 10^7 Btu/sec (the order of 10^4 megawatts) requires either a highly efficient heat transfer mechanism, permitting high surface heat fluxes, or a highly extended heat transfer surface for utilization of lower flux levels. In the case of purely gas-cooled reactors there is no choice but to use the extended heat transfer surface, owing to the relatively low heat transfer coefficients obtainable with gaseous coolants. The types of extended surface mentioned by Rosenblum et al. (4) included porous beds and arrays of closely-spaced flat plates or small holes, all of which present tedious fabrication problems. Since the surface must be protected against chemical attack, the magnitude of the protection problem also increases with that of the heat transfer surface.

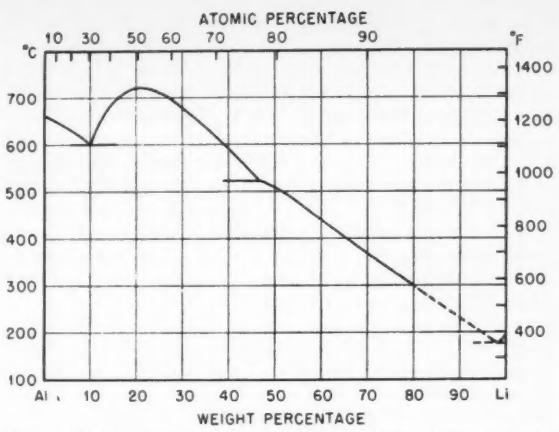

Fig. 6 Liquidus curve for aluminum-lithium (from "Liquid Metals Handbook")

This is not to say that high heat flux rates cannot be realized using gaseous coolants. The experiments of Durham, Neal and Newman (21) demonstrated that heat flux rates of the order of 10^6 Btu/ft² hr could be obtained in forced convection to helium flowing through straight, electrically-heated, $\frac{1}{16}$-in. ID graphite tubes. However, in typical cases the differences between the inner surface temperature and the bulk gas temperature were of the order of 10^3 F, corresponding to effective film coefficients of the order of 10^3 Btu/ft² hr F. Although better performance might be expected using hydrogen or ammonia owing to dissociation effects, it appears that heat removal by gaseous forced convection alone in flow through straight channels involves a significant sacrifice in terms of high temperature drop between tolerable local values in the solid and usable bulk values in the gas, increased complexity, reduced compactness and increased weight. These drawbacks may be overcome by use of porous construction, but not without a considerable development effort.

In contrast to the situation encountered using purely gaseous coolants, the use of water and liquid metals permits order-of-magnitude improvements in the heat transfer condition. The maximum heat flux rates achievable with boiling water (22) and boiling liquid metals (23) are also of the order of 10^6 Btu/ft² hr, but the driving temperature difference required for this flux is only about 10 to 20 F. As an example of more efficient heat removal, approximately 90 per cent of the power required for heating the propellants in the H_2O-Li system of Table 2 is expended in liquid phase heating and vaporization of the propellants.

Component Design

The most important design and handling simplification made possible by the hybrid scheme is that cryogenic fluids are avoided. The hybrid systems would involve "hot" vehicles in which the fuel would be maintained in a liquid state by electrical heaters within the fuel tank, which could be constructed from thin gage metal by conventional fabrication techniques. Tank insulation at the temperatures involved presents no problem beyond the scope of everyday

technology, and might indeed be easier than insulation of a liquid hydrogen tank.

Of the various nuclear systems, the only one which would appear to involve significant advances in pump development is the hydrogen heat transfer system, due to the low density and cryogenic nature of the working fluid. The low density is not only reflected in a greatly increased volumetric capacity requirement relative to the other propellants, as illustrated in Table 2, but also in high pumping head requirements. If for a given flow this head is high enough to require more than one centrifugal stage, loss considerations may indicate the use of an axial-flow design, thus involving increased complexity and weight (24).

The problems of radiation heating of the propellant and of radiation damage to solids (especially to close tolerance turbopump components at cryogenic temperatures), such as were mentioned by Rosenblum et al. (4) in discussion of a hydrogen reactor system, would be mitigated in the case of a hybrid system, not only by the reduced power requirement, but also primarily by the fact that the propellant pump and manifold system operates at a temperature high enough to permit rapid annealing of any radiation damage, and thus could be used to shield more sensitive components. Finally, the availability of water as a propellant component presents opportunities for various design simplifications employing water not only as a thrust chamber and nozzle coolant, but also for reflection, shielding and possibly moderating purposes, and also steam-turbine operation.

Conclusion

The foregoing discussion has presented preliminary performance calculations for chemical propellant systems consisting of water and light metals, assuming sufficient preheat by an external source, such as a nuclear reactor, to vaporize the propellants and thus permit the generation of products with high available enthalpy in the ensuing combustion. The possible advantages over conventional chemical and nuclear propulsion systems to be derived by use of the hybrid nuclear-chemical system include:

1 The performance limitation imposed on light metal fuels by high latent heats of vaporization is removed by the nuclear preheating.

2 The performance limitation imposed on pure nuclear heat transfer systems by mechanical strength properties of the core structure is avoided by operation of the core material at reduced temperature levels.

3 By means of this dual removal of limitations, the hybrid system can achieve high specific impulse values without using low density working fluids.

4 Problems associated with the use and handling of cryogenic fluids are eliminated.

5 Reactor power requirements are relaxed by the utilization of chemical energy to supplement the nuclear energy.

6 Use of propellants with improved heat transfer characteristics and reduced radiation sensitivity can permit simplified thermal and mechanical core and engine design.

A semiquantitative comparison of several chemical, nuclear and hybrid systems was presented, using a simplified criterion for roughly estimating the relative engineering feasibility of employing the various systems to achieve a given flight performance, and it was suggested that the hybrid systems appear potentially attractive enough to warrant more detailed consideration. The low-cost hybrid system water-magnesium appears to involve no development advances beyond today's achievement, but use of the higher performance lithium fuel would involve a problem in material protection equivalent to those involved in the use of hydrogen or ammonia in a pure heat transfer system, as well as increased propellant costs comparable to those of fluorine systems. If the corrosion problem is tractable, still higher performance fuels, such as a slurry of lithium hydride in lithium metal, may be envisaged, but consideration of such system elaborations is beyond the scope of the present prefatory discussion.

References

1 Carter, J. M., "How Much Thrust from Chemical Propellants?," *Aviation Age*, vol. 23, 1955, p. 23.

2 Zwicky, F., "Propellants for Tomorrow's Rockets," ASTRONAUTICS, vol. 2, no. 1, Aug. 1957, p. 45.

3 Tormey, J. F., "Liquid Rocket Propellants—Is There an Energy Limit?," *Ind. & Eng. Chem.*, vol. 49, Sept. 1957, pp. 1339–1343.

4 Rosenblum, M. H., Rinehart, W. T. and Thompson, T. L. "Rocket Propulsion with Nuclear Energy," ARS Preprint no. 559-57, New York, Dec. 1957.

5 Malmstrom, C., Keen, R. and Green, L., Jr., "Some Mechanical Properties of Graphite at Elevated Temperatures," *J. Appl. Phys.*, vol. 22, 1951, pp. 593–600.

6 Green, L., Jr., "Erosion of Graphite by High Temperature Helium Jets," North American Aviation Report no. NAA-SR-77, May 1950.

7 Altman, D. and Penner, S. S., *J. Chem. Phys.*, vol. 17, 1959, p. 56.

8 Penner, S. S., *J. Amer. Chem. Soc.*, vol. 71, 1949, p. 788.

9 Penner, S. S., *J. Franklin Inst.*, vol. 230, 1950, p. 452.

10 Amdur, I., *J. Amer. Chem. Soc.*, vol. 60, 1935, p. 2347.

11 Altman, D. and Carter, J. M., "Expansion Processes," in "Combustion Processes," Princeton University Press, 1956.

12 Wilde, K. A., "Effect of Radical Recombination Kinetics on Specific Impulse of High-Temperature Systems," JET PROPULSION, vol. 28, 1958, p. 119.

13 Rossini, F. D., Wagaman, D. D., Evans, W. H., Levine, S. and Jaffee, I., Series I and II of "Selected Values of Chemical Thermodynamic Properties," Nat. Bur. Standards Circ. no. 500, Washington D. C., 1952.

14 "Selected Values of Chemical Thermodynamic Properties," Series III, Nat. Bur. Standards, looseleaf, 1948–1956.

15 Kelley, K. K., U. S. Bureau of Mines Bulletins, nos. 371 (1934), 383 (1935), 393 (1936) and 476 (1949).

16 Sutton, G. P., "Rocket Propulsion Elements," John Wiley & Sons, New York, 2nd ed., 1956.

17 "Rocket Engine Propellants," *Missiles and Rockets*, Dec. 1956.

18 Shenfil, L., Aerojet-General Corp., private communication.

19 Steinberg, M. A., Horizons, Inc., private communication.

20 Miller, E. C., "Corrosion of Materials by Liquid Metals," in "Liquid Metals Handbook," NAVEXOS-P-733 (rev.), Washington, D. C., June 1952.

21 Durham, F. P., Neal, R. C. and Newman, H. J., "High Temperature Heat Transfer to a Gas Flowing in Heat Generating Tubes at High Heat Flux," Los Alamos Scientific Laboratory, Los Alamos, N. Mex.

22 Bonilla, C. F., "Nuclear Engineering," McGraw-Hill Book Company, Inc., New York, 1957, p. 406.

23 Lyon, R. E., Foust, A. S. and Katz, D. L., "Boiling Heat Transfer with Liquid Metals," Heat Transfer—St. Louis, Chemical Engineering Progress Symposium Series, no. 17, vol. 51, Amer. Inst. of Chem. Engrs., 1955, pp. 41–47.

24 Hlavka, G., Garrett Corp., private communications.

Magnetohydrodynamics and Aerodynamic Heating

RUDOLF X. MEYER[1]

Space Technology Laboratories, Inc.
Los Angeles, Calif.

The basic equations and some fundamental concepts of magnetoaerodynamics are discussed. As an application, the problem of the flow near the stagnation point of a body of revolution is reviewed and an exact solution is given. Data are presented for the heat transfer coefficient at the stagnation point, and for its gradient in the stagnation point region. The magnetic field strength required to accomplish an appreciable reduction of aerodynamic heating in hypersonic flight is discussed, for the case in which ionization is due to thermal motion. Alternatively, methods which involve electrical breakdown of the air are considered.

AT HYPERSONIC speeds, exceeding a flight Mach number of approximately 15, the air behind a normal shock reaches a temperature which is sufficient to ionize the air to an appreciable extent. It is then possible to alter the characteristics of the flow by means of externally applied magnetic fields (1 to 8).[2] Due to the motion of the ionized gas (plasma) through the magnetic lines of force, currents are induced in the gas, which in turn give rise to a force $\vec{j} \times \vec{B}$, per unit volume, acting on the gas. In this expression, $\vec{j}$ is the current density and $\vec{B}$ the magnetic induction. The plasma currents in turn give rise to a magnetic field which adds to the field produced by external currents. $\vec{B}$ represents the total field. The theoretical analysis of the ensuing flow therefore requires in general a solution of Maxwell's equations for the electromagnetic field, coupled with the equations of fluid mechanics containing the additional force term. The equation of energy is also modified, in a manner which will be discussed.

Confining the present considerations to the stationary flow of a fluid of constant properties, the usual equations of magnetohydrodynamics take the form

$$\text{curl } \vec{H} = \vec{j} \qquad [1]$$

$$\text{curl } \vec{E} = 0 \qquad [2]$$

$$\text{div } \vec{B} = 0 \qquad [3]$$

where $\vec{H}$ and $\vec{E}$ are the magnetic and electric field strengths, respectively. Maxwell's equations are supplemented by the constitutive equation

$$\vec{B} = \mu \vec{H} \qquad [4]$$

and Ohm's law for moving, isotropic media

$$\vec{j} = \sigma(\vec{E} + \vec{v} \times \vec{B}) \qquad [5]$$

where

μ = magnetic permeability
σ = conductivity
$\vec{v}$ = velocity

Furthermore

$$\text{div } \vec{v} = 0 \qquad [6]$$

since a fluid of constant density is assumed. Supplementing the Navier-Stokes equation by the magnetic force term

$$\rho \frac{\vec{Dv}}{Dt} = -\text{grad } p + \eta \nabla^2 \vec{v} + \vec{j} \times \vec{B} \qquad [7]$$

where

ρ = density
p = pressure
η = viscosity

Equations [1 to 7] suffice to determine, for instance, the velocity and the current distribution in the fluid. For the purpose of computing the distribution of temperature and rates of heat transfer, consideration must be given to the equation of energy[3]

$$\rho c \frac{DT}{Dt} - \kappa \nabla^2 T = \frac{1}{\sigma} \vec{j}^2 + \Phi \qquad [8]$$

where

c = specific heat per unit mass
T = temperature
κ = thermal conductivity

and

$$\Phi = \tau_{ij} \frac{\partial v_i}{\partial x_j} \qquad \tau_{ij} = \eta \left(\frac{\partial v_i}{\partial x_j} + \frac{\partial v_j}{\partial x_i} \right) \qquad [9]$$

The terms on the left of Equation [8] represent the rate of heat removed per unit volume by convection and by heat conduction, respectively. The terms on the right are the rates of heat added through Joule heating and through viscous dissipation.

Stagnation Point Flow

As an illustration, the rotationally symmetric stagnation point flow is considered. The corresponding two-dimensional case was treated by Neuringer and McIlroy (10). In the present analysis, a rotationally symmetric magnetic field is assumed, which vanishes at a large distance forward of the stagnation point and has a normal component on the surface,

Received July 10, 1958. Part of this paper was presented at the ARS Semi-Annual meeting, Los Angeles, Calif., June 9–12, 1958.

[1] Member of Senior Staff, Physical Research Laboratory.

[2] Numbers in parentheses indicate References at end of paper.

[3] A full discussion of the equation of energy in magnetohydrodynamics, applicable to more general conditions than needed here, is due to Goldstein and to Chu (9).

which is constant. It follows from simple symmetry arguments that a solution exists, for which

$$\begin{aligned} j_r &= j_z = 0 \\ B_\varphi &= 0 \\ v_\varphi &= 0 \\ E_r &= E_z = E_\varphi = 0 \end{aligned} \qquad \text{.....[10]}$$

where r, z and φ indicate the corresponding components in cylindrical coordinates. It is seen that the current flows in circular loops about the z-axis. The magnetic force $\vec{j} \times \vec{B}$ is in the meridional plane, and its direction is such as to impede the motion of the fluid.

The trial solution

$$\begin{aligned} v_r &= rf'(z) \\ v_z &= -2f(z) \\ B_r &= rg'(z) \\ B_z &= -2g(z) \\ \bar{p} - p &= h(z) + r^2k(z) \\ \bar{T} - T &= l(z) + r^2m(z) \end{aligned} \qquad \text{.....[11]}$$

where f, g, h, k, l and m are functions of the coordinate z alone, and where $\bar{p}$ and $\bar{T}$ are the pressure and temperature at the stagnation point, satisfies Equations [1 to 9] identically, resulting in a set of differential equations for these functions. Full details are given elsewhere (11).

The following boundary conditions are imposed on the surface, i.e., at $z = 0$:

1 The normal component of the total magnetic field is constant, i.e., $B_z(0) = \bar{B}$, where $\bar{B}$ is a given constant.

2 The velocity vanishes, i.e., $v_r(0) = v_z(0) = 0$.

3 The surface temperature is constant, i.e., $T(0) = \bar{T}$.

At a large distance from the surface, the following conditions are imposed:

4 The magnetic field vanishes. In particular, it is required that $B_z(\infty) = 0$.

5 The velocity and pressure distributions approach the corresponding distributions for an inviscous, nonmagnetic stagnation point flow. In particular, $v_r(\infty) = ar$, where the constant a is determined by the characteristics of the flow outside the stagnation point region.

6 The temperature is independent of the radius. In particular, $T(\infty) = \bar{T}$ where $\bar{T}$ is a given constant.

Numerical results were obtained by means of a digital computer. Introducing the dimensionless quantities

$$\zeta = \sqrt{\mu\sigma a}\, z \qquad [12]$$

$$F(\zeta) = \sqrt{\frac{\mu\sigma}{a}}\, f(z) \qquad [13]$$

$$G(\zeta) = -\frac{2}{\bar{B}}\, g(z) \qquad [14]$$

typical distributions of velocity and magnetic induction are plotted in Fig. 1. These results depend upon two dimensionless parameters namely

$$\alpha = \eta a(\bar{B}^2/2\mu)^{-1} \qquad [15]$$

$$\beta = \mu\sigma\eta/\rho \qquad [16]$$

In aerodynamic applications, α and β are invariably very small, typically of the order of 10^{-6}. The ratio

$$\gamma = \frac{\beta}{2\alpha} = \frac{\sigma\bar{B}^2}{4\rho a} \qquad [17]$$

which is a measure for the ratio of the magnetic forces to the inertial forces, however, is generally of order 1. Letting α and β tend to zero gives rise to a boundary layer problem (11). The velocity and the magnetic field distributions then depend only upon the single parameter γ. Figs. 2 and 3 represent the two velocity components outside this boundary layer ($\zeta_1 \equiv \zeta$, $F_1 \equiv F$). Similarly, Figs. 4 and 5 give the velocity distribution in the boundary layer, where $\zeta_2 \equiv \beta^{-1/2}\zeta$, and $F_2 \equiv \beta^{-1/2}F$.

As one recognizes from the velocity distributions, an important effect of the magnetic field consists in displacing the flow in the direction of the positive z-axis. The thickness of this magnetic cushion, defined by

$$\bar{\zeta} = \sqrt{\mu\sigma a}\, \bar{z} \qquad \bar{z} = \lim_{z \to \infty} [z - f(z)/a] \qquad [18]$$

is plotted in Fig. 7.

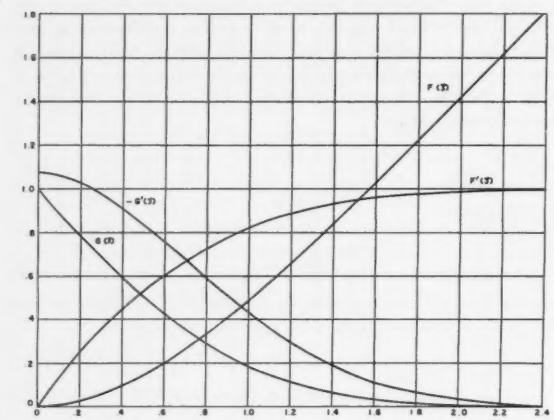

Fig. 1 The functions $F(\zeta)$, $G(\zeta)$ and their derivatives, for $\alpha = \beta = 1$

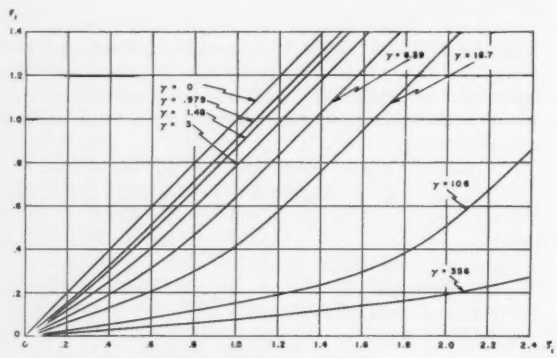

Fig. 2 Function $F_1(\zeta_1)$

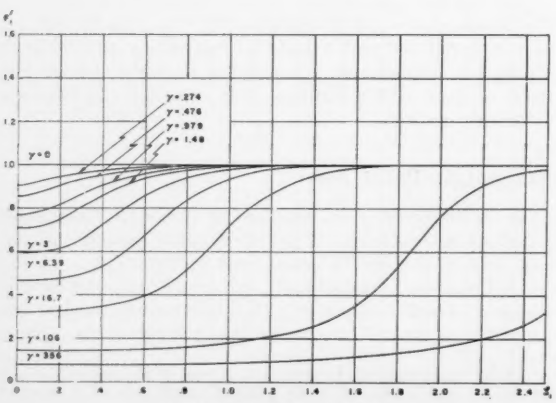

Fig. 3 Function $F_1'(\zeta_1)$

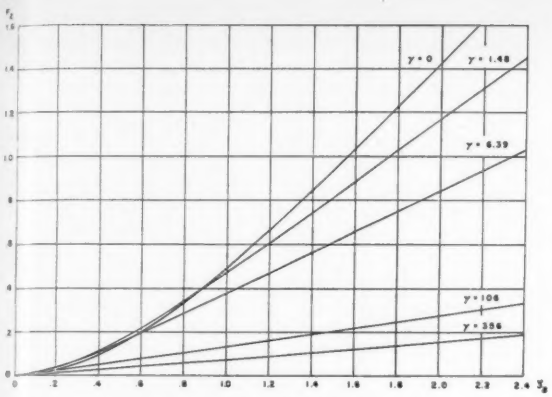

Fig. 4 Function $F_2(\zeta_2)$

Defining the Nusselt number

$$Nu(r) = h(r)\,\frac{1}{\kappa}\left(\frac{\eta}{\rho a}\right)^{1/2} \qquad [19]$$

where $h(r)$ is the heat transfer coefficient, one obtains

$$Nu(r) = Nu^{(0)} + Nu^{(1)}\,\frac{a^2 r^2}{c(\bar{T} - \hat{T})} \qquad [20]$$

The coefficients $Nu^{(0)}$ and $Nu^{(1)}$ have been computed for a Prandtl number of 0.70 and are given in Fig. 8. With increasing magnetic field strength, the rate of heat transfer at the stagnation point is seen to decrease, a result which is in qualitative agreement with the computations by Neuringer and McIlroy (10) for the two-dimensional case. In the nonmagnetic case which corresponds to $\gamma = 0$, the result agrees with data computed by Cohen and Reshotko (12).

$Nu^{(1)}$ increases with increasing field strength, indicating an increased slope of the heat transfer rate considered as a function of the radius. In applications to aerodynamic heating, this is a detrimental effect. The crossover point, at which the advantage of a reduced heat transfer at the stagnation point is canceled by an increased heat transfer at some distance from this point, depends upon the details of the application.

Required Magnetic Field Strength

It is seen that γ must be large (of the order of 100), if an appreciable reduction in heat transfer at the stagnation point is to be achieved. The same does not need to be true, however, for configurations of the magnetic field differing from the one presently considered. The contribution of the plasma currents to the total magnetic field is substantial, as seen from the curves in Fig. 6 where the magnetic field outside the boundary layer is plotted in terms of $G_1(\zeta_1) \equiv G(\zeta)$.

The required field strength depends critically upon the conductivity of the medium. The conductivity of air in thermodynamic equilibrium has been estimated for temperatures up to 24,000 K (Fig. 9). The quotient ρ/ρ_0 in this figure is the ratio of the density to the density at normal temperature and pressure. These data have been computed from the electron collision cross sections (13) and the calculated equilibrium composition of air (14). Details are given in an Appendix to this paper. It must be emphasized that in view of the uncertainty in the presently available data on the appropriate cross sections, the degree of accuracy is small.

In order to permit a quick orientation, the conductivity of air behind a normal shock is plotted in Fig. 10 directly as a function of the flight velocity V and of the altitude H above sea level. Fig. 11 is a plot of the magnitude of the magnetic induction B which is required to make the ratio of the mag-

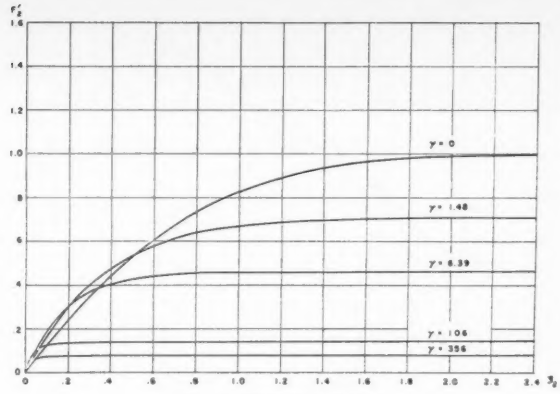

Fig. 5 Function $F_2'(\zeta_2)$

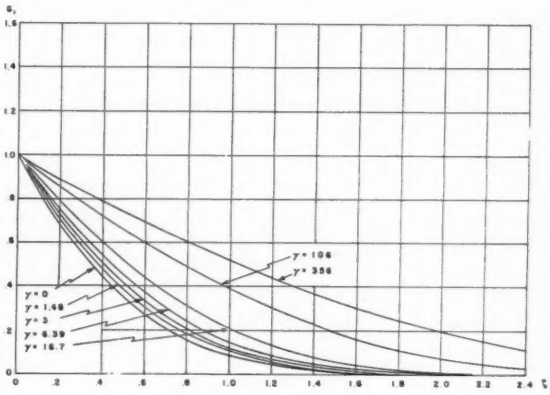

Fig. 6 Function $G_1(\zeta_1)$

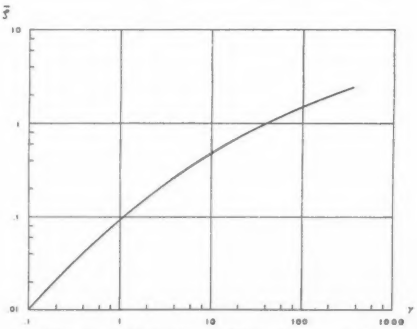

Fig. 7 Magnetic cushion thickness $\bar{\zeta}$

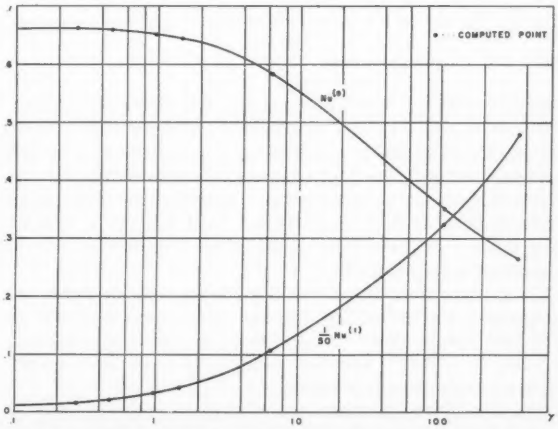

Fig. 8 Nusselt numbers $Nu^{(0)}$ and $Nu^{(1)}$ for $Pr = 0.70$

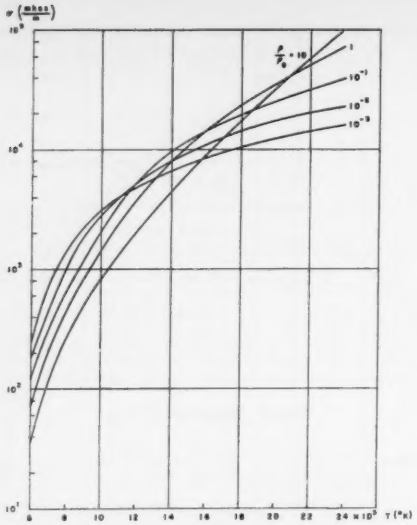

Fig. 9 Estimated electrical conductivity of air

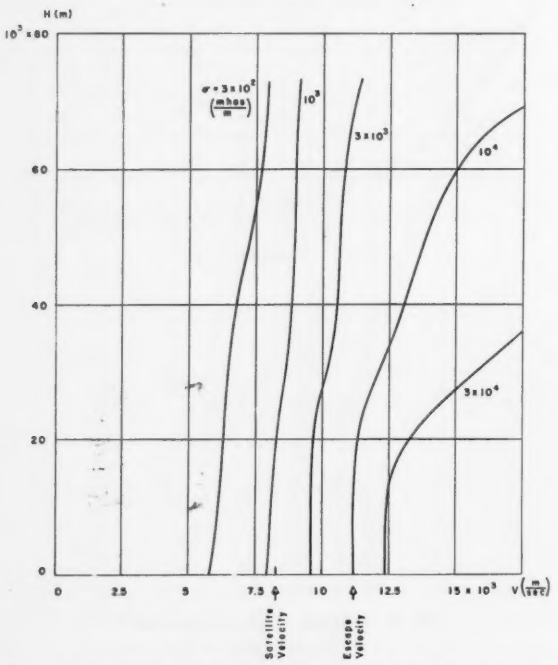

Fig. 10 Estimated electrical conductivity of air behind a normal shock

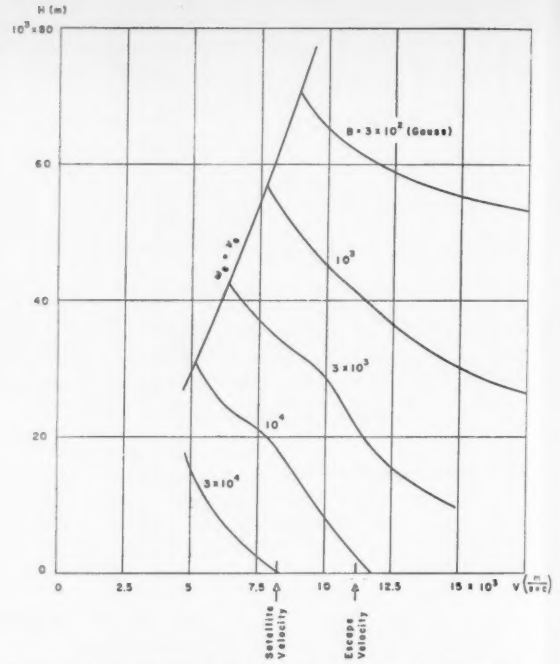

Fig. 11 Required magnitude of magnetic field for $\sigma B^2 l/\rho u = 1$ and $l = 1m$, behind a normal shock in air

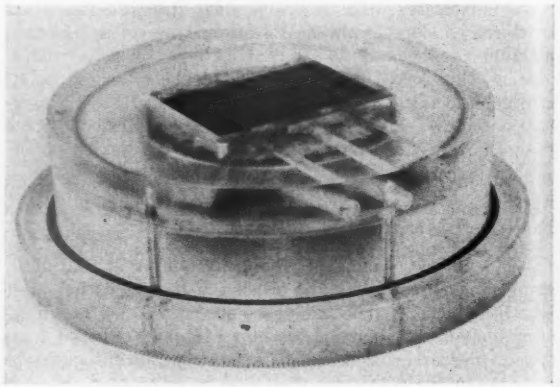

Fig. 12 Model used in glow discharge experiments in a supersonic stream

netic forces to the inertial forces, i.e., $\sigma B^2 l/\rho u$, equal to unity. Here, σ, ρ and u are the conductivity, density and velocity behind a normal shock in air (taking into account dissociation and ionization). l is a characteristic length of the aerodynamic body, and was taken as 1m. With these assumptions, a definite field strength is associated with any given velocity and altitude. The curve labeled by the equation $\omega_e = \nu_e$ is discussed in the Appendix.

It appears from these data that large field strengths are required if the heat transfer at the stagnation point is to be reduced substantially at altitudes for which aerodynamic heating is critical. Different configurations of the magnetic field may be more advantageous.

In some cases, the temperature of the electron gas may be many times greater than the temperature of the gas, corresponding to an effective increase of the conductivity. This is the case with microwave breakdown and glow discharges, for instance. The device shown in Fig. 12 contains a large number of electrodes of alternating polarity, which are imbedded in an aerodynamic surface. It has been found possible to maintain a glow discharge in a supersonic airstream, thereby ionizing the air in the boundary layer. A typical current voltage characteristic is given in Fig. 13.

Appendix

The electrical conductivity of air in thermodynamic equilibrium at temperatures up to about 7000 K is known with considerable certainty from shock tube experiments reported by Lamb and Lin (13). At these temperatures, the

contribution of the positive ions to the total electron collision probability is still relatively small, but becomes increasingly important at higher temperatures.

It appears that no detailed experimental data are available at present for temperatures in excess of 7000 K. On the other hand, many of the contemplated applications of magnetoaerodynamics involve considerably higher temperatures. In this paper, estimates of the conductivity up to 24,000 K are computed. This upper limit was decided upon because it coincides with the limit of Gilmore's computations of the equilibrium composition of air (14).

The usual practice in computing the conductivity of partially ionized gases is to add the Maxwell-averaged total electron collision cross sections (weighted with the number density) of the neutral molecules to a corresponding equivalent cross section of the ions, the latter being computed on the basis of a theory which applies to fully ionized gases. The degree of approximation involved in this assumption is not known. In the case of air, a further element of uncertainty is introduced by the fact that the cross sections of some of the neutral species, notably N, are not known with certainty.

The conductivity σ is expressed by

$$\sigma = \frac{n_e e^2}{m_e \bar{C}_e \sum n_j \bar{Q}_j} \qquad [A\text{-}1]$$

where

n_e = number density of free electrons
e = electronic charge
m_e = electronic mass
n_j = number density of the species j
$\bar{Q}_j$ = Maxwell-averaged total electron collision cross section of the species

$\bar{C}_j = \sqrt{\frac{8kT}{\pi m_e}}$ = the mean speed of the electrons

k = Boltzmann's constant
T = temperature

Thermodynamic equilibrium with an electron temperature equal to the gas temperature is assumed.

The summation in Equation [A-1] is extended over those species, neutrals as well as ions, which contribute appreciably to the total cross section. An inspection of the equilibrium composition of air in the range from 6000 to 24,000 K and a density ratio ρ/ρ_0 (ρ_0 = standard density) varying from 10^{-3} to 10 indicates that the neutrals of major importance are N_2, N and O (14). In view of the approximate nature of the computation, the inclusion of O_2, NO and other even less frequent species would not be warranted. The cross sections for N_2, N and O above an electron temperature of 6000 K are believed to be quite similar and nearly independent of the energy in the range considered. (At much higher temperatures, the effect of the neutrals becomes negligible.) The computations can be based therefore on a common cross section of the neutrals, $\bar{Q}_n$, which was taken as 0.80×10^{-15} cm^2. In view of the uncertainty in the cross-sectional data of N and O, a more detailed computation would not be justified.

The sum over all cross sections, in Equation [A-1], can therefore be expressed as

$$\sum n_j \bar{Q}_j = n_n \bar{Q}_n + n_i \bar{Q}_i = n_{A.\,0} \frac{\rho}{\rho_0} [(N_2 + N + O)\bar{Q}_n + e^- \bar{Q}_i] \qquad [A\text{-}2]$$

where n_n and n_i are the number densities of neutrals and ions, respectively. $n_{A.\,0}$ is the number density of "air atoms" at standard condition, i.e., $n_{A.\,0} = 5.38 \times 10^{19}$ cm^{-3}. N_2, N, O and e^- are the number of N-molecules, N-atoms, O-atoms and free electrons, respectively, per "air atom." The values computed by Gilmore have been used for these fractions.

Within the limits of temperature and density considered here, the effect of doubly ionized ions on the conductivity amounts to less than 8 per cent, and is neglected. Similarly, the effect of O^- is negligible. Consequently, for a neutral plasma

$$n_i = n_e = n_{A.\,0} \frac{\rho}{\rho_0} e^- \qquad [A\text{-}3]$$

a result which was already utilized in the derivation of Equation [A-2].

Spitzer and Härm's (15) results for the conductivity of a fully ionized gas, if written in terms of an equivalent cross section $\bar{Q}_i$ for the positive ions, give

$$\bar{Q}_i = \left(\frac{\pi e^2}{4kT}\right)^2 \frac{\ln (qC_e^2)}{\gamma_E} \qquad [A\text{-}4]$$

for singly ionized ions, where

$$q = \frac{m_e}{2e^3}\left[\frac{kT}{2\pi n_e}\right]^{1/2}$$

and $\gamma_E = 0.582$. C_e is the rms electron velocity

$$C_e = \left(\frac{3kT}{m_e}\right)^{1/2}$$

The results of a computation of σ, based on Equations [A-1 to A-4] are given in Fig. 9. It is noted that the dependence upon density is relatively weak, and that its gradient reverses within the considered temperature interval. Above 24,000 K, the effect of the second ionization becomes increasingly important.

At the lower end of the temperature interval, the computed conductivity agrees with the experimental data of Lamb and Lin (13). The computed values fall inside the experimental scatter. However, this agreement is to be expected, since cross-sectional values were used which are derived from these data.

Gilmore's results for the thermodynamic variables of state of the air behind a normal shock resulting from hypersonic velocities have been used to calculate the conductivity for different flight velocities V and altitudes H above sea level (Fig. 10). For comparison, the velocity of a satellite in a circular orbit of 7×10^6 m radius and the escape velocity have also been indicated.

In many applications of magnetoaerodynamics, the parameter $\sigma B^2 l/\rho u$ plays an important role since it is a measure for the ratio of the magnetic forces to the inertial forces. In general, this parameter must be at least of order 1, if the magnetic field is to produce an appreciable effect.

In order to permit a quick estimate of the typical field strength required in magnetoaerodynamics (assuming thermodynamic equilibrium), Fig. 11 has been drawn. In this figure, the required field strength is given in the case where

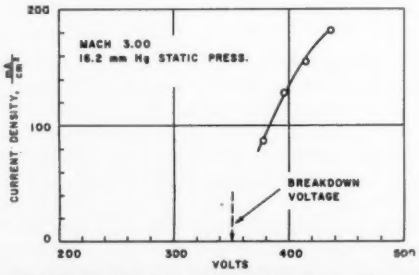

Fig. 13 Typical current-voltage characteristic for glow discharge in supersonic air stream. Copper electrodes, parallel to free-stream velocity. Cathode area = 3 cm^2

the value of this parameter is 1, and for a length $l = 1$m. From conservation of mass

$$\rho u = \rho_\infty V$$

where $\rho_\infty = \rho_\infty(H)$ is the freestream density, and the computation of B as a function of H and V is straightforward.

Equation [A-1] gives σ correctly only in the case of weak fields. Otherwise, the conductivity is no longer described by a scalar quantity. This occurs if the cyclotron frequency ω_e of the electrons is comparable or larger than their collision frequency ν_e. From

$$\omega_e = \frac{Be}{m_e}$$

and

$$\sigma = \frac{n_e e^2}{m_e \nu_e}$$

it follows from equating ω_e and ν_e, that

$$B' = \frac{n_e e}{\sigma} \qquad \text{[A-5]}$$

where B' can be considered as a rough estimate of the maximum field strength B for which Equation [A-1] is still valid. The locus of points in the H-V diagram for which this limiting condition exists, is indicated in the figure. To the left of this curve, $\omega_e > \nu_e$.

Acknowledgment

The author is indebted to Dr. Lee O. Heflinger, who supervised the digital computer programming, and to Dr. Allan B. Schaffer, who obtained the data presented in Fig. 13.

References

1 Resler, E. L., Jr. and Sears, W. R., "The Prospects for Magnetoaerodynamics," *J. Aeron. Sci.*, vol. 25, no. 4, 1958, pp. 235–258.

2 Sears, W. R., "Recent Developments in Magnetoaerodynamics," IAS Summer Meeting, Los Angeles, June 1957.

3 Patrick, R. M., "Magnetohydrodynamics of Compressible Fluids," Ph.D. Thesis, Cornell University, Ithaca, N. Y., 1956.

4 Rossow, V. J., "On Flow of Electrically Conducting Fluids Over a Flat Plate in the Presence of a Transverse Magnetic Field," NACA TN 3971, 1957.

5 Bond, J. W., Jr., "Plasma Physics and Hypersonic Flight," JET PROPULSION, vol. 28, no. 4, 1958, pp. 228–235.

6 Landshoff, R. K. M. (ed.), "Magnetohydrodynamics, A Symposium," Stanford University Press, Stanford, Calif., 1957.

7 Bush, Wm. B., "Magnetohydrodynamic-Hypersonic Flow Past a Blunt Body," Report ARL-7-70, Phys. Res. Lab., The Ramo-Wooldridge Corp., Los Angeles, Calif., 1957.

8 Kemp, N. H., "On Hypersonic Blunt-Body Flow With a Magnetic Field," Res. Report 19, Avco Research Lab., Everett, Mass., 1958.

9 Chu, B. T., "Thermodynamics of Electrically Conducting Fluids and Its Application to Magneto-Hydromechanics," TN 57-350, Wright Air Dev. Center, 1957.

10 Neuringer, J. L. and McIlroy, Wm., "Two Dimensional Flow in the Vicinity of the Stagnation Point of an Incompressible, Viscous, Electrically Conducting Fluid in the Presence of a Magnetic Field," Republic Aviation Corp. Report, 1957.

11 Meyer, R. X., "Rate of Heat Transfer Near the Stagnation Point of a Blunt Body of Revolution, in the Presence of a Magnetic Field," Phys. Res. Lab., Report GM-TR-0127-00016, The Ramo-Wooldridge Corp., Los Angeles, 1958.

12 Cohen, C. B. and Reshotko, E., "Similar Solutions for the Compressible Laminar Boundary Layer With Heat Transfer and Pressure Gradient," NACA Report 1293, 1956.

13 Lamb, L. and Lin, S. C., "Electrical Conductivity of Thermally Ionized Air Produced in a Shocktube," *J. Appl. Phys.*, vol. 28, no. 7, 1957.

14 Gilmore, F. R., "Equilibrium Composition and Thermodynamic Properties of Air to 24,000°K," RM-1543, Rand Corp., Santa Monica, Calif., 1955.

15 Spitzer, L. and Härm, R., "Transport Phenomena in a Completely Ionized Gas," *Phys. Rev.*, vol. 89, no. 5, 1953, pp. 977–981.

Compression Sensitivity of Monopropellants

G. A. MEAD[1]

Air Reduction Company, Inc.
Murray Hill, N. J.

A method for evaluating the sensitivity of liquid monopropellants to initiation of decomposition in the presence of rapidly compressed gas bubbles has been developed. The mechanical design of the equipment and the conditions of experimentation simulate the environment which can occur in actual propellant systems. During the test, a gas bubble in contact with a liquid monofuel sample is compressed rapidly by a gas driven piston. The mass and velocity of the piston are analogous to the mass and velocity of a liquid propellant flowing in an actual propellant system against a dead end. It is postulated that the significant parameter to be associated with decomposition initiation by this type of stimulus is the minimum compressive energy per unit gas bubble volume. A theoretical analysis and experimental data for several monofuels are given in support of this hypothesis. The process of data reduction is described.

BECAUSE monopropellants are necessarily capable of exothermic decomposition, a certain amount of risk is associated with their handling and use. To minimize this hazard, conditions which might result in inadvertent and uncontrolled decompositions must be recognized and avoided. One possible cause of the unintentional initiation of monopropellant decomposition is the rapid compression of small gas bubbles in contact with liquid fuel. Rapid compression can result from mechanical shock to containers of fuel, or from rapid closing of valves in propellant lines containing entrained gas bubbles. Such phenomena are thought to be responsible for a number of accidental explosions. Therefore, a method of estimating the relative sensitivity of various monofuels to this kind of initiation, or, of quantitatively measuring the severity of conditions necessary to cause initiation, should have considerable practical value.

The work described herein is an extension of an investigation begun by the Aerojet-General Corp. (1).[2] Similar equipment has been employed throughout. This equipment was de-

Received July 3, 1958.

[1] Engineer, Combustion and Fuels Technology Section. Member ARS.

[2] Numbers in parentheses indicate References at end of paper.

signed to simulate conditions which might occur in an actual propellant line, and incorporates a device for applying pressure very rapidly to a gas bubble in contact with a liquid propellant sample. In the previous work, results were reported in terms of the rate of pressure rise necessary to cause explosion without a consideration of other thermodynamic parameters. In the present study, an attempt has been made to explain the significance of rate of pressure rise, relating it to other physical conditions of the test in order to estimate the energy input to the sample.

The relative sensitivity of several monopropellants has been measured, and a quantitative scale of sensitivity rating has been developed. It is thought that the method of evaluation should be useful for estimating the sensitivity of experimental monofuels and of explosive liquids in general.

Equipment and Operation

The tester used in this investigation is identical in critical dimensions and similar in construction to that first developed by the Aerojet-General Corp. (1). During the course of this investigation, a few changes have been made to facilitate operation and to improve documentation of the phenomena occurring. A schematic diagram of the test equipment is shown in Fig. 1, and a photograph of the disassembled tester is shown in Fig. 2.

The test sample, consisting of a gas bubble in contact with liquid monofuel, is subjected to rapid compression by a gas driven piston. Driving gas is contained in a high pressure tank and is admitted to the driving cylinder by the rapid opening of a solenoid valve. Since the area of the piston in the driving cylinder is 20 times the area of the piston in the sample chamber, a pneumatic multiplication of 20 results. Maximum driving gas pressure is limited by the strength of the tester body, and with present equipment is about 1000 psi, giving a maximum static pressure in the sample cylinder of 20,000 psi. Rate of pressurization can be varied by adjusting pressure in the driving-gas tank, by varying the size of an orifice in the gas line between the driving-gas tank and the driving cylinder, and by changing the working medium. For example, the use of helium as a driving gas instead of nitrogen, with other conditions being the same, increases the rate of pressure rise in the driving cylinder by a factor of 2.8.

The test chamber itself is formed by the small end of the piston, the walls of the cylinder in which it moves and a burst diaphragm held in place by a bolted retainer (Fig. 2). The burst diaphragm used with recording instrumentation is a 0.1-in. thick heat-treated stainless steel disk which deforms elastically up to at least 20,000 psi. Since the bursting pressure of the steel diaphragm is quite high, there is some danger of damage to the tester when an explosion occurs. Consequently, aluminum diaphragms are usually substituted for steel when testing without the use of recording instrumentation.

The total sample chamber volume is about 1.3 ml. Samples from about 0.4 to 1.1 ml liquid volume and from 0.2 to 0.9 ml bubble volume can be tested. The relative sizes of the two phases in the sample chamber are limited by the accuracy of the liquid phase volume measurement, since bubble volume is estimated by the difference.

The tester is jacketed to provide heating or cooling of the sample, if desired. Piston motion is detected by a slide wire potentiometer. The sliding contacts are fixed to a shaft which is an extension of the driving piston rod. The linear resistor is mounted on the tester body and is stationary with respect to the piston. The variable resistance forms one leg of a resistance bridge. Unbalance of the bridge is amplified electronically, and the resulting signal causes deflection of a galvanometer. A mirror mounted on the galvanometer filament, by deflecting a light beam, allows photographic recording. The rated frequency response of the galvanometer is 1300 cps, so that the maximum piston velocities encountered

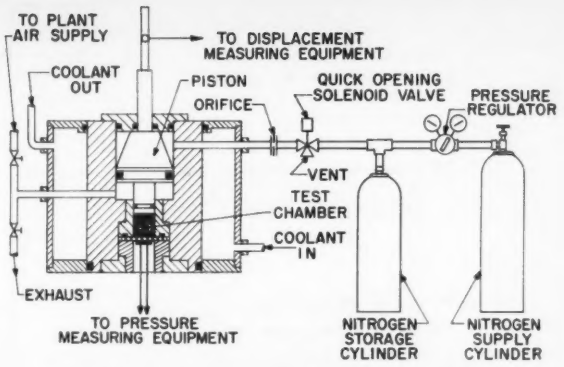

Fig. 1 Rapid compression test equipment

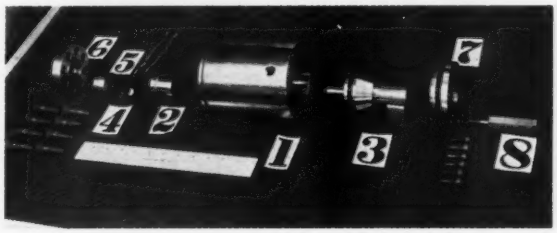

Fig. 2 Rapid compression tester—disassembled view

(1) Body, (2), insert, (3) piston-plunger assembly, (4) strain gage bonded on diaphragm, (5) retainer, (6) flange, (7) cover and (8) linear motion potentiometer.

were well within the range of the instrument.

Instantaneous pressure in the test chamber is sensed by a strain gage cemented to the burst diaphragm. Again, the strain gage forms one leg of a resistance bridge, the unbalance of which is recorded by a system similar to that used to record piston motion.

Analysis of Tester Action

It is generally believed that high temperatures resulting from nearly adiabatic compression are the cause of ignition in the rapid compression tester. The original reason for measuring both pressure rise and piston displacement in the test chamber was that simultaneous readings of these quantities would permit the evaluation of n in the equation

$$\frac{P_f}{P_0} = \left(\frac{V_0}{V_f}\right)^n = \left(\frac{T_f}{T_0}\right)^{\frac{n}{n-1}} \qquad [1]$$

where

P = pressure
V = volume
T = temperature
n = polytropic exponent
0 = initial conditions
f = final conditions

Thus, if the initial gas conditions were known and the pressure and volume of the system could be measured at the time of explosion, a temperature at the instant of explosion could be calculated even though the compression were not adiabatic ($n \neq \gamma$, where γ = specific heat ratio). This analysis has disregarded ignition delay phenomena, which, as will be shown later, can have a substantial effect. Further consideration of the compression process has shown that extremely ac-

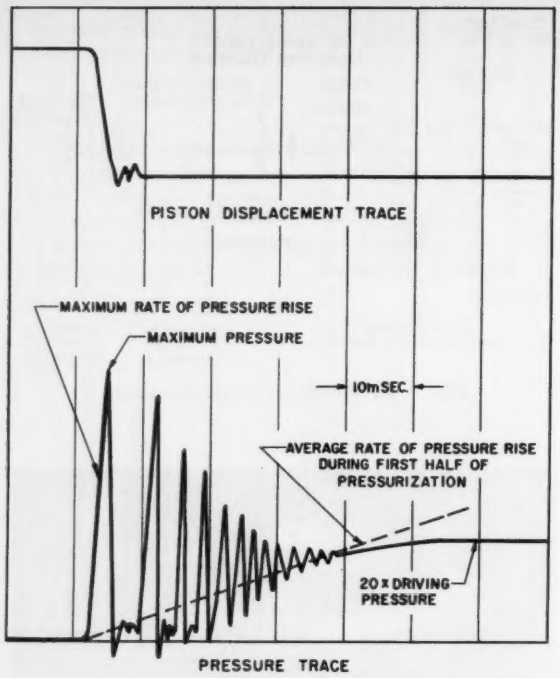

Fig. 3 Typical oscillograph record of blank test on water

curate measurement of piston displacement would be needed to make this calculation, because the volume of compressed gas in the test chamber becomes extremely small at relatively low pressures, and large pressure changes are produced by very small changes in piston displacement. At higher pressures, in the range where explosions usually occur, the difference between piston displacements for adiabatic and isothermal conditions is practically negligible on the scale used to measure total piston travel.

Originally, it was anticipated that smooth pressure traces would be produced, on which a point of initiation could be easily located. A series of such points could be obtained, and the initiation pressure extrapolated to infinite rate of pressure rise, at which point adiabatic conditions would obtain and the specific heat ratio of the gas used to estimate the temperature at the instant of explosion, ignition delays again being disregarded. It was soon observed, however, that very rapid pressure oscillations usually occurred at the start of the pressure-rise cycles. These oscillations could have been anticipated, since the confined gases on each side of the piston could be expected to act essentially like springs. A typical oscillograph record of a blank test on water is shown in Fig. 3. The magnitude of the rate of pressure rise in the first oscillation may be as great as 10^7 psi per sec, and it is not directly related to the average rate of pressure rise, which would be equal to 20 times the rate of pressure rise in the driving chamber. Clearly, if an explosion did occur during the first half of pressure rise, the pressure and rate of pressure rise at that point could not be measured with any accuracy. It was concluded that heavy damping of the system would be necessary to produce smooth pressure traces, but if such damping were incorporated, appreciable deviation from the real situation would result.

To assist in explaining the action of the tester, an expression was derived for the rate of pressure rise on the driving side of the piston in terms of the physical constants of the equipment and driving gas. It was assumed that flow from the high pressure reservoir through the gas release valve and flow restricting orifice was adiabatic, and that the temperature of the gas in the driving chamber remained the same as that in the reservoir throughout the process. Also, it was assumed that the gas pressure in the reservoir was constant, and that driving-chamber volume remained constant. The gas was assumed to be ideal.

Then

$$P = \frac{n_g R_0 T}{V} \qquad [2]$$

$$\frac{dP}{dt} = \frac{dn_g}{dt}\frac{R_0 T}{V} = \frac{m R_0 T}{MV} \qquad [3]$$

where

n_g = number of moles of gas
R_0 = universal gas constant
dP/dt = rate of pressure rise in driving chamber
m = mass rate of gas flow into driving chamber
M = molecular weight of driving gas

Flow between the high pressure reservoir and the driving chamber will be at sonic velocity at the throat (the valve or orifice) until pressure in the driving chamber exceeds the critical fraction of pressure in the reservoir. For nitrogen at room temperature, the critical pressure ratio is 0.528.

For sonic flow (2)

$$m = \frac{A_t P_0 g_c \gamma \sqrt{\left(\frac{2}{\gamma+1}\right)^{\frac{\gamma+1}{\gamma-1}}}}{\sqrt{\frac{g_c \gamma R_0 T_0}{M}}} \qquad [4]$$

where

A_t = throat area
P_0 = reservoir pressure
g_c = gravitational conversion factor
γ = specific heat ratio
T_0 = reservoir temperature

It follows that

$$\frac{dP}{dt} = \frac{A_t P_0}{V}\sqrt{\frac{g_c \gamma R_0 T_0}{M}\left(\frac{2}{\gamma+1}\right)^{\frac{\gamma+1}{\gamma-1}}} \qquad [5]$$

Although all of the assumptions are not exact, the agreement between predicted and observed rates of pressure rise was found to be good. Pressure-rise rates in the test chamber were measured with the test chamber filled with water so that the piston did not move. Smooth pressure traces were obtained. The average difference between observed and calculated rates was less than 10 per cent, which was about the limit of accuracy in estimating the rate of pressure rise from the oscillograph records. The range of pressure-rise rates measured in the test chamber to check the derived expression was from 10,000 to 700,000 psi per sec. Because of the success of the correlation in this range, extrapolation to lower (4000 psi per sec) and higher (1,000,000 psi per sec) rates should introduce no serious errors. Plots of rate of pressure rise vs. driving gas pressure, using helium and nitrogen as working media, for a series of orifices of different areas were prepared and used in subsequent data reduction.

If the pressure rise in the test chamber is rapid, the compression will be nearly adiabatic and a rapid temperature rise will result. There is no conclusive evidence that high pressures or high rates of pressure rise can by themselves initiate explosions, so that what probably is being tested is the sensitivity of propellant vapors to very rapid heating. It is probable that the maximum temperature reached during compression is the quantity of greatest importance in determining whether or not reaction occurs. For an ideal gas, temperature

reached in an adiabatic compression can be related to the energy going into the compression as

$$W = \frac{P_0V_0}{\gamma - 1}\left[1 - \left(\frac{P_f}{P_0}\right)^{\frac{\gamma-1}{\gamma}}\right] \quad [6]$$

Since the compression is adiabatic and the gas is ideal

$$\left(\frac{P_f}{P_0}\right)^{\frac{\gamma-1}{\gamma}} = \frac{T_f}{T_0} \quad [7]$$

and

$$P_0V_0 = n_gR_0T_0 \quad [8]$$

so that

$$W = \frac{P_0V_0}{\gamma - 1}\left(1 - \frac{T_f}{T_0}\right) = \frac{n_gR_0T_0}{\gamma - 1}\left(1 - \frac{T_f}{T_0}\right) \quad [9]$$

where W = work of compression (negative) or expansion (positive).

It can be seen that, in an ideal system, the maximum temperature reached in a compression will be determined by the initial temperature, the specific heat ratio and the quantity of gas being compressed. Therefore, it seemed reasonable to expect that, if a definite minimum temperature would be required for the initiation of a given fuel, the minimum energy input necessary to cause reaction in the rapid compression tester would be directly proportional to the initial gas phase volume of the sample, provided that the tester action actually approached adiabaticity.

The energy input to the test chamber can be evaluated as exactly as the $\int PdV$ expression can be evaluated for the material in the test chamber. This was not practicable with the available instrumentation, as can be seen from examination of Fig. 3. The same difficulties, in somewhat lesser degree, applied to the evaluation of $\int PdV$ on the driving side of the piston.

To estimate the energy input to the sample, it was proposed that gas expanding from the high pressure reservoir imparts kinetic energy to the piston, and the kinetic energy of the piston is expended compressing gas in the test chamber. The analysis given by Lamb (3) for the compression of a spherical bubble surrounded by liquid appears to be relevant.

The correctness of this picture depends on the fact that the opposing force of pressure in the test chamber is usually negligible until the piston has traveled over 90 per cent of the distance from its original position to the surface of the liquid sample, thus allowing the piston to acquire very nearly the velocity which it would attain if the sample chamber were open.

An expression for the piston velocity was developed in terms of the rate of pressure rise on the driving side of the piston and the distance traveled by the piston. The observed result, that rate of pressure rise in the driving chamber was constant throughout the first half of the pressure rise, was used in the expression, since this means that the rate of change of acceleration of the piston will be constant. Denoting this constant by $\dot{a}$

$$\dot{a} = \frac{da}{dt} = \frac{dP}{dt}\frac{A_p}{M_p} \quad [10]$$

where

a = instantaneous acceleration
dP/dt = rate of pressure rise on large end of piston
A_p = area of large end of piston
M_p = mass of piston

integrating

$$a = \int \dot{a}dt = \dot{a}t + a_0 \quad [11]$$

(neglecting gravity, $a_0 = 0$)

$$\text{velocity} = v = \int \dot{a}tdt = \frac{\dot{a}t^2}{z} + v_0 \quad [12]$$

(since initial velocity is zero, $v_0 = 0$)

$$\text{distance traveled} = X = \int \frac{\dot{a}t^2}{2}\,dt = \frac{\dot{a}t^3}{6} + X_0 \quad [13]$$

Combining Equations [10, 12 and 13] and inserting the necessary conversion factors and physical constants leads to the following expression for piston velocity

$$v = 14.9\left(\frac{dP}{dt}\right)^{1/3}X^{2/3} \quad [14]$$

where v is in in. per sec; dP/dt is in psi per sec, and X is in inches.

Actual piston velocities were estimated from measurements on oscillograph traces and were found to average about 0.66 of the predicted rates. Inserting the empirical correction factor gave

$$v = 10.0\left(\frac{dP}{dt}\right)^{1/3}X^{2/3} \quad [15]$$

Average deviation from the empirical equation over a range of measured velocities from 40 to 110 in. per sec was something less than 10 per cent. Although the correction is based on a relatively small number of tests because of difficulties encountered in obtaining consistently legible records, it is thought that the available results are sufficient to verify the prediction that the piston velocity should be proportional to the 1/3 power of the rate of rise of driving pressure and the 2/3 power of the distance traveled, and that any difference between calculated energy input and actual energy input is consistent, if not small.

A model for the reaction initiation and propagation in the compression tester process has been suggested. Temperature in the gas bubble is raised by compression; the heat generated tends to evaporate liquid from the bubble surface, which tends to lower the bubble temperature. Simultaneously, the decrease in bubble volume tends to condense vapor at the interface. From an examination of vapor pressure vs. temperature characteristics of several monopropellants, it appears that the net effect during this stage of the process will almost always be evaporation accompanied by a temperature rise, if most of the material in the gas phase is insoluble in liquid. This occurs when the gas consists of a mixture of fuel vapor and air. However, if the vapor pressure of the liquid were only a weak function of temperature, or if the gas were soluble in the liquid, the net effect could be condensation. Also, during compression, heat is being lost to the mass of the liquid sample and to parts of the equipment in contact with the bubble. If the compression is fast enough, these losses will be negligible.

When the temperature becomes high enough, fuel in the gas phase decomposes, generating heat. Some of this heat can be lost to the liquid sample and tester parts, and some can go into evaporating more liquid. If enough heat is generated in the bubble, the reaction will become self-sustaining.

The situation in the rapid compression tester is complicated by rapid oscillations in pressure, with corresponding oscillations in temperature. However, these are the conditions to which an entrained bubble in an actual propellant line would be subjected by the sudden closing of a valve, in either a pressurized system or a centrifugally-pumped system. Therefore, it appears that the sensitivity of a fuel as measured by the adiabatic compression tester should be a good indication of the sensitivity of the same material in use.

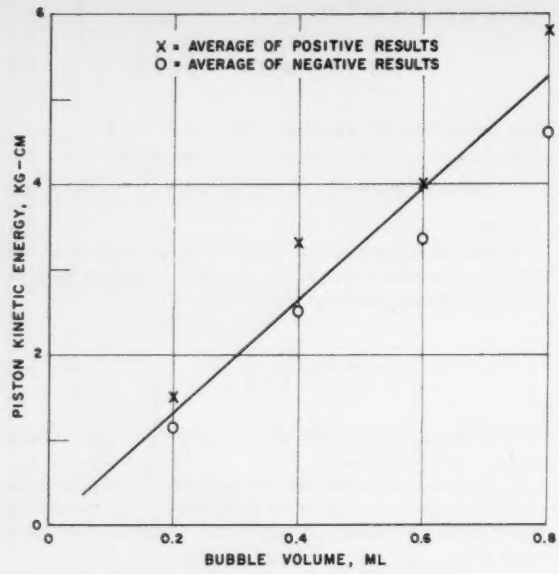

Fig. 4 Compression sensitivity of n-propyl nitrate

Test Procedure and Results

Because a prohibitive amount of time and effort would have been required to obtain oscillograph records of any large number of tests, the correlations discussed above were used to evaluate energy input to the fuel samples. For the reasons previously discussed, it was thought that the energy required to initiate liquid phase explosion in a given fuel would be directly proportional to the gas phase volume of the sample if the tester action actually approached adiabaticity, so two or more bubble volumes were tested for fuels which could be made to decompose. Only two types of results were considered: Positive, in which essentially complete decomposition of the sample occurred; and negative, in which the fuel sample remained apparently unaffected by the test. Undoubtedly, partial decompositions or vapor phase ignitions which did not propagate were obtained occasionally, but results of this type could not be identified with any certainty.

Because other characteristics of n-propyl nitrate have been well documented, it was thought that the results of intensive testing of this material would be of practical interest. The presence of air in the bubble, because of the high specific heat ratio and the possibility of ignition by oxidation, is thought to represent the most severe condition which might be encountered in practice.

Bubble volumes of 0.2, 0.4, 0.6 and 0.8 ml were investigated. A "reversal" technique was employed, starting in the approximate range determined by preliminary tests, increasing or decreasing driving pressure in uniform increments according to the type of result obtained first, until a reversal in result occurred. The direction of pressure change was then reversed, and the procedure continued until the desired number of tests had been completed. A total of 28 tests was made for each of the four bubble volumes. The results are shown in Fig. 4. The average of positive results (after starting a "reversal" series) is indicated by "X"; the average of negative results is indicated by "O" for each bubble volume. The accuracy of the slope is thought to be ±15 per cent. The numerical value is 6.7 kg-cm/ml. At 0.8 ml, positive results were occasionally obtained at energy inputs as low as 3.2 kg-cm, and negative results as high as 5.9 kg-cm, so it appears that in order to obtain a reliable value of the parameter, minimum ignition energy per unit bubble volume, it is necessary either to run several tests at one bubble volume, or a few tests at several bubble volumes.

Satisfactory records of explosions were obtained while testing n-propyl nitrate. Shown in Fig. 5 is a typical record of an explosion caused by an energy input of 6.2 kg-cm to a sample consisting of an 0.9 ml air bubble in contact with 0.55 ml of n-propyl nitrate liquid. It is in agreement with the average value of a fairly large number of tests, and there is a clear indication from the piston displacement trace that rapid reaction started during the first pressure surge, as can be seen by comparison with Fig. 6 which is a record of a test made on water under the same conditions. Fig. 7 shows the effect of an energy input of 4.0 kg-cm to a similar sample of n-propyl nitrate and air bubble, while Fig. 8 shows the result of a blank test on water with the same conditions. From the cusp in the pressure trace and the high rebound of the piston, it appears that reaction started, but quenched rapidly. Fig. 9 is the record of an explosion caused by an energy input of 3.2 kg-cm to another sample consisting of 0.55 ml of liquid n-propyl nitrate in contact with an 0.8 ml air bubble. The result appears unusual for several reasons. First, the explosion was caused by an energy considerably less than the average required for these conditions. Second, there is no evidence of initiation of reaction at the end of the downstroke of the piston. Why the explosion occurred is not known. It can only be repeated that the process of ignition is complex and, admittedly, not very well understood.

Nitromethane was tested in the presence of 0.2, 0.4 and 0.8 ml air bubbles. At the two smaller volumes, only enough tests were made to locate the first reversal in result. At the 0.8 ml bubble volume, a reversal series of 10 tests was made. The average obtained in this series was reasonably well in line with the results at the lower bubble volumes. Since in normal operation the direction of piston motion is straight down toward a stationary liquid surface, it was thought that a difference in results might be observed if the piston were driven upward, accelerating the liquid, and possibly agitating the liquid surface enough to form a large number of small bubbles. No significant difference was noticed. Results of the two types of test are shown in Fig. 10. The sensitivity of nitromethane in the presence of air measured by either type of test would be 10.4 ± 1.7 kg-cm/ml.

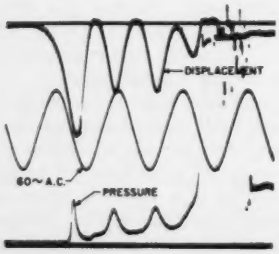

Fig. 5 Record of explosion

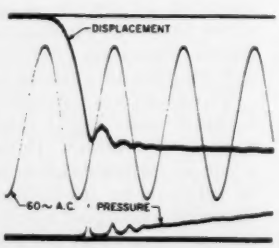

Fig. 6 Blank test record

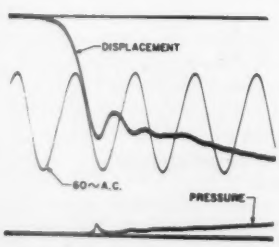

Fig. 7 Record of probable partial decomposition

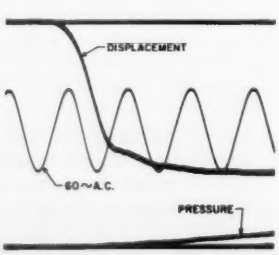

Fig. 8 Blank test record

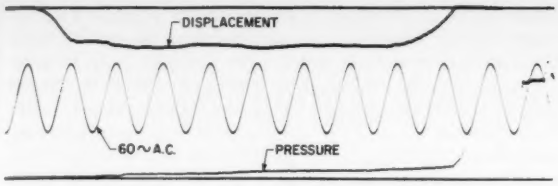

Fig. 9 Record of delayed explosion

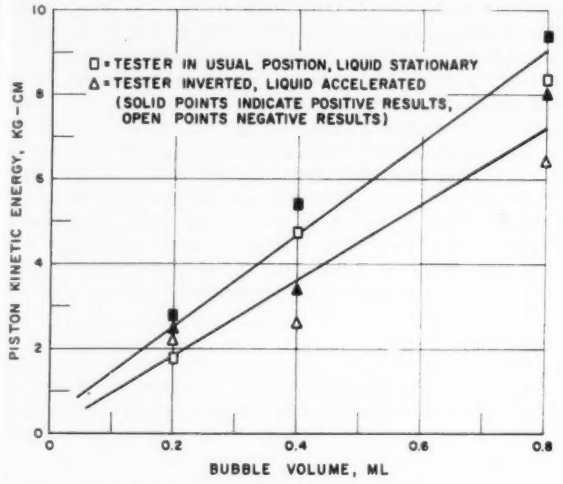

Fig. 10 Sensitivity of nitromethane

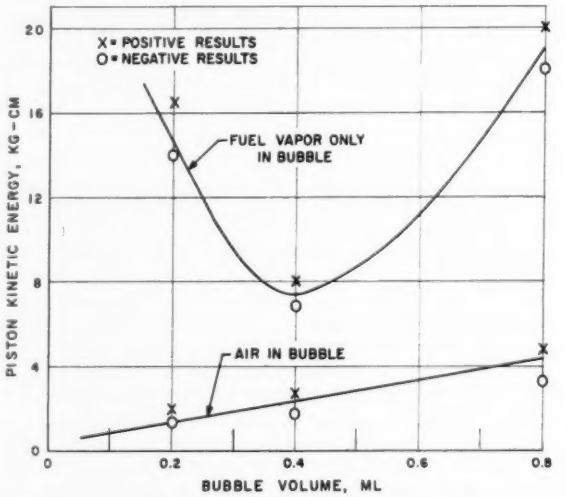

Fig. 11 Sensitivity of 60 per cent ethyl nitrate-40 per cent propyl nitrate

The results obtained for a mixture of 60 per cent ethyl nitrate and 40 per cent propyl nitrate in contact with air bubbles of various size are shown in Fig. 11. Also shown are results for the same material with fuel vapor bubbles of various size. This mixture was the most sensitive of any of the materials tested, and was also the only one which could be made to decompose in the absence of air in the vapor space.

The sensitivity of ethyl-propyl nitrate (and of the other fuels which could be ignited in the presence of air) is clearly much lower in the absence of air. Several explanations are possible for the decreased sensitivity. Among these are the absence of oxygen and the high specific heat of the fuel vapor relative to air. Also, vapor in the presence of a liquid can condense very rapidly. For example, the nitromethane vapor in a 1-ml bubble, in contact with a 1-cm² surface of liquid nitromethane at 20 C could condense in a time on the order of 10^{-4} sec. This would mean, in the compression tests with liquid in the presence of vapor only, that the fuel vapor is being condensed instead of being compressed. This condition, of course, would raise the temperature of the liquid surface, but the temperature rise would be very small compared to that produced in compressing a bubble of insoluble gas with the same amount of energy.

Methylacetylene was made to decompose at bubble volumes of 0.8 and 0.4 ml. For these tests, the liquid sample was loaded at about −40 C and fired at about −30 C. Cooling was effected by circulating trichloroethylene through the tester jacket and a coil immersed in a dry ice-trichloroethylene bath. Negative results were confirmed by the presence of unaffected liquid remaining when the chamber was opened while still cold. Decompositions were indicated by the presence of a compacted carbon pellet in the chamber, and also by pressure in the chamber. The results are shown in Fig. 12. Only enough tests were made to locate the first reversal in result. Since maximum energy input possible with this equipment is not a linear function of bubble volume, there is no special significance attached to the absence of any positive result at 0.2 ml. A test with an 0.8 ml bubble, in which the sample was sealed and allowed to warm to room temperature before firing, gave a negative result at maximum energy input. The vapor pressure of methylacetylene is about 90 psig at room temperature.

Hydrogen peroxide, hydrazine, unsymmetrical dimethyl hydrazine and ethylene oxide (tested both at −20 C and at room temperature) could not be made to decompose by test conditions of maximum severity, i.e., an energy input of 115 kg-cm to an 0.8 ml air bubble, or 144 kg-cm/ml. As far as is

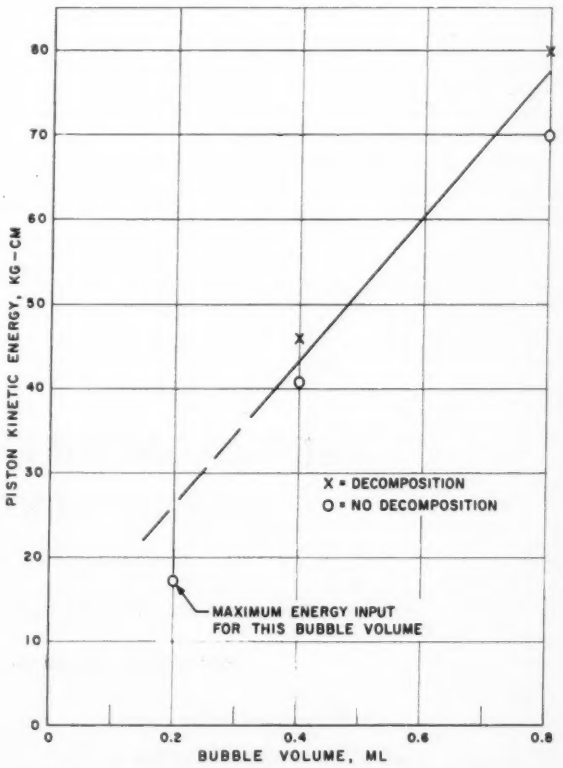

Fig. 12 Sensitivity of methylacetylene at −30 C

known, no accidental explosions which could be blamed on rapid compression have occurred in the handling or use of these materials.

Conclusions

The rapid compression test, in its present state of development, can be used to rate numerically the sensitivity of liquids to ignition in the presence of rapidly compressed air bubbles. The parameter on which the scale of rating is based is the minimum compressive energy per unit bubble volume necessary to cause gas phase ignition followed by propagation to the liquid. The sensitivity scale is thought to be valid and useful because of the simple relationship between the indicated sensitivities of different materials, i.e., if one material is shown to be five times as sensitive as another, it can be ignited by one-fifth as much compressive energy if other conditions are the same. Although the action of the tester is not simple, it appears to simulate closely conditions which might occur in actual propellant systems. For each of the four monopropellants which have been made to ignite or decompose in the presence of air bubbles, it has been found that the sensitivity parameter is constant over the range of bubble volumes (0.2 to 0.8 ml) tested, within the limits of accuracy of the test.

For the materials tested, the sensitivity ratings in the presence of air bubbles are as follows

Monofuel	Sensitivity, kg-cm/ml
60 per cent ethyl nitrate 40 per cent propyl nitrate	4.0 ± 0.8
n-propyl nitrate	6.7 ± 1.2
nitromethane	10.4 ± 1.7
methylacetylene	86 ± 12
hydrogen peroxide	>144
hydrazine	>144
unsymmetrical dimethyl hydrazine	>144
ethylene oxide	>144

All of the fuels which could be ignited in the presence of air bubbles were substantially less sensitive in the presence of fuel-vapor bubbles. It is believed therefore that the tests in the presence of air bubbles represent the most severe conditions which might be met in practice.

Because of the reasonable constancy of the sensitivity parameter over the range of bubble volumes tested, and because of the larger range of energy inputs possible with the larger bubble volumes, it is suggested that the sensitivity of experimental monofuels which were available only in small quantity could be evaluated by a series of tests at the largest bubble volume practicable. Almost certainly, because of the rapid increase of surface to volume ratio with decreasing bubble volume, resulting in increased rate of heat loss, there will be some minimum bubble volume below which the indicated sensitivity parameter will increase very rapidly with decreasing bubble volume. Although this "critical" bubble volume was apparently less than 0.2 ml for the monofuels which could be made to react in the tester, with the possible exception of the ethyl-propyl nitrate mixture in the presence of fuel-vapor bubbles, the possibility of testing experimental materials at bubble volumes below "critical" should be minimized. It is thought that a series of 20 tests, requiring 10 or 15 ml of material, would be ample to establish a reliable sensitivity rating.

There is an evident need for the definition by example of the potentially hazardous range of sensitivity by the selection of two standard fuels, one of which would mark the dangerous limit of sensitivity and one of which would mark the safe limit of sensitivity. Until such a range has been established, the usefulness of the test results will be restricted, and any need for extending the range of the tester will be uncertain.

Acknowledgment

The work described in this paper was performed in partial fulfillment of the requirements of Contract No. AF 33(616)-3433 sponsored by the Rocket Fuels Branch, Propulsion Laboratory, Wright Air Development Center. The cooperation of that group during the course of the investigation and in the release of this information is greatly appreciated. The original design and development of the tester was carried out by the Aerojet-General Corp. Air Reduction Co. personnel who have contributed to the success of this investigation include J. P. Helck, W. B. Moen and D. J. Craig. Especial credit is due to R. A. Miller, who performed most of the recent experimental work.

References

1. Wilson, E. M., "The Stability of Ethylene Oxide," JOURNAL OF THE AMERICAN ROCKET SOCIETY, vol. 23, no. 6, Nov. –Dec. 1953, pp. 368–369.
2. Sutton, G. P., "Rocket Propulsion Elements," John Wiley & Sons, Inc., New York, 2nd ed., 1956, p. 61.
3. Lamb, Sir Horace, "Hydrodynamics," Dover Publications, New York, 6th ed., 1945, p. 122.

Isothermal Compressibility of Liquid Oxygen and RP-1

GEORGE T. Y. CHAO[1]

Dresser Dynamics, Inc.
Northridge, Calif.

The methods for computing the isothermal compressibility for RP-1 and liquid oxygen are presented. Liquid oxygen is a single substance, and RP-1 is a complex petroleum mixture, hence different methods of approach were used in each case. The accuracy of the calculated result is on the order of the experimentally derived result.

THE LIQUID propellant engine system generally consists of one or more tanks to store the propellants, a feed mechanism for forcing the liquids into the thrust chamber, a power source for furnishing the energy required by the feed mechanism and a control device for regulating the propellant flow rates. In order to arrive at a satisfactory feed mechanism design, correct power supply and accurate mass flow rate, it is necessary to know the density of propellants under actual operating conditions. One of the present trends of combustion chamber design in the development of high thrust rocket engines is to increase the chamber pressure. Therefore, the study of compressibility of liquid propellants is one of growing importance.

In general, the compressibility of liquid is small, a few hundred-thousandths of the initial volume (1×10^{-5}) per atm. The difference in volume between that at 1 atm pressure and that under 1000 psi pressure is rather small, generally smaller than the accuracy with which a flowmeter can measure today. Since most rocket engines are now operated at a pressure of less than 1000 psia, it is doubtful that the pressure exerted on the propellants has any influence on the measurement of the specific impulse of the thrust chamber. However, the compressibility of the liquid propellants may have its effects on combustion. Kretschmar (7)[2] has shown that the compressibility of propellants may be related to the pressure transients in the injector system, which, in turn, may couple with natural frequencies of the combustion chamber in such a way that instability and rough combustion result. Since one of the most commonly used propellant combinations consists of liquid oxygen and RP-1, a knowledge of their isothermal compressibilities would be of interest to engine development work. This paper attempts to make a thorough evaluation of the quantitative relation of densities for these propellants under pressurized conditions, and to arrive at a method by which their compressibilities can be determined.

Isothermal Compressibility of Liquid Oxygen

Partington (10) made a comprehensive review of the literature on the compressibility of liquids; no simple and decisive rule could be found to generalize the calculation of compressibility for liquids, even for a pure substance.

There are two types of compressibility for liquids, isothermal and adiabatic, as defined by the following equations

$$K_i = \frac{1}{v}\left(\frac{\partial v}{\partial p}\right)_t \qquad [1]$$

$$K_a = \frac{1}{v}\left(\frac{\partial v}{\partial p}\right)_s \qquad [2]$$

where

K_i = isothermal compressibility
K_a = adiabatic compressibility
s = entropy
p = pressure
v = volume

There are more adiabatic than isothermal compressibility data in the literature. In cases where isothermal compressibilities are needed, some method to convert adiabatic compressibility into isothermal compressibility must be developed. Such conversion may sometimes be difficult or even impossible without sacrificing accuracy.

As shown by thermodynamics

$$\gamma = \frac{C_p}{C_v} = \frac{K_i}{K_a} \qquad [3]$$

$$C_p - C_v = \frac{Tv\alpha^2}{K_i} \qquad [4]$$

From Equations [3 and 4]

$$K_i - K_a = \frac{Tv\alpha^2}{C_p} \qquad [5]$$

where

α = coefficient of liquid volume expansion
C_p = molar heat capacity at constant pressure
C_v = molar heat capacity at constant volume
v = molar volume
T = absolute temperature
γ = ratio of C_p/C_v

Direct application of the above relations to compute K_i from K_a is rather difficult. γ cannot be calculated from C_p and C_v, because C_v of the liquid is almost impossible to measure, and, in turn, is calculated from known values of C_p with Equation [4].

In general, α for many liquids is known for different temperatures at 1 atm pressure. However, since α is a function of both temperature and pressure, values of α at constant temperature will vary with pressure. For example, at zero deg C, α for mercury is 181×10^{-6} at zero pressure, while α is 152×10^{-6} at 7000 kg/cm^2. The difference due to pressure is around 20 per cent. In addition, C_p and v are also functions of both temperature and pressure. For the above mentioned reasons, it is rather difficult to compute K_i and K_a without some approximation, unless the whole set of data on α, C_p and v is known.

Received April 28, 1958.
[1] Head, Chemical Kinetics Section. Member ARS.
[2] Numbers in parentheses indicate References at end of paper.

Table 1 Calculation of K_i for liquid oxygen

Temperature, K	Temperature, F	ρ, gm/cm³	v, cm³/gm	α or $\frac{1}{v}\left(\frac{\partial v}{\partial T}\right)_p$, K × 10^{-3}	α^2, $K^{-2} \times 10^{-6}$	$T\alpha^2$, $K^{-1} \times 10^{-3}$	C_p, cal/gm/K	$C_p\rho$, cal/cm³/K	$T\alpha^2/C_p$, cm³/cal × 10^{-3}	K_i, in.²/lb × 10^{-6}
90	−297.7	1.142	0.8757	4.21	1.772	1.595	0.4059	0.4635	3.441	12.9
85	−306.7	1.167	0.8569	4.15	1.722	1.464	0.4039	0.4714	3.106	11.6
80	−315.7	1.191	0.8396	4.03	1.624	1.299	0.4019	0.4787	2.714	10 4
75	−324.7	1.215	0.8230	3.94	1.552	1.164	0.4008	0.4870	2.390	9.30
70	−333.7	1.239	0.8071	3.82	1.459	1.021	0.3989	0.4942	2.065	8.27
65	−342.7	1.263	0.7918	3.65	1.332	0.8658	0.3972	0.5017	1.726	7.23
60.5	−350.9	1.282	0.7800	3.46	1.197	0.7242	0.3972	0.5092	1.422	6.30

In the case of liquid oxygen, only two point data (8, 12) of α can be found from the literature. Because these two values come from two different sources and only one value lies in the temperature range of interest, neither is adopted in this computation. α values in the whole temperature range and 1 atm pressure can be derived from the density data of Baley (1). The specific volume of the liquid oxygen is plotted vs. temperature on large-scale coordinate paper. Tangent lines are then drawn at various temperatures. In order to avoid errors in drawing these tangent lines, the slopes of the tangents are plotted vs. temperatures to smooth out the differences in drawing tangents. These smoother slopes $(\partial v/\partial t)_p$ at one temperature multiplied by the density of that particular temperature will give the value of α at that temperature. α values derived this way, in addition to the density data from Baley (1) and heat capacity at constant pressure data from Giauque (3) are the only known data which can be utilized for calculating K_i by Equation [5]. All these values are given at 1 atm.

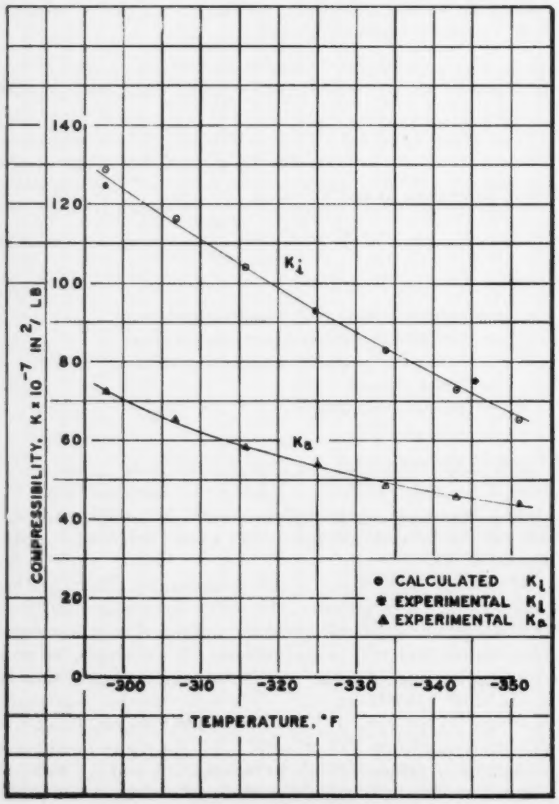

Fig. 1 Compressibility of liquid oxygen

In order to use these data at 1 atm for computation at all pressures, some assumptions must be made. These in turn must be proved sound, and the results of calculations based on these assumptions must be checked with two known experimental values of isothermal compressibility of liquid oxygen.

The logical approach to this problem is to assume $(v\alpha^2/C_p)$ to be a constant at a definite temperature disregarding the change of pressures. The accuracy of this assumption can be proved in the following way: Since the compressibility of liquid oxygen is in the range of 1×10^{-6}, the fluctuation of v due to change in pressure is rather small, less than 1 per cent from that at 1 atm, even at 1000 psia. As to the change of α due to change of pressure, the information can be estimated from Hougen and Watson's chart "Thermal Expansion and Compression of Liquids" (4). In the temperature range of −297.7 to −350.9 F (90 to 60 K), the range of reduced temperature T_r is from 0.396 to 0.583. At $T_r = 0.396$, the ω value[3] read from the chart is 0.1420 at 1460 psia and 0.1415 at zero pressure. The ratio of these two numbers is around 1.0035. Even at the high temperature limit of the range, the corresponding values of ω at 1460 and 0 psia are 0.1270 and 0.1258. This ratio is 1.0095. The "Heat Capacity" chart of (4) also shows that the difference between C_p at 1462 psia and C_p at zero psia is around one-fifth of 1 per cent, in the temperature range of interest. Based on this information, one may be sure that the ratio $\alpha^2/\rho C_p$ is a constant with a maximum error of less than 1 per cent on pressure change. The soundness of the above assumption can be further proved by comparing two calculated values with two experimental values

Temperature, F	Experimental K_i, in.²/lb	Calculated K_i, in.²/lb
−299.7	1.25×10^{-5}	1.29×10^{-5}
−345.5	0.75×10^{-5}	0.72×10^{-5}

Based on the above assumption, results calculated are listed in Table 1 and plotted in Fig. 1. For convenience of engineers in the field, a chart has been made which shows the precise density of liquid oxygen at various pressures with temperature and density as coordinates.

Isothermal Compressibility for RP-1

RP-1 is a special kind of kerosene used in rocket engines; its characteristics are regulated by military specification MIL-F-25576A(USAF), April 8, 1957. In the literature, there is some information about the compressibility of kerosene (13) in general and about the jet fuels (7) in particular. However, such data can only provide the range of compressi-

[3] ω = expansion factor of liquid at P_r and T_r.

bility for RP-1, not the data which can be used for calculating the density of particular samples. Because RP-1 is a mixture not a pure substance, and the military specification gives limited information about RP-1, it is difficult to obtain the data which can be used for estimation even when supported with experiments on a limited number of samples. In such a case, the only way to obtain the necessary data is correlation.

There are three generalized correlation methods in the literature which can possibly be applied here. The "Thermal Expansion and Compressibility of Liquids" chart of (4) probably is the most widely known. It covers a wide range of pressures and temperatures, and can be utilized for estimation up to critical temperatures of a liquid and up to a pressure five times the critical pressure of a liquid. This chart can also be easily used for interpolation. On the other hand, it has many defects. First, it is drawn from a reduced temperature of 1.0 to 0.6 which then has been extrapolated down to 0.4. Information for liquid at temperatures lower than reduced temperature 0.4 cannot be found from the chart. Secondly, the use of the chart requires knowledge of the critical temperature and pressure of the liquid under investigation. However, critical properties are not always known and are generally inaccurate for mixtures. This chart inherits the defects of all generalized charts, namely, inaccuracy. It is good for general estimating and engineering purposes, but not for precision work.

Jessup's correlation (6) of compressibility and thermal expansion of petroleum published in 1930 is probably the best source of information which can be applied here. This method resulted from tests of 14 representative samples of petroleum oils from various sources over the pressure range of 0 to 50 kg/cm² (gage) and the temperature range of 0 to 300 C.

Jessup found from the result obtained on these samples that the compressibility and thermal expansion of two samples of the same specific gravity, but from different sources, differed by more than 30 per cent at high temperatures; whereas oils of the same specific gravity and the same viscosity had the same compressibility and thermal expansion within rather narrow limits.

The parameter used for Jessup's correlation is the volume modulus

$$1/(d\sqrt{\log 1000\, s})$$

where

d = the specific gravity of oils at 60 F
s = the kinematic viscosity at 100 F

As he claimed, the maximum deviations of an observed point from the compressibility curve vs. the independent variable is around 0.1 per cent in volume at 50 kg/cm². After comparing his correlation with the experimental results of Zeitfuchs (14) and Bearce and Peffer (2), he found that the agreement between his correlation and experiment was good.

Jessup's method was studied by Thiele and Kay (11). They reviewed the literature published before 1933 containing data on the expansion of liquid petroleum products at low temperature. They thought these experimental data adequate for application in ordinary engineering estimating purposes. However, these data cannot be considered sufficiently accurate in precision work. Jessup's method was more suitable for extrapolation and interpolation, since it made the volume modulus relation at a given temperature a straight line. However, extrapolation to high values of modulus was not found satisfactory, even at 302 F, since there is considerable curvature at high modulus. At 167 F, the curves are straight for wide ranges of values, and provide a reasonable means for extrapolation.

Thiele and Kay attempted to use the law of corresponding states to extend Jessup's data to high temperatures. They presented a final drawing to show the density as a fraction of the density at 60 F and 1 atm, for gage pressures of 0, 400 and 800 lb per in.², and for values of square of Jessup's modulus up to 2.4. Thiele and Kay also presented an alignment chart from which Jessup's modulus can be quickly found.

In 1946, Jacobson, Ambrosius, Dashiell and Crawford (5) presented a new method of correlation for compressibility of liquid hydrocarbons. The method used by Jacobson et al. is to plot API[4] vs. compressibility with temperature parameters. However, this method can be criticized. API is similar to density which, as shown by Jessup long ago, is not the only determined function of compressibility. Furthermore, the chart presented by Jacobson et al. is far from perfect. The only complete set of data used to determine the characteristics of the curve is at one temperature, 100 F. The other two basic curves at 80 and 30 F used to determine the space of temperature curves were based on calculated, not experimental, values. The reliability of such calculated values is doubtful. Despite the fact that Jacobson's original chart is plotted on a contracted API scale, the points are still scattered around the curves. For this reason, the method of Jacobson et al. cannot be considered to give accuracy.

Based on the above statement and discussion, the author concluded that the only method which can be adopted for estimating the density of RP-1 accurately is Jessup's method and its modified version by Thiele and Kay.

According to the military specification MIL-F-25576A (USAF), the density range of RP-1 is 0.801 to 0.815(60/60). The density range of RP-1 at other temperatures can be estimated by Hougen and Watson's "Thermal Expansion and Compression of Liquids" chart. Because here only the range of density is required, and not the density of the particular sample, the accuracy of the chart is adequate. The maximum and minimum densities at 100 F estimated by this method are 0.800 and 0.785, respectively.

The specification only gives the maximum viscosity of RP-1 at −30 F as 13.9 centipoise. The maximum viscosity at other temperatures can be estimated with decane as a reference material by using the equation, $\log \mu = a \log P + b$ (9). μ is viscosity, P the vapor pressure, and a and b are constants. The maximum viscosity of RP-1 at 100 F estimated by this method is around 2.5 centipoise. Since the specification does not give the minimum viscosity, it can only be estimated from experience in handling RP-1 samples. Experience shows that for 100 F, a good guess for the minimum viscosity is 1.0 centipoise. From the maximum and minimum viscosity and density values of RP-1 at 100 F, the maximum and minimum kinematic viscosities of RP-1 at 100 F were calculated to be 3.185 and 1.250 centistokes. From the value of kinematic viscosity at 100 F and specific gravity at 60 F, the maximum and minimum "volume modulus" of Jessup were calculated to be 0.709 and 0.655.

The narrow range of "volume modulus" of RP-1 further simplifies the application of Jessup's method to RP-1. The above mentioned method fails at high temperatures when the compressibility-volume modulus straight line is extended to high volume modulus. However, this is not the case for RP-1 within the narrow limit of volume modulus between 0.655 and 0.709. The straight line relation can be sure to hold even at high temperatures for RP-1. In this case, Thiele and Kay's modifications do not apply.

The only chance for heating RP-1 in the rocket engine before it is atomized from the injector is in the passages of the regenerative cooling system of the thrust chamber. Because of the short period of passage through the cooling jacket, the final temperature coming to the injector is never too high. This is generally below 572 F, the highest temperature which Jessup's experiment covered. The highest pressure used in his experiment covers the pressure limit in the present-day rocket engine. The lower temperature limit of his data is zero deg C. In order to take care of the cooling of RP-1 by liquid oxygen in certain rocket system arrangements, the lower temperature of his data is extended to −40 F.

[4] Abbreviation of American Petroleum Institute gravity, related to specific gravity by deg API= [(141.5)/(spec. gr. at 60/60)]-131.5.

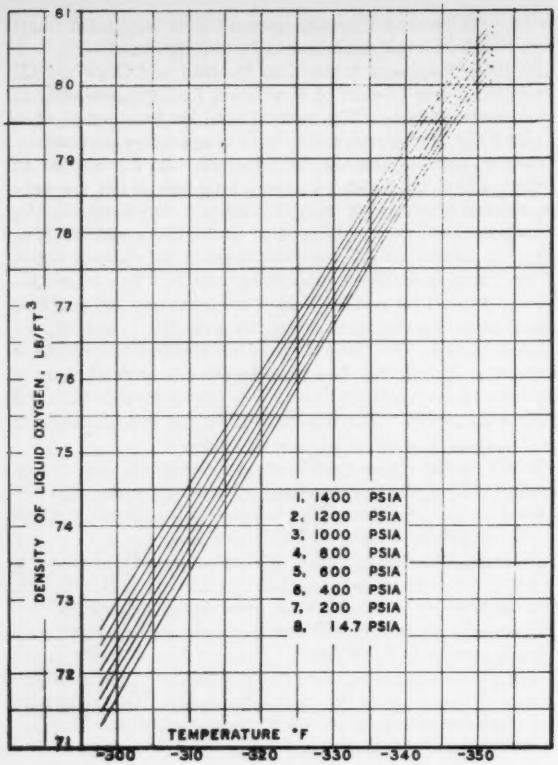

Fig. 2 Density of liquid oxygen under pressure

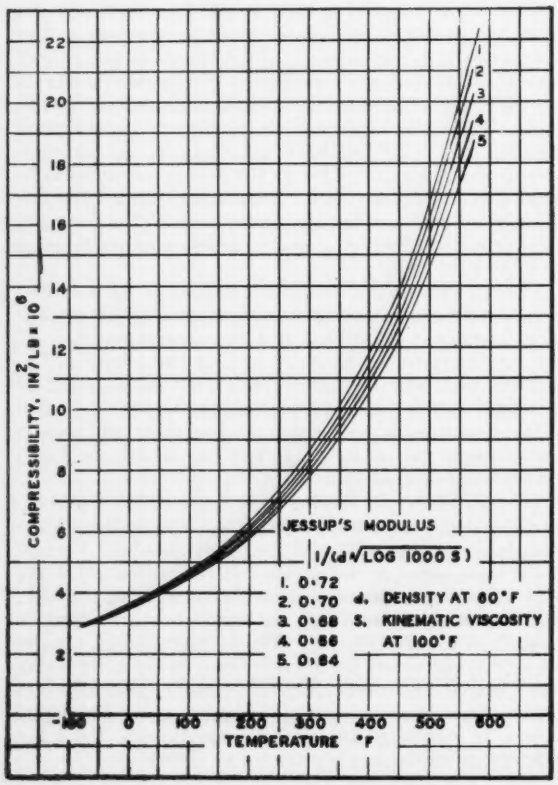

Fig. 3 Isothermal compressibility of RP-1

Table 2 Average compressibility of RP-1 at various temperatures under pressures up to 500 kg/cm²

Volume modulus	Compressibility × 10⁶, in.²/lb, temperatures, F					
	32	86	167	302	437	572
0.64	3.78	4.29	5.27	7.80	11.80	18.60
0.66	3.82	4.34	5.38	8.02	12.15	19.45
0.68	3.86	4.41	5.48	8.25	12.55	20.21
0 70	3.89	4.46	5.60	8.46	12.95	21.00
0.72	3.92	4.54	5.71	8.69	13.35	21.80

From Jessup's experimental data, mean compressibility vs. volume modulus at various temperatures can be plotted. The mean compressibility in the range of volume modulus between 0.64 and 0.72 is found for every 0.02 unit of volume modulus. For engineering application, the units of compressibility are converted into in.²/lb from cm²/kg, and temperature units are converted into deg F from deg C. The result is summarized in Table 2.

The data in Table 2 are plotted in Fig. 3. Fig. 3 can further simplify the use of Jessup's method for test stand application. At temperatures below 100 F the difference in compressibilities within the limit range of volume modulus is within the accuracy of his experiment. Therefore, it is accurate enough to take the average compressibility within the limit range of volume modulus at one temperature to represent the compressibility of all samples of RP-1 at that particular temperature. Fig. 4 is a chart by which the volume correction for specific volume of RP-1 based on the specific gravity measurement at the measuring temperature at 1 atm can be found. It is the author's opinion that any chart presented in this paper is limited only to correction, not the final density or specific volume. Because the correction is rather small compared with the specific gravity or specific volume itself, the wide range of specific gravity variation of RP-1 itself and its variation at various temperatures prevents the accurate readings of the specific gravity directly from a chart of reasonable size. However, the specific gravity of RP-1 under pressure can be easily calculated by the equation

$$S_{t,p} = \frac{1}{1/S_{t,r} - v_c \times T_c \times P} \qquad [6]$$

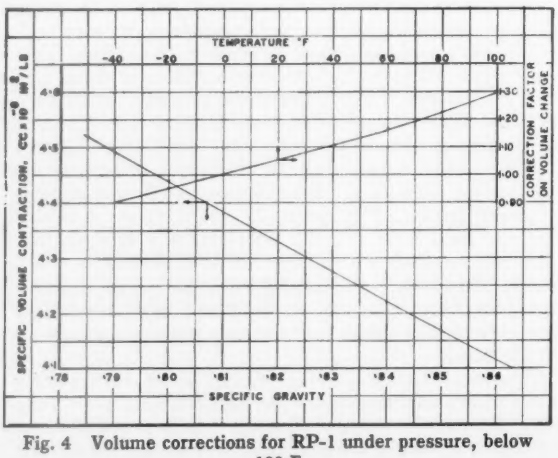

Fig. 4 Volume corrections for RP-1 under pressure, below 100 F

where

$S_{t,p}$ = sp. gr. of RP-1 at temperature t F and pressure p lb/in.²
$S_{t,1}$ = sp. gr. of RP-1 at temperature t F and 1 atm
v_c = volume correction from Fig. 4. in cm³ × 10^{-6} in.²/lb
T_c = temperature correction from Fig. 4 at the measuring temperature
p = pressure of RP-1 in lb/in.²

The calculation can be faster with the help of a table of reciprocals of numbers, and the product $v_c \times T_c \times p$ can be calculated with a slide rule without affecting the accuracy of the final result.

At a temperature higher than 100 F, the simplified method above cannot be used without sacrificing a certain amount of accuracy, because of the increasing effect of Jessup's modulus on compressibility with increasing temperature. For example, at 100 F, the compressibility change within the range of Jessup's modulus is from 4.42 to 4.70 × 10^{-6} in.²/lb, while at 550 F, the compressibility change within the same range of Jessup's modulus is 17.3 to 20.0 × 10^{-6} in.²/lb. However, the utilization of the compressibility of RP-1 at high temperature is not for daily routine work at the test stand, but rather for application in designing when one has more time to calculate for the purpose of accuracy. The following equation can be used in this case to calculate the actual specific gravity after the compressibility has been found from Fig. 3

$$S_{t,p} = \frac{1}{1/S_{t,1}(1 - C \times p)} \qquad [7]$$

where C is the compressibility in in.²/lb × 10^{-6} from Fig. 3 at measuring temperature t of RP-1 with its characteristic "volume modulus." Density of RP-1 at 60 F and kinematic viscosity at 100 F are the additional data required for the calculation of the density of RP-1 at measuring temperature t under pressure p.

Conclusions

Liquid oxygen is a single substance, while RP-1 is a complex petroleum mixture. This paper presents methods to calculate the isothermal compressibility in both cases. The same technique presented in this paper can be applied to investigate the isothermal compressibility for other propellants. The present approach serves to reduce the amount of experimental work through the use of data from published literature. However, such published data should be subjected to analysis in order to insure that the accuracy of the calculated result is comparable to that derived from experiments.

References

1 Baley, E. C. C. and Donnan, F. G., "The Variation with Temperature of the Surface Energies and Densities of Liquid Oxygen, Nitrogen, Argon and Carbon Monoxide," *J. Chem. Soc.*, London, vol. 81, 1902, pp. 907–923.

2 Bearce, H. W. and Peffer, E. L., "Density and Thermal Expansion of American Petroleum Oils," Nat. Bur. Standards, Tech. Paper 77, 1916.

3 Giauque, W. F. and Johnston, H. L., "The Heat Capacity of Oxygen from 12 K to Its Boiling Point and Its Heat of Vaporization," *J. Amer. Chem. Soc.*, vol. 51, 1929, pp. 2300–2321.

4 Hougen, O. A. and Watson, K. M. "Chemical Process Principle Charts," John Wiley & Sons, Inc., New York, 1951.

5 Jacobson, E. W., Ambrosius, E. E. Dashiell, J. W. and Crawford, C. L., "Compressibility of Liquid Hydrocarbons," *Oil and Gas J.*, vol. 44, no. 3, 1946, pp. 109–110.

6 Jessup, R. S., "Compressibility and Thermal Expansion of Petroleum Oils in the Range 0 to 300 C," *Bur. Standards, J. Res.*, vol. 5, 1930, p. 985–1039.

7 Kretschmar, G. G., "The Isothermal Compressibilities of Some Rocket Propellant Liquids and the Ratios of the Two Specific Heats," JET PROPULSION, vol. 24, 1954, pp. 175–179.

8 Mellor, J. W., "A Comprehensive Treatise on Inorganic and Theoretical Chemistry," vol. 1, Longmans, Green and Co., Ltd., London, p. 365.

9 Othmer, D F. and Cornwell, J. W., "Correlating Viscosity and Vapor Pressure of Liquids," *Ind. and Engng. Chem.*, vol. 37, 1945, pp. 1112–1115.

10 Partington, J. R., "An Advanced Treatise on Physical Chemistry. Vol. II, The Property of Liquids," Longmans, Green and Co., Ltd., London, 1955, 2nd ed.

11 Thiele, E. W. and Kay, W. B., "Densities of Hydrocarbon Mixtures," *Ind. and Engng. Chem.*, vol. 25, 1933, pp. 894–898.

12 Washburn, E. W. (ed.), "International Critical Tables of Numerical Data, Physics, Chemistry and Technology," vol. 1, McGraw-Hill Book Co., Inc., New York, p. 102.

13 *Ibid.*, vol. II, p. 146.

14 Zeitfuchs, E. H., "Thermal Expansion of California Petroleum Oil," *Ind. and Engng. Chem.*, vol. 17, 1925, pp. 1280–1282.

An Attitude Control System for Space Vehicles

WALTER HAEUSSERMANN[1]

Army Ballistic Missile Agency
Huntsville, Ala.

An attitude control system, applicable to any size space vehicle, is proposed which uses expulsion charges to compensate for initial disturbances. Final fine control is exerted by a low power flywheel reaction-type servo system which makes use of a specially designed d-c servo motor with an impedance-type commutator and transistor control. The d-c servo motor is able to work in vacuum. It is shown how the control system can be stabilized without direct derivatives of the attitude information; therefore, the system also supports stabilization when manually controlled. Some possibilities are mentioned to derive attitude information for space and Earth fixed reference systems.

THE ATTITUDE control system for a space vehicle must be designed to meet requirements (1,2)[2] which differ so much from those of the control system for the booster stages that independent control systems will be preferable for both applications.

Presented at the ARS Semi-Annual Meeting, Los Angeles, Calif., June 9–12, 1958.

[1] Director Guidance and Control Laboratory, Development Operations Division. Member ARS.

[2] Numbers in parentheses indicate References at end of paper.

Some of the major requirements for a three-axis attitude control system for a space vehicle are:

Required features:

1 Ability to compensate for the relatively high initial angular impulse resulting from the last separation process.

2 Automatic control as well as assistance to manual reorientation.

3 Continuous operational duty must be possible.

4 Control system must have a lifetime at least equal to

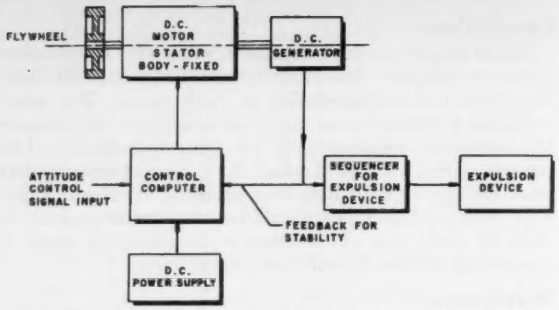

Fig. 1 Functional diagram of a one-axis control system

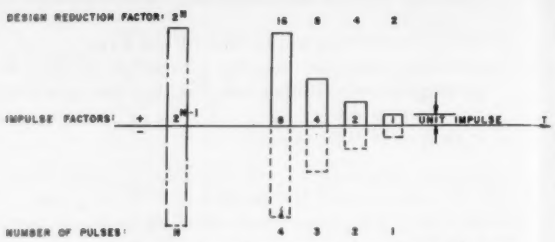

Fig. 2 Magnitude and sequence of expulsion charges

the lifetime of the space vehicle as determined by its main missions.

5 Necessary power should be as small as possible and be drawn on small satellites from solar cells delivering d-c, on larger vehicles from nuclear power supplies or solar cells.

Desirable features:

1 Control system should be able to work in vacuum.

2 The principles of control should be applicable to small and large space vehicles.

3 The system should be able to withstand accelerations during ascent of at least 6 g for manned satellites, and high accelerations during ascent as occurring on instrumented satellites.

Proposed Attitude Control System

Several methods of exerting control torques are possible. One which appears most attractive has been selected in the following description. It uses the inertial reaction torque principle.

For the attitude control of each of the three mutually perpendicular axes, a separate control system is proposed, since such a solution gives minimum cross coupling effects between the three individual torque producing systems.

The principle of the scheme of such a one-axis control system is shown in the functional diagram Fig. 1.

The attitude control signal as derived from a sun sensor, an infrared horizon sensor, a supervised gyro, or from a manual control, is amplified in a control computer and accelerates a d-c motor with a flywheel. The stability of this system can be improved if either the first derivative of the input attitude signal or the flywheel velocity is fed back.

The requirement to overcome the initial unpredictable angular impulse, caused by separation from the booster, can only be met by the described angular reaction system if the integrated reaction torque or the corresponding flywheel rpm change is tolerable. In order to avoid unfavorable design limitations and large constant friction losses of the system, it is proposed that the initial angular impulse be almost completely compensated by an expulsion or thrust device which is controlled by the flywheel speed. By proper staggering of the magnitude of the angular impulses and by selection of the number of steps, a considerable reduction in the torque requirements, and therefore in the overall flywheel system parameters, can be gained. The lower limit for the design parameters is finally given by factors, such as the minimum desired loop frequency, system sensitivity, transient disturbances due to moving parts or bodies in the space vehicle, etc.

The proposed expulsion scheme has been selected to achieve simplicity for the sequencer and for the control of the expulsion charges. The magnitudes, or "impulse factors," of the impulses are given in Fig. 2 with the time sequence in which they must be fired. Two sets of N expulsion charges are provided for plus and minus angular impulse directions. Regardless of the magnitude of the initial disturbance which must be reduced, N pulses will always be fired in the sequence shown on the time scale of Fig. 2. The magnitude of each individual charge is twice the magnitude of the following charge, and its sign will be determined by the direction of the flywheel rotation.

Thus the indicated impulse factors are multiples of the last charge impulse, which may be called "unit impulse." This unit impulse must be small enough to diminish the angular momentum of the space vehicle to a remaining value which can be transferred to the flywheel. Therefore, the maximum angular impulse, which finally must be compensated by an average speed of the flywheel, is equal to the unit impulse.

The design reduction factor, which may be defined as the ratio of maximum angular impulse of the space vehicle to the impulse which can be compensated by the flywheel alone, is also indicated in Fig. 2. It is equal to the ratio of maximum allowable initial angular impulse to the unit impulse.

It can be expected that the resulting flywheel speed will be reduced after some time due to eddy current damping of the flywheel if the space vehicle travels through magnetic fields. This effect should be considered in the design and layout of the flywheel system.

The flywheel-motor arrangement shown in Fig. 1 demands special design features to fulfill the necessary and desirable requirements; in particular, the d-c motor and the d-c generator must be designed in such a way that they will work without mechanical commutators. In order to explain the proposed modifications, the motor design will be discussed first. It is obvious that a d-c motor can have its armature winding in the stationary part and its field excitation in the rotor, if the armature current is conducted through sliprings to rotating brushes which transfer the current to the stationary commutator, which is connected to the stationary armature winding. A brushless solution is obtained by replacing the "slipring-rotating-brushes-stationary-commutator" system with an "impedance-commutator-transistor switch" system in which the impedance commutator controls the transistor-switching due to its air gap variations, which are a function of the stator to rotor positioning. An oscillator is necessary to excite the impedance commutator; however, this control circuit requires practically no power because it only controls the operation of the transistors which perform the high power transfer to the stationary armature.

Fig. 3a shows a cross section of the impedance-commutator-motor assembly; the motor uses permanent magnets for field excitation in order to avoid sliprings, excitation power and heat dissipation problems. Fig. 3b indicates the air gap variation of the impedance commutator developed along its circumference.

Fig. 4 gives the schematic diagram for a one-axis control system. The proposed impedance commutator is, in principle, a generator with an amplitude modulated output. The demodulated output voltage gives the three-phase signal for

the control gate of the armature motor current. The armature carries the motor winding and a generator winding in the same slots. The a-c voltage, which is induced in the generator winding, is proportional to the speed of the flywheel. The rectification of this voltage is controlled by the demodulated output of the impedance commutator which also controls the commutation of the motor current. The rectified voltage of the generator winding provides the velocity feedback signal used for damping and also furnishes information to trigger the sequencer for the expulsion device through a controlled gate.

The derivation in the next paragraph shows that the system is stable due to the effect of the induced emf of the motor. Therefore, in the case of some calculated examples with suitable numerical system data, no velocity feedback signal had to be applied to stabilize the control system.

Control System Characteristics

The following derivations are based on the assumption of an idealized control system, the components of which do not have any time lag, friction, saturation or other nonlinearities. Furthermore, coupling terms of the three mutually perpendicular control axes are considered to be negligible. The equation of torques about the axis to be controlled gives

$$I_1\ddot{\phi} + I_2\ddot{\alpha} = 0 \qquad [1]$$

where

I_1 = moment of inertia to be controlled
I_2 = moment of inertia of rotor (including flywheel, etc.)
ϕ = angular displacement of space vehicle, input signal[3]
α = angular displacement of rotor[3]
Dots written above variables denote time derivatives

The equilibrium of voltages in the armature circuit of the d-c servo motor gives

$$f(\phi, \alpha) + e(\dot{\phi} - \dot{\alpha}) + kI_1\ddot{\phi} = 0 \qquad [2]$$

where

$f(\phi, \alpha)$ = control voltage applied to the armature of the servo motor
$= a_0\phi + a_1(\dot{\phi} - \dot{\alpha})$ according to Fig. 4 [3]
$e(\dot{\phi} - \dot{\alpha})$ = emf of servo motor
$kI_1\ddot{\phi}$ = ohmic voltage drop in armature circuit due to control current proportional to its corresponding torque $I_1\ddot{\phi}$

The characteristic equation of the system of Equations [1, 2 and 3] is

$$s^2 + \frac{a_1 + e}{k}\left(\frac{1}{I_1} + \frac{1}{I_2}\right)s + \frac{a_0}{kI_1} = 0 \qquad [4]$$

In order to describe the system completely, it should be mentioned that the characteristic equation actually contains a factor of s^2, which has been canceled out on Equation [4]. The two poles at $s = 0$ allow for two initial conditions with respect to α and $\dot{\alpha}$. The initial displacement α of the flywheel is of no concern, whereas the initial value of the flywheel speed $\dot{\alpha}$ is zero in order to have symmetrical starting conditions for the operating range of the control system. Thus, the stability of the flywheel control system is sufficiently described by Equation [4].

Equation [4] indicates that the system behaves like a damped pendulum with the undamped natural frequency

$$f = \frac{1}{2\pi}\sqrt{\frac{a_0}{kI_1}} \qquad [4a]$$

and the relative damping ratio

$$\zeta = \frac{1}{2}\frac{a_1 + e}{\sqrt{ka_0/I_1}}\left(\frac{1}{I_1} + \frac{1}{I_2}\right) \qquad [4b]$$

[3] Measured in space direction fixed system, as desired by control mission.

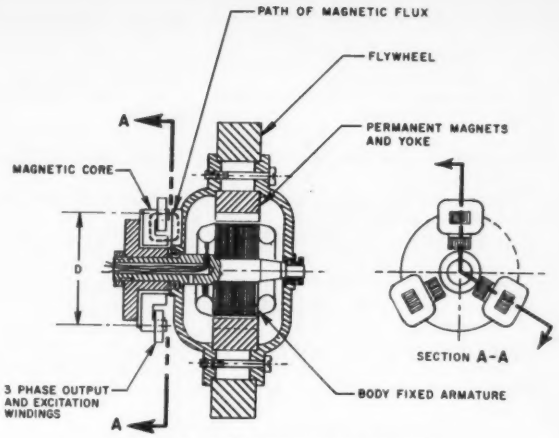

Fig. 3a Impedance-commutator-motor

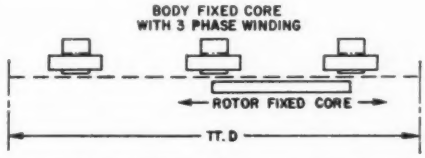

Fig. 3b Air gap variation of impedance-commutator-motor

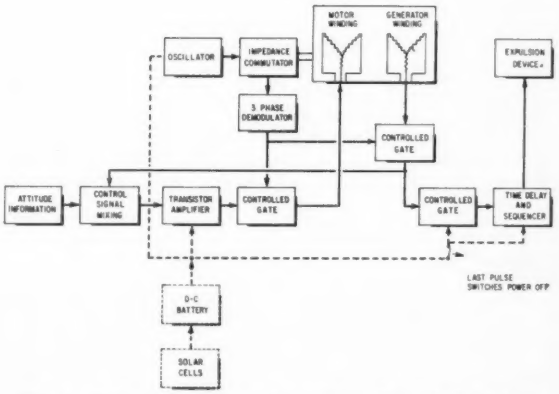

Fig. 4 Schematic diagram for a one-axis control system

The described motor works most efficiently like any d-c motor with a proportional control system. However, the available power sources are constant voltage sources. Thus, highly efficient control inverters and amplifiers have to be developed. Most promising is the use of pulse modulated transistor and controlled rectifier-type amplifiers.

The use of control characteristics with a properly selected dead zone or an on-off behavior will further improve the efficiency of the control circuit, because no power is required during the dead zone interval.

Preliminary design results are very favorable. The weight of all the flywheels for a three-axis control system contributes less than 0.5 per cent to the weight of the space vehicle. It can be expected that the total weight contribution, which includes the weight of the control circuitry, the servo motors, and the expulsion devices (however, no weight of the

Table 1 Feasible methods for attitude sensing

Resulting type of coordinate direction	Medium to be sensed	From	Attitude sensor
space fixed direction	visible light	stellar bodies	light direction sensitive cell (5,6)
direction fixed to center of emitting body	visible light, infrared light	sun, planet, moon	light and infrared direction sensitive cell (5,6)
direction fixed to center of body shadowing cosmic rays	cosmic rays (if no radiation belt present)	planet, moon	cosmic ray sensor (3)
magnetic field vector direction	geomagnetic field (application questionable due to el. currents in ionosphere)	Earth	magnetic compass
direction fixed to gravitational field vector	gravitational field	orbited body	satellite body or pendulum (4)
direction fixed normal to orbit plane	(Angular velocity of satellite due to attitude control direction fixed to center of orbited body)		rate gyro
relative velocity direction, acceleration	gas	atmosphere	angle-of-attack indicator, accelerometer
determined by signal, reference direction determined by space vehicle to Earth transmitter or receiver line	RF signals	Earth	RF receiver, either on Earth or in space vehicle (distance for attitude sensing is limited by length of base line)

attitude sensing devices and the power supply) can be kept within 3 to 5 per cent of the vehicle weight.

A motor with impedance commutator has been built and works satisfactorily. Analog computer studies have been carried out to determine optimum conditions for the combination of the expulsion and the flywheel systems. The results are as expected and confirm the feasibility of the proposed attitude control system.

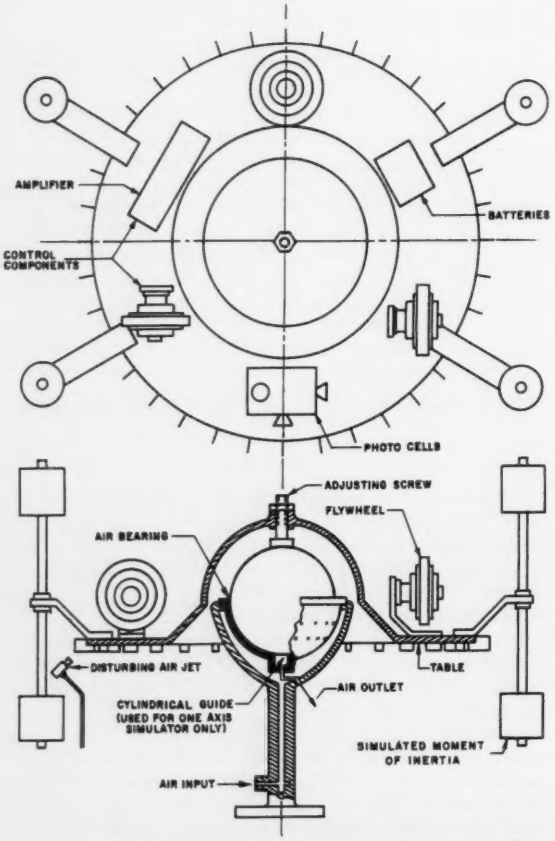

Fig. 5 Control system test table

Attitude Sensing

In order to attitude control a body in space, attitude angles must be sensed with respect to a selected reference system. Such a reference coordinate system can be established by means:

1 Within the space vehicle. For this purpose inertial devices alone are available, which maintain a space direction fixed system.

2 Outside the space vehicle, such as by any radiating field, potential field or field with matter.

Due to limitations in the performance of instruments, the accuracy of inertial devices is not sufficient to retain their measuring system for a long time in space fixed position. In order to avoid drift of the measuring system, it is mandatory to supervise it as mentioned under item 2 above. Thus the inertial system will be of benefit if interruptions of the supervisory information will occur as due to shadowing effects, etc., or if by averaging of a noisy supervisory signal, better attitude information can be obtained.

Information sources outside the space vehicle can be used to establish space fixed reference systems, celestial body (including the Earth) aligned systems, or a combination of both. Some feasible attitude sensors for different outside information sources with the resulting type of coordinate direction are given in Table 1.

The most favorable combination for a three-axis attitude sensing system can only be selected with the space vehicle mission, its path, the resulting accuracy requirements, weight, power and volume allowances in proper consideration.

For certain space vehicle missions, it may be possible to use a two-axis attitude control system, and a limited angular rate around the third axis, the roll axis, can be tolerated, or a specified angular rate may be required. Then it becomes necessary to use an input signal to the roll axis control system which depends on the spin rate. In this case the attitude sensor will be replaced by an angular rate sensor, e.g., a rate gyroscope if a small angular speed is requested, or an accelerometer if a specified angular rate is demanded. The feedback loop, which is shown in Fig. 4, producing the angular rate damping terms becomes unnecessary.

Appendix Simulation of the Attitude Control Loop

It is desirable to investigate first the complete one-axis sys-

tem under the influence of expected initial disturbances and with respect to its overall behavior due to inherent and built-in nonlinearities. The frictionless support of the simulated moment of inertia of the space vehicle can be accomplished by an air bearing as indicated in Fig. 5. The mounting table represents the space vehicle and carries the complete one-axis control system, including batteries. The attitude signal can be derived from an optical pickup, such as in real application or from a simulated inductive pickup. The initial disturbance or the first angular impulse may be introduced by an air jet.

Simulation of the three-axis control system behavior can be achieved with the complete control system mounted on the table, which is now supported by a spherical bearing without the cylindrical guide (see Fig. 5). The simulating device will serve to study coupling effects if large attitude angles occur, such as during the period of alignment to a reference system or during the period of changing from one reference system to another.

References

1 Roberson, R. E., "Attitude Control of a Satellite Vehicle—An Outline of the Problem," presented at the Eighth IAF congress, Barcelona, Spain, Oct. 1957.

2 Roberson, R. E., "Torques on a Satellite Vehicle from Internal Moving Parts," *J. Appl. Mech.*, June 1958, p. 196.

3 Stuhlinger, E., "Control and Power Supply Problems of Instrumented Satellites," JET PROPULSION, vol. 26, 1956, p. 364.

4 Oberth, H., "A Precise Attitude Control for Artificial Satellites," ABMA publication, 1957.

5 Wallmark, J. Torkel, "A New Semiconductor Photocell Using Lateral Photoeffect," *Proc. IRE*, April 1957, p. 474.

6 Wallmark, J. Torkel, "Photocell Measures Light Directions," *Electronics*, July 1957, p. 165.

Application of Astronomical Perturbation Techniques to the Return of Space Vehicles[1]

ROBERT M. L. BAKER Jr.[2]

Aeronutronic Systems, Inc.
Newport Beach, Calif.

An application of astronomical perturbation techniques is made to the return of space vehicles from satellite, lunar and interplanetary missions. Such techniques increase the accuracy of the computations and shorten the computational times required. The proposed variation-of-parameters perturbation method is illustrated by applying it first to the standard problem of a gravitational orbit perturbed by drag and, subsequently, by applying it to the inverse problem of a gravity-free drag orbit perturbed by gravity. The perturbation method is employed specifically in the analysis of the return from space voyages, and it is concluded from other comparative calculations that the perturbation computations are 3 to 10 times faster and are 11 to 165 times more accurate than the nonperturbation computations.

THE MANY integration steps that are required in a numerical integration lead to the accumulation of end figure error. The usual re-entry trajectory calculations, i.e., step-by-step numerical integration of the total accelerations acting on the vehicle—known to astronomers as Cowell's method—have been especially subject to this difficulty. Furthermore, the many integration steps involve too much calculation time. In the case of perturbation methods, one integrates only the departures from a reference orbit. Thus, only a few steps are necessary in those phases of the vehicle's flight when the perturbative forces are small instead of the very many steps required when all the forces are included in the integrand. (It has been found that, in this case at least, the advantage of having fewer steps more than compensates for the disadvantages of using the perturbation formulas which are not always as simple or symmetrical as the nonperturbation formulas, see (11).[3])

The reference orbit that is to be perturbed is usually chosen as the orbit that best depicts the gross motion of an object. All forces not taken into account in this gross motion are then categorized as perturbative forces. It is usually advisable to utilize as the reference orbit, an orbit that can be integrated analytically in closed form at the outset without requiring a step-by-step numerical procedure.

These considerations immediately led astronomers to the utilization of the two-body Keplerian orbit as the reference orbit for the study of planetary perturbations. All forces exerted by drag, other planets, etc., are then incorporated as perturbative forces that tend to change the orbital parameters, such as eccentricity, semimajor axis, etc., of the two-body orbit.

Comparative computations of the problem discussed in the fifth section of this paper have demonstrated that, in this particular case, the perturbation method requires one-fifth to one-thirtieth fewer integration steps than does Cowell's method, and, hence, proceeds 3 to 10 times faster. It should be noted also that the accumulation of end figure error cannot be overcome by simply increasing the number of digits carried in the computation, because such a procedure merely conceals the inherent round-off errors of any tabular data included in the integrand (e.g., atmospheric density). As pointed out by Dirke Brouwer (1) the end figure error of a double integration

Received July 15, 1958.

[1] This paper represents a portion of a dissertation submitted in partial fulfillment of the requirements for the degree of Doctor of Philosophy at the University of California, Los Angeles.

[2] Staff Member; also Acting Assistant Professor of Astronomy, University of California. Member ARS.

[3] Numbers in parentheses indicate References at end of paper.

increases in proportion to the three halves power of the number of integration steps; hence, the perturbation techniques proposed here should provide answers with between $5^{3/2}$ and $30^{3/2}$ or between about 11 and 165 times more accuracy than would the commonly employed nonperturbation techniques.

The need for extremely accurate and rapid computations of re-entry trajectories has arisen, in part, out of the requirements for return from voyages into space, e.g., when the recovery of a human being is involved, a fast, accurate orbit determination is mandatory. Even in other re-entry problems, the computational efficiency usually afforded by perturbation techniques (which have often been employed advantageously by astronomers (9)) should also be taken advantage of by missile designers.

Perturbation Analysis

In essence, the following perturbation analysis utilizes the technique of the variation of parameters,[4] which involves the continuous correction ("rectification") of a reference orbit such that at every instant the reference orbit is tangent to the true orbit. This technique can be best illustrated by first applying it to the standard problem of a purely gravitational two-body orbit perturbed by drag, and subsequently by applying the technique to the inverse problem of a rectilinear gravity-free, drag orbit perturbed by gravity. Fig. 1 and the following two subsections illustrate a comparison of these two applications. As the vehicle's path is perturbed, its motion is represented by a series of osculating or continuously varying reference orbits. Perturbative forces cause a change in the parameters that specify the orbit and, consequently, cause a progression from one osculating orbit to the next.

The notation and formulation of the following subsections are based largely upon the work of Herrick (2).

Drag Perturbation of a Drag-Free, Gravity Orbit

If we denote the perturbative derivative by the grave symbol (`), and define

- $\dot{s}$ = the speed of the object tangential to its trajectory (in terms of surface circular-satellite speed)
- r = the radial distance of the object from the geocenter (in Earth radii)
- a = the semimajor axis of the osculating ellipse
- $\dot{s}^{\grave{}}$ = the perturbative acceleration tangential to the trajectory of the object (e.g., resulting from drag)
- $a^{\grave{}}$ = the perturbation in the semimajor axis

then the perturbative derivative[5] of the well-known *vis-viva* or energy integral

$$\dot{s}^2 = \frac{2}{r} - \frac{1}{a} \qquad [1]$$

becomes

$$2\dot{s}\dot{s}^{\grave{}} = a^{\grave{}}/a^2 \qquad [2]$$

From Equation [2] we find that

$$a^{\grave{}} = 2a^2\dot{s}\dot{s}^{\grave{}} \qquad [3]$$

[4] Instead of a variation-of-parameters technique, one could also profitably employ an "Encke" perturbation technique (see (8)).

[5] I.e., if f is a function of the independent variable τ, and certain variable parameters $P_1, P_2, \ldots P_i \ldots$, then

$$\frac{df}{d\tau} = \frac{\partial f}{\partial \tau} + \sum \frac{\partial f}{\partial P_i}\frac{dP_i}{d\tau}$$

Symbolically, the terms of this equation are identified by $df/d\tau = \dot{f} + f^{\grave{}}$, where the parameters P_i vary only because of perturbative forces. See chapter 17 of (2).

DRAG-PERTURBED ELLIPTICAL ORBIT

GRAVITY-PERTURBED RECTILINEAR ORBIT

INITIAL ORBITS ———
PERTURBED OSCULATING ORBITS – – – –

Fig. 1 Variation-of-parameters technique

Taking the derivative of the semi-lactus rectum or parameter p where

$$p = a(1 - e^2) \qquad [4]$$

we have

$$p^{\grave{}} = 2a^2\dot{s}\dot{s}^{\grave{}}(1 - e^2) - 2aee^{\grave{}} \qquad [5]$$

where e = the eccentricity of the osculating ellipse.

By the law of areas (or the principle of the conservation of angular momentum)

$$p = r^2(rv)^{\cdot} \qquad [6]$$

where $\dot{v}$ = the angular speed of the true anomaly v. (For geocentric orbits v is the angle between the object and the perigee measured, at the geocenter.)

Again perturbative differentiation yields

$$p^{\grave{}} = 2r^4\dot{v}v^{\grave{}} \qquad [7]$$

but, since drag is a perturbation that is tangential to the trajectory and, furthermore, since it is the only perturbative force to be considered, we find that

$$r\dot{v}^{\grave{}} = \dot{s}^{\grave{}}\cos\theta = \dot{s}^{\grave{}}r\dot{v}/\dot{s} \qquad [8]$$

where θ is the angle of elevation, i.e., the angle between the tangent to the trajectory and local horizontal plane.

Hence, Equation [7] becomes

$$p^{\grave{}} = 2p\dot{s}^{\grave{}}/\dot{s} \qquad [9]$$

If we employ the equation of the osculating ellipse

$$p/r = 1 + e\cos v \qquad [10]$$

and solve for $e^{\grave{}}$, then we find that

$$e^{\grave{}} = \frac{2\dot{s}^{\grave{}}}{\dot{s}}(\varepsilon + \cos v) \qquad [11]$$

Equation [11] agrees with previous computations made by Moulton (3) and Herrick (2). (Moulton's more complex equation reduces to [11] if Eqs. [1 and 10] of this paper are substituted into the fifth equation of problem 4, p. 405 of (3).) Similar expressions for $v^{\grave{}}$, etc., may be obtained in a straightforward manner.

Perturbations of a Gravity-Free, Drag Orbit

In the case of re-entry orbits, the drag forces predominate, and it is therefore advisable to discard the two-body orbit and substitute in its stead a purely gravity-free, drag orbit.[6] Because all the drag forces are directed opposite to the velocity vector, the orbit will be rectilinear. The orbital parameters, perigee distance[7] and the longitude of perigee $\tilde{\omega}$ vary only

[6] The changeover from the gravitational to the drag reference orbit should take place when the drag accelerations exceed the gravitational accelerations.

[7] The distance from the center of the Earth to the point of nearest approach of the orbit to the Earth.

because of gravitational perturbative forces. Integrations of these parameters yield a complete history of the trajectory (see (4)). Lift forces, normal to the trajectory, also can be easily included in the new perturbation scheme.

It is necessary to consider the rectilinear orbit only with respect to a spherically symmetrical Earth; therefore, the one angle $\tilde{\omega}$ and one distance x are the only parameters needed to specify the orbit. (Of course, considerations of the asphericity of the Earth, rotation and periodic fluctuations in the Earth's atmosphere, and gravitational anomalies can be included also in the perturbation analysis.) Another quantity (e.g., y or v) is required to give the position of the object on this orbit.

Consider the coordinate system shown in Fig. 2. The rather unconventional labeling of the coordinate axes is employed in order to preserve the direction of the x-axis toward perigee.

Let the grave symbol ($\grave{}$) also denote perturbative variation of a quantity with respect to time in which the variation results from gravity. Thus, the radial and transverse perturbative accelerations are

$$\dot{r}^{\grave{}} = -1/r^2 \qquad r\dot{v}^{\grave{}} = 0 \tag{12}$$

Because the osculating orbit is by definition the one along which the vehicle is instantaneously traveling, there exists no instantaneous change in the radial distance r and the true longitudinal of the vehicle l; therefore, since $l = v + \tilde{\omega}$, we find that

$$l^{\grave{}} = v^{\grave{}} + \tilde{\omega}^{\grave{}} = 0 \quad \text{or} \quad \tilde{\omega}^{\grave{}} = -v^{\grave{}} \tag{13}$$

Of course $r^2 = x^2 + y^2$; $x = r\cos v$, and $y = \sin v$. Accordingly, we find that

$$x^{\grave{}} = -yv^{\grave{}} = +y\tilde{\omega}^{\grave{}} \tag{14}$$

Through reference to Fig. 2, we observe that $\dot{r} = r\dot{v}\tan v$. Therefore, since $r\dot{v}^{\grave{}} = 0$

$$\dot{r}^{\grave{}} = (r\dot{v}\sec^2 v)v^{\grave{}} \tag{15}$$

and, consequently

$$v^{\grave{}} = -\left(\frac{1}{r^2}\right)\frac{\cos^2 v}{r\dot{v}} \tag{16}$$

But $\cos v/r\dot{v} = 1/\dot{y}$, whereas $r\cos v = x$ so that

$$v^{\grave{}} = -\frac{1}{r^3}\frac{x}{\dot{y}} \quad \text{or} \quad \tilde{\omega}^{\grave{}} = \frac{x}{\dot{y}r^3} \tag{17}$$

(see footnote 8).
Thus

$$x^{\grave{}} = xy/\dot{y}r^3 \tag{18}$$

But

$$\dot{y}^{\grave{}} = \frac{\dot{r}^{\grave{}}y}{r} = -\frac{y}{r^3} \tag{19}$$

Since $dx/d\tau = \dot{x} + x^{\grave{}} = x^{\grave{}}$, and $dx/d\tau = (dx/dy)(dy/d\tau) \times (x \rightarrow \tilde{\omega})$, the perturbation derivatives with respect to y as the independent variable (denoted by $'$) are, similarly

$$\tilde{\omega}' = x/(\dot{y} + y^{\grave{}})\dot{y}r^3 \tag{20}$$

and

$$x' = xy/(\dot{y} + y^{\grave{}})\dot{y}r^3 \tag{21}$$

Let us examine the behavior of Equations [17, 18 and 19] in two limiting cases. First, assume that the object is approaching the Earth along a rectilinear orbit through the geocenter and that there is no drag. In this case $d\dot{y}/d\tau = -y^{\grave{}}r^3$, while x and, consequently, $x^{\grave{}}$ and $\tilde{\omega}^{\grave{}}$ are zero. Second, assume that the object is circling the Earth in a drag-free environment. In the case of a circular satellite $\dot{y} = 1/\sqrt{r}$ and $x = r$, therefore, $\tilde{\omega}^{\grave{}} = 1/r^{3/2}$, and $x^{\grave{}} = 0$. From another point of view, the x-axis would be rotating around the Earth just fast enough to keep pace with the object, so that the speed relative to the perturbed axis is zero; hence, $\dot{y} + y^{\grave{}} = 0$. But, as can be easily shown (see Eq. [14]), $y^{\grave{}} = -x\tilde{\omega}^{\grave{}}$, therefore $\dot{y} = x\tilde{\omega}^{\grave{}} = 1/\sqrt{r}$. All of the preceding results are in agreement with conventional theory.

[8] It should be recognized that $\dot{y} + y^{\grave{}}$ is the speed of the object with respect to the perturbed x-axis.

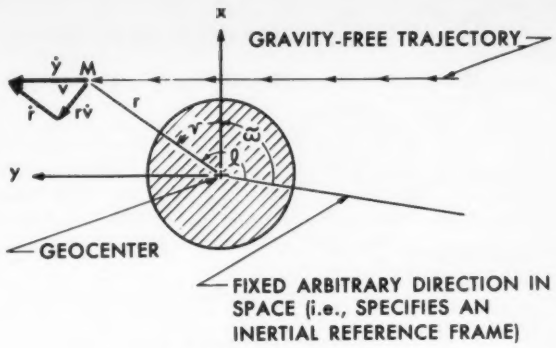

Fig. 2 Coordinate system

Inclusion of Lift in the Gravitational Perturbation Scheme

In certain high speed re-entry problems, the vehicle may be expected to exhibit lift as well as drag. If we denote the lift acceleration (directed normally to the velocity of the vehicle) by L, then, from Fig. 3.

$$\dot{r}^{\grave{}} = L\cos v - 1/r^2 \tag{22}$$

$$r\dot{v}^{\grave{}} = -L\sin v \tag{23}$$

Also $\tan v = r\dot{v}/\dot{r}$, or $\dot{r} = r\dot{v}\tan v$, so that differentiation yields $\dot{r}^{\grave{}} = r\dot{v}^{\grave{}}\tan v + r\dot{v}\sec^2 v v^{\grave{}}$. Substituting the previously determined values of $\dot{r}^{\grave{}}$ and $r\dot{v}^{\grave{}}$, we obtain

$$L\cos v - \frac{1}{r^2} = -L\sin v\tan v + r\dot{v}v^{\grave{}}\sec^2 v \tag{24}$$

Solving for $v^{\grave{}}$, we find that

$$v^{\grave{}} = \frac{L\cos v - \dfrac{\cos^2 v}{r^2}}{r\dot{v}} \tag{25}$$

or, in terms of x, y and r

$$v^{\grave{}} = (L - x/r^3)/\dot{y} \tag{26}$$

From Fig. 3 we observe that $x = r\cos v$; therefore

$$x^{\grave{}} = r\sin vv^{\grave{}} = -yv^{\grave{}}$$

Hence

$$x^{\grave{}} = \frac{y}{\dot{y}}\left(\frac{x}{r^3} - L\right)$$

whereas

$$\tilde{\omega}^{\grave{}} = -v^{\grave{}} = \frac{1}{\dot{y}}\left(\frac{x}{r^3} - L\right) \tag{27}$$

Of course, $\dot{y}^{\grave{}}$ remains unchanged.

The perturbational derivations with respect to y as the in-

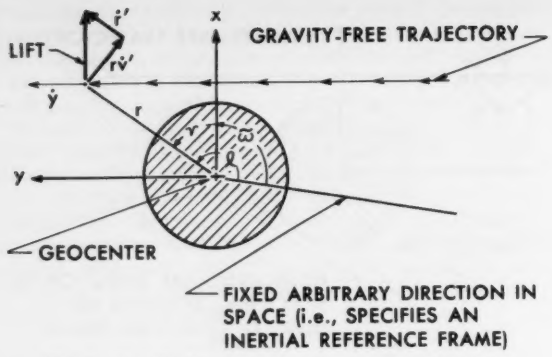

Fig. 3 Coordinate system for the incorporation of lift

dependent variable (denoted by′) are

$$\tilde{\omega}' = \frac{1}{\dot{y}(\dot{y} + y\grave{})}\left(\frac{x}{r^3} - L\right) \qquad [28]$$

$$x' = \frac{y}{\dot{y}(\dot{y} + y\grave{})}\left(\frac{x}{r^3} - L\right) \qquad [29]$$

Formulation of the Drag-Perturbation Equations

We have determined the perturbation variations in the parameters specifying the rectilinear gravity-free orbit in the preceding sections and it now remains to incorporate these into equations suitable for computation. Since all the motion of the vehicle is directed along the y-axis, the basic drag equation of motion is given by

$$\frac{d\dot{y}}{d\tau} = \ddot{y} + \dot{y}\grave{} = -\left[\frac{C_{D_0}A_0\rho_0 V_{c_0}^2}{2g_0 m_0}\right]\sigma\gamma\mu\alpha\dot{y}^2 - \frac{y}{r^3} \triangleq -D_0^2\sigma\gamma\mu\alpha\dot{y}^2 - \frac{y}{r^3} \qquad [30]$$

where

C_{D_0} = the reference value of the drag coefficient
A_0 = the initial projected frontal area of the vehicle
m_0 = the initial mass of the vehicle
g_0 = the acceleration of gravity at unit distance (979.81979 cm/sec²)
ρ_0 = the sea-level atmospheric density (1.225×10^{-3} gm/cm³)
$\sigma = \rho/\rho_0$
$\gamma = C_D/C_{D_0}$
$\mu = m_0/m$
$\alpha = A/A_0$
$\dot{y}$ = the speed of the vehicle with respect to atmosphere

ρ, C_D, A and m represent, respectively, the true value of the atmospheric density, drag coefficient, projected frontal area and mass of the vehicle.

Actually, γ can be expected to be a function primarily of the three variables T_s, σ and $\dot{y}$ (where T_s is the surface temperature of the vehicle). These variables will determine the transitional and continuum variation of the drag coefficient. In certain re-entry problems in which the transitional variation and compressibility variation of C_D (and hence of γ) occur at different points along the trajectory, it is possible to separate γ into two factors[9]

$$\gamma = \gamma(\sigma)\gamma(\dot{y}) \qquad [31]$$

$\gamma(\sigma)$ specifies the variation of the drag coefficient during the transition from free molecule to continuum flow, and is strongly a function of the local molecular mean-free path, and consequently, is a function of the density ratio σ (5). $\gamma(\dot{y})$ specifies the variation of C_D with the Mach number, and hence is properly a function of $\dot{y}$ (assuming that the local speed is nearly constant).

If it is assumed that $\mu\alpha$ remains constant and equal to unity during re-entry[10] and that the gross variation of $\sigma\gamma(\sigma)$ and $\gamma(\dot{y})$ (for supersonic speeds), respectively, can be represented by

$$\sigma\gamma(\sigma) = C_0 + C_2\sigma^2 + C_4\sigma^4 + \ldots \qquad [32]$$

and

$$\gamma(\dot{y}) = A + B/\dot{y} + \ldots \qquad [33]$$

(where for $C_{D0} = 0.92$ and mean sonic speed = 320m/sec, $A = 1$ and $B = 6.84 \times 10^{-3}$ for a fit to the data of (12)) then

$$\frac{d\dot{y}}{d\tau} = -D_0^2\left(A + \frac{B}{\dot{y}}\right)\gamma(\sigma)\sigma\dot{y}^2 - D_0^2\left[\gamma(\dot{y}) - \left(A + \frac{B}{\dot{y}}\right)\right]\gamma(\sigma)\sigma\,\dot{y}^2 - \frac{y}{r^3} \qquad [34]$$

One can proceed by either integrating with respect to time τ, or distance, y. For nearly circular satellite orbits (in which $dy/d\tau$ and y are close to zero) direct integration of Equations [17, 18 and 34] with τ as independent variable is advantageous. In this case, one integrates the first term in Equation [34] analytically (as per Eq. [42]—with $P = 0$) and integrates the second and third perturbational terms of Equation [34] numerically to obtain $\dot{y}$; a second integration of $dy/d\tau = \dot{y} + y\grave{} = \dot{y} - x\tilde{\omega}\grave{}$ is then required to obtain y. On the other hand, for either large $\dot{y}^2$ or small x^2 (i.e., for either high speeds, e.g., meteorites, or large angles of elevation, θ) the employment of y as independent variable is advantageous. In this latter case one proceeds as follows

$$\frac{dy}{d\tau}\frac{d\dot{y}}{dy}\frac{1}{\left(A + \frac{B}{\dot{y}}\right)\dot{y}^2} = -D_0^2\gamma(\sigma)\sigma - \left\{\frac{D_0^2}{\left(A + \frac{B}{\dot{y}}\right)}\left[\gamma(\dot{y}) - \left(A + \frac{B}{\dot{y}}\right)\right]\gamma(\sigma)\sigma + \frac{y}{\left(A + \frac{B}{\dot{y}}\right)\dot{y}^2r^3}\right\} \qquad [35]$$

where $dy/d\tau = \dot{y} + y\grave{} = \dot{y} - x^2/\dot{y}r^3$, and we define

$$\frac{dP}{dy} \triangleq -\left\{\frac{D_0^2}{\left(A + \frac{B}{\dot{y}}\right)}\left[\gamma(\dot{y}) - \left(A + \frac{B}{\dot{y}}\right)\right]\gamma(\sigma)\sigma + \frac{y}{\left(A + \frac{B}{\dot{y}}\right)\dot{y}^2r^3}\right\} \Bigg/ \left(1 - \frac{x^2}{\dot{y}^2r^3}\right) - D_0^2\gamma(\sigma)\sigma\left[\frac{x^2}{\dot{y}^2r^3} + \left(\frac{x^2}{\dot{y}^2r^3}\right)^2 + \ldots\right] \qquad [36]$$

Since this last equation includes all of the perturbational terms, the basic integral for $\dot{y}$ becomes simply

$$\int_{\dot{y}_0}^{\dot{y}} \frac{d\dot{y}}{(A\dot{y} + B)} = -D_0^2\int_{y_0}^{y}\gamma(\sigma)\sigma dy - \int_{y_0}^{y}\frac{dP}{dy}\,dy \qquad [37]$$

where the zero subscript denotes the initial values of position

[9] In meteoritic analysis, it is convenient to include also a factor γ_{ab} that specifies the variation of C_D which results from the reaction of ablated molecules, i.e., the "reverse rocket" effect. See, e.g., (6).

[10] The variation of $\mu\alpha$ has been included, however, in the referenced works (6).

(y) and speed ($\dot{y}$). Integration yields

$$\dot{y} = \left[\dot{y}_0 + \frac{B}{A}\right] \exp\left[-AD_0^2 \int_{y_0}^{y} \gamma(\sigma)\sigma dy - AP\right] - \frac{B}{A} \quad [38]$$

Since $r^2 = x^2 + y^2$, we can in turn represent $\sigma\gamma(\sigma)$ by

$$\sigma\gamma(\sigma) = Y_0 + Y_2 y^2 + Y_4 y^4 + \ldots \quad [39]$$

where

$$Y_0 = C_0 + C_2 x^2 + C_4 x^4 + \ldots$$
$$Y_2 = C_2 + 2C_4 x^2 + 3C_6 x^4 + \ldots$$
$$Y_4 = C_4 + 3C_6 x^2 + 6C_8 x^4 + \ldots$$
$$Y_6 = C_6 + 4C_8 x^2 + 10C_{10} x^4 + \ldots, \text{etc.}$$
$$\ldots\ldots\ldots\ldots\ldots\ldots \quad [40]$$

Employing the summation notation, we will set

$$\sigma\gamma(\sigma) = \sum_{i=0}^{i=n} Y_{2i} y^{2i}$$

and observe that

$$-AD_0^2 \int_{y_0}^{y} \sigma\gamma(\sigma) dy = -AD_0^2 \sum_{i=0}^{i=n} \frac{Y_{2i} y^{2i+1}}{2i+1}\bigg|_{y_0}^{y} \quad [41]$$

in which it is recognized that Y_{2i} is a function of the parameter x.

In practice it is found advisable to change the constants $C_0, C_2, C_4, \ldots$, within a few levels of the atmosphere, in order to avoid an excessive number of terms.

Finally then, we can establish the equation for $\dot{y}$ as

$$\dot{y} = \left[\dot{y}_0 + \frac{B}{A}\right] \exp\left[-AD_0^2 \sum_{i=0}^{i=n} \frac{Y_{2i} y^{2i+1}}{2i+1}\bigg|_{y_0}^{y} - AP\right] - \frac{B}{A} \quad [42]$$

Thus given y and P (and the initial conditions $\dot{y}_0$ and y_0), $\dot{y}$ can be explicitly determined in closed form.

The computation with y as the independent variable proceeds by integrating

$$\bar{\omega} = \bar{\omega}_0 + \int_{y_0}^{y} \bar{\omega}' \, dy \quad [43]$$

$$x = x_0 + \int_{y_0}^{y} x' dy \quad [44]$$

$$P = \int_{y_0}^{y} \frac{dP}{dy} \, dy \quad [45]$$

where the initial value of P is set equal to zero.

Applications and Conclusions

The perturbation and computational approaches of the foregoing sections are justified only if they lead to faster and more accurate calculations. Consequently, other comparative calculations were performed in which the conventional integration of all the forces (Cowell's method) and the perturbation scheme were employed on the same problem. The problems chosen for analysis are discussed in (6 and 10), and the Runge-Kutta integration method coupled with the Adams correction procedure (7) was employed in the actual computations.

In every computation of this particular problem, the conventional calculations (even though their equations were slightly simpler and more symmetric) required from 3 to 10 times more computer time than did the perturbation computations; furthermore, the many extra integration steps involved in the nonperturbation methods caused a gradual accumulation of end figure error. It is concluded, therefore, that there exist definite advantages to the application of astronomical perturbation techniques to the computations of the return trajectories of space vehicles.

Acknowledgment

During the preparation of this paper, I have profited from many constructive suggestions, criticisms and ideas contributed by others. Professor Samuel Herrick of the Department of Astronomy of the University of California, Los Angeles, has given me many helpful suggestions, especially in regard to perturbation techniques, and has always encouraged and stimulated my work. Dr. Eric Durand of Aeronutronic Systems, Inc. made possible the early completion of this paper by allowing me to utilize the Aeronutronic computer, and by sponsoring much of my research. Prof. Dirk Brouwer carefully read through the manuscript.

References

1 Brouwer, D., "On the Accumulation of Errors in Numerical Integration," *Astronomical J.*, vol. XLVI, no. 16, 1937. pp. 149–153.

2 Herrick, S., "Astrodynamics," Van Nostrand (to be published 1959).

3 Moulton, F. R., "An Introduction to Celestial Mechanics," MacMillan Co., New York. 1914.

4 Baker, R. M. L., Jr., "Drag Interactions of Meterorites with the Earth's Atmosphere," unpublished paper presented at the Twentieth Meeting of the Meteoritical Society, Univ. of Calif., Los Angeles, Sept. 24, 1957.

5 Baker, R. M. L., Jr. and Charwat, A F., "Transitional Correction to the Drag of a Sphere in Free Molecule Flow," *Phys. Fluids*, vol. 1, no. 2, 1958, pp. 73–81; *see also* Baker, R. M. L., Jr., "Transitional Aerodynamic Drag of Meteorites," *Astrophysical J.*, May, 1959.

6 Baker, R. M. L., Jr., "Drag Interactions of Meteorites with the Earth's Atmosphere," Doctoral Dissertation, University of California, Los Angeles, May 1958; *see also* "Sputtering as It Is Related to Hyperbolic Meteorites," *J. Appl. Phys.*, April, 1959.

7 Adams, E., "A Method for Interval Control and Correction with Runge-Kutta Integration," in "Math. Tab. and Other Aids to Comp." (to be published).

8 Baker, R. M. L., Jr., "Encke's Method and Variation of Parameters as Applied to Reentry Trajectories," Proc. of Amer. Astronautical Soc., Western Regional Meeting, Aug. 18–19, 1958.

9 Herrick. S. and Baker, R. M. L., Jr., "Recent Advances in Astrodynamics," Jet Propulsion, vol. 28, no. 10, 1958, pp. 649–654.

10 Baker, R. M. L., Jr., "Accuracy Required for a Return from Interplanetary Voyages," to be published *J. Brit. Interplanet. Soc; see also* "Emphemeral Natural Satellites of the Earth," *Science*, vol. 128 no. 3333, Nov. 14, 1958.

11. Porter, J. G., "A Comparative Study of Perturbation Methods," *Astronomical J.*, vol. 63 no. 10, 1958, pp. 405-406; *see also* "Planetary Coordinates for the Years 1960-1980," Her Majesty's Stationery Office, London, pp. vii to xix.

12 Hodges, A. J., "The Drag Coefficient of Very High Velocity Spheres," *J. Aeron. Sci.*, vol. 24, no. 3, 1957, pp. 549-555.

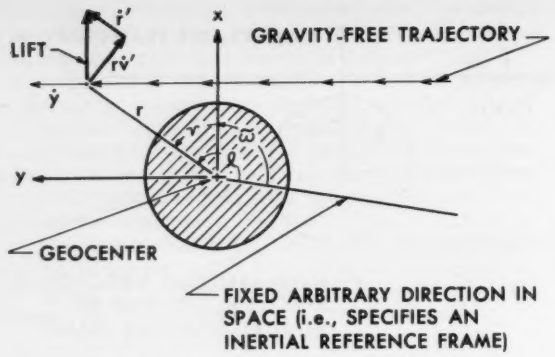

Fig. 3 Coordinate system for the incorporation of lift

dependent variable (denoted by$'$) are

$$\tilde{\omega}' = \frac{1}{\dot{y}(\dot{y} + y^{\backprime})}\left(\frac{x}{r^3} - L\right) \qquad [28]$$

$$x' = \frac{y}{\dot{y}(\dot{y} + y^{\backprime})}\left(\frac{x}{r^3} - L\right) \qquad [29]$$

Formulation of the Drag-Perturbation Equations

We have determined the perturbation variations in the parameters specifying the rectilinear gravity-free orbit in the preceding sections and it now remains to incorporate these into equations suitable for computation. Since all the motion of the vehicle is directed along the y-axis, the basic drag equation of motion is given by

$$\frac{d\dot{y}}{d\tau} = \ddot{y} + \dot{y}^{\backprime} = -\left[\frac{C_{D_0}A_0\rho_0 V_{c_0}^2}{2\zeta_0 m_0}\right]\sigma\gamma\mu\alpha\dot{y}^2 - \frac{y}{r^3} \triangleq -D_0^2\sigma\gamma\mu\alpha\dot{y}^2 - \frac{y}{r^3} \qquad [30]$$

where

C_{D_0} = the reference value of the drag coefficient
A_0 = the initial projected frontal area of the vehicle
m_0 = the initial mass of the vehicle
g_0 = the acceleration of gravity at unit distance (979.81979 cm/sec^2)
ρ_0 = the sea-level atmospheric density (1.225×10^{-3} gm/cm^3)
$\sigma = \rho/\rho_0$
$\gamma = C_D/C_{D_0}$
$\mu = m_0/m$
$\alpha = A/A_0$
$\dot{y}$ = the speed of the vehicle with respect to atmosphere

ρ, C_D, A and m represent, respectively, the true value of the atmospheric density, drag coefficient, projected frontal area and mass of the vehicle.

Actually, γ can be expected to be a function primarily of the three variables T_s, σ and $\dot{y}$ (where T_s is the surface temperature of the vehicle). These variables will determine the transitional and continuum variation of the drag coefficient. In certain re-entry problems in which the transitional variation and compressibility variation of C_D (and hence of γ) occur at different points along the trajectory, it is possible to separate γ into two factors[9]

$$\gamma = \gamma(\sigma)\gamma(\dot{y}) \qquad [31]$$

$\gamma(\sigma)$ specifies the variation of the drag coefficient during the transition from free molecule to continuum flow, and is strongly a function of the local molecular mean-free path, and consequently, is a function of the density ratio σ (5). $\gamma(\dot{y})$ specifies the variation of C_D with the Mach number, and hence is properly a function of $\dot{y}$ (assuming that the local speed is nearly constant).

If it is assumed that $\mu\alpha$ remains constant and equal to unity during re-entry[10] and that the gross variation of $\sigma\gamma(\sigma)$ and $\gamma(\dot{y})$ (for supersonic speeds), respectively, can be represented by

$$\sigma\gamma(\sigma) = C_0 + C_2r^2 + C_4r^4 + \ldots \qquad [32]$$

and

$$\gamma(\dot{y}) = A + B/\dot{y} + \ldots \qquad [33]$$

(where for $C_{D0} = 0.92$ and mean sonic speed = 320m/sec, $A = 1$ and $B = 6.84 \times 10^{-3}$ for a fit to the data of (12)) then

$$\frac{d\dot{y}}{d\tau} = -D_0^2\left(A + \frac{B}{\dot{y}}\right)\gamma(\sigma)\sigma\dot{y}^2 - D_0^2\left[\gamma(\dot{y}) - \left(A + \frac{B}{\dot{y}}\right)\right]\gamma(\sigma)\sigma\,\dot{y}^2 - \frac{y}{r^3} \qquad [34]$$

One can proceed by either integrating with respect to time τ, or distance, y. For nearly circular satellite orbits (in which $dy/d\tau$ and y are close to zero) direct integration of Equations [17, 18 and 34] with τ as independent variable is advantageous. In this case, one integrates the first term in Equation [34] analytically (as per Eq. [42]—with $P = 0$) and integrates the second and third perturbational terms of Equation [34] numerically to obtain $\dot{y}$; a second integration of $dy/d\tau = \dot{y} + y^{\backprime} = \dot{y} - x\tilde{\omega}^{\backprime}$ is then required to obtain y. On the other hand, for either large $\dot{y}^2$ or small x^2 (i.e., for either high speeds, e.g., meteorites, or large angles of elevation, θ) the employment of y as independent variable is advantageous. In this latter case one proceeds as follows

$$\frac{dy}{d\tau}\frac{d\dot{y}}{dy}\frac{1}{\left(A + \frac{B}{\dot{y}}\right)\dot{y}^3} = -D_0^2\gamma(\sigma)\sigma - \left\{\frac{D_0^2}{\left(A + \frac{B}{\dot{y}}\right)}\left[\gamma(\dot{y}) - \left(A + \frac{B}{\dot{y}}\right)\right]\gamma(\sigma)\sigma + \frac{y}{\left(A + \frac{B}{\dot{y}}\right)\dot{y}^3r^3}\right\} \qquad [35]$$

where $dy/d\tau = \dot{y} + y^{\backprime} = \dot{y} - x^2/\dot{y}r^3$, and we define

$$\frac{dP}{dy} \triangleq -\left\{\frac{D_0^2}{\left(A + \frac{B}{\dot{y}}\right)}\left[\gamma(\dot{y}) - \left(A + \frac{B}{\dot{y}}\right)\right]\gamma(\sigma)\sigma + \frac{y}{\left(A + \frac{B}{\dot{y}}\right)\dot{y}^3r^3}\right\} \Bigg/ \left(1 - \frac{x^2}{\dot{y}^2r^3}\right) - D_0^2\gamma(\sigma)\sigma\left[\frac{x^2}{\dot{y}^2r^3} + \left(\frac{x^2}{\dot{y}^2r^3}\right)^2 + \ldots\right] \qquad [36]$$

Since this last equation includes all of the perturbational terms, the basic integral for $\dot{y}$ becomes simply

$$\int_{\dot{y}_0}^{\dot{y}} \frac{d\dot{y}}{(A\dot{y} + B)} = -D_0^2\int_{y_0}^{y}\gamma(\sigma)\sigma dy - \int_{y_0}^{y}\frac{dP}{dy}\,dy \qquad [37]$$

where the zero subscript denotes the initial values of position

[9] In meteoritic analysis, it is convenient to include also a factor γ_{ab} that specifies the variation of C_D which results from the reaction of ablated molecules, i.e., the "reverse rocket" effect. See, e.g., (6).

[10] The variation of $\mu\alpha$ has been included, however, in the referenced works (6).

(y) and speed ($\dot{y}$). Integration yields

$$\dot{y} = \left[\dot{y}_0 + \frac{B}{A}\right] \exp\left[-AD_0^2 \int_{y_0}^{y} \gamma(\sigma)\sigma dy - AP\right] - \frac{B}{A} \qquad [38]$$

Since $r^2 = x^2 + y^2$, we can in turn represent $\sigma\gamma(\sigma)$ by

$$\sigma\gamma(\sigma) = Y_0 + Y_2 y^2 + Y_4 y^4 + \ldots \qquad [39]$$

where

$$\begin{aligned} Y_0 &= C_0 + C_2 x^2 + C_4 x^4 + \ldots \\ Y_2 &= C_2 + 2C_4 x^2 + 3C_6 x^4 + \ldots \\ Y_4 &= C_4 + 3C_6 x^2 + 6C_8 x^4 + \ldots \\ Y_6 &= C_6 + 4C_8 x^2 + 10C_{10} x^4 + \ldots, \text{ etc.} \end{aligned}$$

$$\ldots\ldots\ldots\ldots\ldots\ldots\ldots\ldots\ldots\ldots \qquad [40]$$

Employing the summation notation, we will set

$$\sigma\gamma(\sigma) = \sum_{i=0}^{i=n} Y_{2i} y^{2i}$$

and observe that

$$-AD_0^2 \int_{y_0}^{y} \sigma\gamma(\sigma) dy = -AD_0^2 \sum_{i=0}^{i=n} \frac{Y_{2i} y^{2i+1}}{2i+1}\Bigg|_{y_0}^{y} \qquad [41]$$

in which it is recognized that Y_{2i} is a function of the parameter x.

In practice it is found advisable to change the constants $C_0, C_2, C_4, \ldots$, within a few levels of the atmosphere, in order to avoid an excessive number of terms.

Finally then, we can establish the equation for $\dot{y}$ as

$$\dot{y} = \left[\dot{y}_0 + \frac{B}{A}\right] \exp\left[-AD_0^2 \sum_{i=0}^{i=n} \frac{Y_{2i} y^{2i+1}}{2i+1}\Bigg|_{y_0}^{y} - AP\right] - \frac{B}{A} \qquad [42]$$

Thus given y and P (and the initial conditions $\dot{y}_0$ and y_0), $\dot{y}$ can be explicitly determined in closed form.

The computation with y as the independent variable proceeds by integrating

$$\tilde{\omega} = \tilde{\omega}_0 + \int_{y_0}^{y} \tilde{\omega}' \, dy \qquad [43]$$

$$x = x_0 + \int_{y_0}^{y} x' dy \qquad [44]$$

$$P = \int_{y_0}^{y} \frac{dP}{dy} \, dy \qquad [45]$$

where the initial value of P is set equal to zero.

Applications and Conclusions

The perturbation and computational approaches of the foregoing sections are justified only if they lead to faster and more accurate calculations. Consequently, other comparative calculations were performed in which the conventional integration of all the forces (Cowell's method) and the perturbation scheme were employed on the same problem. The problems chosen for analysis are discussed in (6 and 10), and the Runge-Kutta integration method coupled with the Adams correction procedure (7) was employed in the actual computations.

In every computation of this particular problem, the conventional calculations (even though their equations were slightly simpler and more symmetric) required from 3 to 10 times more computer time than did the perturbation computations; furthermore, the many extra integration steps involved in the nonperturbation methods caused a gradual accumulation of end figure error. It is concluded, therefore, that there exist definite advantages to the application of astronomical perturbation techniques to the computations of the return trajectories of space vehicles.

Acknowledgment

During the preparation of this paper, I have profited from many constructive suggestions, criticisms and ideas contributed by others. Professor Samuel Herrick of the Department of Astronomy of the University of California, Los Angeles, has given me many helpful suggestions, especially in regard to perturbation techniques, and has always encouraged and stimulated my work. Dr. Eric Durand of Aeronutronic Systems, Inc. made possible the early completion of this paper by allowing me to utilize the Aeronutronic computer, and by sponsoring much of my research. Prof. Dirk Brouwer carefully read through the manuscript.

References

1 Brouwer, D., "On the Accumulation of Errors in Numerical Integration," *Astronomical J.*, vol. XLVI, no. 16, 1937. pp. 149–153.

2 Herrick, S., "Astrodynamics," Van Nostrand (to be published 1959).

3 Moulton, F. R., "An Introduction to Celestial Mechanics," MacMillan Co., New York. 1914.

4 Baker, R. M. L., Jr., "Drag Interactions of Meteorites with the Earth's Atmosphere," unpublished paper presented at the Twentieth Meeting of the Meteoritical Society, Univ. of Calif., Los Angeles, Sept. 24, 1957.

5 Baker, R. M. L., Jr. and Charwat, A F., "Transitional Correction to the Drag of a Sphere in Free Molecule Flow," *Phys. Fluids*, vol. 1, no. 2, 1958, pp. 73–81; *see also* Baker, R. M. L., Jr., "Transitional Aerodynamic Drag of Meteorites," *Astrophysical J.*, May, 1959.

6 Baker, R. M. L., Jr., "Drag Interactions of Meteorites with the Earth's Atmosphere," Doctoral Dissertation, University of California, Los Angeles, May 1958; *see also* "Sputtering as It Is Related to Hyperbolic Meteorites," *J. Appl. Phys.*, April, 1959.

7 Adams, E., "A Method for Interval Control and Correction with Runge-Kutta Integration," in "Math. Tab. and Other Aids to Comp." (to be published).

8 Baker, R. M. L., Jr., "Encke's Method and Variation of Parameters as Applied to Reentry Trajectories," Proc. of Amer. Astronautical Soc., Western Regional Meeting, Aug. 18–19, 1958.

9 Herrick, S. and Baker, R. M. L., Jr., "Recent Advances in Astrodynamics," JET PROPULSION, vol. 28, no. 10, 1958, pp. 649–654.

10 Baker, R. M. L., Jr., "Accuracy Required for a Return from Interplanetary Voyages," to be published *J. Brit. Interplanet. Soc; see also* "Emphemeral Natural Satellites of the Earth," *Science*, vol. 128 no. 3333, Nov. 14, 1958.

11. Porter, J. G., "A Comparative Study of Perturbation Methods," *Astronomical J.*, vol. 63 no. 10, 1958, pp. 405-406; *see also* "Planetary Coordinates for the Years 1960-1980," Her Majesty's Stationery Office, London, pp. vii to xix.

12 Hodges, A. J., "The Drag Coefficient of Very High Velocity Spheres," *J. Aeron. Sci.*, vol. 24, no. 3, 1957, pp. 549-555.

Technical Notes

Thrust of a Conical Nozzle[1]

ELLIS M. LANDSBAUM[2]

Jet Propulsion Laboratory, California Institute of Technology, Pasadena, Calif.

The equations for calculating the thrust of a conical nozzle, originally presented by Malina, are reviewed. The correct use of the equations is demonstrated. The usual improper use of these equations results in a slight error. Although the error is negligible, the correct method should be more widely known.

THE THRUST obtained from a conical nozzle is usually represented by

$$F = \lambda \dot{m} v_e + (P_e - P_a)A_e \qquad [1]$$

where

$$\lambda = 1 + \cos\frac{\alpha}{2} \qquad [2]$$

and α is the half-angle of the expansion cone. The other symbols have their usual meaning and are further identified in the nomenclature. Malina[3] correctly presented the original derivation of both equations. Usually, the values of v_e and P_e, for use in Equation [1], are based on the plane area and the assumption of axial flow at the exit. This is incorrect, and, although the difference in values is not large, the correct values of v_e and P_e are based on the spherical area obtained from the assumption of radial flow at the exit. Since the above statements are not clear without reference to the derivation of the equations, the derivation, essentially as originally presented by Malina, is repeated in this paper.

Determination of Thrust

The thrust propelling a rocket may be related to the momentum and pressure forces acting in the axial direction at the nozzle exit and assuming uniform axial flow

$$F = \dot{m} v_e + (P_e - P_a)A_e \qquad [3]$$

As P_a the atmospheric pressure is unaffected by the flow conditions, it will be neglected in the remainder of the derivation.

At the exit of a conical nozzle, represented in Fig. 1, the flow conditions will be neither axial nor constant across nozzle exit A_p, and

$$F_v = \int [(\dot{M}_p v_p)_x + P_p]dA_p \qquad [4]$$

The variables cannot be integrated in closed form, and numerical integration is necessary. Since there is no net force

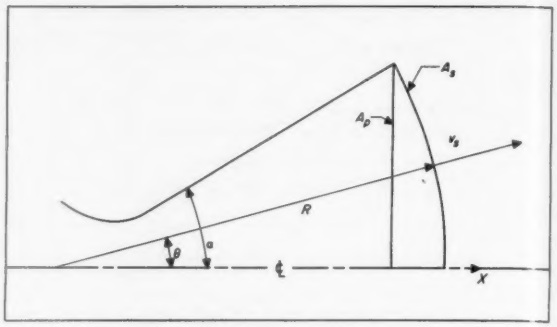

Fig. 1 Radial flow of a conical nozzle

across the control surfaces A_p and A_s, the thrust can also be determined by integrating across area A_s

$$F_v = \int [(\dot{M}_s v_s)_x + (P_s)_x]dA_s \qquad [5]$$

If radial flow is assumed to exist at the exit, along the spherical area A_s, the variables of Equation [5] are all constant, and the following equations can be written

$$\dot{M} = \frac{\dot{m}}{A_s} = \rho_s v_s \qquad [6]$$

$$(M_s v_s)_x = \rho_s v_s^2 \cos\theta \qquad [7]$$

$$(P_s)_x = P_s \cos\theta \qquad [8]$$

$$dA_s = 2\pi R^2 \sin\theta d\theta \qquad [9]$$

$$F_v = \int_0^\alpha [\rho_s v_s^2 + P_s]2\pi R^2 \sin\theta \cos\theta d\theta \qquad [10]$$

$$F_v = [\rho_s v_s^2 + p_s]\pi R^2 \sin^2\alpha \qquad [11]$$

$$A_p = \pi R^2 \sin^2\alpha \qquad [12]$$

$$F_v = \left[\dot{m} v_s \frac{A_p}{A_s} + P_s A_p\right] \qquad [13]$$

$$\frac{A_p}{A_s} = \frac{(1 + \cos\alpha)}{2} \qquad [14]$$

finally

$$F_v = \lambda \dot{m} v_s + P_s A_p \qquad [15]$$

or

$$F_v = \lambda(\dot{m} v_s + P_s A_s) \qquad [16]$$

It is evident that the values of v_e and P_e for use in Equation [1] are those which are related to the area A_s, not the area A_p.

The calculation of the thrust coefficient, for use in the following equation

$$F_v = C_{F_v} P_c A_t \qquad [17]$$

is then

$$(C_{F_v})_{A_p} = \frac{1 + \cos\alpha}{2}(C_{F_v})_{A_s}$$

Received Nov. 4, 1958.

[1] This paper presents the results of one phase of research carried out at the Jet Propulsion Laboratory, California Institute of Technology, under Contract no. DA-04-495-Ord 18, sponsored by the Department of the Army, Ordnance Corps.

[2] Research Engineer, Solid Rockets. Member ARS.

[3] Malina, F., "Characteristics of the Rocket Motor Unit Based on the Theory of Perfect Gases," *J. Franklin Inst.*, vol. 230, 1940, p. 433.

EDITOR'S NOTE: The Technical Notes and Technical Comments sections of ARS JOURNAL are open to short manuscripts describing new developments or offering comments on papers previously published. Such manuscripts are published without editorial review, usually within two months of the date of receipt. Requirements as to style are the same as for regular contributions (see masthead page).

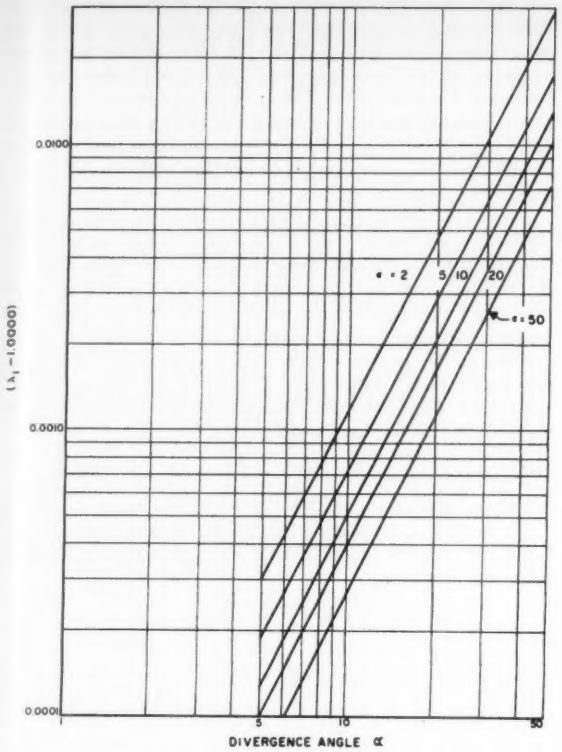

Fig. 2 Correction factor for divergence loss of a conical nozzle, $\gamma = 1.22$

It is readily seen that the use of equations such as

$$F_v = \lambda C_{F_v} P_c A_t \qquad [18]$$

or

$$F = \lambda C_F P_c A_t$$

where the thrust coefficients are calculated in the usual manner, results in a slightly greater error than does the incorrect use of Equation [1].

The correction term is a function of ϵ, α and γ, since the change in thrust coefficient between A_p and A_s is a function of these variables. In order to use the vacuum thrust coefficient, related to A_p, the following can be written

$$F_v = \lambda_1 \frac{(1 + \cos \alpha)}{2} (C_{F_v})_{A_p} P_c A_t$$

The value of λ_1 is presented in Fig. 2 as a function of the area ratio ϵ and expansion angle α for a gas with $\gamma = 1.22$. Decreasing γ results in a slight increase in λ_1. The parameter λ_1 represents the error resulting from the use of Equation [18].

Conclusions

If nozzle optimization is redone using the equations correctly, a nozzle of slightly smaller area ratio and slightly larger expansion angle will be obtained. Since the variation of λ_1 with ϵ and α is very small, the difference will probably not be noticeable. The error from neglecting λ_1 in determining the thrust of a conical nozzle is small over the range of exit areas and expansion angles usually of interest. This will result in a slightly more conservative design, since λ_1 is greater than one. However, one should be aware of the correct calculation for determining the thrust of a conical nozzle.

Nomenclature

- A = area
- C_F = thrust coefficient
- F = thrust
- M = mass flow per unit area
- $\dot{m}$ = mass flow
- P = absolute pressure
- v = velocity of exhaust gas
- α = expansion angle
- γ = specific heat ratio
- ϵ = area ratio
- λ = thrust coefficient correction term = $(1 + \cos \alpha)/2$
- λ_1 = thrust coefficient correction term
- ρ = density of gas

Subscripts

- a = atmosphere
- e = exit
- p = plane
- s = spherical
- v = vacuum

Determination of Transient Pressure Flow Relationship by Momentum Measurements[1]

EDWARD J. CROKE[2] and JERRY GREY[3]

Princeton University, Princeton, N. J.

A momentum-sensitive device was used to measure the transient flow rate through a rocket motor injector. The relationship between instantaneous pressure drop and flow rate was measured under conditions of artificially induced small sinusoidal oscillations at various frequencies. The observed phase shift of flow rate behind pressure drop agreed quite well with previous theoretical predictions (1,2),[4] but some discrepancy was observed between the predicted and observed amplitude ratios.

THE PROBLEM of instantaneous liquid flow rate measurement in transient systems has appeared many times in the literature. One rather specialized need for this measurement became apparent in 1952, in connection with rocket combustion instability studies, in which it was necessary to measure the instantaneous efflux of propellant from the injector orifices of a liquid propellant rocket motor. This need resulted in the experimental evaluation of a number of transient flowmeters (3), including various forms of electromagnetic, angular momentum, hotwire and pressure drop devices (e.g., see (4) for discussion). None of these schemes proved suitable, and a theoretical calculation was used to determine instantaneous flow rate from existing instantaneous pressure drop methods (1,2). This paper describes an experimental technique used to check the validity of the theoretical calculation.

Received Dec. 16, 1958.

[1] Part of a program under the direction of Professor L. Crocco, sponsored by U. S. Navy Bureau of Aeronautics, Contract NOas 53-817-c.

[2] Research assistant, Department of Aeronautical Engineering.

[3] Assistant Professor of Aeronautical Engineering. Member ARS.

[4] Numbers in parentheses indicate References at end of paper.

Apparatus

The experimental setup, shown schematically in Fig. 1, consisted of a pressurized water tank supplying a rocket injector through a cavitating venturi and a piston-type flow-modulating device. The water jet from the injector (actually a converging group of 12 individual jets) impinged on a T-shaped collector tube (see Fig. 1) so that the total axial momentum of the jet appeared as a thrust load on the collector. The collector was mounted on a cantilever beam to which four high sensitivity Baldwin C-7 strain gages were attached. Thus the strain gage signal was directly proportional to the instantaneous momentum of the jet. The measured natural frequency of the strain beam was 700 cps and hence was adequate for the 60 to 140 cps range of forcing frequencies used. The injector pressure drop was measured by a Li-Liu transducer located in the injector manifold (the injector exhausted to atmosphere; hence the pressure drop and manifold pressure were identical).

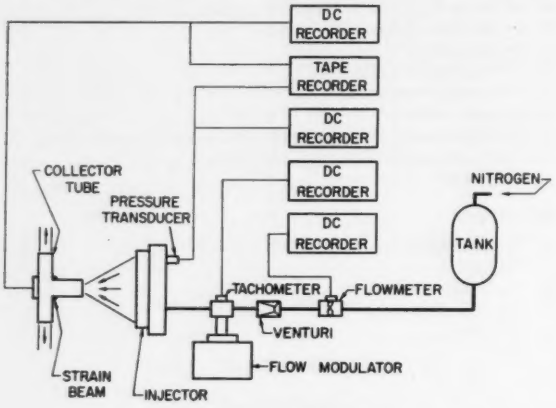

Fig. 1 Diagram of apparatus

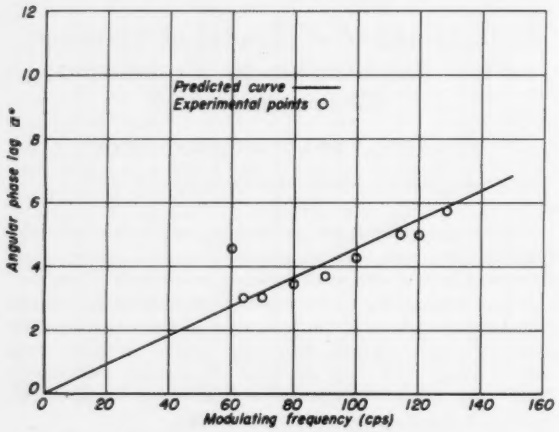

Fig. 2 Inertial phase lag vs. modulating frequency

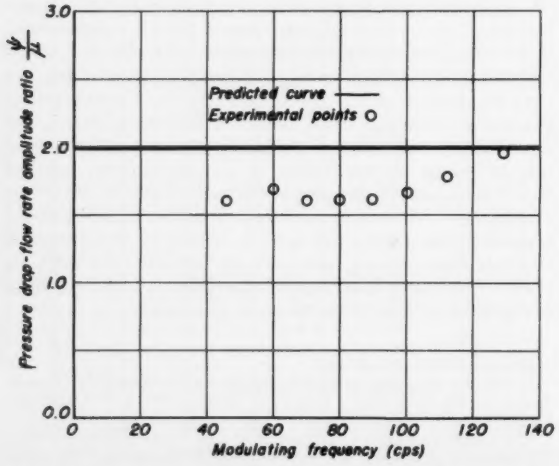

Fig. 3 Pressure drop-flow rate amplitude ratio vs. frequency

The tests consisted of varying the small amplitude sinusoidal forcing frequency produced by the flow modulator, and measuring the amplitude ratio and phase difference between the resulting flow and pressure drop signal oscillations. The fixed time displacement required for the steady-state flow component to traverse the distance between the injector orifice and the collector was obtained from turbine flowmeter and jet diameter measurements. Details of the apparatus development, final configuration, procedures, calibration techniques, etc., are included in detail in (5).

Discussion

It has been shown in (1,4, etc.) that for small sinusoidal oscillations of an incompressible fluid, the instantaneous fractional pressure drop ψ and the instantaneous fractional flow rate μ are related by

$$\frac{\psi}{\mu} = \frac{2}{\cos \alpha} e^{i\alpha}$$

where ψ and μ are defined by

$$\Delta p = \overline{\Delta p}(1 + \psi)$$

$$\dot{m} = \bar{\dot{m}}(1 + \mu)$$

The phase lag α of flow behind pressure drop results from the fluid inertia, and hence is a function of orifice dimensions, steady-state fluid velocities, and fluid density. Values of α, as computed theoretically (2) for the specific orifices used in the present experimental study, appear as the curve of Fig 2. The experimental values of α obtained from the apparatus of Fig. 1 agree quite well with the theoretical predictions of (1) and (2). Comparison of the theoretical and experimental amplitude ratios, shown in Fig. 3, indicate that the experimental values are somewhat low. However, it must be remembered that the amplitude might be expected to be rather sensitive to such indeterminate but consistent factors as location of the pressure pickup with respect to a true stagnation region, effect of oscillations on the velocity distribution in the jet and on entrainment of surrounding air, etc.

Conclusions

Measurement of transient liquid flow rates has been accomplished by the use of a momentum sensitive "flowmeter" at frequencies up to 140 cps.

The validity of the theoretical flow-pressure relationship for simple orifices (1,2) has been established by direct measurement of instantaneous flow rate and pressure for a specific configuration. Agreement between experimental and theoretical phase lags was excellent, but only fair correlation with predicted amplitudes was obtained.

References

1 Crocco, L. and Grey J., "Combustion Instability in Liquid Propellant Rocket Motors," Princeton University Aeronautical Engineering Report no. 216c, Appendix A, Jan. 1953.

2 Matthews, G. B., "Determination of Combustion Time Lag Parameters in a Liquid Bipropellant Rocket Motor," Princeton University Aeronautical Engineering Report no. 372, Appendix C, March 1957.

3 Davis, W. S., "Research on the Hot-Wire and a Momentum Sensitive Device for Transient Water Flow Phase Measurements," Princeton University Aeronautical Engineering Report (to be published).

4 Grey, J. and Liu, F. F., "Methods of Flow Measurement," JOURNAL OF THE AMERICAN ROCKET SOCIETY, vol. 23, May-June 1953, p. 133.

5 Croke, E. J., "Measurement of the Inertial Flow Phase Lag in an Orifice System by Means of a Momentum Sensitive Transient Flowmeter," Princeton University Aeronautical Engineering Report (to be published).

Similitude Treatment of Hypersonic Stagnation Heat Transfer[1]

DANIEL E. ROSNER[2]

AeroChem Research Laboratories, Inc., Princeton, N. J.

Using the "similarity" between heat and mass transport an expression for the convective heat transfer rate at the nose of a blunt body is developed for dissociated but "chemically frozen" laminar flow with arbitrary surface catalytic activity. The result is shown to be identical in structure with recent solutions to the boundary layer equations.

THE LAMINAR boundary layer equations for the case of hypersonic stagnation point flow with no gas phase atom recombination have been integrated by Lees (1)[3] and Fay and Riddell (2) for a "fully" catalytic surface, and by Goulard (3) and Scala (4) for surfaces of arbitrary catalytic activity. As an example, with the assumptions $\rho\mu$ = constant, $h_e \gg h_w$, Goulard gives the heat transfer rate as

$$\dot{q} = 0.664(\beta\rho_e\mu_e)^{1/2}(Pr_\lambda)^{-2/3}h_e\{1 + [(Le)^{2/3}\varphi - 1]\alpha_e Q/h_e\} \quad [1]$$

where the factor

$$\varphi = [1 + 0.664(k_w\rho_w)^{-1}(\beta\rho_e\mu_e)^{1/2}(Pr_D)^{-2/3}]^{-1} \quad [2]$$

is a correction for the fact that the steady-state atom concentration α_w at the wall need not, for all combinations of catalytic activity and flight conditions, be small compared to the value α_e at the outer edge of the boundary layer. The purpose of this note is to indicate that a result of identical structure may easily be obtained using an elementary chemical engineering approach to this problem. This simplified approach suggests applications to related problems (5) in the calculation of energy transfer rates in partially dissociated gases, using existing "low-speed" and "undissociated" heat transfer data.

Analysis

If we write the contribution due to ordinary conduction as

$$\dot{q}_\lambda = (St_\lambda)\rho_\infty U_\infty(\bar{h}_e - \bar{h}_w) \quad [3]$$

and the contribution due to atom diffusion to the wall as the product of the heat of recombination and the mass transfer rate

$$\dot{q}_D = Q(St_D)\rho_\infty U_\infty(\alpha_e - \alpha_w) \quad [4]$$

then the net heat transfer $\dot{q}$ will be the sum of these two rates. From similitude theory, we assume that the Stanton number St_D for mass transport is obtainable from the Stanton number St_λ for heat transport by making the replacement: $Pr_\lambda \rightarrow Pr_D$ (Pr_D is commonly referred to as the Schmidt number). This is asymptotically exact for the low-speed, constant property case when the free stream concentration of reactant is small compared to unity.

For a laminar flow at the blunt nose of a body of revolution St_λ can be approximated, for example, by Sibulkin's incompressible fluid formula (6), applied to the stagnation region behind the normal shock

$$St_\lambda = 0.763(\rho_\infty U_\infty)^{-1}(\beta\rho_e\mu_e)^{1/2}(Pr_\lambda)^{-0.6} \quad [5]$$

If the subscripts λ are replaced by D, we obtain the corresponding Stanton number for mass transport, which is then introduced into the diffusive contribution $\dot{q}_D$ to the net energy transfer. Furthermore, if the surface recombination kinetics are described by a first order rate law (3) of the form

$$\dot{R}_w = k_w\rho_w\alpha_w \quad [6]$$

then, in the steady state, the conservation equation for atoms at the gas-solid interface may be written

$$k_w\rho_w\alpha_w = 0.763(\beta\rho_e\mu_e)^{1/2}(Pr_D)^{-0.6}(\alpha_e - \alpha_w) \quad [7]$$

This relation may be considered to determine the "eigenvalue" of the atom concentration at the wall. If this value for α_w is introduced into the Equation [4] and use is made of the fact that the enthalpy h of the partially dissociated gas is comprised everywhere of the sum $\bar{h} + \alpha Q$, then the net heat transfer rate $\dot{q} = \dot{q}_\lambda + \dot{q}_D$ becomes

$$\dot{q} = 0.763(\beta\rho_e\mu_e)^{1/2}(Pr_\lambda)^{-0.6}(h_e - h_w)\{1 + \varphi[(Le)^{0.6} - 1] \times \alpha_e Q/(h_e - h_w)\} \quad [8]$$

where φ is again a correction factor of the form $\mathcal{C}/(1 + \mathcal{C})$; $\mathcal{C}$ being the relevant "catalytic parameter" (7)

$$\mathcal{C} = k_w\rho_w[0.763(\beta\rho_e\mu_e)^{1/2}(Pr_D)^{-0.6}]^{-1} \quad [9]$$

This result should be compared to Goulard's result (Eq. [1]) the latter being based upon the assumption of a highly cooled wall ($h_e \gg h_w$). It is observed that when the complete driving force ($h_e - h_w$) is retained in place of just h_e, the catalytic correction factor φ should modify the entire term ($Le^{0.6} - 1$) and not just the Lewis number term. This can be verified by checking the reasonableness of the limiting case $\varphi \rightarrow 0$, since $\dot{q}$ must approach $\dot{q}_\lambda$ in the absence of surface catalysis.[4]

By way of further comparison, the "fully" catalytic wall investigated by Fay and Riddell (2) corresponds to the limiting case $\varphi \rightarrow 1$. It is interesting then to write down the suggested correlation equation which best represented their numerical integrations

$$\dot{q} = 0.763\left(\frac{\rho_w\mu_w}{\rho_e\mu_e}\right)^{0.1}(\beta\rho_e\mu_e)^{1/2}(Pr_\lambda)^{-0.6}(h_e - h_w) \times \left\{1 + [(Le)^{0.63} - 1]\frac{\alpha_e Q}{h_e}\right\} \quad [10]$$

Upon setting φ in Equation [8] equal to unity, and comparing the result with Equation [10] it will be noted that, apart from the correction factor for variable $\rho\mu$, these equations are virtually identical. Since detailed calculations indicate that, at most, $\rho\mu$ at the wall is five times the value at the outer edge of the boundary layer, the fact that this ratio is raised to the $1/10$ power in Equation [10] makes the corresponding correction of the order of only 5 per cent.

It appears then that relatively simple techniques of the type adopted here, guided by some "exact" numerical results for extreme cases, can provide a realistic approach to related problems. Conversely, these techniques should facilitate the "correlation" of machine calculations.

Nomenclature

- $\mathcal{C}$ = catalytic parameter (Eq. [9])
- $\bar{h}$ = sensible or "frozen" enthalpy of the mixture
- h = enthalpy of the mixture
- k_w = rate constant for surface atom recombination
- Le = "frozen" Lewis number ($Le = Pr_\lambda/Pr_D$), assumed constant
- Pr = "frozen" Prandtl number, assumed constant
- $\dot{q}$ = heat transfer rate
- Q = heat of recombination, assumed constant
- $\dot{R}_w$ = mass rate of atom recombination at surface
- St = Stanton number

Received Dec. 15, 1958.

[1] This research was supported by the United States Air Force through the Air Force Office of Scientific Research of the Air Research and Development Command under Contract no. AF 49-(638)-300.

[2] Research Scientist. Member ARS.

[3] Numbers in parentheses indicate References at end of paper.

[4] Note that in this limiting process $(h_e - h_w) \rightarrow (\bar{h}_e - \bar{h}_w)$ since $\alpha_w \rightarrow \alpha_e$.

U = fluid velocity relative to body
α = mass fraction of atoms in mixture
β = inviscid velocity gradient at the nose
ρ = density of fluid
μ = absolute viscosity of fluid

Subscripts

∞ = before normal shock
e = at outer edge of the boundary layer
w = at the wall (surface of body)
λ = pertaining to thermal conduction
D = pertaining to concentration diffusion

References

1 Lees, L., "Laminar Heat Transfer Over Blunt-Nosed Bodies at Hypersonic Flight Speeds," JET PROPULSION, vol. 26, April 1956, pp. 259–269.
2 Fay, J. A. and Riddell, F. R., "Theory of Stagnation Point Heat Transfer in Dissociated Air," *J. Aeron. Sci.*, vol. 25, no. 2, Feb. 1958, p. 73.
3 Goulard, R. J., "On Catalytic Recombination Rates in Hypersonic Stagnation Heat Transfer," JET PROPULSION, vol. 28, no. 11, Nov. 1958, pp. 737–745.
4 Scala, S. M., "Hypersonic Heat Transfer to Surfaces Having Finite Catalytic Efficiency," General Electric Co., Aerophysics Laboratory Research Memorandum 4, M.O.S.D. 57SD646, July 1957.
5 Rosner, D. E., "Steady Surface Temperature in Dissociated High-Speed Gas Flows," AeroChem Research Laboratories, Inc., TP-9, Dec. 3, 1958. To appear in *J. Aero/Space Sci.*
6 Sibulkin, M., "Heat Transfer Near the Forward Stagnation Point of a Body of Revolution," *J. Aeron. Sci.*, vol. 19, no. 8, Aug. 1952, pp. 570–571.
7 Rosner, D. E., "Chemical Frozen Boundary Layers with Surface Reaction," Princeton University, Aeronautical Engineering Report no. 419, March 1958. To appear in *J. Aero/Space Sci.*

Motion Units to Simplify Space Travel Computations

BEMROSE BOYD[1]

General Motors Corp., Milwaukee, Wisc.

UNDER the special conditions of constant acceleration and zero initial velocity, we have

$$V = at \qquad [1]$$

This is a basic mathematical relationship and is valid in any consistent set of units. It can be nondimensionalized by use of a reference velocity V_r

$$\frac{V}{V_r} = \frac{at}{V_r} \qquad [2]$$

Furthermore, the quantities can be expressed in arbitrary units if proper conversion factors are incorporated

$$V' = K_1 V \qquad [3a]$$

$$a' = K_2 a \qquad [3b]$$

$$t' = K_3 t \qquad [3c]$$

$$\frac{V'}{V_r} = \frac{K_1}{K_2 K_3 V_r} a't' = Ka't' \qquad [4]$$

If V_r is chosen to be the velocity of light, and a' is measured in units of Earth gravity and t' in years, the composite coefficient K has the numerical value 1.03. Thus, within an accuracy of 3 per cent, the original equation (Eq. [1]) is valid in these units with V replaced by the ratio V'/V_r

$$\frac{V'}{V_r} \cong a't' \qquad [5]$$

The ratio V'/V_r might be given a designation such as "lux number" in analogy to Mach number.

Equation [5] shows that, except for relativistic effects, an acceleration of 1 g applied continuously for one year would bring a body up to the velocity of light. Similarly an acceleration of 10^{-3} g for one year or 1 g for 10^{-3} year (8.8 hr) would produce a terminal velocity of this fraction (10^{-3}) of the velocity of light, or 670,000 mph. Considering the velocity of light as a fundamental limitation on a physical system, the above relationship facilitates an understanding of values of thrust and travel time required for various space travel missions.

These units of generalized velocity, acceleration and time which lead to the simplified form of Equation [5] are particularly useful in conjunction with distances expressed in light-years as is done in some areas of astronomical usage. The mean distance of the Earth from the sun is 1.58×10^{-5} light-years (8.3 light-min), and the distance to Pluto, the farthest planet, is 6.26×10^{-4} light-years (5.6 light-hr), whereas the distance to Proxima Centauri, one of the nearest stars, is 4.3 light-years.

It is evident that there is a big step between the minor planets (Mercury, Venus, Earth, Mars) and the major planets (Jupiter, Saturn, Uranus, Neptune, Pluto), and a much greater step between the limits of the solar system and any stellar or extra-solar body. All space travel is presently acceleration-limited by virtue of thrust limitation. To the extent that this limitation is removed by developments in nuclear propulsion or utilization of radiation, travel outside the solar system will be velocity-limited. Travel within the solar system might continue to be acceleration-limited as a result of practical considerations of human tolerances, economics, etc.

Received Dec. 15, 1958.

[1] Research Associate, Advanced Design and Development Department.

A Short Form Method for Determining Near-Circular Orbit Quantities

JOSEPH N. BENEZRA[1]

Boeing Airplane Co., Seattle, Wash.

A method is presented that allows quick and accurate determination of the precision with which a satellite must be injected into a "near-circular" orbit so that apogee and perigee remain within preselected limits. Various orbital quantities of interest are presented as functions of injection velocity and attitude "errors," given the injection altitude. The sensitivities of these orbital quantities to velocity or attitude errors are given as functions of the errors themselves and the injection altitude.

GIVEN the injection altitude of a satellite, it is possible to determine the effect of velocity and attitude injection errors on various orbital quantities, such as perigee and apogee velocities and altitudes, period, etc. (By "errors" is meant simply the differences ΔV, ψ between the injection quantities of velocity and attitude and those corresponding to a circular orbit at the injection altitude.) Singer (1)[2] has done this rigorously for apogee and perigee altitudes. Jensen (2) briefly discusses by numerical example the sensitivity of apogee and perigee altitudes as well as orbit period to injection errors. Both Jensen (2) and Arnowitz (3) deal with the question of injection errors which can be tolerated in order to restrain the satellite to orbit within specified apogee and perigee limits.

Received March 18, 1958.

[1] Aerodynamics Engineer, Pilotless Aircraft Division. Member ARS.

[2] Numbers in parentheses indicate References at end of paper.

The short form presented here is obtained by applying standard perturbation techniques to basic equations. It has the advantage of expressing the orbit quantities listed below and their sensitivity to injection errors as explicit functions of the injection errors and injection altitude:

Eccentricity, semimajor axis, period, energy per unit mass.

Velocity and altitude at apogee and perigee.

Method

An expression for orbit eccentricity in terms of injection conditions is (see Fig. 1)

$$\epsilon = \left[1 - 2\frac{V^2}{V_c^2}\left(1 - \frac{V^2}{2V_c^2}\right)\cos^2\psi\right]^{1/2} \qquad [1]$$

Applying standard perturbation technique by letting $V = V_c + \Delta V$ and $\cos^2\psi \cong 1 - \psi^2$ it can be easily shown that Equation [1] becomes

$$\epsilon \cong \left[\psi^2 + 4\left(\frac{\Delta V}{V_c}\right)^2\right]^{1/2} \qquad [2]$$

where

$$V_c = \left(\frac{gR^2}{r}\right)^{1/2}$$

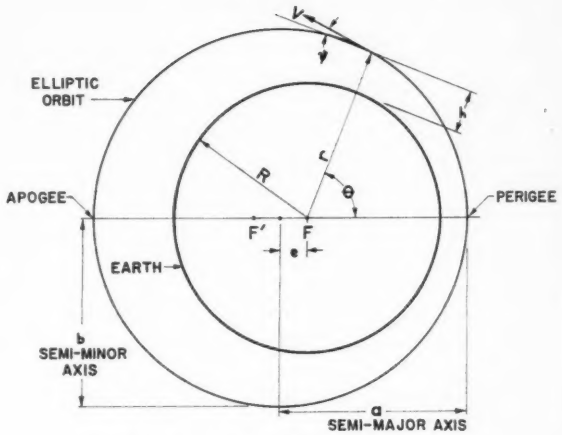

Fig. 1 Elliptic orbit characteristics

Table 1 Expressions for near-circular orbit quantities

Quantity	$\Delta V \neq 0, \psi \neq 0$ General case	$\Delta V = 0, \psi = 0$ Circular orbit
ϵ	$\left[\psi^2 + 4\left(\frac{\Delta V}{V_c}\right)^2\right]^{1/2}$	0
$\frac{b}{a}$	$\left[1 - \psi^2 - 4\left(\frac{\Delta V}{V_c}\right)^2\right]^{1/2}$	1
$\frac{h_A}{R}$	$\left(1 + \frac{h}{R}\right)\left(1 + 2\frac{\Delta V}{V_c}\right)(1 - \psi^2)(1 + \epsilon + \epsilon^2) - 1$	$\frac{h}{R}$
$\frac{h_P}{R}$	$\left(1 + \frac{h}{R}\right)\left(1 + 2\frac{\Delta V}{V_c}\right)(1 - \psi^2)(1 - \epsilon + \epsilon^2) - 1$	$\frac{h}{R}$
$\frac{V_A}{V_c}$	$\left(1 - \frac{\Delta V}{V_c}\right)\left(1 + \frac{\psi^2}{2}\right)(1 - \epsilon)$	$1 = \frac{1}{V_c}\left(\frac{gR}{1 + \frac{h}{R}}\right)^{1/2}$
$\frac{V_P}{V_c}$	$\left(1 - \frac{\Delta V}{V_c}\right)\left(1 + \frac{\psi^2}{2}\right)(1 + \epsilon)$	1
$\frac{V_P}{V_A} = \frac{\frac{h_A}{R} + 1}{\frac{h_P}{R} + 1}$	$1 + 2\epsilon + 2\epsilon^2$	1
$\frac{V_P - V_A}{V_c}$	$2\left(1 - \frac{\Delta V}{V_c}\right)\left(1 + \frac{\psi^2}{2}\right)\epsilon$	0
$\frac{h_A}{h_P}$	$\frac{2\left(1 + \frac{h}{R}\right)\epsilon}{\left(1 + \frac{h}{R}\right)\left(1 + 2\frac{\Delta V}{V_c}\right)(1 - \psi^2)(1 - \epsilon + \epsilon^2) - 1} + 1$	1
$\frac{h_A - h_P}{R}$	$2\left(1 + \frac{h}{R}\right)\left(1 + 2\frac{\Delta V}{V_c}\right)(1 - \psi^2)\epsilon$	0
$\frac{a}{R}$	$\left(1 + \frac{h}{R}\right)\left[1 + 2\frac{\Delta V}{V_c} + 5\left(\frac{\Delta V}{V_c}\right)^2\right]$	$1 + \frac{h}{R}$
$\frac{T}{T_c}$	$\left[1 + 3\frac{\Delta V}{V_c} + 9\left(\frac{\Delta V}{V_c}\right)^2\right]$	$1 = \frac{2\pi\left(\frac{R}{g}\right)^{1/2}\left(1 + \frac{h}{R}\right)^{3/2}}{T_c}$
$\frac{E}{E_c}$	$\left[1 + \frac{2\frac{\Delta V}{V_c} + \left(\frac{\Delta V}{V_c}\right)^2}{1 + 2\frac{h}{R}}\right]$	$1 = \frac{\frac{gR}{2}\left(1 + \frac{h}{R + h}\right)}{E_c}$

Table 2 Sensitivities of near-circular orbit quantities

Derivative	$\Delta V \neq 0,\ \psi \neq 0$ General case	Derivative	$\Delta V \neq 0,\ \psi \neq 0$ General case
$\frac{\partial \epsilon}{\partial \psi}$	$\frac{\psi}{\epsilon}$	$\frac{\partial (V_P/V_A)}{\partial (\Delta V/V_c)}$	$8\left(\frac{\Delta V}{V_c}\right)\left(\frac{1}{\epsilon}+2\right)$
$\frac{\partial \epsilon}{\partial (\Delta V/V_c)}$	$\frac{4(\Delta V/V_c)}{\epsilon}$	$\frac{\partial (V_P/V_A)}{\partial \psi}$	$2\psi\left(\frac{1}{\epsilon}+2\right)$
$\frac{\partial (h_A/R)}{\partial (\Delta V/V_c)}$	$\left(1+\frac{h}{R}\right)\left\{2(1+\epsilon+\epsilon^2)+4\left(\frac{1}{\epsilon}+2\right)\left[\frac{\Delta V}{V_c}+2\left(\frac{\Delta V}{V_c}\right)^2\right]\right\}$	$\frac{\partial (h_A/h_P)}{\partial (\Delta V/V_c)}$	$8\left(\frac{1}{h/R}+1\right)\frac{\Delta V/V_c}{\epsilon}$
$\frac{\partial (h_P/R)}{\partial (\Delta V/V_c)}$	$\left(1+\frac{h}{R}\right)\left\{2(1-\epsilon+\epsilon^2)-4\left(\frac{1}{\epsilon}-2\right)\left[\frac{\Delta V}{V_c}+2\left(\frac{\Delta V}{V_c}\right)^2\right]\right\}$	$\frac{\partial (h_A/h_P)}{\partial \psi}$	$2\left(\frac{1}{h/R}+1\right)\frac{\psi}{\epsilon}$
$\frac{\partial (h_A/R)}{\partial \psi}$	$\left(1+\frac{h}{R}\right)\left(1+2\frac{\Delta V}{V_c}\right)\frac{\psi}{\epsilon}$	$\frac{\partial (h_A/R - h_P/R)}{\partial (\Delta V/V_c)}$	$4\left(1+\frac{h}{R}\right)\left[\frac{2(\Delta V/V_c)}{\epsilon}\left(1+2\frac{\Delta V}{V_c}\right)+\epsilon\right]$
$\frac{\partial (h_P/R)}{\partial \psi}$	$-\left(1+\frac{h}{R}\right)\left(1+2\frac{\Delta V}{V_c}\right)\frac{\psi}{\epsilon}$	$\frac{\partial (h_A/R - h_P/R)}{\partial \psi}$	$2\left(1+\frac{h}{R}\right)\left(1+2\frac{\Delta V}{V_c}\right)\frac{\psi}{\epsilon}$
$\frac{\partial (V_A/V_c)}{\partial (\Delta V/V_c)}$	$\frac{4(\Delta V/V_c)}{\epsilon}\left(\frac{\Delta V}{V_c}-1\right)+\epsilon-1$	$\frac{\partial (V_P/V_c - V_A/V_c)}{\partial (\Delta V/V_c)}$	$4\left[\frac{2(\Delta V/V_c)}{\epsilon}\left(1+2\frac{\Delta V}{V_c}\right)+\epsilon\right]$
$\frac{\partial (V_P/V_c)}{\partial (\Delta V/V_c)}$	$-\frac{4(\Delta V/V_c)}{\epsilon}\left(\frac{\Delta V}{V_c}-1\right)+\epsilon+1$	$\frac{\partial (V_P/V_c - V_A/V_c)}{\partial \psi}$	$2\left(1+2\frac{\Delta V}{V_c}\right)\frac{\psi}{\epsilon}$
$\frac{\partial (V_A/V_c)}{\partial \psi}$	$-\left(1-\frac{\Delta V}{V_c}\right)\frac{\psi}{\epsilon}$	$\frac{d(a/R)}{d(\Delta V/V_c)}$	$2\left(1+\frac{h}{R}\right)\left(1+5\frac{\Delta V}{V_c}\right)$
$\frac{\partial (V_P/V_c)}{\partial \psi}$	$\left(1-\frac{\Delta V}{V_c}\right)\frac{\psi}{\epsilon}$	$\frac{d(T/T_c)}{d(\Delta V/V_c)}$	$3\left(1+6\frac{\Delta V}{V_c}\right)$
$\frac{d(V_P/V_A)}{d\epsilon}$	$2(1+2\epsilon)$	$\frac{d(E/E_c)}{d(\Delta V/V_c)}$	$\frac{2}{1+2(h/R)}\left(1+\frac{\Delta V}{V_c}\right)$

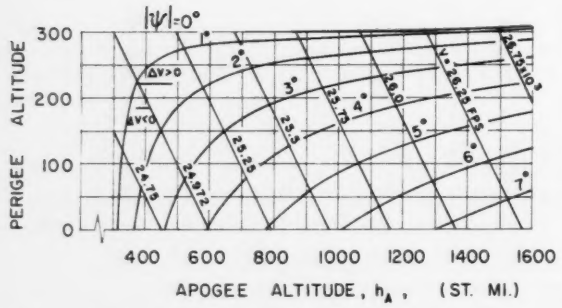

Fig. 2a Effect of injection velocity V and attitude ψ on apogee and perigee altitudes; injection at 300 statute miles altitude

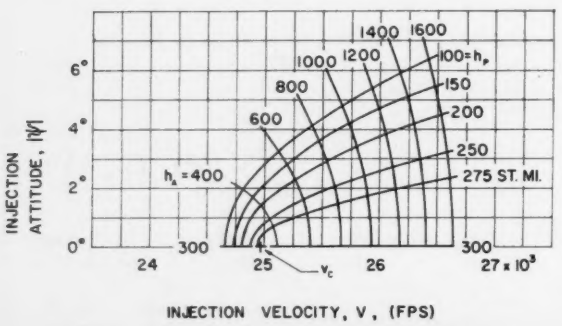

Fig. 2b Concluded—injection at 300 statute miles

From the polar equation of the ellipse and conservation of moment of momentum we obtain for the apogee and perigee altitudes

$$h_p^A = \frac{r^2V^2\cos^2\psi}{gR^2(1 \mp \epsilon)} - R \qquad [3]$$

Again, letting $V = V_c + \Delta V$, etc., Equation [3] becomes

$$\frac{h_p^A}{R} \cong \left(1+\frac{h}{R}\right)\left(1+2\frac{\Delta V}{V}\right)(1-\psi^2)(1 \pm \epsilon + \epsilon^2) - 1 \qquad [4]$$

If $\psi = 0$, Equation [4] shows immediately that perigee occurs at injection when $\Delta V > 0$, and that apogee occurs at injection when $\Delta V < 0$. It is interesting to note that when $\Delta V = 0$, $\psi \neq 0$ injection is automatically at one end of the minor axis.

Since

$$a = \frac{rgR^2}{2gR^2 - rV^2} \qquad [5]$$

and $V^2 = V_c^2 = gR^2/r$, it follows that $r = a$, which can occur at only two points on the ellipse, i.e., at either end of the minor axis.

From Equations [2 and 4], it is possible to plot curves of apogee as a function of perigee altitude showing lines of constant injection attitude and velocity. Alternately, curves may be plotted of injection attitude as a function of injection velocity (given the injection altitude) for constant values of apogee and perigee altitude. These plots are shown in Figs. 2a and 2b for an injection altitude of 300 statute miles. From the curves, tolerances may be established on injection attitude and velocity when apogee and perigee are held within designated limits.

Results

Summarized in Table 1 are quantities pertaining to near-circular orbits expressed in dimensionless form as functions of injection errors in velocity and attitude. Those involving apogee and perigee velocities are derived from Equations [3 and 4]. The expression for semimajor axis a may be derived from [5], whence follows the expressions for orbit period using Kepler's Third Law. It will be noted that the expression for orbit period depends only upon the velocity and altitude at injection, as would be expected.

By differentiating the expressions in Table 1 with respect to either attitude or velocity error, the sensitivities are obtained; these have been tabulated in Table 2.

Accuracy

This scheme of determining various orbit quantities should be sufficiently accurate for preliminary performance work. As the injection errors (or eccentricity) become smaller, the accuracy improves; this is apparent from Fig. 2a. It may be seen that for small positive velocity injection errors, perigee occurs at the injection altitude for zero attitude error. However, as the velocity error increases, perigee is seen to occur slightly above the injection altitude. Rigorously, of course, perigee occurs precisely at injection altitude regardless of the magnitude of the injection velocity ($V > V_c$). A quick indication of the relative accuracy of the method may be had from the following examples:

Suppose a satellite is injected with $\psi = 0.07$ rad; $V = 26{,}000$ fps; $h = 300$ statute miles. The circular velocity at this altitude $V_c = 24{,}972$ fps. From Equation [1], $\epsilon = 0.1092$. The approximate expression, Equation [2], gives $\epsilon \cong 0.1081$. The discrepancy between the two is -1.0 per cent.

It is instructive to consider another example. The Naval Research Laboratory reported that the Army's first Explorer satellite, on the basis of its first 32 runs around the Earth, goes out as far as 1587 statute miles and comes in as close as 219 miles. From these figures the velocities at apogee and perigee may be computed using Kepler's laws; they are 20,282 fps and 26,938 fps, respectively. The period is 114.818 min. To obtain the corresponding figures from the approximate method, the eccentricity of the orbit is first computed.

From Table 1, $(h_A/R + 1)/(h_P/R + 1) \cong 1 + 2\epsilon + 2\epsilon^2$, whence $\epsilon \cong 0.1426$.[3] Since actual injection data are not known, it may be assumed for computation purposes that injection takes place anywhere between apogee and perigee. For simplicity, assume that injection occurs at perigee. The circular orbit velocity at this altitude is 25,214 fps. From Table 1

$$V_P^A \cong V_c\left(1 - \frac{\epsilon}{2}\right)(1 \mp \epsilon)$$

giving 20,078 fps and 26,756 fps for apogee and perigee velocity, respectively. Again from Table 1

$$T \cong T_c\left(1 + \frac{3}{2}\epsilon + \frac{9}{4}\epsilon^2\right) = 115.16 \text{ min}$$

where

$$T_c = 2\pi\left(\frac{R}{g}\right)^{1/2}\left(1 + \frac{h_P}{R}\right)^{3/2} = 91.419 \text{ min}$$

the period of a circular orbit at perigee altitude. Comparing the results of the approximate and rigorous methods we find:

discrepancy in $V_A = -1.01$ per cent
discrepancy in $V_P = -0.68$ per cent
discrepancy in $T = +0.30$ per cent

Higher order terms have been retained in the expression presented in both Tables 1 and 2 because, in general, they enhance the accuracy of the results in case the injection errors may not be, mathematically speaking, small. The expressions may be further simplified at the discretion of the user.

[3] The eccentricity may be determined directly in this example from the relationship $\epsilon = (r_A - r_P)/(r_A + r_P) = 0.1409$. Using this slightly more accurate value of ϵ the resulting discrepancies in V_A, V_P and T are even less.

Nomenclature

a	=	semimajor axis
b	=	semiminor axis
e	=	linear eccentricity $[a^2 - b^2]^{1/2}$
E	=	total energy per unit mass; zero potential energy reference at Earth's surface
F, F'	=	foci of ellipse
g	=	acceleration of gravity at Earth's surface, 32.174 fps^2 at 45 deg latitude
h	=	injection altitude, orbit altitude
r	=	injection radius
R	=	Earth's radius, 20.855×10^6 ft at 45 deg latitude
T	=	orbit period
V	=	injection velocity, orbital velocity
ΔV	=	velocity excess or defect, $V - V_c$
ϵ	=	eccentricity, $[1 - (b/a)^2]^{1/2}$
θ	=	geocentric angle
ψ	=	injection attitude, orbit direction angle (angle formed by tangent line to orbit and local horizontal)

Subscripts

A	=	apogee
c	=	circular orbit corresponding to injection altitude
P	=	perigee
^A_P	=	apogee, perigee

References

1 Singer, S. F., "Studies of a Minimum Orbital Unmanned Satellite of the Earth (MOUSE), Part II: Orbits and Lifetimes of Minimum Satellites," *Astronautica Acta*, vol. II, no. 3, 1956, pp. 125–144.

2 Jensen, Jorgen, "Satellite Ascent Mechanics," Jet Propulsion, vol. 26, no. 5, May 1956, p. 359.

3 Arnowitz, Leonard, "The Vanguard Control System," Astronautics, vol. 2, no. 3, Oct. 1957, pp. 34–35.

General Equation for Rocket Velocity

SYLVAN RUBIN[1]

Stanford Research Institute, Menlo Park, Calif.

IT HAS been suggested that high rocket velocities can be attained by means of propulsion systems producing very high exhaust velocities, such as ion propulsion. In comparison with conventional chemical rocket motors, such systems introduce two new independent variables:

1 The exhaust velocity may be varied, independently of the specific energy of the fuel.

2 The fuel and the propellant may be different materials, with different masses and rates of consumption.

An equation for the final velocity of a rocket using any propulsion system is derived, in terms of the exhaust velocity, the specific energy of the fuel, and the mass ratios of fuel and propellant to the rocket mass at burnout. The calculation is made for a single stage rocket.

It is shown that the final rocket velocity is a maximum when the exhaust velocity is equal to the fuel kinetic velocity. Since the fuel kinetic velocity is approximately equal to the exhaust velocity of a conventional rocket motor using the same fuel, the conventional motor yields the maximum rocket velocity for a given fuel. In other words, the specific impulse of the propellant should be matched to the specific impulse of the fuel.

For exhaust velocities greater than the fuel kinetic velocity, the *final rocket velocity is inversely proportional to the exhaust velocity.*

Received Dec. 22, 1958.

[1] Senior Physicist, Physics Dept.

Assumptions

1 The exhaust velocity is freely variable, independent of the fuel properties, but constant throughout the propulsion phase.

2 All the fuel and propellant to be used are initially loaded in the rocket, and they are consumed in a constant proportion, equal to their initial loading ratio, so that both are completely consumed at the end of the propulsion phase. It should be noted that all or part of the used fuel may be used for propellant. Therefore, the propellant mass defined in the equations is only the initially inert portion of the propulsive material.

3 Used fuel, if not expelled as propellant, is jettisoned continuously during the propulsion phase.

4 The exhaust jet is unidirectional, with no momentum going into lateral or divergent flow velocity components.

5 Gravitational and drag forces are neglected.

Calculation

The equations for the differential momentum balance and for the conversion of fuel energy to kinetic energy are most readily stated in a coordinate system momentarily stationary with respect to the rocket.

$$\text{Momentum: } -c\,dp = d[(M + p + f)V] = (M + p + f)dV \quad [1]$$

$$\text{Energy: } -dE = e\,df = \frac{1}{2}c^2\,dp \quad [2]$$

Combining the above equations

$$dV = -\frac{2e\,df}{c(M + p + f)} \quad [3]$$

Since fuel and propellant are used in a constant ratio

$$p + f = \alpha f$$

where

$$\alpha = 1 + (P/F)$$

$$V_b = -\frac{2e}{c}\int_F^0 \frac{df}{(M + \alpha f)} = \frac{2e}{c\alpha}\ln\frac{M + \alpha F}{M} = \frac{v_k^2}{c}\left(\frac{R_f}{R_p + R_f}\right)\ln(1 + R_p + R_f) \quad [4]$$

It is evident that if no further restrictions are applied, the burnout velocity will generally be inversely proportional to the exhaust velocity, and proportional to the square of the fuel kinetic velocity. However, for most rockets of practical interest, there will be further restrictions, so that this general equation must be considered to give an upper limit to the possible burnout velocity.

The simplest restriction is obtained for a conventional chemical rocket, where the fuel and propellant are identical. In this case $c = v_k$, and $\alpha = 1$, giving the conventional equation for burnout velocity.

A very important restriction applies to all cases in which $c < v_k$, arising from the necessity for supplying enough inert propellant mass to carry off all the energy as kinetic energy. The minimum additional inert propellant P is given by the equation for energy balance

$$\frac{1}{2}F v_k^2 = \frac{1}{2}(F + P)c^2$$

On substituting this restriction into Equation [4]

$$V_b = c\ln(1 + R_p + R_f) \quad [5]$$

which is again identical with the equation for a chemical rocket. This gives a smaller upper limit to burnout velocity than Equation [4] for $c < v_k$.

These two limiting curves for burnout velocity correspond to the two conditions of: (a) limited total energy and more than sufficient propellant mass; (b) limited propellant mass and more than sufficient energy. Because of the way v_k is defined, the transition point between these two conditions occurs at $c = v_k$, where the two limiting curves intersect. If additional mass or additional energy could be obtained in flight, it would be possible to continue on the ascending branch of the corresponding curve to a higher burnout velocity, but without such a process, the maximum possible burnout velocity occurs at $c = v_k$.

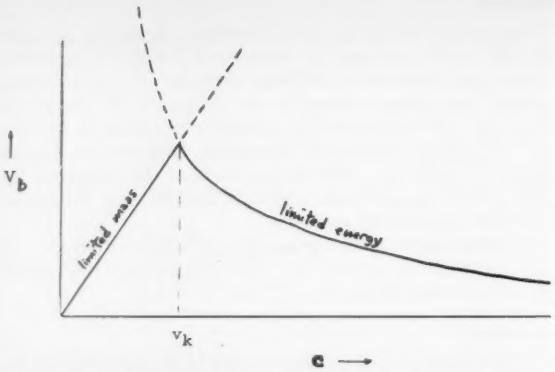

Fig. 1 Upper limits to rocket burnout velocity V_b as a function of varying exhaust velocity c for a fixed fuel kinetic velocity v_k. For any value of c, the lowest limit is the actual limit, indicated by the solid line

Conclusions

It is evident that the greatest final velocity will be given to a rocket if the specific impulse of the propellant is equal to the specific impulse of the fuel.

The physical reasons for this behavior are quite obvious, after one has the equations. In the high exhaust velocity region, increasing exhaust velocity causes a greater fraction of the available energy to be expended on the propellant, and correspondingly less supplied to the rocket. This is also pointed out by Oberth[2] showing that impulse is *inversely* proportional to particle velocity for a given energy input. In the low velocity region, reduction of exhaust velocity is accomplished essentially by diluting the fuel with inert propellant, which obviously can only diminish the rocket velocity.

Burning a chemical fuel in a conventional rocket motor is the most efficient propulsion system for obtaining maximum rocket velocity from that particular fuel. Ion propulsion systems are useful for utilization of high energy fuels which cannot be directly burned, such as nuclear fuels. The ion velocity must equal the fuel kinetic velocity to obtain maximum effectiveness. For example, the kinetic velocity corresponding to full utilization of the fission energy of pure U^{235} is 1.2×10^9 cm per sec (about 0.7 Mev per nucleon).

These results do not apply, of course, to space vehicles designed to obtain energy from their environment during propulsion, as by means of solar batteries or solar radiation pressure.

Nomenclature

- c = exhaust velocity
- V = rocket velocity (variable)
- V_b = final rocket velocity
- e = specific energy of fuel (available work per unit mass)
- v_k = kinetic velocity of fuel, defined by $e = \frac{1}{2}v_k^2$
- E = energy supplied by fuel (variable)
- M = rocket mass (less fuel and propellant)
- f = remaining fuel mass (variable)
- F = total fuel mass
- p = remaining propellant mass (variable)
- P = total propellant mass
- R_f = F/M (fuel-mass ratio)
- R_p = P/M (propellant-mass ratio)

[2] Oberth, H., "Wege Zur Raumschiffahrt," Oldenbourg, Munich, 3rd ed., 1929, p. 410, Equation 237.

Technical Comments

Reply to Crocco's Criticism of the Zucrow-Osborn Paper

M. J. ZUCROW[1] and J. R. OSBORN[2]

Purdue University, Lafayette, Ind.

IN THE December 1958 issue of JET PROPULSION there appeared a Technical Note hereafter designated as Reference (1).[3] The authors of (1) presented the results they obtained from an experimental study of combustion pressure oscillations of the longitudinal mode. They conducted their experiments with an approximately 250-lb thrust liquid propellant rocket motor burning 95 per cent ethyl alcohol and liquid oxygen. The authors of this discussion were greatly interested in the results presented in (1) since they had performed similar experiments with a rocket motor burning premixed gases; their experiments were reported in (2).

We were pleased to note that, in the ranges where the results obtained by (1) could be compared with our own experimental results, the agreement was satisfactory. For the guidance of the reader, it is pointed out that most of the results published in (2) were obtained approximately two years ago and were reported at three different symposia (3,4,5) on liquid rocket combustion stability, and that those symposia were attended by one or more of the authors of (1).

In the section "Discussion" the authors of (1) make the following statement with regard to the effect of combustion chamber length on combustion pressure oscillations. We quote, "Note this existence of an upper limit clearly invalidates oscillation-producing mechanism advanced by Zucrow and Osborn (2) as discussed by Crocco (6) since this mechanism cannot account for the observed cessation of oscillations with increasing chamber lengths." We will show later in this discussion that not only is that statement incorrect, but the possible existence of such an *upper critical combustion chamber length* was postulated by Osborn and Schiewe some time ago (7).

We now turn our attention to a Technical Comment which appeared in the same issue of JET PROPULSION. That article (6), by Prof. L. Crocco of Princeton University, is entitled "Comments on the Zucrow-Osborn Paper on Combustion Oscillations" (2).

In a Comment of more than 1500 words by Crocco upon a paper reporting experimental data and results, he did not make a single comment concerning the experiments themselves. In his first paragraph he makes the assertion concerning his own theories that "in the United States and abroad . . . the mechanism (time lag theory) on which these theories are based have been accepted as correct." To the senior author this is a surprising statement. The senior author and other investigators, to cite a few (8,9,10,11,12,13), have challenged those theories at practically every symposium held on combustion stability. In fact, the primary reason for initiating a research program on combustion pressure oscillations at Purdue University can be attributed to the conviction of the senior author of this discussion that the time lag theory was insufficient for explaining the complex phenomena associated with high-frequency combustion pressure oscillations.

In the second paragraph of his comments Crocco implies in a somewhat disparaging tone that the experimental techniques used at Purdue are similar to those used at Princeton. He then correctly points out that the Purdue experiments were conducted with rocket motors burning premixed gases. We are of the opinion, and our progress indicates, that from the standpoints of obtaining basic information (1), simplifying the experimental procedures, increasing the speed of conducting the experiments, and economy, there are a great many advantages in using premixed gaseous rocket motors.

In the third paragraph of the aforementioned Comment, Crocco presents his summary of the conclusions to be reached from our experiments. In that summary he interprets our conclusions under five numbered items. Since there is no disagreement with Item 1 we will discuss only the remaining four.

Item 2. He states that we conclude that "The tendency toward instability . . . , and therefore (it) increases with decreasing frequency." We made no such statement in our paper (2). As a matter of fact, the statement is inconsistent with our data on the effect of combustion chamber length. Apparently Prof. Crocco misunderstood our experimental objectives and also our physical explanation of the existence of a (lower) *critical combustion chamber length*, that is, the length of combustion chamber below which no combustion pressure oscillations were detected. Our experiments on the effect of combustion chamber length were conducted for the purpose of determining the (*lower*) critical combustion chamber length. Consequently, our discussion and comments are applicable only to the range of lengths we investigated. We refer Prof. Crocco to our conclusion ((2), p. 658). "Experimenters using liquid bipropellant rocket motors have also noted that long combustion chambers tended to initiate combustion pressure oscillations of the longitudinal mode more readily than do short ones" (14). The above statement is correct and refers to rocket motors of *practical* lengths and having the lengths we investigated. For Crocco's comment to be consistent with our data and physical explanation it should read "and therefore (the tendency toward instability) increases with decreasing frequency for combustion chamber lengths near the (lower) critical length." Any other conclusion is invalid and incomplete. The authors are also of the opinion that the frequency of the combustion pressure oscillations should not be considered to be an independent variable.

Item 3. This item, which is also concerned with the effect of combustion chamber length, is again an incorrect conclusion drawn by Crocco from our experiments, *and not by us.* His statement, "Oscillations with a pressure amplitude that steadily increases with increasing chamber length," as in the case of Item 2 is inconsistent with our data and physical explanation. Table 1, reproduced from (2), summarizes the results of our investigation of the effects of combustion chamber length.

Table 1 Typical reduced data from the study on the effect of chamber length for superheated propane and air

Chamber length	Type of oscillation	Frequency of oscillations, cps	Amplitude of oscillations, psi
28	shock (L)*	570	22
22.3	shock (L)	685	22
16.3	shock (L)	948	17
12.6	sinusoidal (L)	1219	4

Values for the variables: Equivalence ratio, 1.2 ± 0.08; propane line pressure drop, 158 ± 8 psi; air line pressure drop, 150 ± 10 psi; mean combustion pressure, 45 psia ± 2 psi.

*L indicates a longitudinal mode of oscillation.

Received Jan. 10, 1959.

[1] Professor of Gas Turbines and Jet Propulsion, School of Mechanical Engineering. Fellow Member ARS.

[2] Assistant Professor of Mechanical Engineering. Member ARS.

[3] Numbers in parentheses indicate References at end of paper.

The table shows that the pressure amplitudes of the oscillations were identical for a 22- and 28-in. long combustion chamber, and that the rapid change in the amplitude of the oscillations occurred near the critical length. The error arose from the same considerations we have discussed under Item 2 above. As pointed out earlier in this discussion, we have for some time been aware of the possible existence of an (*upper*) critical combustion chamber length, that is, a length beyond which there would be no combustion pressure oscillations. What is noteworthy, however, is that our former graduate student R. M. Schiewe arrived at the above conclusion by applying the very mechanism which Prof. Crocco asserts cannot explain the existence of the upper critical combustion length. We quote from a report by Osborn and Schiewe (7): "It is conceivable, however, that if the combustion chamber were made sufficiently long the pressure disturbance will be considerably attenuated before it can traverse twice the length of the combustion chamber. Thus the returning pressure wave could be too weak for raising the temperature and pressure of the unburned and burning mixture significantly, and, therefore, there would be no amplification of the pressure disturbance." Because the upper critical combustion chamber length was considerably longer than the lengths of practical rocket motors, we did not deem it of sufficient importance to determine it experimentally. We are glad to learn, however, that the authors of (1) have determined its existence experimentally.

Item 4. This is concerned with our prognostication that the mechanism by which the transverse modes of combustion pressure oscillation arise is probably similar to that influencing the longitudinal modes. Prof. Crocco presents a long discussion which completely ignores the discussions presented in our paper (2).

Item 5. We used the phrase "a type of detonation wave" to make a distinction between a Chapman-Jouguet wave and a shock wave with combustion taking place behind the wave. We are still unconvinced that our choice of words is incorrect (15).

In the closing paragraph of his comments (6) Crocco implies that we have no right to advance a new mechanism for explaining combustion instability in rockets. He also implies that we have not made even "a limited perusal" of the published literature. Such remarks are irrelevant and inaccurate. Furthermore, they contribute nothing to improving our understanding of the complicated phenomena associated with combustion pressure oscillations. Reference (16) of this discussion, listed as (6) in our paper (2), shows that we have made a rather complete study of the literature.

We sincerely regret that we were not given the opportunity of reading Prof. Crocco's comments before they appeared in the December 1958 issue of JET PROPULSION. Consequently, we were denied the opportunity of publishing our reply in the same issue.

References

1 Crocco, L., Grey, J. and Harrje, D. T., "On the Importance of the Sensitive Time Lag in Longitudinal High-Frequency Rocket Combustion Instability," JET PROPULSION, vol. 28, no. 12, Dec. 1958, pp. 841–843.

2 Zucrow, M. J. and Osborn, J. R., "An Experimental Study of High-Frequency Combustion Pressure Oscillations," JET PROPULSION, vol. 28, no. 10, Oct. 1958, pp. 654–659.

3 Air Force Office of Scientific Research, Seventh Symposium on Liquid Rocket Combustion Instability, Princeton, N. J., May 27–28, 1957. (Confidential)

4 Zucrow, M. J. and Osborn, J. R., "An Experimental Study of High Frequency Combustion Pressure Oscillations in a Gaseous Bipropellant Rocket Motor," Fourth Formal Symposium on Liquid Rocket Combustion Instability, Los Angeles, Calif., Dec. 9–10, 1957, to be published. (Confidential)

5 Air Force Office of Scientific Research, Ninth Symposium on Liquid Rocket Combustion Instability, Denville, N. J., June 17–18, 1958. (Confidential)

6 Crocco, L., "Comments on the Zucrow-Osborn Paper on Combustion Oscillations," JET PROPULSION, vol. 28, no. 12, Dec. 1958, pp. 843–844.

7 Osborn, J. R. and Schiewe, R. M., "An Experimental Investigation of High Frequency Combustion Pressure Oscillations in a Gaseous Biopropellant Rocket Motor," Purdue University Report no. I-58-1, June 1958, p. 40.

8 Zucrow, M. J., Panel Discussion, Symposium on Combustion Instability in Liquid Rocket Engines, U. S. Naval Air Rocket Test Station, Report no. 42, April 1954, p 317. (Confidential)

9 Zucrow, M. J., Panel Discussion, Third Conference on Liquid Propellant Rocket Combustion Instability, Princeton University, Oct. 18, 1955, p. 341. (Confidential)

10 Karlovitz, B., "Combustion Instability Induced by Turbulence,' Symposium on Combustion Instability in Liquid Rocket Engines," U. S. Naval Air Rocket Test Station, Report no. 42, April 1954, p. 118. (Confidential)

11 Ellis, H. B. and Pickford, R. S., "High-Frequency Combustion Instability," Aerojet-General TN-17, Sept. 1956. (Confidential)

12 Lewis, B., Panel Discussion, Symposium on Combustion Instability in Liquid Rocket Engines, U. S. Naval Air Rocket Test Station, Report no. 42, April 1954, p. 313. (Confidential)

13 Sarmaras, D. G., "Discussion of High Frequency Combustion Instability in Rockets with Distributed Combustion," in "Fourth Symposium on Combustion," The Williams and Wilkins Co., Baltimore, Md., 1953, p. 879.

14 Berman, K. and Cheney, S. H., Jr., "Rocket Motor Instability Studies," JET PROPULSION, vol. 25, no. 10, Oct. 1955, p. 513.

15 Lewis, B., Discussion of Paper of Reference 4, Fourth Formal Symposium on Liquid Rocket Combustion Instability, Los Angeles, Dec. 9–10, 1957, to be published. (Confidential)

16 Osborn, J. R. and Zucrow, M. J., "An Unclassified Literature Survey on Combustion Pressure Oscillations in Liquid Propellant Rocket Motors," Purdue University report TM57-1, June 1957.

17 Osborn, J. R. and Zucrow, M. J., "A Literature Survey on Combustion Pressure Oscillations in Liquid Propellant Rocket Motors," Purdue University report TM57-2, June 1957. (Confidential)

And Now the Editor Has His Say

LIKE the unwary referee in a TV wrestling match, your editor was jostled by one of the combatants in the Crocco-Zucrow fray. Prof. Zucrow in the above Comment questions our editorial policy, implying that we should have shown him Prof. Crocco's Technical Comment (JET PROPULSION, December 1958) before we published it. So now we have to explain our policy and defend our decision.

We consider it to be an established fact that intellectual controversy is a strong stimulus to scientific progress. The history of science is full of such examples. The argument over the nature of the primary cosmic rays in the 1930's spurred many physicists to perform searching experiments that ultimately added much to our knowledge, and the disputes at meetings of the American Physical Society at the time often became quite heated. No one would have suggested that these disputes ought to have been settled "behind the scenes" or that the disputants should have cleared their arguments with each other beforehand.

The position of your editor is that publishing such Comments in the ARS JOURNAL when they are not defamatory helps to clarify the issues for the benefit of our readers, and in our view, the JOURNAL exists for the benefit of its readers. We therefore published Crocco's criticism of Zucrow's paper and also Zucrow's defense against Crocco's criticism. We earnestly recommend to those of our readers interested in rocket combustion that they read both Technical Comments: We ourselves learned a lot about the scientific issues at stake, and we are grateful to both authors for it.

—**Martin Summerfield**

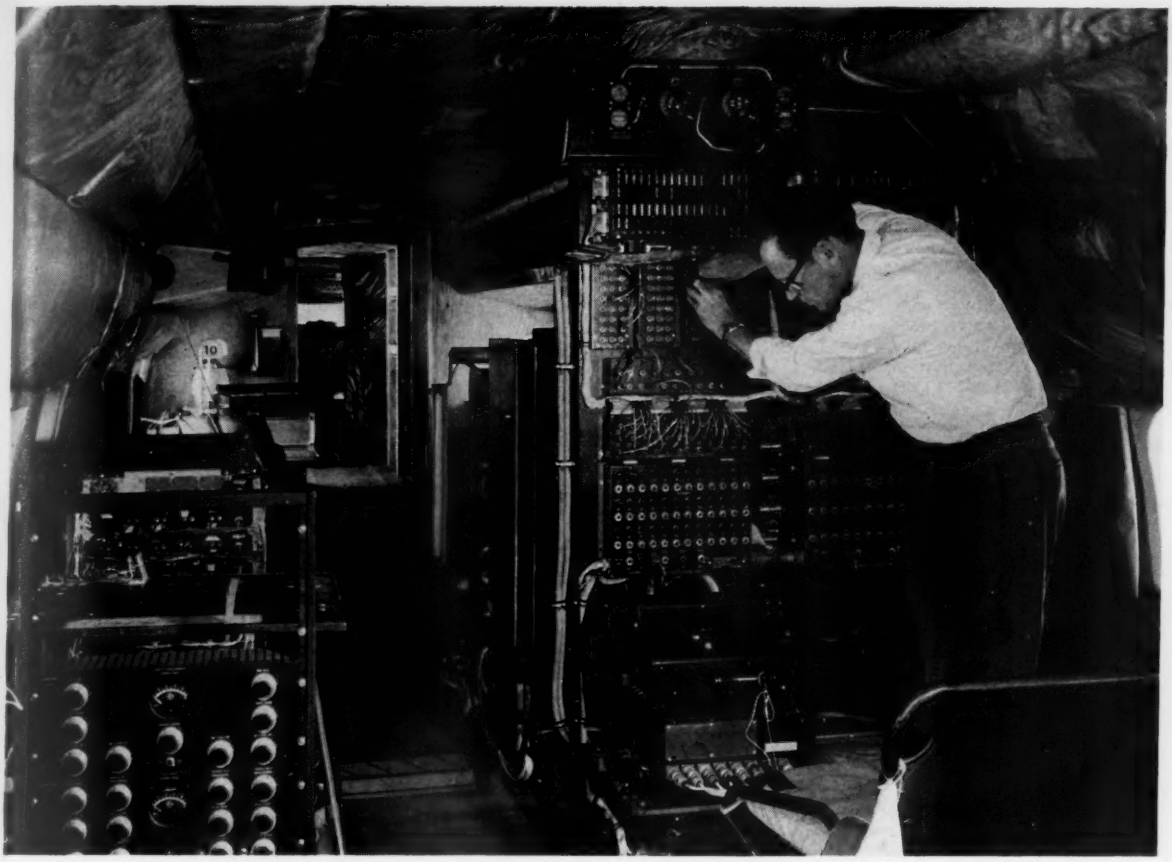

This is the cabin interior of Lockheed's test Electra airplane. The engineer adjusts control panel for oscillographic recorder at lower right.

"WE USE DU PONT LINO-WRIT 4 FOR OUR MOST CRITICAL TESTS"

—Dynamics Flight Test Laboratory,
Lockheed Aircraft Corporation, Burbank, California

Here's a report from a Lockheed Group Engineer. "The photorecording papers we use have to deliver dependable performance while combining a high enough degree of emulsion sensitivity to handle special tests. We started using Lino-Writ 4 early in 1957 and now use about 2000 feet per week.

"The first advantage we noticed was Lino-Writ's extra thinness which allows us to load almost 100% more footage in a 12-inch magazine than we could before. This meant that we could run longer tests without interruption and obtain a correspondingly larger volume of test data from each flight."

Other advantages of Lino-Writ 4 cited by Lockheed: it can be used as an intermediate in making diazo reproductions; it is strong and durable, capable of withstanding stresses incurred in processing; no quality problems with either exposed or unexposed rolls because of high temperature and humidity storage conditions—even the oldest records are still clear and thoroughly legible.

Isn't it time you investigated the Lino-Writ line for *your* oscillographic installation?

E. I. du Pont de Nemours & Co. (Inc.), Photo Products Department, Wilmington 98, Delaware. In Canada: Du Pont of Canada Limited, Toronto.

DU PONT
REG. U.S. PAT. OFF.

This advertisement was prepared exclusively by Phototypography.

Better Things for Better Living . . . *through Chemistry*

New Patents

George F. McLaughlin, *Contributor*

Self vaporization of liquid fuels by partial oxidation (2,864,233). J. G. Tschinkel, Huntsville, Ala., assignor to the U. S. Army.

Method of vaporizing a normally stable liquid fuel taken from the class consisting of isopropyl alcohol and xylene. The process comprised vaporizing a mixture of the fuel and phenylhydrazine by reacting the mixture with a peroxide compound.

Buoyed rate gyro (2,865,206). T. R. Quermann, Huntington Station, N. Y., assignor to United Aircraft Corp. (Ketay Dept., Norden Div.)

Unheated floated rate gyro for controlling servomechanisms and stabilization systems in missiles. Stability is maintained by means of a bellows, slotted spring steel damping cylinder and a fixed cam surface. The gyro is a component of Atlas, Polaris, Titan and Snark missiles.

Rocket motor liquid propellant (2,865,727). J. W. DeDapper, Los Angeles, Calif., assignor to North American Aviation, Inc.

Fuel comprised of not less than 80 per cent (by weight) turpentine, and the remainder an ethereal liquid in which up to 4.5 per cent lithium aluminum hydride is dissolved, and which is mixed with turpentine.

Flame holding device (2,866,314). A. Korti, N. Woodbury, Conn., assignor to United Aircraft Corp.

Flameholder mounted in the combustion chamber, movable from an external position between a flame holding position and a streamlined position.

Variable exhaust nozzle actuator (2,866,315). K. K. Schakel, Cincinnati, Ohio, assignor to Kett Corp.

Hydraulic device for a gas turbine engine afterburner. The exhaust nozzle is variable within a first range for normal operation, and movable through a second range to fully open condition for afterburner operation.

Thrust reversing and silencing (2,866,316). G. B. Towle, R. L. Vasquez and A. E. Wetherbee Jr., Newington, Conn., assignors to United Aircraft Corp.

Exhaust walls including small nozzles spaced for directing gases aft. Segmental plates about the nozzle axis, pivoted at their downstream ends, swing outward to reverse part of the gases from the nozzles.

Fuel turbidimeter (2,866,378). H. D. Warshaw and E. Nerheim, Minneapolis, Minn., assignors to the U. S. Navy.

Device for determining turbidity of a fluid by measuring scattered light as a function of turbidity. The intensity of light, introduced through a quartz rod and the fluid, produces a reading on an ammeter.

Automatic jet engine starter (2,866,385). K. W. Miller, Granada Hills, Calif., assignor to Northrop Aircraft, Inc.

Ground equipment with multiple-position stepping switches connected to individual control switches on the aircraft. Sequence stepping means are operable when a given desired condition is reached, and switches are turned off to a static condition as before starting the engine.

EDITOR'S NOTE: Contributions from Professors E. R. G. Eckert, J. P. Hartnett, T. F. Irvine Jr. and P. J. Schneider of the Heat Transfer Laboratory, University of Minnesota, are gratefully acknowledged.

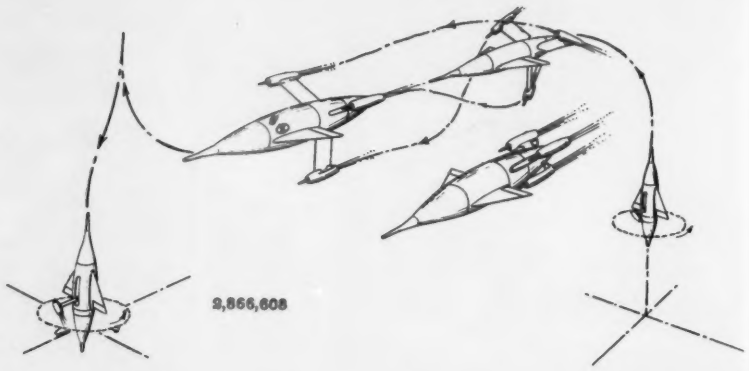

Vertical takeoff aircraft with jet driven rotor (2,866,608). L. H. Leonard, Inglewood, Calif.

Jet engines installed at the tips of propeller blades mounted for rotation about the longitudinal axis of the fuselage. Blades and engines may be folded into a position parallel with each other by means of a pivotal connection between each engine and its associated blade.

Data computer for converting oscillograph traces into direct-reading records (2,866,596). E. G. Hoefs and G. T. Litton, Dallas, Texas, assignor to Chance Vought Aircraft, Inc.

Potentiometer mounted on a carriage movable longitudinally over an oscillogram, and a stylus on the carriage transversely movable for following the trace. A computer connected between a movable contact connected to the stylus is responsive to movement of the stylus.

Aircraft jet thrust control (2,866,610). J. E. M. Taylor, Cleveland, Ohio.

Deflector member located outside, and aft of, a jet engine to intercept the jet stream. The angle of impact may be varied between zero and 90 deg to effect variations in the proportion of reverse thrust and lift.

Mechanical stick force producer (2,966,611). H. B. Thompson, Redondo Beach, Calif., assignor to Northrop Aircraft, Inc.

Pilot's attitude control including means for producing a differential ratio between ram air pressure and static pressure on the airplane in flight. The resulting force tends to center the control in neutral position.

Automatic steering system (2,866,930). C. Russell, Milldale, Conn., assignor to Bendix Aviation Corp.

Steering means, course setting means and controls for automatically maintaining a dirigible craft on a preset course. Fol-

(*continued on page 227*)

Target indicating mechanism (2,866,967). L. M. Bernbaum, Philadelphia, Pa.

Fixed target detection system for performing sequential search of successive sectors in discrete steps. Means responsive to target signal input to produce a vertical deflection on a spaced line observed on a visual indicator.

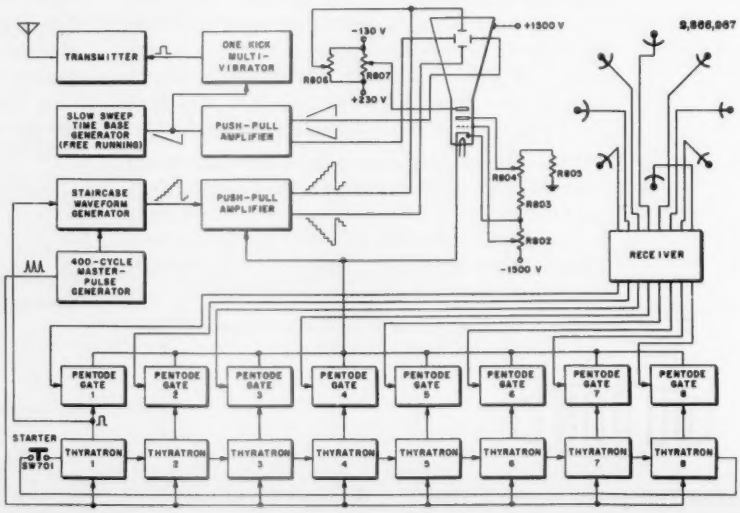

(left) Pop-up test of Navy Polaris IRBM.

(below left) One of the Santa Cruz test stands with dynamic thrust mount to simulate flight environment. Vibration oscillator functions during static firings.

(below right) Large centrifuge for environmental testing has unique shaker attachment to provide vibration simultaneously with high G-loadings.

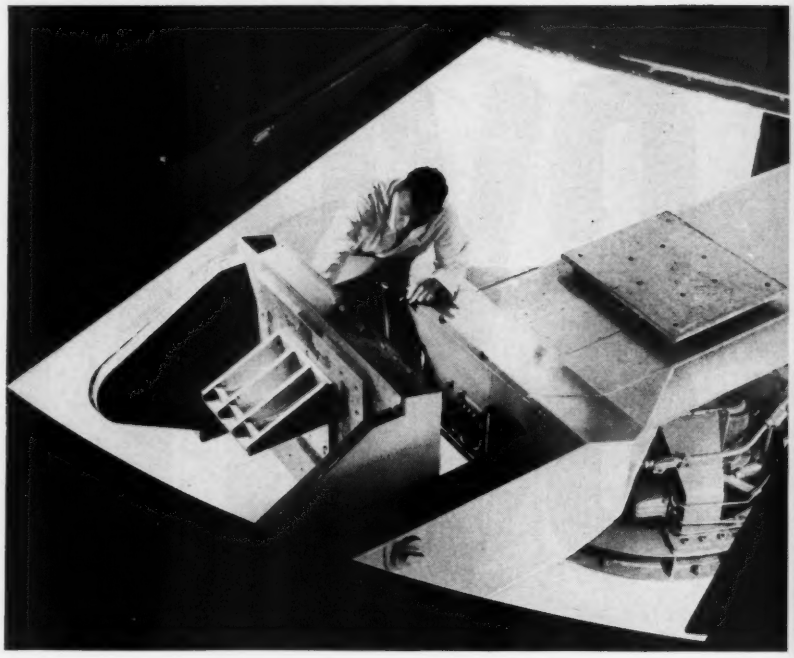

TEST / Expanding the Frontiers of Space Technology

Testing is a vital part of every stage in the development of missile and space programs at Lockheed Missiles and Space Division.

The Division maintains one of the most completely equipped missile and space test laboratories in the world. Equipment includes: altitude, temperature and humidity chambers; shaker and vibration systems; G-accelerators; and apparatus capable of performing chemical, metallurgical, plastic, heat transfer, hydraulic, pneumatic, shock, acceleration, sinusoidal and random vibration, structural, electrical, and electronic tests. Static field testing; research and development testing on controls; testing in ordnance and hydraulics and high-pressure gas and propulsion systems are conducted at the 4,000 acre, company-owned test base in the Ben Lomond mountains near Santa Cruz, California.

As weapon systems manager for such major, long-term projects as the Navy Polaris IRBM; Discoverer Satellite; Army Kingfisher; Air Force Q-5 and X-7; and other important research and development programs, Lockheed is engaged in expanding the frontiers of technology in all areas.

Flight testing is conducted at Cape Canaveral, Florida; Alamogordo, New Mexico; and Vandenberg AFB near Santa Maria, California; in a unique manner. All components and sub-systems of a new project are initially tested on known-performance, production missiles. Thus, when the final system is ready for first flight, its individual components already have flight-tested reliability. This new concept of flight testing is a major contribution and has enabled Lockheed to produce extremely complex missile systems in record time and at greatly reduced expense.

Underwater launch tests—including studies of cavitation, wave simulation and skip motion—are carried on at the Sunnyvale facility and at the Navy test base on San Clemente Island. In addition, structural and other tests are performed at Hunter's Point Naval Shipyard, California.

If you are experienced in any of the various phases of testing, we invite your inquiry. Positions also are available in physics, mathematics, chemistry, or one of the engineering sciences. Write: Research and Development Staff, Dept. C-25, 962 W. El Camino Real, Sunnyvale, California.

"The organization that contributed most in the past year to the advancement of the art of missiles and astronautics." NATIONAL MISSILE INDUSTRY CONFERENCE AWARD

Lockheed / **MISSILES AND SPACE DIVISION** /

SUNNYVALE, PALO ALTO, VAN NUYS,
SANTA CRUZ, SANTA MARIA, CALIFORNIA
CAPE CANAVERAL, FLORIDA · ALAMOGORDO, NEW MEXICO

low-up means regulates the controls to change the course setting and inactivate the follow-up.

Directional system sensitive to rates of turn (2,866,934). H. W. Whitehead, Marblehead, Mass., assignor to General Electric Co.

Inertial directional reference means maintaining a stable spatial orientation. A slaving control corrects directional information upon departure of the reference means from a predetermined course. The turn signal interrupts operation of the slaving control when the signal exceeds a preset amplitude.

Automatic tracking circuits (2,866,966). E. L. C. White, Iver, England, assignor to Electrical & Musical Industries, Ltd.

Position defining pulses generated by four electrical wave forms which repeatedly pass through a predetermined reference value. Pulses are derived from voltage variations set up across a load impedance connected to a point of fixed potential.

Non-propulsion attachment for rockets (2,866,413). C. R. Roquemore, China Lakes, Calif., assignor to the U. S. Navy.

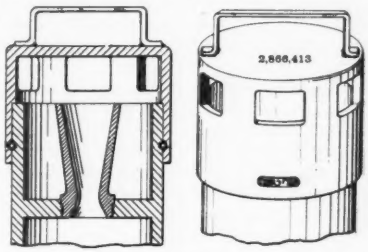

Thrust nullifier for a rocket having a launcher retainer groove near its rear end. Gas from the rocket issues through holes in the wall in such radial directions that no transverse forces are applied to the rocket.

Launching control device (2,867,153). J. Hirsch, Pacific Palisades, Calif., assignor to Aerophysics Development Corp.

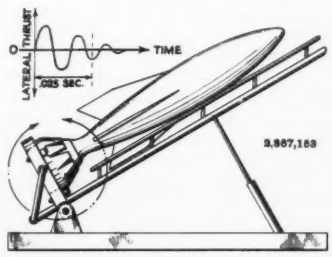

System for gradually releasing a rocket propelled missile on a launching frame. Spring force on fingers gripping an adapter in alignment with the CG of the missile is retarded for a period greater than the period during which initial transient thrust eccentricities exist.

Boundary layer control (2,867,392). W. P. Lear, Pacific Palisades, Calif., assignor to Lear, Inc.

Hollow airfoils divided into compartments on either side of the longitudinal axis, and predetermined areas of the airfoil surfaces having apertures between the compartments and the external atmosphere. Air pumps are arranged to supply equal boundary layer capacity to both sides of the axis.

Book Reviews

Ali Bulent Cambel, Northwestern University, *Associate Editor*

Behaviour of Metals at Elevated Temperatures, Institution of Metallurgists, London, 1957, 122 pp.

Reviewed by J. P. Frankel
University of California

This volume contains the four lectures that comprised the Institution of Metallurgists Refresher Course given at Llandudno in October 1956. The lecture titles were: Engineering Properties of Metals at High Temperatures, Effect of Temperatures up to 450C on Metals, Non-Ferrous High Temperature Materials, and High Temperature Steels.

With the exception of some data on S. A. P., the mixture of aluminum and its oxide, the discussions concentrate on metals and alloys, excluding metal ceramic mixtures.

The first lecture is an excellent summary of the import of materials properties on engineering design procedures; the remaining lectures deal with specific temperature ranges and materials properties. This volume is of particular interest to the airframe and engine designer, since it discusses thoroughly the problem of material selection for short time high temperature applications. The interests of designers in the long time application fields are by no means neglected, however.

In short, the book is commended to the designer and others who have not the opportunities to follow closely developments in the rapidly changing materials field. The only drawback, from the point of view of the reader in the U.S., is the use of British alloy data for representation of the basic principles. In many cases, as the book itself points out, the characteristic behavior of particular alloys is quite sensitive to composition; accordingly, the American reader must use this book primarily as an overall guide rather than a source of data. The book may be considered as an excellent pocket guide to the exotic field of High Temperature Metallurgy whose inhabitants obey strange laws, but tend to be somewhat friendly when understood, and quite amenable to exploitation.

The Exterior Ballistics of Rockets, by L. Davis Jr., J. W. Follin Jr. and L. Blitzer, Van Nostrand Co., Princeton, 1958, v + 457 pp. $8.50.

Reviewed by A. E. Fuhs
Northwestern University

This book is a modified version of a previously classified U.S. Navy publication of the same title. Most ofthe book was written immediately following World War II and considers the exterior ballistics of solid fuel rockets without moving control surfaces. The theoretical analysis evolved simultaneously with a wartime experimental program; hence the book is based on tested techniques. The methods of solving ballistic problems, which are presented by this clearly written book, are still pertinent today. Problems associated with more complex rocket systems can be solved by an extension of the basic treatment given in this book.

Before we consider in detail the material included in the book, let us examine some of its features. In order to adequately develop the mathematical theory it is necessary to introduce an enormous array of symbols. To help the reader, a list of symbols is provided, and the section where the symbol is first introduced is indicated. In many cases the formulas are derived in alternate ways. The physical significance of each mathematical result is discussed sufficiently to give the reader insight into its meaning. Typical values for the various parameters are given to help fix in mind the order of magnitude of the terms. Precise derivations are given from which more useful approximate expressions are developed. Solutions are usually shown both in graphical and analytical form. The book is divided into two parts (fin- and spin-stabilized rockets) each preceded by an introductory chapter.

The force system acting on the rocket consists of gravity, jet and aerodynamic forces. Assuming these forces to be known, the theory necessary to predict the trajectory is given. The trajectory can be considered to be composed of different segments, namely, launching, motion during burning and motion after burning. Each segment of the tracjectory is considered fully, including launching from stationary sites and moving aircraft.

To be able to understand the book, the reader should be familiar with vector analysis, elementary differential equations and the basic concepts from analytical mechanics. Where other mathematical tools are needed, the necessary background is presented.

Random Vibration, edited by Stephen H. Crandall, The Technology Press, Cambridge, 1958, 390 pp.

Reviewed by Robert L. Sutherland
University of Wyoming

This book, consisting of the notes for the M.I.T. special summer program on Random Vibration, covers a range of topics including theory of random processes, response to random vibration, instrumentation for random vibration analysis, simulation equipment and associated problems, and recommended design procedure for equipment subjected to random loading. There are also discussions somewhat more general in subject matter rather than specifically concerned with random vibration theory, such as in the chapters on structural damping, fatigue of metals and examples of stochastic processes of mechanical origin. Hence it might well be titled (for example) "Considerations in the Design of Equipment Subjected to Random Loading." Nevertheless, all sections contribute to the development and understanding of the overall picture of random vibration and associated problems.

As pointed out by several of the contributing authors, random vibration represents an involved and not completely understood subject. However, certain aspects of the theory are not entirely new, since electrical engineers have already encountered the complexities of random phenomena in their studies of noise in signal transmission. The current necessity for the understanding of random mechanical vibration is largely a result of the high level of noise and vibration energy generated by powerful rocket and jet engines of recent development. Thus the inclusion of chapters devoted to the response of structures to jet noise and the estimation of sound-induced missile vibrations is both timely and significant.

The fundamental approach (including necessary limitations) to the designation and analysis of random processes in general and random vibration in particular is presented in chapters 2 and 4. The most conveniently handled representation of random excitation is that of the Gaussian probability distribution; the resulting power spectrum and probability distribution of the response is presented. The discussion of instrumentation for random vibration analysis is both thoroughly and ably handled, and the final chapter consisting of four papers on the random vibration design problem is an interesting, appropriate and complementary conclusion for this collection of notes.

In common with the usual compilation of papers by a number of authors, a certain amount of discontinuity of development and non-uniformity of style is unavoidable. This is overshadowed, however, by the value of the material as a reference source of information for engineers and scientists dealing with design and analytical problems involving random processes. A helpful addition would have been the inclusion of a good subject index, which would add greatly to the book's usefulness as a reference text.

Landing Gear Design, by H. G. Conway, Chapman and Hall Ltd., London, 1958, viii + 342 pp. Distributed in America by Macmillan Co., New York.

Reviewed by James J. Kauzlarich
Worcester Polytechnic Institute

This monograph on airplane landing gears is the first such treatment of this subject in book form known to the reviewer. The author has attempted to give a full coverage emphasizing practical design advice. The context is principally historical, treating recent landing gear designs in detail. This reviewer feels that the material is a light treatment of the subject having little depth in discussing topics

of current interest, e.g., wheel shimmy, skidding, stability, etc. As the title implies, the book covers many disciplines of engineering. In particular, the landing gear tires, wheels, brakes and shock absorbers are treated in separate chapters. In addition, there are chapters on energy absorption, general layout of the landing gear, retraction and landing gear stressing. In each chapter the important requirements for the particular element of the landing gear under discussion are summarized. This is usually followed with example calculations based on simplified analysis or empirical results. In cases where empirical data are used, the reference is given, but without comment. There is no separate bibliography.

The discussion of typical landing gear designs includes American, British and Germ n design practices. However, the author has, in general, ignored the extensive resear h activities concerning landing gear problems that have been conducted in America. The Wright Air Development Center and the Langley Aeronautical Laboratory, in addition to the very extensive facilities of private companies, have made many significant contributions on the subject. For example, the author has overlooked the analytical treatment of landing gear wheel shimmy including extensive testing of the theory that has been successfully conducted by the Wright Air Development Center (see *J. Aeron. Sci.*, vol. 21, p. 793).

In summary, "Landing Gear Design," is a book that may be useful to the novice aeronautical engineer or student, but does not cover the subject in sufficient depth to be very useful for the experienced designer confronted with a critical design problem. The book does, however, serve the useful purpose of giving the reader a broad perspective of the subject.

Technical Literature Digest

M. H. Smith, *Associate Editor*, and M. H. Fisher, *Contributor*
The James Forrestal Research Center, Princeton University

Jet and Rocket Propulsion Engines

The Hot Water Rocket, by Otto Mühlhäuser, *Raketentechnik und Raumfahrtforschung*, vol. 2, no. 2, April 1958, pp. 38–44 (in German).

Altitude-test-chamber Investigation of Performance of a 28-inch Ram-jet Engine, IV: Effect of Inlet-air Temperature, Combustion-chamber-inlet Mach Number, and Fuel Volatility on Combustion Performance, by Robert W. Kahn, Shigeo Nakanishi and James L. Harp Jr., *NACA Res. Mem.* E51D11, July 1951, 27 pp. (Declassified from Confidential by authority of *NACA Res. Abstr.* 127, p. 13, 6/5/58.)

Altitude Test Chamber Investigation of Performance of a 28 inch Ram Jet Engine, III: Combustion and Operational Performance of Three Flame Holders with a Center Pilot Burner, by Thomas B. Shillito, George G. Younger, and James G. Henzel Jr., *NACA Res. Mem.* E50J20, Feb. 1951, 30 pp. (Declassified from Confidential by authority of *NACA Res. Abstr.* 127, p. 18, 6/5/58.)

A Proposed Ram-jet Control System Operated by Use of Diffuser Pressure Recovery, by Maxime A. Faget. *NACA Res. Mem.* L52E05D, Sept. 1952, 19 pp. (Declassified from Confidential by authority of *NACA Res Abstr.* 127, p. 18, 6/5/58.)

Vanguard Engine, by Louis Michelson, *Missiles and Rockets*, vol. 3, May 1958, pp. 139, 141–142.

Some Actuator Disc Theories for the Flow of Air through an Axial Turbo Machine, by J. H. Horlock, *Gt. Brit., Aeron. Res. Council. Rep. & Mem.* 3030 (formerly *ARC Tech. Rep.* 15491), 1958, 31 pp.

A Study of High Energy Level, Low Power Output Turbines, *American Machine and Foundry Co., Turbo Div., Rep.* 1196, 1 Feb. 31 Dec. 1957, 181 pp. 63 figs.

A Study of Liquid Boric Oxide Particle Growth Rates in a Gas Stream from a Simulated Jet Engine Combustor, by Paul C. Setze, *NACA Res. Mem.* E55120a, April 1957, 41 pp. (Declassified from Confidential by authority of *NACA Res. Abstr.* 126, p. 31, 5/2/58.)

Thermopropulsive Characteristics of High-speed Thrust Generators, by A. F. Charwat, *Aero-Space Engineering* (formerly *Aeron. Engng. Rev.*), vol. 17, June 1958, pp. 45–48.

Hydrogen Peroxide Injection Boosts Jet Thrust 120%, by L. E. Varadi, *Aviation Age*, vol. 29, June 1958, pp. 54–58.

Better Turbopump Design Ups Aircraft Range, by Joseph Bendersky, *Aviation Age*, vol. 29, June 1958, pp. 72–77.

Power Sources for Space Explored, by James A. Fusca, *Aviation Week*, including *Space Technology*, vol. 68 June 16, 1958, pp. 234–241.

Advanced Propulsion Research Speeded *Aviation Week*, including *Space Technology*, vol. 68, June 16, 1958, pp. 277–280.

Propellant Vaporization as a Criterion for Rocket-engine Design: Experimental Effect of Fuel Temperature on Liquid-oxygen-Heptane Performance, by M. F. Heidmann, *NACA Res. Mem.* E57E03, July 1957, 21 pp. (Declassified from Confidential by authority of *NACA Res. Abstr.* 126, p. 32, 5/2/58.)

A Study of Injection Processes for Liquid Oxygen and Gaseous Hydrogen in a 200-pound-thrust Rocket Engine, by Carmon M. Auble, *NACA Res. Mem.* E56125a, Jan. 1957, 32 pp. (Declassified from Confidential by authority of *NACA Res. Abstr.* 126, p. 32, 5/2/58.)

Injection Principles for Liquid Oxygen and Heptane Using Two-element Injectors, by Marcus F. Heidmann, *NACA Res. Mem.* E56D04, June 1956, 30 pp. (Declassified from Confidential by authority of *NACA Res. Abstr.* 126, p. 31, 5/2/58.)

Combustion Instability in Liquid Propellant Rocket Motors, 23d Quarterly Progress Report for the Period 1 Nov. 1957 to 31 Jan. 1958, *Princeton Univ., Dept. Aeron. Engng., Rep.* 216-w, March 1958, 45 pp., 2 tabs., 22 figs.

Investigation of Internal Film Cooling of 1000 - pound - thrust Liquid -ammonia-Liquid-oxygen Rocket-engine Combustion Chamber, by Gerald Morrell, *NACA Res. Mem.* E51E04, July 1951, 42 pp. (Declassified from Confidential by authority of *NACA Res. Abstr.* 115, p. 11, 5/22/57.)

Temperature Surveys of Rocket Motor Combustion Chambers, by Dwight I. Baker, *Calif. Inst. Tech., Jet Prop. Lab., Progr. Rep.* 24–5, Nov. 1952, 23 pp. (Declassified from Restricted by authority of *CIT-JPL Public.* 38, p. 18, 1/3/55.)

Small Power Plants for Use in Space, by Louis Rosenblum, *Aero-Space Engng.*, vol. 17, July 1958, pp. 30–33, 51.

Booster Propulsion for Space Vehicles, by Richard S. Wentink, *Aero-Space Engng.*, vol. 17, July 1958, pp. 40–45, 51.

How Do Small Gas Turbines Scale? by Dennis P. Edkins. *Aviation Age*, vol. 30, July 1958, pp. 38–39, 41–45.

Preliminary Survey of Propulsion Using Chemical Energy Stored in the Upper Atmosphere, by Lionel V. Baldwin and Perry L. Blackshear. Appendix D: Heat Transfer and Friction Drag, by James F. Schmidt, *NACA TN* 4267, May 1958, 73 pp.

An Analysis of Ram-jet-engine Time Delay Following a Fuel-flow Disturbance, by Fred A. Wilcox and Arthur R. Anderson, *NACA Res. Mem.* E55D22, June 1955, 38 pp. (Declassified from Confidential by authority of *NACA Res. Abstr.* 126, pp. 31, 5/2/58.)

Effect of Mechanically Induced Sinusoidal Air-flow Oscillations on Operation of a Ram-jet Engine, by E. E. Dangle, A.

EDITOR'S NOTE: Contributions from Professors E. R. G. Eckert, J. P. Hartnett, T. F. Irvine Jr. and P. J. Schneider of the Heat Transfer Laboratory, University of Minnesota, are gratefully acknowledged.

J. Cervenka and Eugene Perchonok, *NACA Res. Mem.* E54D01, June 1954, 24 pp. (Declassified from Confidential by authority of *NACA Res. Abstr.* 126, p. 29, 5/2/58.)

Internal Flow and Burning Characteristics of 16 Inch Ram Jet Operating in a Free Jet at Mach Numbers 1.35 and 1.73, by Eugene Perchonok and John M. Farley, *NACA Res. Mem.* 51C16, May 1951, 37 pp. (Declassified from Confidential by authority of *NACA Res. Abstr.* 126, p. 26, 5/2/58.)

Summary of Scale-model Thrust-reverser Investigation, by John H. Povolny, Fred. W. Steffen and Jack G. McArdle, *NACA Rep.* 1314, 1957, 14 pp. (Supersedes TN 3664.)

Effect of Fuel-orifice Diameter on Performance of Heptane-oxygen Rocket Engines, by Richard J. Priem and Martin Hersch, *NACA Res. Mem.* E57126, Feb. 1958, 20 pp. (Declassified from Confidential by authority of *NACA Res. Abstr.* 126, p. 33, 5/2/58.)

Injection Principles for Liquid Oxygen and Heptane Using Nine-element Injectors in an 1800-pound-thrust Rocket Engine, by Richard F. Neu, *NACA Res. Mem.* E57E13, July 1957, 27 pp. (Declassified from Confidential by authority of *NACA Res. Abstr.* 126, p. 32, 5/2/58.)

Aerodynamics of Jet Propelled Missiles

Wind Tunnel Tests at Mach Numbers 1.5 and 2.0 on Models of a 2.75 Inch Folding Fin Rocket, by B. F. Jaeger, F. H. Knemeyer and G. M. Schroedter, *NAVORD Rep.* 1284, (*NOTS* 354) Feb. 1951, 18 pp. (Declassified from Confidential by authority of NOTS ltr 7506-BJS:nh, Reg. 75-53839 dtd 19 May 58, Ref. OPNAV INST 5510.1A, Art. 0408 dtd 2 Oct. 54.)

The Supersonic Lift on Blunt and Sharp Trailing Edge Folding Fins in Combination with a Long Body, by Marvin L. Luther and G. M. Schroedter, *NAVORD Rep.* 1317, (*NOTS* 391) June 1951, 12 pp. (Declassified from Confidential by authority of NOTS ltr 7506-BJS:nh. Reg. 75-53839 dtd 19 May 58. Ref. OPNAV INST 5510.1A. Art. 0408 dtd 2 Oct. 54.)

Cross Wind Firing of Rockets: An Experimental Survey, by William R. Haseltine, *NAVORD Rep.* 1181, (*NOTS* 237), Sept. 1949, 16 pp. (Declassified from Confidential by authority of NOTS ltr 7506-BJS:nh. Reg. 75–53839 dtd 19 May 58. Ref. OPNAV INST 5510.1A. Art. 0408 dtd 2 Oct. 54.)

The Employment of Aerodynamic Forces to Obtain Maximum Range of a Rocket Missile, by D. F. Lawden, *Aeron. Quart.* vol. 9, May 1958, pp. 97–109.

The Shock Pattern of a Wing-body Combination, Far from the Flight Path, by F. Walkden, *Aeron. Quart.*, vol. 9, May 1958, pp. 164–194.

Exploratory Investigation of Aerodynamic Effects of External Combustion of Aluminum Borohydride in Airstream Adjacent to Flat Plate in Mach 2.46 Tunnel, by Robert G. Dorsch, John S. Serafini and Edward A. Fletcher, *NACA Res. Mem.* E57E16, July 1957, 91 pp. (Declassified from Confidential by authority of *NACA Res. Abstr.* 126, p. 33, 5/2/58.)

Exploratory Investigation of Static- and Base-pressure Increases Resulting from Combustion of Aluminum Borohydride Adjacent to Body of Revolution in Supersonic Wind Tunnel, by John S. Serafini, Robert G. Dorsch and Edward A. Fletcher, *NACA Res. Mem.* E57E15, Oct. 1957, 49 pp. (Declassified from Confidential by authority of *NACA Res. Abstr.* 126, p. 32, 5/2/58.)

Combustion of Aluminum Borohydride in a Supersonic Wind Tunnel, by Edward A. Fletcher, Robert G. Dorsch and Melvin Gerstein, *NACA Res. Mem.* E55F07, Aug. 1955, 12 pp. (Declassified from Confidential by authority of *NACA Res. Abstr.* 126, pp. 31, 5/2/58.)

Note on Ballistic Trajectories and Orbits, by Richard F. Hughes, *J. Aeron. Sci.*, vol. 25, May 1958, pp. 330-331.

On the Character of the Instability of the Laminar Boundary Layer Near the Nose of a Blunt Body, by A. M. Kuethe, *J. Aeron. Sci.*, vol. 25, May 1958, pp. 338–339.

A Program of Systemic Wind Tunnel Tests of Long, Fin Stabilized Rocket Models, by G. M. Schroedter, L. T. Jagiello and B. F. Jaeger, *NAVORD Rep.* 1049, (*NOTS* 169), Nov. 1948, 28 pp. (Declassified from Confidential by authority of NOTS ltr 7507-BJS:nh, Reg. 75-53839 dtd 19 May 58, Ref. OPNAV INST 5510.1A. Art. 0408 dtd 2 Oct. 54.)

Experimental Studies of Forces, Pressure Distributions and Viscous Effects on Long Inclined Bodies of Revolution at Mach 2.96, by C. S. Brown, M. L. Luther and G. M. Schroedter, *NAVORD Rep.* 1281, (*NOTS* 351), Feb. 1951, 60 pp. (Declassified from Confidential by authority of NOTS ltr 7506-BJS:nh Reg.

75-53839 dtd 19 May 58. Ref. OPNAV INST 5510.1A. Art. 0408 dtd 2 Oct. 1954.)

Investigation of the Laminar Aerodynamic Heat-transfer Characteristics of a Hemisphere-cylinder in the Langley 11-inch Hypersonic Tunnel at a Mach Number of 6.8, by Davis H. Crawford and William D. McCauley, *NACA Rep.* 1323, 1957, 21 pp. (Supersedes *TN* 3706.)

Forces and Moments on Oscillating Slender Wing Body Combinations at Supersonic Speed, Part II: Applications and Comparison with Experiment, by Haim Kennet, Holt Ashley and Robert L. Stapleford, *MIT, Fluid Dynamics Res. Group. Rep.* 57-5 (*AFOSR-TN*-114; *ASTIA AD* 152022), Dec. 1957, 55 pp.

Effect of Wing Camber and Twist at Mach Numbers from 1.4 to 2.1 on the Lift, Drag, and Longitudinal Stability of a Rocket-powered Model Having a 52.5° Sweptback Wing of Aspect Ratio 3 and Inline Tail Surfaces, by Warren Gillespie Jr., *NACA Res. Mem.* L56C16, May 1956, 29 pp. (Declassified from Confidential by authority of *NACA Res. Abstr.* 126, p. 35, 5/2/58.)

Low Amplitude Damping-in-pitch Characteristics of Tailless Delta-wing-body Combinations at Mach Numbers from 0.80 to 1.35 as Obtained with Rocket-powered Models, by Charles T. D'Aiutolo, *NACA Res. Mem.* L54D29, June 1954, 34 pp. (Declassified from Confidential by authority of *NACA Res. Abstr.* 126, p. 34, 5/2/58.)

Transonic Flight Test of a Rocket-powered Model to Determine Propulsive Jet Influence on the Configuration Drag, by Carlos A. deMoraes, *NACA Res. Mem.* L54D27, June 1954 16 pp. (Declassified from Confidential by authority of *NACA Res. Abstr.* 126, p. 34, 5/2/58.)

Experimental Effects of Propulsive Jets and Afterbody Configurations on the Zero-lift Drag of Bodies of Revolution at a Mach Number of 1.59, by Carlos A. deMoraes and Albin M. Nowitzky, *NACA Res. Mem.* L54C16, Apr. 1954, 32 pp. (Declassified from Confidential by authority of *NACA Res. Abstr.* 126, p. 34, 5/2/58.)

Aerodynamics of Slender Bodies at Mach Number of 3.12 and Reynolds Numbers from 2×10^6 to 15×10^6, II: Aerodynamic Load Distributions of Series of Five Bodies Having Conical Noses and Cylindrical Afterbodies, by John R. Jack and Lawrence I. Gould, *NACA Res. Mem.* E52C10, May 1952, 28 pp. (Declassified from Confidential by authority of *NACA Res. Abstr.* 126, p. 57, 5/2/58.)

Low-speed Measurement of Static Stability and Damping Derivatives of a 60° Delta-wing Model for Angles of Attack of 0° to 90°, by Donald E. Hewes, *NACA Res. Mem.* L54G22a, Sept. 1954, 30 pp. diagrs., photo., tab. (Declassified from Confidential by authority of *NACA Res. Abstr.* 127, p. 20, 6/5/58.)

Wind-tunnel Investigation of the Use of Spoilers for Obtaining Static Longitudinal Stability of a Canard-missile Model in Reverse Flight, by Herman S. Fletcher, *NACA Res. Mem.* L54E05, June 1954, 15 pp., diagrs., tab. (Declassified from Confidential by authority of *NACA Res. Abstr.* 127, p. 19, 6/5/58.)

Rocket Trajectory Equations and Differential Corrections in Spherical Coordinates, by E. F. Dobies, *Calif. Inst. of Techn., Jet Propulsion Lab., Progr. Rep.* 20-233, March 1958, 12 pp.

The Interaction of Shock Waves and Turbulent Boundary Layers, by Andrew G. Hammitt, *J. Aeron. Sci.*, vol. 25, June 1958, pp. 345-356.

Note on the Lift of Slender Nose Shapes According to Newtonian Theory, by J. D. Cole, *J. Aeron. Sci.*, vol. 25, June 1958, pp. 399.

The Wave Drag of Nonlifting Combinations of Thin Wings and "Non Slender" Bodies, by L. M. Sheppard, *Gt. Brit., Aeron. Res. Council. Rep. & Mem.* 3-76 (formerly *ARC Tech. Rep.* 19319; *Royal Aircr. Estab., TN Aero* 2496), 1958, 17 pp.

Investigation of Factors Affecting the Control and Stability of High Speed Aircraft and Missiles. A Review of Work Conducted in This Field (9/1/52 to 2/28/1958), by Phrixos Theodorides, *Univ. of Maryland, Inst. for Fluid Dynamics and Appld. Math., Tech. Rep.* BN-129 (*AFOSR-TR*-58-52; *ASTIA AD* 154215), April 1958, 12 pp.

The Pressure Drag Due to Turbulent Separation on Bodies of Revolution with Varying Boundary Layer Thickness, by Erik G. M. Petersohn, *Sweden, Aeron. Res. Inst., Rep.* 75, 1957, 9 pp.

Aerodynamic Characteristics at Supersonic Speeds of a Series of Wing-body Combinations Having Cambered Wings with an Aspect Ratio of 3.5 and a Taper Ratio of 0.2. Effects of Sweep Angle and Thickness Ratio on the Aerodynamic Characteristics in Pitch at M-2.-1, by Ross B. Robinson, *NACA Res. Mem.* L52E09, July 1952, 27 pp., diagrs., photos., 2 tabs. (Declassified from Confidential by authority of *NACA Res. Abstr.*

127, p. 18, 6/5/58.)

Aerodynamic Characteristics at Supersonic Speeds of a Series of Wing-body Combinations Having Cambered Wings with an Aspect Ratio of 3.5 and a Taper Ratio of 0.2. Effects of Sweep Angle and Thickness Ratio on the Static Lateral Stability Characteristics at M-1.60, by M. Leroy Spearman and John H. Hilton Jr., *NACA Res. Mem.* L51K15a, Jan. 1952, 31 pp., diagrs., 2 tabs. (Declassified from Confidential by authority of *NACA Res. Abstr.* 127, p. 17, 6/5/58.)

Effect of Camber on the Drag of a Body of Revolution, by Robert R. Dickey, *NACA Res. Mem.* A56E23, Oct. 1956, 8 pp., diagrs., tabs. (Declassified from Confidential by authoriy of *NACA Res. Abstr.* 127, p. 12, 6/5/58.)

Forces and Moments on Pointed and Blunt-nosed Bodies of Revolution at Mach Numbers from 2.75 to 5.00, by David H. Dennis and Bernard E. Cunningham, *NACA Res. Mem.* A52E22, Aug. 1952, 47 pp., diagrs., photos, 11 tabs. (Declassified from Confidential by authority of *NACA Res. Abstr.* 127, p. 12, 6/5/58.)

Exact Solution of the Neumann Problem. Calculation of Non-circulatory Plane and Axially Symmetric Flows about or within Arbitrary Boundaries, by A. M. O. Smith and Jesse Pierce, *Douglas Aircraft Co., Inc., Rep.* ES 26988, April 1958, 106 pp.

A Numerical Method for Evaluation Wave Drag, by Maurice S. Cahn and Walter B. Olstad, *NACA TN* 4258, June 1958, 13 pp., diagrs., tabs.

Low-speed Measurements of Rolling and Yawing Stability Derivatives of a 60° Delta-wing Model, by Joseph L. Johnson Jr., *NACA Res. Mem.* L54G27, Dec. 1954, 17 pp., diagrs., tab. (Declassified from Confidential by authority of *NACA Res. Abstr.* 127, p. 20, 6/5/58.)

Conditions Governing the Initial Slope of a Sonic Line on a Blunt Body, by Andrew Hammitt and John J. Sullivan, *Princeton Univ., Dept. Aeron. Engng., Rep.* 408 (*Wright Air Devel. Center, TN* 58–73; *ASTIA AD* 151066), Feb. 1958, 6 pp., 3 figs.

An Experimental Investigation at a Mach Number of 2.01 of the Effects of Body Cross-section Shape on the Aerodynamic Characteristics of Bodies and Wing-body Combinations, by Harry W. Carlson and John P. Gapcynski, *NACA Res. Mem.* L55E23, July 1955, 29 pp., diagrs., 2 tabs. (Declassified from Confidential by authority of *NACA Res. Abstr.* 127, p. 21, 6/5/58.)

Investigation of the Effects of Body Indentation and of Wing-plan-form Modification on the Longitudinal Chaacteristics of a 60° Swept-wing-body Combination at Mach Numbers of 1.41, 1.61 and 2.01, by John R. Sevier Jr., *NACA Res. Mem.* L55E17, July 1955, 37 pp., diagrs., tabs. (Declassified from Confidential by authority of *NACA Res. Abstr.* 127, p. 20, 6/5/58.)

General Variational Theory of the Flight Paths of Rocket Powered Aircraft, Missiles and Satellite Carriers, by Angelo Miele, *Purdue Univ., School of Aeron. Engng., Rep* A-58-2 (*AFOSR-TN*-58-246; *ASTIA AD* 154148), Jan. 1958, 57 pp., 11 figs.

Aerodynamic Characteristics at Supersonic Speeds of a Series of Wing-body Combinations Having Cambered Wings with an Aspect Ratio of 3.5 and a Taper Ratio of 0.2. Effect at M-2.-1 of Nacelle Shape and Position on the Aerodynamic Characteristics in Pitch of Two Wing-body Combinations with 47° Sweptback Wings, by Cornelius Driver, *NACA Res. Mem.* L52F03, July 1952, 27 pp., diagrs., photos., tab. (Declassified from Confidential by authority of *NACA Res. Abstr.* 127, p. 18, 6/5/58.)

Aerodynamic Characteristics at Supersonic Speeds of a Series of Wing-body Combinations Having Cambered Wings with an Aspect Ratio of 3.5 and a Taper Ratio of 0.2. Effects of Sweep Angle and Thickness Ratio on the Static Lateral Stability Characteristics at M-2.01, by Clyde V. Hamilton, *NACA Res. Mem.* L52E23, Aug. 1952, 37 pp., diagrs., 2 tabs. (Declassified from Confidential by authority of *NACA Res. Abstr.* 127, p. 18, 6/5/58.)

An Experiment on Flat Plate Turbulent Boundary Layer Flow—the Effect of Local Fluid Addition on Friction and Velocity Distribution, by H. Barrow, *J. Roy. Aeron. Soc.*, vol. 62, Feb. 1958, pp. 135–138.

Heat Transfer Through the Laminar Boundary Layer on a Circular Cylinder in Axial Incompressible Flow, by D. E. Bourne and D. R. Davies, *Quart. J. Mech. and Appl. Math.*, Feb. 1958, pp. 52–66.

Recovery Temperatures and Heat Transfer Near Two-dimensional Roughness Elements at Mach 3.1; by P. F. Brinich, *NACA TN* 4213, Feb. 1958, 20 pp.

On the Diffusion of a Chemically Reactive Species in a Laminary Boundary Layer Flow, by P. L. Chambre and J. D. Young, *Phys. of Fluids,* vol. 1, Jan.-Feb. 1958, pp. 48–56.

Combustion in the Laminar Boundary Layer of Chemically Active Sublimating Surfaces, by M. R. Denison and D. A. Dooley, *J. Aeron. Sci.*, vol. 25, April 1958, pp. 271–272.

A Method for Computing the Turbulent Boundary Layer When a Longitudinal Pressure Gradient is Present, by K. K. Fediaevskii and A. S. Ginevskii, *Sov. Phys.-Tech. Phys.*, Feb. 1957, pp. 275–291.

Transient Temperature Distribution in Aircraft Structures, by I. Frank., *J. Aeron. Sci.*, vol. 25, April 1958, pp. 265–267.

On the Heat Transfer to Constant Property Laminar Boundary Layer with Power-Function Free-stream Velocity and Wall-temperature Distribution, by I. Imai, *Quart. J. Appl. Math.*, April 1958, pp. 33–45.

Some Effects of Bluntness on Boundary-layer Transition and Heat Transfer at Supersonic Speeds, by W. E. Moeckel, *NACA Rep.* 1312, 1957, 14 pp.

An Extension of the Linearized Theory of Supersonic Flow Past Quasi-cylindrical Bodies, with Applications to Wing-body Interference, by R. C. Lock, *J. Fluid Mech.*, vol. 4, May 1958, pp. 33–63.

Heat Transfer and Fluid Flow

The Three Dimensional Flow Field of an Axial Compressor Blade Row-Subsonic, Transonic and Supersonic, by James Elliot McCune, *Cornell Univ., Grad. School of Aeron. Engng.* (*AFOSR-TN*-58-72; *ASTIA AD* 148116 and 148117), Feb. 1958, 259 pp.

Measurement of the Effect of an Axial Magnetic Field on the Reynolds Number of Transition in Mercury Flowing through a Glass Tube, by Michel Bader and William C. A. Carlson, *NACA TN* 4274, May 1958, 8 pp.

A Performance Analysis of Methods for Handling Excess Inlet Flow at Supersonic Speeds, by Donald P. Hearth and James F. Connors, *NACA TN* 4270, May 1958, 26 pp.

Droplet Impingement and Ingestion by Supersonic Nose Inlet in Subsonic Tunnel Conditions, by Thomas F. Golder, *NACA TN* 4268, May 1958, 56 pp.

Summary of Experimental Heat-transfer Measurements in Turbulent Flow for a Mach Number Range from 0.87 to 5.05, by Maurice J. Brevoort and Barbara D. Arabian, *NACA TN* 4248, May 1958, 43 pp.

A Preliminary Investigation of Methods for Improving the Pressure-recovery Characteristics of Variable-geometry Supersonic-subsonic Diffuser Systems, by Lowell E. Hasel and Archibald R. Sinclair, *NACA Res. Mem.* L57H02, Oct. 1957, 57 pp. (Declassified from Confidential by authority of *NACA Res. Abstr.* 126, p. 37, 5/2/58.)

Internal Performance Characteristics of Short Convergent-divergent Exhaust Nozzles Designed by the Method of Characteristics, by H. George Krull and William T. Beale, *NACA Res. Mem.* E56D27a, July 1956, 17 pp. (Declassified from Confidential by authority of *NACA Res. Abstr.* 126, p. 32, 5/2/58.)

Matching of Auxiliary Inlets to Secondary-air Requirements of Aircraft Ejector Exhaust Nozzles, by Donald P. Hearth, Gerald W. Englert and Kenneth L. Kowalski, *NACA Res. Mem.* E55D21, Aug. 1955, 39 pp. (Declassified from Confidential by authority of *NACA Res. Abstr.* 126, p. 30, 5/2/58.)

Heat Transfer from Surfaces on Non-uniform Temperature, by J. T. Stuart, *J. Fluid Mech.*, vol. 4, May 1958, pp. 1–21.

On the Theory of Vortex Flow, by K. H. Müller, *ZAMM*, vol. 38, May-June 1958, pp. 179–186 (in German).

On the Calculation of Radial Turbine Cascade Flow, by W. H. Isay, *ZAMM*, vol. 38, May-June 1958 pp. 209–219 (in German).

Laminar Heat Transfer Around Blunt Bodies in Dissociated Air, by N. H. Kemp, P. H. Rose and R. W. Detra, *AVCO Mfg. Corp., AVCO Res. Lab., Res. Rep.* 15, May 1958, 31 pp., 5 figs.

Experimental Investigation of Heat Transfer by Forced Convection from the Hot Gas to a Cooled Stainless Steel Radial in Flow Gas Turbine Rotor, by Thomas R. Swartwout, *Purdue Univ., Jet Prop. Center, Rep.* F-58-2, Jan. 1958, 69 pp.

On the Strength Distribution of Noise Sources Along a Jet, by H. S. Ribner, *Univ. of Toronto, Inst. Aerophys., Rep.* 51, April 1958, 19 pp., 7 figs.

UTIA Air Duct Facility for Investigation of Vibration Noise Inducted by Turbulent Flow Past a Panel (Boundary Layer Noise), by L. Maestrello, *Univ. of Toronto, Inst. Aerophys., TN* 20, April 1958, 5 pp., 2 tabs., 11 figs.

Note on Acoustic Energy Flow in a Moving Medium, by H. S. Ribner, *Univ. of Toronto, Inst. Aerophys., TN* 21, April 1958, 6 pp., 2 figs.

The Interaction of a Plane Strong Shock Wave with a Steady Magnetic Field, by J. H. deLeeuw, *Univ. of Toronto, Inst. Aerophys., Rep.* 49, March 1958, 47 pp., 3 tabs., 29 figs.

Laminar Flow in an Annulus with Porous Walls, by A. S. Berman, *Atomic Energy Comm.*, K-1324, June 1957, 31 pp.

Relaxation Phenomena in Air Between 3000 and 8000° K, by M. Camac, J. Camm, J. Keck and C. Petty, *AVCO Mfg. Corp., AVCO Res. Lab., Res. Rep.* 22, March 1958, 30 pp.

Forced-convection Heat-transfer Characteristics of Molten Flinak Flowing in an

Inconel X System, by Milton D. Grele and Louis Gedeon, *NACA Res. Mem.* E53L18, Feb. 1954, 23 pp. (Declassified from Secret by authority of *NACA Res. Abstr.* 127, p. 24, 6/5/58.)

On the Thermal Conduction Equation for Self-heating Materials with Surface Cooling, by P. H. Thomas, *Trans. Faraday Soc.*, vol. 54, Jan. 1958, pp. 60–65.

Some Shock Tube Experiments on the Chemical Kinetics of Air at High Temperatures, by S. Feldman, *J. Fluid Mech.*, Dec. 1957, pp. 225–242.

Effect of Oxygen Recombination on One-dimensional Flow at High Mach Numbers, by S. P. Heims, *NACA TN* 4144, Jan. 1958, 52 pp.

Radiant Heat Exchange in a Gas-filled Enclosure, by H. C. Hottel and E. S. Cohen, *AIChE J.*, vol. 4, no. 1, March 1958, pp. 3–14.

Dynamics of a Dissociating Gas, (III) Non-equilibrium Theory, by N. C. Freeman, *NATO AGARD Rep.* 133, July 1957, 21 pp.

On the Relation of Surface Friction and Heat Transfer, by E. A. Sidorov, *Sov. Phys.-Tech. Phys.*, March 1957, pp. 499–504.

An Analysis of the Turbulent Boundary-layer Characteristics on a Flat Plate with Distributed Light-gas Injection, by M. W. Rubesin and C. C. Pappas, *NACA TN* 4149, Feb. 1958, 43 pp.

The Influence of Surface Injection on Heat Transfer and Skin Friction Associated with the High-speed Turbulent Boundary Layer, by M. W. Rubesin. *NACA RM* A55L13, Feb. 20, 1956, 16 pp.

Heat Transfer in Isotropic Turbulence During the Final Period of Decay, by D. W. Dunn and W. H. Reid, *NACA TN* 4186, June 1958, 68 pp.

Prandtl Number Effects on Unsteady Forced-convection Heat Transfer, by E. M. Sparrow and J. L. Gregg, *NACA TN* 4311, June 1958, 14 pp.

Thermodynamic Properties and Composition of Air by Dissociation Equilibrium, by H. J. Kaeppeler and H. G. L. Krause, *Forschugsinst. f. Physik der Strahlantriebe, Mitteil.* 1, 1954, 40 pp., 22 figs. (in German.)

A Graphical Method for Solution of Freezing Problems, by P. S. Longwell, *AIChE J.*, vol. 4, no. 1, March 1958, pp. 53–57.

Heat and Momentum Transfer in the Flow of Gases Through Packed Beds, by M. B. Glaser and G. Thodos, *AIChE J.*, vol. 4, no. 1, March 1958, pp. 63–67.

Heat Transfer from Horizontal Cylinders to a Turbulent Air Flow, by B. G. van der Hogge Zijnen, *Appl. Sci. Res.*, Sec. A., no. 2–3, 1958, pp. 205–223.

Heat Transmission to Fluids with Low Prandtl Numbers for Flow Through Tube Banks, by R. D. Cess and R. J. Grosh, *ASME Trans.*, vol. 80, no. 3, April 1958, pp. 677–682.

Heat Transfer to Fluids with Low Prandtl Numbers for Flow Across Plates and Cylinders of Various Cross Section, by R. J. Grosh and R. D. Cess, *ASME Trans.*, vol. 80, no. 3, April 1958, pp. 667–671.

Heat Transfer Rates to Cross-flowing Mercury in a Staggered Tube Bank (II), by C. L. Rickard, O. E. Dwyer and D. Dropkin, *ASME Trans.*, vol. 80, no. 3, April 1958, pp. 646–651.

Shock Wave Photography of Large Subjects in Daylight, by H. E. Edgerton, *Rev. Sci. Instr.*, vol. 29, no. 2, Feb. 1958, pp. 171–172.

Measurement of Metal Heat Conduc-

tivity in a Wide Range of Temperature During a Single Experiment, by O. A. Kraev, *Teploenergetika*, vol. 4, no. 12, Dec. 1957, pp. 69–72 (in Russian).

Unsteady Heat Convection Near a Horizontal Cylinder, by G. A. Ostroumov, *Sov. Phys-Tech. Phys.*, Oct. 1957, pp. 2627–2641.

Natural Convection Heat Transfer in Regions of Maximum Fluid Density, by R. S. Schechter and H. S. Isbin, *AIChE J.*, vol. 4, no. 1, March 1958, pp. 81–89.

Heat Transfer in Nucleate Boiling (II) New Correlating Equation, by K. Nishikawa, *Trans. Japan Soc. Mech. Engrs.*, vol. 22, Aug. 1956, pp. 557–561.

Heat Transfer in Nucleate Boiling (III) Effect of Pressure, by K. Nishikawa, *Trans. Japan Soc. Mech. Engrs.*, vol. 22, Aug. 1956, pp. 562–570.

On the Stability of Boiling Heat Transfer, by N. Zuber, *ASME Trans.*, vol. 80, April 1958, pp. 711–718.

Heat Transfer to Supercritical Water, by N. L. Dickinson and C. P. Welch, *ASME Trans.*, vol. 80, April 1958, pp. 746–752.

Experimental Velocity and Temperature Profiles for Air in Turbulent Pipe Flow, by C. A. Sleicher Jr., *ASME Trans.*, vol. 80, no. 3, April 1958, pp. 693–698.

Turbulent Heat Transfer in the Thermal Entrance Region of a Pipe with Uniform Heat Flux, by E. M. Sparrow, T. M. Hallman and R. Siegel, *Appl. Sci. Res.*, sect. A, no. 1, 1958, pp. 37–52.

Fluid Friction in Noncircular Ducts, by J. E. Walker, G. A. Whan and R. R. Rothfus, *AIChE J.*, vol. 3, Dec. 1957, pp. 484–489.

Heat Transfer to Flow in a Round Tube with Arbitrary Velocity Distribution, by I. R. Whiteman and W. B. Drak, *ASME Trans.*, vol. 80, no. 3, April 1958, pp. 728–736.

Convective Heat Transfer from High-temperature Air Inside a Tube, by H. E. Zellnik and S. W. Churchill, *AIChE J.*, vol. 4, no. 1, March 1958, pp. 37–42.

Quasilinear Heat Flow, by N. E. Friedmann, *ASME Trans.*, vol. 80, no. 3, April 1958, pp. 635–641.

Graphical and Numerical Methods for Heat Conduction with Unsteady-state Ambient Temperature or Heat Generation, by Y. Katto, *Trans. Japan Soc. Mech. Engrs.*, vol. 22, Aug. 1956, pp. 525–529.

Formulae and Approximations for Aerodynamic Heating Rates in High Speed Flight, by R. J. Monaghan, *Gt. Brit., Aeron. Res. Council, Curr. Pap.* 360, Oct. 1955, 1957, 53 pp.

On Heat Transfer in Laminar Boundary-layer Flows of Liquids Having a Very Small Prandtl Number, by G. W. Morgan, A. C. Pipkin and W. H. Warner, *J. Aeron. Sci.*, vol. 25, March 1958, pp. 173–180.

Incompressible Two-dimensional Stagnation-point Flow of an Electricaly Conducting Viscous Fluid in the Presence of a Magnetic Field, by J. L. Neuringer and W. McIlroy, *J. Aeron. Sci.*, vol. 25, March 1958, pp. 194–198.

Measurement of Turbulent Heat Transfer Rates on the Aft Portion and Blunt Base of a Hemisphere-cylinder in the Shock Tube, by J. Rabinowixz, *Calif. Inst. Tech., Guggenheim Aeron. Lab., Mem.* 41, Nov. 1957, 24 pp.

Hypersonic Heat Transfer to Catalytic Surfaces, by S. M. Scala, *J. Aeron. Sci.*, vol. 25, April 1958, pp. 273–275.

Steady Temperature of a Plane Plate in a Reacting Gas Flow, by E. P. Vaulin, *Sov. Phys.-Dokl.*, March-April 1957, pp. 187–191.

Film Boiling from Vertical Tubes, by Y. Y. Hsu and J. M. Westwater, *AIChE J.*, vol. 4, March 1958, pp. 58–62.

Effect of Superatmospheric Pressures on Nucleate Boiling of Organic Liquids, by R. B. Mesler and J. T. Banchero, *AIChE J.*, vol. 4, March 1958, pp. 102–113.

Heat Transfer in Nucleate Boiling (1) Effective Stirring Length of Bubbles, by K. Nishikawa and M. Kawano, *Japan Soc. Mech. Engrs. Trans.*, vol. 22, Aug. 1956, pp. 551–556.

Far Noise Field of Air Jets and Jet Engines, by Edmund E. Callaghan and Willard D. Coles, *NACA Rep.* 1329, 1957, 18 pp. (Supersedes *TN* 3590; *TN* 3591.)

Some Measurements Bearing on the Principle of Operation of Jet Silencing Devices, by G. M. Corcos, *Douglas Aircr. Co., Rep.* SM-23114, March 1958, 39 pp.

The Compressible Flow through Cascade Actuator Discs, by J. H. Horlock, *Aeron. Quart.*, vol. 9, May 1958, pp. 110–130.

Turbulent Mixing of Two Streams of Different Gases, by L. G. Napolitano, *L'Aerotecnica*, vol. 37, Dec. 1957, pp. 301–310 (in Italian).

Application of the Integral Methods to Study of the Laminar Motion of a Non-reacting Binary Gas Mixture, by A. Pozzi, *L'Aerotecnica*, vol. 37, Dec. 1957, pp. 311–320 (in Italian).

Experimental Data on Turbulent Wall Jets, by A. Sigalla, *Aircr. Engng.*, vol. 30, May 1958, pp. 131–134.

The Contra-flow Gas-to-gas Heat Exchanger, by J. S. Turton, *Aircr. Engng.*, vol. 30, May 1958, pp. 135–141.

The Effect of Shock Waves on the Isentropic Efficiency of Convergent-divergent Nozzles, by B. W. Martin and F. J. Bayley, *Roy. Aeron. Soc. J.*, vol. 62, May 1958, pp. 377–382.

On Heat Transfer in Slip Flow, by Stephen H. Maslen, *J. Aeron. Sci.*, vol. 25, June 1958, pp. 400–401.

On Hypersonic Stagnation-point Flow with a Magnetic Field, by Nelson H. Kemp, *J. Aeron. Sci.*, vol. 25, June 1958, pp. 405–407.

Macroscopic Foundation of Plasma Dynamics, by Taro Kihara, *Phys. Soc. Japan J.*, vol. 13, May 1958, pp. 473–481.

Externally Pinched Plasma, by Tihiro Ohkawa and Taro Kihara, *Phys. Soc. Japan J.*, vol. 13, May 1958, pp. 482–483.

The Instability of a Pinched Fluid with a Longitudinal Magnetic Field, by M. Kruskal and J. L. Tuck., *Roy. Soc., Proc.*, vol. A245, June 3, 1958, pp. 222–237.

A Radial Heat-flow Apparatus for Liquid Thermal Conductivity Determinations, by A. R. Challoner, H. A. Gundry and R. W. Powell, *Roy. Soc. Proc.*, vol. A245, June 3, 1958, pp. 259–267.

On Some Fundamentals in Magneto-fluid-mechanics, by Eugene E. Covert, *MIT, Naval Supersonic Lab., Tech. Rep.* 247, March 1958, 300 pp.

Magneto-gasdynamics of Hypersonic Couette Flow, by Z. O. Bleviss, *Douglas Aircr. Co., Rep.* SM 23098, Feb. 1958, 56 pp.

Attenuation in a Shock Tube Due to Unsteady-boundary-layer Action, by Harold Mirels, *NACA Rep.* 1333, 1957, 19 pp. (Supersedes *TN* 3278.)

Measurements of the Effect of Surface Cooling on Boundary Layer Transition on a 15° Cone, Part I: Tests at M = 2 and 3 in an 8" x 9" Wind Tunnel at RAE-Bedford, by A. C. Browning, J. F. W. Crane and R. J. Monaghan, *Gt. Brit., Aeron. Res. Council, Curr. Paper* 381 (formerly *ARC Tech. Rep.* 19836; *Roy. Aircr. Estab., TN Aero* 2527).

An Experimental Study of the Turbulent Boundary Layer on a Shock-tube Wall, by Paul B. Gooderum, *NACA TN* 4243, June 1958, 63 pp., diagrs., photos., tab.

Stall Propagation in a Cascade of Airfoils, by Anthony R. Kriebel, Harry S. Seidel and Richard G. Schwind, *NACA TN* 4134, June 1958, 122 pp.

Cooling Characteristics of a Transpiration-cooled Afterburner with a Porous Wall of Brazed and Rolled Wire Cloth, by William K. Koffel, *NACA Res. Mem.* E54E25, Aug. 1954, 68 pp. (Declassified from Confidential by authority of *NACA Res. Abstr.* 127, p. 15, 6/5/58.)

The Structure of a Hydromagnetic Shock in Steady Plane Motion, by G. S. S. Ludford, *Univ. of Maryland, Inst. for Fluid Dynam. and Appl. Math., TN BN-131 (AFOSR-TN* 58–418; *ASTIA AD* 158221), April 1958, 23 pp.

Design and Operation of a Sodium to Lithium to Air Heat Transfer System, by A. R. Crocker, R. L. Potter, R. J. Spera, T. D. McLay and S. H. Esleeck, *Atomic Energy Comm., APEX* 327, Aug. 1957, 195 pp.

The Analytical Determination of the Local Heat Transfer Characteristics of Gases Flowing Turbulently in the Thermal Entrance Region of a Circular Duct with Large Temperature Differences between the Gas and the Duct Wall, by Helmut Wolf and M. J. Zucrow, *Project Squid*,

Tech. Rep. PUR-35-M (available only on microcards).

Induced Air Flows in Fuel Sprays, by Hikmet Binark and W. E. Ranz, *Project Squid, Tech. Rep.* PSU-1-P (*ASTIA AD* 156507), April 1958, 25 pp. (available only on microcards).

Internal Characteristics and Performance of Several Jet Deflectors at Primary-nozzle Pressure Ratios up to 3.0, by Jack G. McArdle, *NACA TN* 4264, June 1958, 107 pp.

Measurements on the Velocity of Sound in Oxygen Gas under High Pressure, by A. van Itterbeek and J. Zink, *Appl. Sci. Res.*, vol. A7, no. 5, 1958, pp. 375–385.

On Simple Waves in Perfect and Dissociating Gases: Theory and Application, by Haim Kennet, *MIT, Fluid Dynam. Res. Group. Rep.* 58.1 (*AFOSR-TN-58-302*), Feb. 1958, 49 pp.

Measurements of the Velocity Distribution in a Plane Turbulent Jet of Air, by B. G. van der Hegge Zijnen, *Appl. Sci. Res.*, sect. A, vol. 7, no. 4, 1958, pp. 256–276.

Measurements of the Distribution of Heat and Matter in a Plane Turbulent Jet of Air, by B. G. van der Hegge Zijnen, *Appl. Sci. Res.*, sect. A, vol. 7, no. 4, 1958, pp. 277–292.

Measurements of Turbulence in a Plane Jet of Air by the Diffusion Method and by the Hot-wire Method, by B. G. van der Hegge Zijnen, *Appl. Sci. Res.*, sect. A, vol. 7, no. 4, 1958, pp. 293–313.

Magnetohydrodynamics: Hope for Space, by J. S. Butz Jr., *Aviation Week*, vol. 68, May 12, 1958, pp. 48–50.

Time Delay between High-speed Pellets and Associated Luminosity and Ionization, by P. E. Tucker, R. A. Davidson, and W. S. Patridge, *J. Appl. Phys.*, vol. 29, May 1958, pp. 868–870.

Hydromagnetic Effects on Stagnation-point Heat Transfer, by Joseph L. Neuringer and William McIlroy, *J. Aeron. Sci.* vol. 25, May 1958, pp. 332–334.

Magnetohydrodynamic Analysis of Heat Transfer Near a Stagnation Point, by Vernon J. Rossow, *J. Aeron. Sci.*, vol. 25, May 1958, pp. 334–335.

Calculation of Shock Hugoniots and Related Quantities for Nitrogen and Oxygen, by R. A. Alpher and H. D. Greyber, *Physics of Fluids*, vol. 1, March-April 1958, pp. 160–161.

Turbulence Measurement in Electrically Conducting Fluids, by Salamon Eskinazi, *Physics of Fluids*, vol. 1, March-April 1958, pp. 161–162.

Pumping and Drag Characteristics of an Aircraft Ejector at Subsonic and Supersonic Speeds, by Gerald G. Gorton, *NACA Res. Mem.* E54D06, June 1954, 19 pp. (Declassified from Confidential by authority of *NACA Res. Abstr.* 126, p. 29, 5/2/58.)

Investigation of Performance of Several Double-shroud Ejectors and Effect of Variable-area Exhaust Nozzle on Single Ejector Performance, by C. W. Ellis, D. P. Hollister and H. D. Wilsted, *NACA Res. Mem.* E52D25, July 1952, 25 pp. (Declassified from Confidential by authority of *NACA Res. Abstr.* 126, p. 27, 5/2/58.)

Internal Performance Characteristics of Variable-throat Plug- and Vaned-type Convergent-divergent Nozzles, by H. George Krull, Fred W. Steffen and Carl C. Ciepluch, *NACA Res. Mem.* E53D09, June 1953, 34 pp. (Declassified from Confidential by authority of *NACA Res. Abstr.* 126, p. 28, 5/2/58.)

Preliminary Experimental Investigation of Transpiration Cooling for an Afterburner with a Sintered, Porous Stainless-steel Combustion-chamber Wall, by William K. Koffel, *NACA Res. Mem.* E53-DO8, June 1953, 47 pp. (Declassified from Confidential by authority of *NACA Res. Abstr.* 126, p. 28, 5/2/58.)

Exploratory Tests of Transpiration Cooling of a Porous 8° Cone at M = 2.05 Using Nitrogen Gas, Helium Gas, and Water as the Coolants, by Leo T. Chauvin and Howard S. Carter, *NACA Res. Mem.* L55C29, June 1955, 22 pp. (Declassified from Confidential by authority of *NACA Res. Abstr.* 126, p. 35, 5/2/58.)

Theoretical Study of the Effect of the Non-ideality of a Dense Shocktube Driver Gas with Special Reference to Non-uniform Shocktubes, by A. E. Seigel, *NAVORD Rep.* 5707 (*Naval Ord. Lab., Ball. Res. Rep.* 5), Nov. 1957, 35 pp.

Schlieren Evaluation of a Shock Tube for Pressure Gage Performance, by Stuart M. Hauser, *Calif. Inst. Techn., Jet Prop. Lab., Rep.* 20-115, Nov. 1957, 49 pp.

Combustion, Fuels and Propellants

Observations on the Kinetics of the Ionization of Alkali Metals in Flame Gases, by P. F. Knewstubb and T. M. Sugden, *Faraday Soc. Trans.*, vol. 54, March 1958, pp. 372-380.

The Thermal Reaction between Hydrogen and Nitrogen Dioxide, Part IV: Thermal Ignitions of Hydrogen and Nitrogen Dioxide, by P. G. Ashmore and B. P. Levitt, *Faraday Soc. Trans.*, vol. 54, March 1958 pp. 390-393.

The Dielectric Constant of a Compressed Gas Mixture, by A. D. Buckingham and R. E. Raab, *Faraday Soc. Trans.*, vol. 54, May 1958, pp. 623-628.

Elementary Processes in the Radiochemical Excitation of Gaseous Oxygen, by K. J. Laidler and E. Kerry Gill, *Faraday Soc. Trans.*, vol. 54, pp. 633-639.

Mixing and Chemical Reaction in the Laminar Wake of a Flat Plate, by S. I. Cheng and A. A. Kovitz, *J. Fluid Mech.*, vol. 4, May 1958, pp. 64-80.

Applications of Thermodynamic Constants and Data to Gaseous Mixing at Elevated Temperatures (Flames, Engines and Propulsion Systems), by G. Ribard and N. Manson, *France, Ministere de l'Air, Publications Scientifiques et Techniques*, no. 341, 1958, 194 pp. (in French).

Performance Estimation of the Coolant Fuel System, by L. Greiner, J. Rabinowicz and A. Zuckerman, *Odin Assoc., Tech. Rep.* 100-1 (*AFOSR-TR-58-43; ASTIA AD* 154150), Dec. 1957, 33 pp.

Evaluation of Some Analytical Procedures for Solid Rocket Oxidants, Part I, by E. A. Burns and R. F. Muraca, *Calif. Inst. Tech., Jet Prop. Lab., Mem.* 20-158, June 1958, 17 pp.

Ignition Limits of Hydrogen Peroxide Vapor at Pressures above Atmospheric, by C. N. Satterfield, F. Feakes and N. Sekler, *Mass. Inst. Tech., Dept. Chem. Engng., Rep.* 53, June 1958, 9 pp.

I. Macromolecular Symposium, Prague, Sept. 1957; II. Soviet Polymer Seience, 1957, Condensed Report, by H. F. Mark, *Solid Propellant Info. Agency*, July 1958, 50 pp.

Relation between Gas Absorptivities and Emissivities, by D. Olfe and S. S. Penner, *Calif. Inst. Tech., Daniel and Florence Guggenheim Jet Prop. Center, Tech. Rep.* 27, June 1958, 4 pp.

High Energy Solid Fuels May Be Hydrids, by Michael Yaffee, *Aviation Week*, vol. 68, June 23, 1958, pp. 47, 50-51.

Some Aspects of Detonation, Part I: Detonation Velocity and Chemical Constitution by A. R. Martin and H. J. Yallop; Part II: Detonation Velocity as a Function of Oxygen Balance and Heat of Formation, by A. R. Martin and H. J. Yallop, *Faraday Soc. Trans.*, vol. 54, pt. 2, Feb. 1958, pp. 257-271.

New Method for Reducing Data on Interior Ballistic Trajectories, by Tadeusz Leser and John Lanahan, *Aberdeen Proving Ground, Ballistic Res. Labs., Rep.* 1024, Aug. 1957, 41 pp.

Theoretical Performance of Liquid Ammonia with Liquid Oxygen as a Rocket Propellant, by Sanford Grodon and Alan R. Glueck, *NACA Res. Mem.* E58A21, May 1958, 84 pp.

Theoretical Rocket Performance of Liquid Methane with Several Fluorine-Oxygen Mixtures Assuming Frozen Composition, by Sanford Gordon and Michael E. Kastner, *NACA Res. Mem.* E58B20, May 1958, 44 pp.

New Formulas for Rapid Calculation of Linear Burning Rates of Solid Propellants, by William F. Wallace, *Picatinny Arsenal, Samuel Feltman Ammunition Labs,. Tech. Rep.* 2488, April 1958, 40 pp.

Studies of OH, CO, CH, and C_2 Radiation from Laminar and Turbulent Propane-air and Ethylene-air Flames, by Thomas P. Clark, *NACA TN* 4266, June 1958, 23 pp., diagrs., photos.

Flame Structure Studies, IV: Premixed Carbon Monoxide Combustion, by Raymond Friedman and Robert G. Nugent, *Project Squid, Tech. Rep.* ARC-3-P (*ASTIA AD* 156505), 18 pp., April 1958 (available only on microcards).

Considerations Pertaining to Spherical Vessel Combustion, by J. Grummer, E. B. Cook and T. A. Kubala, *Project Squid, Tech. Rep.* BUM-25-P (*ASTIA AD* 156947), April 1958, 18 pp. (available only on microcards).

Composition Traverses in Curved Laminar Fronts, by George H. Markstein, *Project Squid, Tech. Rep.* CAL-75-P (*ASTIA AD* 156503), April 1958, 21 pp. (available only on microcards).

The Decay of Radical Radiation, by Edward T. Child and Kurt Wohl, *Project Squid, Tech. Rep.* DEL-9-P (*ASTIA AD* 156506), April 1958, 23 pp. (available only on microcards).

Spectrographic Studies of Laminar Flames, II, by Raymond Kushida and Kurt Wohl, *Project Squid, Tech. Rep.* DEL-10-P (*ASTIA AD* 156504), April 1958 (available only on microcards).

Optical Studies of Structure of Turbulent Flames, by Kurt Wohl and Rajah H. Atalla, *Project Squid, Tech. Rep.* DEL-11-P (*ASTIA AD* 156948), April 1958, 20 pp. (available only on microcards).

Two Dimensional Effects in Gaseous Detonation Waves, by James A. Fay and Gerhard Opel, *Project Squid, Tech. Rep.* MIT-16-P (*ASTIA AD* 153326), March 1958, 5 pp. (available only on microcards).

Ionization in Detonation Waves, by Satyaki Basu and James A. Fay, *Project Squid, Tech. Rep.* MIT-17-P (*ASTIA AD* 156502), April 1958, 16 pp. (available only on microcards).

On the Structure of Detonation Waves, by T. C. Anderson, *Project Squid. Tech. Rep.* MICH-4-M (*ASTIA AD* 156509), April 1958, 19 pp. (available only on microcards).

Anomalous Extinction Phenomena in

Solid Propellant Burning, by Donald L. Reid, Kimball P. Hall and Martin Summerfield, *Project Squid, Tech. Rep.* PR-77-P (*ASTIA AD* 156501), April 1958, 19 pp. (available only on microcards).

Investigation of Liquid Fluorine-Liquid Ammonia Propellant Combination in a 100-pound-thrust Rocket Engine, by Edward A. Rothenberg and Howard W. Douglass, *NACA Res. Mem.* E53E08, July 1953, 31 pp. (Declassified from Confidential by authority of *NACA Res. Abstr.* 127, p. 14, 6/5/58.)

The Analysis of Red Fuming Nitric Acid, II: Determination of Water by the Karl Fischer Titration, by E. A. Burns and R. F. Muraca, *Calif. Inst. Tech., Jet Prop. Lab., Progr. Rep.* 20-344, Jan. 1958, 8 pp.

A Statistical Theory of Chemical Reaction Rates, by James Keck, *AVCO Mfg. Corp., AVO Res. Lab., Res. Rep.* 20, April 1958, 18 pp.

The Reactions of Hydrogen Atoms with Oxygen, by B. deB. Darwent, and V. J. Krasnansky, *Project Squid, Tech. Rep.* CUA-1-P (*ASTIA AD* 157195), April 1958, 18 pp. (available only on microcards).

Diffusion and Heterogeneous Reaction, I: The Dynamics of Radical Reactions, by Henry Wise and Clarence M. Ablow, *Project Squid, Tech. Rep.* SRI-1-P (*ASTIA AD* 156508), March 1958, 17 pp. (available only on microcards).

Infrared Absorptivities and Emissivities of Gases, by A. Thomson, W. J. Hooker and S. S. Penner, *Calif. Inst. Tech., Daniel and Florence Guggenheim Jet Prop. Center, Tech. Rep.* 26, June 1958, 6 pp.

Micro Determination of Nitrogen in Organic Compounds, by E. M. Bens, *NAVORD Rep.* 5865 (*NOTS* 1988), April 1958, 26 pp.

The Determination of Unsaturation in Polypropylene Glycols, by E. A. Burns, R. F. Muraca and F. Chang, *Calif. Inst. Techn., Jet Prop. Lab., Progr. Rep.* 20-345, Jan. 1958, 12 pp.

Internal Ballistics of a High Velocity Light Gas Gun, by M. S. Sodha and V. K. Jain, *Appl. Sci. Res.*, vol. A7, no. 5, 1958, pp. 351–357.

On the Internal Ballistics of a Supergun (Hochdrukpumpe), by V. A. Jain and M. S. Sodha, *Appl. Sci. Res.*, vol. A7, no. 5, 1958, pp. 369–374.

Liquids vs. Solids, by Kurt R. Stehling, *Aviation Age,* vol. 29, June 1958, pp. 22–23, 90–91, 94–95.

Advances Made in Conventional Fuels, by Michael Yaffee, *Aviation Week,* including *Space Technology,* vol. 58, June 16, 1958, pp. 267–272.

High Temperature Radiation Chemistry of Hydrocarbons, by P. J. Lucchesi, B. L. Tarmy, R. B. Long, D. L. Baeder and J. P. Longwell, *Ind. Engng. Chem.*, vol. 50, June 1958, pp. 879–884.

Gaseous Detonations, X: Study of Reaction Zones, by John P. Chesick and G. B. Kistiakowsky, *J. Chem. Phys.*, vol. 28, May 1958, pp. 956–961.

Basic Considerations in the Combustion of Hydrocarbon Fuels with Air, Propulsion Chemistry Division, edited by Henry C. Barnett and Robert R. Hibbard. **Chap. I: Atomization and Evaporation of Liquid Fuels,** by Charles C. Graves and Donald W. Bahr. **Chap. II: Flow and Mixing Processes in Combustion Chambers,** by Wilfred E. Scull and William R. Mickelsen. **Chap. III: Ignition and Flammability of Hydrocarbon Fuels,** by Frank E. Belles and Clyde C. Swett. **Chap. IV: Laminar Flame Propagation,** by Gordon L. Dugger, Dorothy M. Simon and Melvin Gerstein. **Chap. V: Turbulent Flames,** by Melvin Gerstein and Gordon L. Dugger. **Chap. VI: Flame Stabilization,** by Gordon L. Dugger and Melvin Gerstein. **Chap. VII: Diffusion Flames,** by Richard S. Brokaw and Melvin Gerstein. **Chap. VIII: Oscillations in Combustors,** by Perry L. Blackshear Jr. and Warren D. Rayle. **Chap. IX: Smoke and Coke Formation in the Combustion of Hydrocarbon-air Mixtures,** by Rose L. Schalla and Robert R. Hibbard. *NACA Rep.* 1300, 1957, 259 pp.

Double Waves in Gaseous Detonations, by Mark Cher and G. B. Kistiakowsky, *Harvard Univ., Dept. Chem.*, March 1958, 15 pp., 3 figs.

Chemically Frozen Boundary Layers with Surface Reaction, by D. E. Rosner, *Princeton Univ., Dept. Aeron. Engng., Rep.* 419, March 1958, 17 pp.

The Spark Ignition of Dust Clouds, by Lloyd E. Line Jr., Harold A. Rhodes and Thomas E. Gilmer Jr., *Experiment Inc., TP*-129, March 1958, 12 pp., 10 figs.

Shock Tube Studies of Acetylene Compounds, by W. J. Hooker, *Calif. Inst. Techn., Daniel and Florence Guggenheim Jet Prop. Center, Tech. Rep.* 7 (*AFOSR-TN*-58-293: *ASTIA AD* 154202), April 1958, 10 pp., 5 figs.

The Reaction Rate Law in Non-Uniform Flows, by D. E. Rosner, *Princeton Univ., Dept. Aeron. Engng., Rep.* 420, Nov. 1957, 10 pp.

On the Effect of Preliminary Vaporization on the Completeness and Stability of Combustion of a Fuel Spray, by V. Y. Basevich, *Akademiia Nauk SSSR, Izvestia, Otdelenie Tekhnicheskikh Nauk,* no. 2, Feb. 1958, pp. 26–32 (in Russian).

Effect of Pressure on the Normal Velocity of the Propagation of Flames, by S. A. Gol'denberg and V. S. Pelevin, *Akademiia Nauk SSSR, Izvestia, Otdelenie Tekhnicheskikh Nauk,* no. 2, Feb. 1958, pp. 33–41 (in Russian).

The Pressure - Volume - temperature Properties of Fluorobenzene, by D. R. Douslin, R. T. Moore, J. P. Dawson and Guy Waddington, *Am. Chem. Soc. J.*, vol. 80, May 5, 1958, pp. 2031–2038.

Flow Field of Bunsen Flame, by M. S. Uberoi, A. M. Kuethe and H. R. Menkes, *Physics of Fluids,* vol. 1, March-April 1958, pp. 150–158.

NACA Probes Fluorine Uses, by Alfred J. Zaehringer, *Missiles and Rockets,* vol. 3, May 1958, pp. 104–105.

Stopping Time—the Photography of Explosives, by Charles H. Bagley, *SRI J.*, vol. 2, no. 1, 1958, pp. 27–32.

Materials of Construction

Outlook for 600 Deg. F. Silicone Rubbers, by J. F. Dellaria, *Aviation Age,* vol. 29, June 1958, pp. 60–64.

Sheet Steels for High-speed Aircraft and Missiles, by A. L. Feild and M. E. Carruthers, *Aero-Space Engng.* (formerly *Aeron. Engng. Rev.*), vol. 17, June 1958, pp. 41–44.

Regularities in Creep and Hot Fatigue Data, Part II, by K. F. A. Walles and A. Graham, *Gt. Brit., Aeron. Res. Council, Curr. Paper* 380 (formerly *Nat. Gas Turbine Estab. Rep.* R190), Dec. 1956, 46 pp., 97 figs.

Elastomeric Mountings for High Temperatures, by R. P. Thorn, *Aviation Age,* vol. 30, July 1958, pp. 66–69.

Index to Advertisers